INVENTOR EDITION PATENT IEP A96B1C59-67B6-433C-AA2D-37E5C0F4D790

Inventor and proprietor: **Yuri Feldman**, e-mail: **yuri@liftoplane.com**

Published at **April 11, 2023** under URL:
https://www.liftoplane.com/publications/IEP_A96B1C59-67B6-433C-AA2D-37E5C0F4D790.pdf
referenced on the Web-page: **https://www.liftoplane.com/Patenting.htm**

Priority: **June 26, 2015**, originated from the USA application **US 14/751,180** published at **December 29, 2016** as **US20160376003A1**

Effective date for property rights: **December 29, 2016** that commences the **20 years** period.

Title: **AIRCRAFT**

International Patent Classification (IPC):
B64C 39/00 *(2006.01)* ***B64C 11/06*** *(2006.01)* ***B64C 13/08*** *(2006.01)* ***B64C 13/14*** *(2006.01)*
G06F 17/10 *(2006.01)* ***B64D 43/00*** *(2006.01)* ***G05D 1/10*** *(2006.01)* ***G01P 13/02*** *(2006.01)*
B64C 13/34 *(2006.01)* ***B64C 31/028*** *(2006.01)*

Cooperative Patent Classification (CPC):
B64C 39/005; B64C 11/006; B64C 13/08; B64C 13/14; B64C 13/34; B64D 43/00; G05D 1/101; G01P 13/025; G06F 17/10; B64C 31/028

Prior art documents cited:
US 2045233 A **US 5100080 A** **US 6932296 B2**

ABSTRACT

A concept of performing a powered flight by performing a work against gravity using a gliding wing as a steady support is introduced, namely the "flying elevator" concept, resulted in an aircraft presented that uses the prolate movement of the cyclorotor wings, where steering of these wings utilizes a four-gears pitch steering scheme managed on the base of "pitch-gain-skew" freedoms controlled respectively from the side of angular trimmers for handling the aircraft. The aircraft implements this concept in its handling evaluated and optimized for particular flight operations, using presented modeling aspects, their simulation for an entire flight and analyzing of the reported result. Handling rules are presented. A biangular handling mode based on the angles of attack serves the pilot manipulation with joystick of flight computer to actuate the trimmers, and the fuselage follows the direction of its flight, using a stream deviation tube for a feedback.

<u>**100**</u>

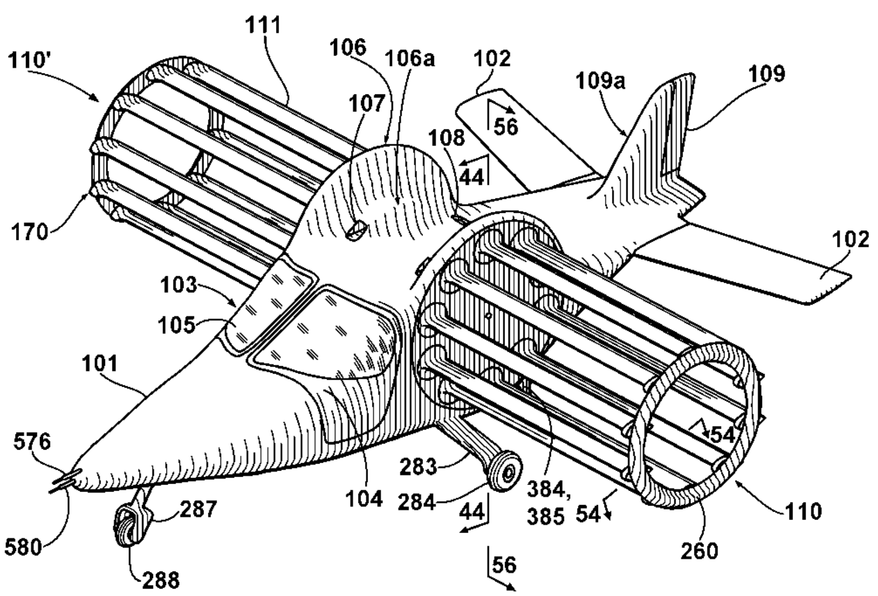

IEP A96B1C59-67B6-433C-AA2D-37E5C0F4D790

AIRCRAFT

FIELD OF THE INVENTION

[0001] The presented invention generally relates to short takeoff and landing aircraft. In particular, the present invention relates to such an aircraft that uses a pair of rotors of parallel-oriented rotating wings to obtain an overall aerodynamic force with the required components in the vertical and horizontal directions, enough to accomplish the entire flight instead of a pair of stationary wings and separate propulsors. The invention also relates to a steering those wings on the rotors and to a handling of the entire aircraft.

BACKGROUND OF THE INVENTION

[0002] Contemporary aviation in its history had a remarkable time when the first aircraft for powered flight was invented. Looking only from the point of view of the powering, this invention can be considered as an application of a rotated wings actuator, known as a propeller, for a non-powered glider. Prior this time, the propeller was well known for use in marine applications, and its successful adaptation to air applications ushered in the era of airplanes and defined a common point of view on any kind of aircraft. The cornerstone of this common point of view is a considering of neediness of a some kind of a powered propulsion for any kind of a powered flight. And for characterizing an ability or performance of such propulsion a coefficient of the propulsion efficiency is used. This coefficient was known prior the time as a part of the momentum theory of actuators, which was successfully applied to the marine applications and was developed by W.J.M. Rankine, A.G. Greenhill and R.E. Froude. And therefore, the propeller of the airplane is no exception to this. Other performance characteristic of the airplane was well known from the time of the non-powered flight as a glide ratio. Also, it can be substituted by its equal counterpart as a lift to drag ratio, and it is widely used when referring to the performance of the contemporary airplanes and gliders. And the total performance of an aircraft can be considered as the product of both of the mentioned coefficients. Progress in the creation of the high performance airplanes still is today neediness, but this progress is saturated after the long way of the airplanes optimization. One of the last steps of such optimization was the migrating to use of the turbofan engines in the park of contemporary airplanes, which have a significant advantage over the used before turbojet engines. This advantage is permitted by having the higher propulsion efficiency in the full accordance with the momentum theory of actuators. However, the propulsion efficiency of the turbofan in the time of cruise is only about 50 percent, since its fan stage only partially participates in the overall propulsion.

[0003] Other types of aircraft were also under consideration, but only a few of them succeeded in practical use. One of them is a helicopter, which propulsion efficiency in time of cruise of more than 90 percent, but its lift to drag ratio is too low to compete with the airplane. Autogiro also has a too low lift to drag ratio and also uses a separate propeller for propulsion, so its propulsion efficiency is below 80 percent. Nevertheless, it is still used for the flights.

[0004] Ornithopters were also in development. They have a big advantage in the performance, permitting to have the propulsion efficiency of more than 95 percent and the high lift to drag ratio, but they have a big drawback: the oscillations from its flapping wings are inevitable propagated to its fuselage, so such a flight is not comfortable for humans. Also, they need transmissions with a very high applied force, especially for the big scale aircraft. Nevertheless, this type of “aircraft” is successfully used by birds.

[0005] Aircraft with parallel movement of wings over circular pathway are known as cyclorotor aircraft. They have been in development for a long time since the beginning of the twentieth century, but so far have not succeeded for human flight. Currently, they are used only for small-scale models, without a great advantage over small-scale helicopter models. Nevertheless, cyclorotor actuators themselves have succeeded in marine applications. The non-succeeding of the cyclorotors for aircraft was mainly caused by a misunderstanding of their abilities upon migrating the elements of theory and practice for the development of airplanes and helicopters to their development. A main principal point in this misunderstanding is the particular kind of the direct relation between powering and propulsion for an airplane. The cyclorotors can also operate in this particular case, but they cannot leverage their potential by this way. Nevertheless, this mode of operation permits to have abilities for using a short runway, which are also known as the Short Takeoff and Landing operations (STOL).

[0006] Presented invention is originated from some concept of the inventor, which is explained in the detailed description of the application, and from which a generalized relation between the powering and propulsion follows. And the development of the presented invention resulted from a correct understanding of the application of this generalized relation on the cyclorotor aircraft and from the correct implementation of mentioned concept in an aircraft with high propulsion efficiency, moderate glide ratio and ability for STOL operations.

SUMMARY OF THE INVENTION

[0007] The present invention provides an aircraft with high propulsion efficiency, moderate gliding efficiency, the ability to perform short takeoff and landing (STOL) and also having cruise speed up to subsonic limit. Another aspect of the invention is presented in the aircraft as the use of high torque electric engines to power the actuators of the aircraft with the possibility of recuperation energy with high efficiency under descent, deceleration or both such operations simultaneously of this aircraft.

[0008] The aircraft is based on an improved variant of the cyclorotor aircraft, where improvements include the use of improved steering mechanics of the pitching of the wings of the rotors and the use of intermediate support rings to increase the aspect ratio of this aircraft. As an aspect of the invention this improving of steering mechanics is performed by using a displaceable four-gears scheme with a set of groove followers inside a common groove coaxial with a central gear instead of a displaceable three-gears scheme with multiple radial connected links. The improvement allows the use of a large number of wings per rotor, sufficient to maintain a low level of remaining vibrations for a comfortable flight. Also, an additional aspect of the invention is a method for decreasing these vibrations by applying specific patterns of electric current in the coils of the engines through an engine controller.

[0009] The core value of the invention is presented in the application by disclosing a correct attitude of understanding the operation of a generic cyclorotor aircraft by considering the use such an aircraft as the best variant for implementing an abstract scheme with ideal powering. This abstract scheme is referenced in the application as a "flying elevator" concept of performing a powered flight by performing a work against gravity using a gliding wing as a steady support. The concept is presented here with detail analysis, including flight simulation results for other variants for implementing this concept. Also, a preferred embodiment of the invention was subjected to a detailed analysis of the forecast after modeling the flight before presenting it. The details of the multi-tier modeling the flight are also presented here as aspects of the invention.

[0010] Another aspect of the invention is handling of the aircraft. The handling is presented here in two levels. The first is a low level vector of three components, where these components are introduced at the detailed description as a Pitch, Gain and Skew for each rotor of the both sides of the aircraft, which is referenced as PGS-state or simply PGS. The rotor possesses additional mechanics for decomposing the PGS vector on its components independently. The additional mechanics is also a separate aspect of the invention. Another aspect of the invention with respect to handling is a set of control and indication trimmers connected to the output shafts of these decomposing mechanics. These trimmers permit to control each component with high precision over a high dynamic range, by using up to three coaxial scales rotating simultaneously. Each of the trimmers can be handled electromechanically by a servo or manually in the case of an unattended electricity outage. The second handling level is a two-components biangular set with Skew as an additional component. The values of this set are meaningful angles of attack at some points of wings occurrence of the presented rotor, which are located on the Skew line. For the pilot, the exact meaning of these points can be irrelevant, but the values of this set are significant. In comparison with conventional airplane, they can be corresponded to the position of the elevator and the position of the flaps. Also, they can have meaning of the elevator and the ailerons for the turn operations. And the next aspect of the invention is the architecture of the software, which acts together with a flight computer to match the servos of trimmers with the actual winding speed of the rotors and the airspeed of the aircraft for having kinematically correct angles of attack near these specific points, using these values from the second handling level. These kinematic angles of attack differ from the actual angles of attack on some values induced by the wings interference and the inflow, but it is irrelevant for the pilot, since they are fixed for a particular aerodynamic speed and a winding speed of the rotor, for a known flight operation. The application provides a broad set of handling parameters for the presented aircraft, for many typical operations of the entire flight. And that can be repeated for any other particular implementation, using the presented simulation scheme.

[0011] Another aspect of the invention is a redundancy of the powering and steering of the rotors. The aircraft possesses abilities to perform turns with the same winding speed of the rotors on each side. In many cases it is a coordinated turn, but it can also perform a flat turn during the finalizing of the landing sequence. So the next aspect of the presented invention prescribes to connect the shafts of the both rotors together. So the aircraft can fly on one engine in a case if the other engine or its controller has an electrical malfunction. Also, these benefits apply to the shaft locking mechanism of each rotor, used in case of gliding or any serious problem. The steering of the rotors possesses the redundancy from the said multiple levels of the handling, which have different impacts from different levels of malfunction.

[0012] Another aspect of the presented invention is a system for providing a steady reference base for the rotors' steering operations, in a case of using the said biangular set. It is referenced as a stream following system that permits to have the fuselage oriented in the direction of the airstream. The system consists from two stabilators managed electromechanically, a controller, a pair of pressure sensors and a special Stream Deviation Tube (SDT), which is introduced in the detailed description as a separate aspect of the presented invention. The system is normally functioning by a negative feedback through this controller with an option of a computer management. But it can be handled manually in a case of an electricity outage, by using a separate trimmer and a pneumatic Stream Deviation Indicator (SDI).

[0013] An additional aspect of the presented invention is a construction of the fuselage for cooling the engines and to provide a simple setup for the engines and rotors. Also a power gear is excluded from the design of the preferred embodiment, since the high shaft moment on the rotors requires to use a high-pressure oil system for such a gear. Using of high torque electric engines instead it solves this problem, where each engine has a large diameter and a small thickness. A further additional aspect of the presented invention is the placement of accumulators along each side of the fuselage space near the rotors on movable racks, which permits to compensate for a load variation and also keeps the central fuselage space relatively free. Another additional aspect of the presented invention is an option with a combustion engine coupled with a generator and placed after the rotors, which utilizes the warm cooling air from the rotors' engines for combustion the fuel with an additional intake and has an exhaust along the trailing edge of the fuselage.

[0014] These as well as other features of the presented invention will be better appreciated by reference to the following detailed descriptions and drawings.

BRIEF DESCRIPTION OF THE DRAWINGS

[0015] FIG. **1** is a diagram of an explanation the "flying elevator" concept;

[0016] FIG. **2**A is an elevation view of a "Wired wings" configuration of a "flying elevator" system with one wired wing;

[0017] FIG. **2**B is an elevation view of a "Wired wings" configuration of a "flying elevator" system with two equal wired wings;

[0018] FIG. **2**C is an elevation view of a "Wired wings" configuration of a "flying elevator" system with two wired wings at separate levels;

[0019] FIG. **2**D is an elevation view of a "Wired wings" configuration of a "flying elevator" system with a glider connected to one wired wing;

[0020] FIG. **3** is a perspective view of a central node of the intermediate wired wing of the system shown in FIG. **2**C;

[0021] FIG. **4** is a diagram of common constraints used in the wired wings simulations;

[0022] FIGS. **5**A, **5**B, **5**C and **5**D are resulted flight profiles and plots of the handling and acceleration values from the flight dynamics simulations for the "wired wings" configurations shown in FIGS. **2**A, **2**B, **2**C and **2**D respectively;

[0023] FIG. **6** is a side elevation view of a "conveyer wings" configuration of a "flying elevator" aircraft;

[0024] FIG. **7** is a side elevation view of a cyclorotor configuration of a "flying elevator" aircraft;

[0025] FIG. **8** is a diagram of an explanation the PGS-state for a considered cyclorotor aircraft;

[0026] FIG. **9** is a kinematic and clearance scheme of the presented rotor in a neutral gain of steering of wings' pitching;

[0027] FIG. **10** is a kinematic and clearance scheme of the presented rotor in a high negative gain of steering of wings' pitching;

[0028] FIG. **11** is a kinematic and clearance scheme of the presented rotor in a high positive gain of steering of wings' pitching;

[0029] FIG. **12** is an overall geometric chart for an explanation the four-gears pitch steering scheme;

[0030] FIG. **13** is a detailed geometric chart for deducing a formula for the pitch variation angle in the four-gears pitch steering scheme;

[0031] FIG. **14** is a formula-deducing chart for the pitch variation angle;

[0032] FIG. **15** is a data flow chart with definitions for an end-use application of the formula for the pitch variation angle;

[0033] FIG. **16** is a plot of the pitch deviation distribution over all wings' positions of the rotor for a wide set of the radial offsets of the central gear for the normal assembling;

[0034] FIG. **17** is a plot of the pitch deviation distribution over all wings' positions of the rotor for a wide set of the radial offsets of the central gear for the inverted assembling;

[0035] FIGS. **18**A and **18**B are comparative charts of the assembling of the four-gears pitch steering scheme for the normal and inverted variants respectively;

[0036] FIG. **19** is a plot of the pitch deviation in the main and opposite positions dependently from a radial offset of the central gear for the inverted assembling;

[0037] FIG. **20** is a plot of the angular gain changing dependently from a radial offset of the central gear and from a linear normalized gain for the inverted assembling;

[0038] FIG. **21** is a diagram of an explanation of the biangular handling of an aircraft with the presented rotor with respect to airflow conditions;

[0039] FIG. **22** is a plot of the distributions angles of attack, pitches and intermediate angles over all wings' positions of the rotor and an explanation the relationship between the biangular handling and the PGS-state;

[0040] FIG. **23** is a plot of the distribution of pitches over all wings' positions of the rotor relative to the biangular handling pitch distribution in the operational mode when airflow conditions are ignored;

[0041] FIG. **24**A is a diagram of the relationship between biangular values, PGS, wings pitching, winding speed, thrust and airflow condition in the “propelling” rotor operation mode in the case of horizontal propelling during acceleration on the runway;

[0042] FIG. **24**B is a diagram of the relationship between biangular values, PGS, wings pitching, winding speed, thrust and airflow condition in the “propelling” rotor operation mode in the event of a vertical takeoff attempt;

[0043] FIGS. **25**A, **25**B, **25**C and **25**D are exemplary plots of the airfoil section coefficients and aggregations in the entire 360° range of angles of attack used in the flight dynamics simulation for the CL, CD, CFx and CFy respectively;

[0044] FIG. **26** is an explanatory chart for definition components of a thrust specific area with respect to the aircraft geometry;

[0045] FIG. **27** is an explanatory chart for definition an inflow and a thrust specific angle with respect to airflow conditions;

[0046] FIG. **28** is a data flow chart with definitions for calculating the thrust specific area and the inflow;

[0047] FIG. **29** is an explanatory chart for defining terms used in calculation wings' interference with respect to the superposition of the vorticity of foreign wings with a segment of the current wing;

[0048] FIG. **30** is an explanatory chart for a formula used for consolidating an interference induced speed vector over the entire wing;

[0049] FIG. **31** is an explanatory chart for a formula used for approximating a center of vorticity of a wing dependently from angle of attack;

[0050] FIG. **32** is an explanatory chart with deducing formulas for calculating a vorticity induced speed vector from a sourced wing to a particular linear segment of a destined wing;

[0051] FIG. **33** is a data flow chart with definitions for calculating a state of the interference corrected airflow of the entire rotor;

[0052] FIG. **34** is an overall data flow chart for a state machine used for the flight dynamics simulation of an aircraft with the presented rotor;

[0053] FIG. **35** is a data definition chart for particular components of the aircraft entire state;

[0054] FIG. **36**A is a data flow chart for querying altitude conditions;

[0055] FIG. **36**B is a data flow chart for updating a predicted state;

[0056] FIG. **36**C is a data flow chart for updating an airflow state;

[0057] FIG. **36**D is a data flow chart for updating a winding state;

[0058] FIG. **36**E is a data flow chart for the first part of updating a dynamic state;

[0059] FIG. **36**F is a data flow chart for the remained part of updating a dynamic state;

[0060] FIG. **36**G is a data flow chart for updating a kinematic state;

[0061] FIG. **36**H is a data flow chart for updating a power state;

[0062] FIG. **36I** is a data flow chart for updating a rotor's phase;

[0063] FIG. **36**J is a data flow chart for the first part of updating a report state;

[0064] FIG. **36**K is a data flow chart for the remained part of updating a report state;

[0065] FIG. **37** is a data definition chart for constraints used in the simulation;

[0066] FIG. **38** is a chart of a Rotor State Indicator (RSI) with an explanation its elements, which is used in the reporting of the result of the simulation;

[0067] FIG. **39** is a definition chart of a designation of flags of a handling state used in the reporting of the result of the simulation;

[0068] FIG. **40**A is a chart reporting a result of the simulation for a flight operation, "Beginning acceleration on runway";

[0069] FIG. **40**B is a chart reporting a result of the simulation for a flight operation, "Before takeoff";

[0070] FIG. **40**C is a chart reporting a result of the simulation for a flight operation, "After takeoff at 0.5 meters";

[0071] FIG. **40**D is a chart reporting a result of the simulation for a flight operation, "Getting initial altitude and speed at 12 meters";

[0072] FIG. **40**E is a chart reporting a result of the simulation for a flight operation, "Getting cruise speed in ascent at 75 meters";

[0073] FIG. **40**F is a chart reporting a result of the simulation for a flight operation, "Ascending to cruise altitude at 400 meters";

[0074] FIG. **40**G is a chart reporting a result of the simulation for a flight operation, "Ascending to cruise altitude at 3900 meters";

[0075] FIG. **40**H is a chart reporting a result of the simulation for a flight operation, "Cruise at altitude 4016 meters";

[0076] FIG. **40I** is a chart reporting a result of the simulation for a flight operation, "Gliding at altitude 3700 meters";

[0077] FIG. **40**J is a chart reporting a result of the simulation for a flight operation, "Recuperative descent at altitude 600 meters";

[0078] FIG. **40**K is a chart reporting a result of the simulation for a flight operation, "Approaching at altitude 202 meters";

[0079] FIG. **40**L is a chart reporting a result of the simulation for a flight operation, "Enter in descent for landing at 165 meters";

[0080] FIG. **40**M is a chart reporting a result of the simulation for a flight operation, "Dropping the speed at altitude 82 meters";

[0081] FIG. **40**N is a chart reporting a result of the simulation for a flight operation, "Dropping the speed at altitude 30 meters";

[0082] FIG. **40**O is a chart reporting a result of the simulation for a flight operation, "Dropping the speed at altitude 20 meters";

[0083] FIG. **40**P is a chart reporting a result of the simulation for a flight operation, "Dropping the speed and descent at altitude 6 meters";

[0084] FIG. **40**Q is a chart reporting a result of the simulation for a flight operation, "Dropping the speed and descent at altitude 2 meters";

[0085] FIG. **40**R is a chart reporting a result of the simulation for a flight operation, "Before touchdown at altitude 0.2 meters";

[0086] FIG. **40**S is a chart reporting a result of the simulation for a flight operation, "Touchdown";

[0087] FIG. **40**T is a chart reporting a result of the simulation for a flight operation, "Begin aerial braking on runway";

[0088] FIG. **40**U is a chart reporting a result of the simulation for a flight operation, "Continue aerial braking on runway";

[0089] FIG. **40**V is a chart reporting a result of the simulation for a flight operation, "Finalizing aerial braking on runway";

[0090] FIG. **41**A is a plot of a result of the simulation of the cruise flight operation, illustrating a deviation of the components of the normalized acceleration and a deviation of the external moment ratio depending on the minor phase of the rotor;

[0091] FIG. **41**B is a plot of a result of the simulation of the cruise flight operation, illustrating a deviation of the internal moment ratio and normalized winding speed depending on the minor phase of the rotor;

[0092] FIG. **42** is a chart of a tabular result of the aircraft turn analysis based on the simulation data of different flight operations;

[0093] FIG. **43** is a perspective view of a preferred embodiment of the aircraft in accordance with the present invention;

[0094] FIG. **44** is a fragmentary cross-sectional view taken along the line **44—44** of FIG. **43** in the direction indicated generally and broken into parts with a placement map and an overall low scale imaging diagram;

[0095] FIG. **44**A is the top left part of the cross-sectional view of FIG. **44**;

[0096] FIG. **44**B is the central left part of the cross-sectional view of FIG. **44**;

[0097] FIG. **44**C is the bottom left part of the cross-sectional view of FIG. **44**;

[0098] FIG. **44**D is the top right part of the cross-sectional view of FIG. **44**;

[0099] FIG. **44**E is the central right part of the cross-sectional view of FIG. **44**;

[0100] FIG. **44**F is the bottom right part of the cross-sectional view of FIG. **44**;

[0101] FIG. **45** is an outer side plan view of an earring assembly;

[0102] FIG. **46** is an elevation view of the earring assembly shown from the direction of the left side of FIG. **45**;

[0103] FIG. **47** is a longitudinal-sectional view taken along the line **47—47** of FIG. **45** in the direction indicated generally;

[0104] FIG. **48** is a fragmentary plan view of an extracted rotor taken from its mating side and broken into parts with a placement map and an overall low scale imaging diagram of the entire rotor;

[0105] FIG. **48**A is the upper part of the view of FIG. **48**;

[0106] FIG. **48**B is the lower part of the view of FIG. **48**;

[0107] FIG. **49** is a fragmentary radial-sectional view taken along the line **49—49** of FIG. **48**A in the direction indicated generally;

[0108] FIG. **50** is a fragmentary cross-sectional view taken along the line **50—50** of FIG. **48**A in the direction indicated generally;

[0109] FIG. **51** is a fragmentary cross-sectional view taken along the line **51—51** of FIG. **48**A in the direction indicated generally;

[0110] FIG. **52** is a fragmentary cross-sectional view taken along the line **52—52** of FIG. **48**A in the direction indicated generally;

[0111] FIG. **53** is a fragmentary cross-sectional view taken along the line **53—53** of FIG. **48**A in the direction indicated generally;

[0112] FIG. **54** is a fragmentary radial-sectional view taken along the line **54—54** of FIG. **43** in the direction indicated generally;

[0113] FIG. **55** is a fragmentary plan view shown from the direction of the ring's side of FIG. **54** and oriented similar as in FIG. **43;**

[0114] FIG. **56** is a fragmentary longitudinal-sectional view taken along the line **56—56** of FIG. **43** in the direction indicated generally;

[0115] FIG. **57** is a partial view of FIG. **56** from the magnification circle labeled with the number **57**;

[0116] FIG. **58** is a partial view of FIG. **56** from the magnification circle labeled with the number **58**;

[0117] FIG. **59** is a fragmentary longitudinal-sectional view taken in the same orientation and direction as for FIG. **56** and showing a tail compartment of a stabilators' steering transmission;

[0118] FIG. **60** is a cut-away fragmentary cross-sectional view taken along the line **60—60** of FIG. **56** in the direction indicated generally and showing only aircraft handling transmissions connected to a cockpit;

[0119] FIG. **61** is an elevation view of the cockpit toward the flight direction with fragmentary included connected transmissions, and which can be considered as a continuation of FIG. **60**;

[0120] FIG. **62** is an upper plan view of a joystick pad of the cockpit;

[0121] FIG. **63** is a composed plan view of the scales of all kinds of trimmers;

[0122] FIG. **64** is a plan view of the scale of a Stream Deviation Indicator (SDI);

[0123] FIG. **65**A is a placement plan view of a left PGS trimmers block taken from the face side direction;

[0124] FIGS. **65**B, **65**C and **65**D are placement plan views of a WST-trimmer, SP-trimmer and L-trimmer, respectively, taken from the face side direction;

[0125] FIG. **66** is a cross-sectional view of a P-trimmer with a transmission, taken along the line **66—66** of FIG. **65**A in the direction indicated generally;

[0126] FIG. **67** is a fragmentary cross-sectional view of an S-trimmer without transmission, taken along the line **67—67** of FIG. **65**A in the direction indicated generally;

[0127] FIG. **68** is a fragmentary cross-sectional view of a G-trimmer without transmission, taken along the line **68—68** of FIG. **65**A in the direction indicated generally;

[0128] FIG. **69** is a fragmentary cross-sectional view of a WST-trimmer without encoder transmission, taken along the line **69—69** of FIG. **65**B in the direction indicated generally;

[0129] FIG. **70** is a fragmentary cross-sectional view of an SP-trimmer without transmission, taken along the line **70—70** of FIG. **65**C in the direction indicated generally;

[0130] FIG. **71** is a fragmentary cross-sectional view of an L-trimmer without transmission, taken along the line **71—71** of FIG. **65**D in the direction indicated generally;

[0131] FIG. **72** is a forward elevation view of a Stream Deviation Tube (SDT);

[0132] FIG. **73** is a fragmentary longitudinal-sectional view of the SDT taken along the line **73—73** of FIG. **72** in the direction indicated generally;

[0133] FIG. **74** is a cross-sectional view of the SDT taken along the line **74—74** of FIG. **73** in the direction indicated generally;

[0134] FIG. **75** is a cross-sectional view of the SDT taken along the line **75—75** of FIG. **73** in the direction indicated generally;

[0135] FIG. **76** is a functional block-diagram of an in-flight management of the presented aircraft;

[0136] FIG. **77** is a fragmentary radial-sectional view of an optional intermediate ring taken in the direction and orientation similar as for the end ring in FIG. **54**;

[0137] FIGS. **78**A and **78**B are fragmentary perspective views of winglets installed on the rotor for variants of a straight and forwardly swept direction, respectively;

[0138] FIG. **79** is a fragmentary plan view of a base part of an extracted wing based on a symmetrical airfoil accommodated to use in the presented aircraft, taken in the direction perpendicular to a chord and axis of this wing;

[0139] FIG. **80** is a fragmentary cut-away view of a placement of a combustion engine accommodated to use in the presented aircraft with relation to all powering and cooling components.

DETAILED DESCRIPTION

[0140] Prior to describing the details of the preferred embodiment, a discussion of a related matter is given to correctly understand the functionality of the type of aircraft to which the preferred embodiment belongs.

[0141] Principal aspects of the invention were originated from the following thought experiment, which I imagined one day.

[0142] Consider an elevator (or lift), which is going up on some wire that is winding in a drum of this elevator by a power of its own engine. And now also consider that the other end of this wire is fixedly connected to some wing or lightweight glider that is gliding down. Also consider that the horizontal components of the speeds of both the elevator and the glider are equal, as well as the movement of both without acceleration. Additionally, suppose that the aerodynamic drag of the elevator and the wire is negligible. So this system will be in the presented movement while exists a free length of the wire. But for now, let's stay away from the problem of limited time of the movement and look at the instantaneous characteristics of this system.

[0143] The system has a certain center of gravity (CG), which moves forward at the same horizontal speed as both components of this system, and will move up if the elevator is going up at a speed exceeding the vertical speed of the glider that glides down. And so a potential energy of the entire system will increase due to a work performed by the engine of the elevator. Now the system can be considered, from the point of view the increasing energy, as if it were a some aircraft in the ascent, where the powering is at 100 percent mechanical.

But such assumption may not be sound well for some people familiar with the realm of aircraft. Indeed, we know, a powered aircraft should have a something for the propulsion it forward, like a propeller, a turbojet engine or a rotor of a helicopter handled for the forward flight. On the other hand, it will not sound such surprisingly for people more familiar with the aspects of non-powered flight, for example for people with experience in sailplanes flying, hang gliding or paragliding. They know that any non-powered glider is propelled forward by gravitational force using energy from decreasing its altitude. More than, they have experience ascending in the rising air of a dynamic or thermal nature. This rising air acts as the elevator in the considered thought experiment in a purely mechanical way. And when the glider is going up in the rising air, it still continues to glide down relative to the air itself under the propulsive force of gravity, having a certain gliding angle. Also, such people know how to switch the direction of this propulsive force to decelerate the glider upon landing.

[0144] So, the considered system possesses some equivalence with a glider placed into rising air, and the power of the elevator acts there as the power of this rising air. And now we can find that the system possesses a powered lift instead of the powered propulsion of an airplane. And the gravitational propulsive component of the system is powered by increasing the altitude of the CG from the lift power. Also, we can find that a correct particular implementation of such an abstract concept of a "flying elevator" will have a great advantage over a conventional airplane. It is a very high propulsion efficiency, since the powered propulsion will be excluded from the scope of such a system as much as possible with a related loss of power in it.

[0145] Now, before going forward, let's look at FIG. **1**, which explains this concept in detail. There and elsewhere, I use the arrow sign to denote a vector. Also, I use the "^" sign to denote a normalized vector, i.e. a vector of unit length, the dot-product of which on some other vector is simply a projection scale of one vector onto the direction of the other.

[0146] There the glider **801** is connected by the wire **804** with the elevator **803**. The glider has a speed vector VG and undergoes a gravitational force GF, the value of which is formulated in the first upper equation, where the vector G is gravitational acceleration, and the masses of the elevator and the glider are denoted as ML and MG, respectively. The gravitational force GF is fully compensated by a full aerodynamic force AF, as it formulated by the second upper equation. The third equation represents a strain force of the wire SF, which is the opposite of a gravitational force of the elevator only. The aerodynamic force can be decomposed into two components: a component perpendicular to the airflow direction, which is a lifting force LF; and a component in the direction opposed to a source of airflow, which is a drag force DF. The gravitational force GF has a projection GP0 on the gliding direction, the value of which is formulated in the fourth upper equation. The GP0 force exactly compensates for the drag force DF, and so it acts as a propulsive force, as it is reflected in the fifth equation. I will reference the GP0 force as a primary gravitic propulsion force. The sixth upper equation represents another side of the using the lifting force LF as a thrust force TF, which is applicable in the realm of helicopter aircraft and also in some explanations of the presented invention. And this equation presents a simple way to calculate it by subtracting the drag force from the full aerodynamic force, vectorially.

[0147] The full speed of the elevator is simply the algebraic vectorial sum of the gliding vector VG and a winding lifting speed vector VL. The CG point on the wire represents the center of gravity of the entire system itself. This point has its own speed vector V, the value of which is formulated by the weighting equation in the center of the diagram. In the current example the CG point is placed on the wire, but in more complex cases, it can simply be placed in space. And so, it isn't attributed to a some element of the system, it is attributed to the entire system. The CG point possesses the mass of the entire system, so the balance of the AF force and the GF force can also be considered there. But the AF force is referenced there by another name as a power lifting force PLF, which means that the CG point is a subject of some lifting. It is reflected in the first equation of the lower group. We will encounter a duality of actuation of the lifting force PLF by projecting it onto the vector V. It brings a lift-propulsion LP, which is represented in the second equation. Also, a projection of the primary gravitic propulsion GP0 onto the vector V brings an entire gravitic propulsion GP, which is represented in the third lower equation. The fourth equation represents a consumed power CPWR as the dot-product of the strain force SF on the elevator's winding speed VL. Having this power, we can calculate two vectors. The first is a power lifting speed PLS, which is represented in the fifth equation. And the second is a consumed thrust CT, which is represented in the sixth equation. Also, we can see that the sum of the both kinds of the propulsion is equal to the consumed thrust, as it is represented in the seventh equation. These PLS and CT represent a duality of powering the system. For the first we can say as presence a lift powering, but for the second we can say as presence a thrust or propulsion powering. But we should understand that they are connected by the common power value CPWR, which is a scalar quantity, and so, it doesn't represent a particular force doing the work. There is simply an exchange of the power between the elevator and the gravity field by increasing or compensating the altitude of the CG.

[0148] Let us now look at a particular case where the CG has only horizontal movement. It will be corresponded to an aircraft on a cruise. The LP for this case is equal to zero. And the system goes forward only by the gravitic propulsion GP, but a power for this propulsion is provided by the elevator. In this case the absolute propulsion efficiency will be defined by a loss of the moment of airstream through a downwash of the glider. But this loss is already included in the balance of the entire drag as induced drag. However, the direction of the entire drag is not exactly parallel to the horizontal flight path direction of the CG, leading to the existence of a small projection of the small downwash onto this flight path, and consequently to existence a very small remained loss, which is less than 1 percent, actually. So, the propulsion efficiency relative to the non-powered wing will be more than 99 percent.

[0149] Let us now look at the case when the elevator is not working. It will be simply a gliding. The LP will be exactly compensated by the GP and so the CT will be equal to zero in the full accordance with the non-powered flight.

[0150] There is also another interesting variant of applying of the "flying elevator" concept, now for the analysis of the induced drag itself during gliding. From the lifting line theory, it is known that the induced drag is created by a vortex associated with the wings of the finite span. It is known as a "horseshoe" vortex. This vortex creates some complex induced deviation of the base flow. This component, at the near infinity in the downstream direction has a vertical direction and is known as downwash. Also, this component in the vicinity of the wings themselves is known as inwash or inflow. This inflow also points down in the in the direction opposite to the lift force, but it is half as much as the downwash. Since this component represents a loss, it is mapped for practical use to those induced drag by a reposition of the actual aerodynamic force to the reference frame of the non-disturbed stream in far infinity. But on the other hand, it can be considered as a kind of a permanent sinking air. This sinking air can be considered as a negative powering, where the potential energy is going back to a power source. But the power source there is the gravity field itself, which provides the propulsion to compensate for the airfoil section drag. But the powering of the "horseshoe" vortex also needs an energy. And so, we can see that the gravity power there is split in two ways. The first is simply compensation for the airfoil section drag, such as profile drag. And the second is the powering of the "horseshoe" vortex that performs a self servicing for this powering by placing the glider inside of the sinking air of the inflow. It looks interesting, but what a useful thing can be extracted from that? It is horizontal acceleration. The horizontal acceleration of the glider will be powered only by the first component that is the gravitic propulsion, since the "horseshoe" vortex stole the second for its own servicing. For using this feature we should consider a gliding of the glider inside its own inflow. For such a gliding a corresponding gliding angle exists. It can be referenced as a local gliding angle (LGA) of the glider. Now consider, we have some implementation of the "flying elevator" concept in a some aircraft. A particular flight of such an aircraft can be decomposed to a "glider" component and a "lift" component. Let's name the "glider" component as embedded virtual glider or simply a virtual glider. So, said LGA can be obtained from this virtual glider. Knowing this is useful for understanding when the aircraft will accelerate or decelerate for any particular flight operation. A real glider cannot instantly change its LGA to correct its acceleration, since such a change is linked to a change in the flight path stabilized by the entire mass of the glider. But the virtual glider can do this simply by changing a handling of its actuator.

[0151] Another interesting thing that this concept can provide is the ability for a recuperation energy with the same level of efficiency as spending it on the flight. To do this, we only need to switch the direction of the winding lift speed, and the aircraft will enter in a recuperative descent. More than, the "glider" can simply exchange an exceptional speed to an additional altitude, and that altitude can be wound back for gaining energy. Doing both of these actions at the same time, we can perform a recuperative deceleration too.

[0152] Now let's look how the "flying elevator" concept applies to the known types of aircraft. Let's look on an airplane on a cruise flight. The airplane will have zero flight path angle due the cruise operation. And so, the projection of the gravitational force onto the drag direction is also zero, which disables the actuation of the gravitic propulsion. The airplane compensates for the drag using a separate actuator, such as a propeller, turbojet or turbofan engine. The separate actuator has a significantly smaller thrust specific area than the wings of the airplane. From the lifting line theory, it is known that the thrust specific area of the wings themselves, which create the downwash, is almost equal to the area of the circle which diameter is based on the wingspan. The separate actuator of the airplane has a high outflow speed, which limits its propulsion efficiency. For the propeller, this efficiency practically lies in the range of 0.5 - 0.8. Also, the propellers perform badly at speeds close to subsonic. The turbojet engines perform well at the subsonic speeds, but their propulsion efficiency lies in the range of 0.2 - 0.3. The turbofan engines in the subsonic flight have a propulsion efficiency of the fan itself about 0.7, for the nozzle - only about 0.25, and the overall - about 0.5. But the low nozzle propulsion efficiency is partially compensated by a high thermal efficiency of the nozzle stage itself, which is about 0.65. So, its overall efficiency relative to fuel energy is about 0.37. Now we can see that having the propulsion efficiency near to 100 percent can elevate the overall efficiency up to 0.4-0.45.

[0153] Next we can analyze an autogiro on cruise. Projection of the gravitational force onto the plane of the blades of its rotor is not equal zero. But, nevertheless, it performs as a wing of an airplane, having a complete zero effect of the gravitational force on the movement of the blades, and a separated additional actuator is also used there for propulsion.

[0154] Let's now look at a helicopter in a cruise flight. There is a different picture. Its rotor is actuated on such manner that the blades are in a flapping motion over the entire turn. Their wingtips lie on a common surface inclined at an angle toward the direction of flight. So, a part of the entire thrust is horizontal and performs horizontal propulsion. But, we can see a difference in the gliding of the blades at different phases of rotation. A wing begins gliding down toward the direction of flight. It undergoes a gravitic propulsion with an increased magnitude of aerodynamic force. And the helicopter itself is going up like an elevator powered by the engine of its rotor. After that, the direction is switched, and the wing is flaring up with a decreased magnitude of aerodynamic force. And the helicopter is going down like an elevator with reduced power consumption. The difference in the powering for both of the considered phases, based on the vertical component of the rotor's thrust, can be considered as a lifting with a PLS compensating for the sink rate of the embedded glider during the gravitic propulsion. Also, for the duality of representation, we can consider the horizontal component of the entire thrust as the consumed thrust - CT. And a core feature of a helicopter, which permits that, is the common actuation area for those actions, due to using its rotor as a common actuator. So, a helicopter is kind of aircraft, which can be referenced as self-actuating aircraft (SAA), because it does not need a separate actuator for the propulsion. It uses for that the same actuator as for providing the sustaining forces. Thus, the propulsion feature of such aircraft has a large thrust specific area, low outflow and high propulsion efficiency.

[0155] Now we can see that a helicopter is an example of the SAA aircraft, which reflects the "flying elevator" concept in its operation. But a helicopter isn't an optimal implementation of this concept, because it was designed for a different target. It was designed for vertical flight in the first order and for horizontal flight in the second. But the concept itself was formulated to design an aircraft with the ideal propulsion for cruise flight. And a particular drawback of the helicopter in the implementation of this concept is the weak gliding ability of its rotor.

[0156] After understanding the existence of the SAA aircraft, we can look for other examples of this kind. I suppose, it can be understood that the birds' flight is an example of this kind. Indeed, the birds have only one actuator for both sustain and propulsion actions - their wings. Also, some birds can reach very high speeds in horizontal flight. It is the gravitic propulsion of a simple glider, which allows that. They can never reach that only by a flapping their wings in a weightlessness environment. They use this flapping mainly to lift themselves, compensating for the glide-sinking rate. There were attempts to build ornithopters that mimic the birds' flight. But I suppose that the trend isn't correct. The birds' flight has a big drawback for using it for people. This is a high level of the oscillated acceleration, mainly in the vertical direction. Birds are well accustomed to it, but it would be a variant of an uncomfortable flight for humans.

[0157] Therefore, now is the time to find the correct implementation of the "flying elevator" concept. After I formulated this concept, I tried to implement it in a straightforward manner: as a some system of wings connected to a common fuselage by their wires with the possibility of winding these wires. I reference such a system as "wired wings" configuration. I considered the following four variants of this kind.

[0158] FIG. **2**A represents the simplest variant with only one wing **801** connected by a wire **804** to a fuselage **806**. The fuselage has a powered winding system **807**, which is placed inside the fuselage next to its CG. This winding system also has locking capabilities when it is motionless. Also, the fuselage has a stabilizer **809** that permits adjusting its attitude during the flight. The wing **801** is designed with elements providing longitudinal and transverse stability, like a hang glider wing, and has a central node **810**, where the wire **804** is connected, with the possibility of moving the connection point in the longitudinal and transverse directions under remote control, which processes the handling commands from the pilot.

[0159] FIG. **2**B represents a variant with two wings equal to the wing **801** in FIG. **2**A, which are connected by wires **804** and **805** to a common fuselage **806**, which is differed from the fuselage in FIG. **2**A, having a set **808** from two winding systems instead of one. Here, the wings are referenced as Wing 1 and Wing 2 with winding speeds WS1 and WS2, respectively. In this configuration, there is the problem of transition of one wing in the vicinity of the wire of another. An avoidance of this is too tricky to handle. Thus, this practically disables the use of this aircraft. Nevertheless, this configuration is useful for a flight simulation analysis.

[0160] FIG. **2**C represents a variant where the neighbor wire avoidance problem of the variant of FIG. **2**B is resolved by permanently placing one wing over the other, and wire **805** from the upper Wing 2 passes through a pulley of an enhanced central node **811** of the lower Wing 1.

[0161] FIG. **2**D represents a variant like as of FIG. **2**A, but the fuselage **806** has its own Wing 1 pivotally connected to the fuselage, and the upper wing is referenced as Wing 2. So, the fuselage here becomes a glider. Also, the stabilizer **809** here is moved up to a tail from the proximity of the main wing. The main wing here is pictured as a kind of a symmetrical airfoil to decrease its steering moment, although for the simulation I used an asymmetric airfoil. Also, a standard glider scheme can be used here, having a fixed main wing and a stabilizer with an elevator surface.

[0162] A variant of implementation of the central node **811** is shown in FIG. **3**. The node has two longitudinal rods **812** mounted on the Wing 1 at their ends with clamping supports **813**. A caret **820** can move on the rods **812** in the longitudinal direction interfacing with these rods by a pair of slipping supports **821** per each rod. Each pair of the slipping supports **821** is connected to a side base **822** on the left side and **823** on the right side. All slipping supports **821** have cross oriented holes for clamping the ends of the rods **824** on the forward and rearward sides of the caret **820**. The forward and rearward rods **824** carry slipping supports **825** and **826**, respectively. These supports have elements that allow them to be pivotally connected to a common frame **827**, oriented perpendicular to the direction of the rods **824**. Also, the elements of these pivotal connections constrain a fixed distance between the supports **825** and **826** equal to the distance between each of the supports **821** on each side of the caret **820**. The frame **827** carries a pulley assembly **828** pivotally mounted inside the frame on a shaft **829**. The pulley assembly **828** consists of a pair of equal cheeks **830** connected by shafts **831**, **829** and **832** and pulleys **833** on these shafts between the cheeks **830**. The placement of the shafts **831** and **832** is symmetrical relative to the shaft **829** with a common rearward displacement. The lower shaft **831** also pivotally carries an earring **834** outside the cheeks **830**. The earring **834** is connected to the end of the wire **804**. The wire **805** enters in the pulley assembly **828** from the rear and around the upper side of the lower pulley **833**. After it, the wire **805** follows around the forward side of the central pulley **833** and exits out and up around the lower side of the upper pulley **833**. The forward slipping support **825** has a continuation with a threaded hole, on its upper side. A transverse screw **835** passes through this hole along the forward rod **824** from a servo **836** placed on the right side base **823**. The servo **836** provides the movement of the slipping supports **825** and **826** with the frame **827**. A wall segment **837** with a threaded hole is placed on the left side base **822**. A longitudinal screw **838** passes through this hole along the left rod **812** from a servo **839** placed near of the forward left clamping support **813**. The servo **839** provides the movement of the caret **820**. This implementation provides a zero-moment footprint on the entire Wing 1 from the wires, since its kinematic scheme has a two-axis gimbal in the center. The central nodes **810** are implemented as simplified variants of the node **811**: without pulleys.

[0163] All four variants of the "wired wings" configuration were tested in a flight dynamics simulation program. I used angles of attack (AoA) of the wings and the winding speeds as input handling parameters. In addition, I brought the simulation as close as possible to reality by including the strain dynamics of the wires themselves, as well as the aerodynamic drag of the wires and the fuselage. The self-explaining diagram in FIG. **4** represents constraints of the "wired wings" simulations, grouped by their modalities. I tried to find optimal handling parameters for each variant of the aircraft.

[0164] I prepared the result of these simulations in a form of composite charts, where the upper side presents a flight profile of each component of the respective aircraft, including the wires that keep connectivity of the data. Also, there is a labeling of the numbers of the resulted samples, one per five. The lower part is a plot composed from the handling AoA of the respective wings and components of the acceleration of the fuselage, which are normalized on the gravitational acceleration. The horizontal axis of this plot is simply the number of a sample corresponding to the number labeled on the flight profiles. I placed labels of the sampling in appropriate places instead of the axis itself. Also, keep in mind that the zero lifting AoA for the used airfoil is about -4°. The result of the entire simulation is represented in four components of FIG. **5**.

[0165] FIG. **5**A represents the result for one wired wing connected to the fuselage. This configuration has some similarities with the bird's flight. There is only one possibility to recover the altitude of the wing, because the wing is only one. It is a partial weightlessness for a short time. But the bird has an advantage in this operation, because its wings aren't "wired". So, to keep the aircraft at least in horizontal flight, I need to use a high magnitude of the winding speed. By that, the vertical acceleration changes from 3g when the fuselage is going up with increased AoA to -1g when the fuselage is going down with decreased AoA. The horizontal acceleration changes from 0.3g to -1.4g. Let's look at sample 18, where the phase of the positive powering begins, when the fuselage has a significant sink after a partial fall. The wing is placed significantly more forward than the fuselage, so the accelerating force is inclined and acts as an inertial force. The horizontal component of the inertial force inclines the normal gravitational vertical, so it becomes an inertial vertical. The fuselage begins to accelerate in both directions. The slowly flying wing promptly reaches the speed of the fuselage under the gravitic acceleration, and they continue to move together, keeping a constant inclination of the wire up to sample 35. Now the fuselage has a significant positive vertical speed and increased horizontal speed. On sample 39 the phase is finished, the wing and fuselage are almost upright, but I don't switch to the negative powering phase. I locked the wire and wait for the vertical speed of the fuselage to be maximal. During this intermediate phase the wing accelerates and undergoes pendulum oscillations with a short period, which are reflected in the oscillations of the acceleration. On sample 53 the recovery phase begins. By this time the horizontal speed of the fuselage decreased. Previous recovery phase begins on sample 7. AoA was decreased to -1°, and to -3° on the next sample. Prior to this, the wing was in strong acceleration due to the high inclined flight path and has reached high speed. The high speed has induced a high aerodynamic force reflected in the mentioned vertical acceleration of 3g, which was possible since the wire was locked. Remember that there is a slipping constraint of 1.4g without this locking. In the recovery phase the wing continues to move forward and up, winding out the wire. Its flight path angle switches to the positive direction and the gravitational force begins to decelerate it. The speed of the wing significantly drops, and also the aerodynamic force. The fuselage enters in almost weightlessness and begins to increase its sink until the end of this phase. So, it isn't a comfortable flight. Also, it is too dangerous.

[0166] FIG. **5**B represents the result for two equal wings connected to the fuselage. This aircraft permits less level of the oscillations of the acceleration, below 2g for the vertical component and 0.5g for the horizontal with both signs. The positive phase of one wing overlaps with the recovery phase of the other. But this overlapping induces mutual dependence in phases. This dependence leads to a higher resonance of long-periodic pendulum oscillations of the fuselage and wings. So, the amplitude of the speed-oscillations for the wings is very high, because the mass of the wings is small. This leads to the periodical occurrences of very low speeds of the wings, when a wing almost cannot support its own weight. This is very dangerous, since the wire begins to become forceless at the end of the recovery phase.

[0167] FIG. **5**C represents the result of simulation for the aircraft with two wings at separate levels. This aircraft performs a bit better than it needs for a cruise flight. The Wing 1 through the pulley assembly of the central node applies additional constraints on the horizontal position of the upper wing and vice versa. So, the amplitude of the horizontal oscillations of the wings is reduced significantly. Here I succeeded in the simple handling of the aircraft. Each wing has AoA of 5° while the fuselage goes up toward it. And in this time the opposite wing has AoA of -1.5°, when it is flaring up, winding its wire out. However, this regular pattern of the handling isn't symmetrical. The phase with the upper sustaining wing is longer than the phase with its recovering. The vertical acceleration is reduced there to a range from -0.3g to 0.65g, and the horizontal acceleration - to a range from -0.3g to 0.15g. Also, these accelerations have the pattern of decrementing oscillations replenished after each transition between the handling phases. I use a low winding speed here, so the phases are long, permitting to see details of these oscillations. However, the system has a drawback: the winding speed that I use is maximal. An additional increasing in the winding speed leads to a transition to a mode of highly increased and irregular fluctuations with a significant loss of altitude and to increasing of the rotational energy of the entire system, i.e., to a high-entropy behavior. So, gaining the cruise altitude for this variant is still problematic.

[0168] FIG. **5**D represents the result of simulation for the glider with an additional wired wing. This aircraft performs a just enough for a cruise flight. The pattern of the handling is also regular like for FIG. **5**C, but there is a prolonged intermediate state for both main and recovery AoAs of the wired wing only. The system has a prolonged recovery phase, when the glider is mainly sustained by its own wing with AoA of 6°, and the wired wing is flaring up with AoA from -2.5° to -2°. After this, a shortened lifting phase occurs, when the wing of the glider is idle with AoA of -2.5°, and the wired wing sustains the glider with AoA from 3° to 6°. The vertical acceleration here lies in the range from -0.28g to 0.18g, and the horizontal acceleration - in the range from -0.17g to 0.15g. Although the winding speed that used here is higher than for the previous variant, the short powering phase doesn't permit to gain cruise altitude at all.

[0169] So finally, the "wired wings" configurations permit to have only an aircraft with the ability to perform a cruise flight, low ability to gain cruise altitude and zero ability to perform operations on the runway for takeoff. These limitations follow from the constraint of the self-sustaining abilities of the wired wings themselves, and from the lack of control of their angular kinetic energy relative to the center of gravity of the entire aircraft. So, for the correct implementation of the "flying elevator" concept, there needs an aircraft with wings that are being fully controlled in their movement and steering. Ideally, the wings of such an aircraft should be in some conveying movement with a certain winding speed along their pivots, where their path has a segment where the lift powering is performed, and another segment to perform a simple return to the upper position, maintaining a low level of aerodynamic force. So, I designed a variant of such a "conveyer" configuration, which is represented in FIG. **6**.

[0170] There, an aircraft **850** is pictured in cruising flight and has a standard fuselage **851** with an upper tail stabilator **852**, which is used to compensate for variations of the moment of the "conveyer" actuators **860** on both sides in a wide range of flight operations. The pathway of the wings **861** on the actuator is a rounded rectangle, which is inclined backward at an angle of the Skew from its vertical position. This inclining is used to distribute a load of the lifting wings along the fuselage direction, and to reduce the overall height of the aircraft and the driving force of the entire actuator along its pathway. The pathway of the actuator has a segment "I", where the lift powering performs, a segment "II", where the recovering of the altitude of the wings performs, a segment "III" to perform a transition from the recovering to the powering, and a segment "IV" to perform a transition from the powering to the recovering. Also, due to the duality representation of the power, the lifting segment "I" can be considered as performing a propulsion powering. And also, the same possibility exists for segment "II", when its wings have a negative load. Such a negative load was not possible in the "wired wings" configurations, but now it is possible for this aircraft. I suppose that the number of the wings per the actuator pictured there is close to optimal, since having a smaller number can lead to a high level of vibrations, and having a larger number leads to too weak wings. I also assume that the separation of the wings pictured there is also close to optimal, in order to have a compact enough actuator with a fairly low level of wings' interference.

[0171] Although from the operational point of view, this aircraft looks perfect, it has a significant drawback. It is almost impossible to implement. The main challenge for this is to solve the problem of the presence the illustrated movement of the wings with their simultaneous rigidness and their long length for the desired high aspect ratio. Indeed, the aircraft should have a high aspect ratio of the wings (AR) in order to be effective enough. But its wings must be rigid enough to withstand the high load on the segment "I" and the high level of centrifugal forces on the segments "III" and "IV". The best method to get sufficient rigidness is to bring the wings to a common support at their free ends. Doing this for a circular path can simply be resolved by a ring. But that doesn't work here. Thus, one way to resolve this problem is to place the wings between two fuselages, which has many disadvantages, such as the presence of additional transverse elements for the frame rigidness. I cannot exclude that one day this problem will be resolved, but currently I don't have a multi-tiered correct solution for this.

[0172] So, the remained way to correctly implement the "flying elevator" concept in an aircraft is to use a circular actuator. An exemplary variant of this kind aircraft is represented in FIG. **7**. The aircraft **700** has a fuselage **701** that is similar to the fuselage of the previous aircraft, and now a stabilator **702** is used to compensate for variations of the moment implied by the circular actuator of the aircraft, which I reference as a rotor **110**. The rotor has the same number of wings **111** as the previous aircraft, and the same wings' separation. Now those specific segments of the wings pathway have an overlapped placement, since the lifting ability of a wing has some variativity over the forward side of this pathway, so do those equivalent propulsion abilities of the negative loaded wings on the rear side of this pathway. Also, the mentioned ring, which provides rigidness to the rotor, is not shown here so as not to obscure the wings **111** in the view.

[0173] The next step in the implementation of the target aircraft is to solve the problem of steering the wings on the rotor. But before doing this, it will be useful to define some system to refer to the particular state of this steering. So I did, and I reference it as PGS-state or just PGS. An explanation of the definition of PGS is represented as a diagram in FIG. **8**.

[0174] The diagram images the rotor wings in some particular state of steering. The main idea of it is: the state is simply kinematic characteristics that are irrelevant to the current airflow condition. And so, it can be considered as a low level of handling of the aircraft. This may not be very convenient for use by the pilot, but at first it is intended only to have an exact reference. A straightforward way for it is to have the number of pitches equal to the number of wings. From the simulation examples we know that the aircraft can be handled by switching AoA from lifting value to recovery value and vice versa. But this AoA is a characteristic of the airflow condition, which will be out of the scope of the desired state. Nevertheless, consider that the desired state of the pitches can have some symmetry corresponding to a symmetrical state of these AoAs with some functional mapping between both states. So if the state of these AoAs can be characterized with two values in two opposed points and intermediate values between their, also the state of the pitches can be characterized in the same manner, where the intermediate values will be reflected by some function, which will depend on the particular implementation of the steering itself and will stay out of the scope of the referencing to the state of the pitches. In such a case, the referenced state will be reduced to only three parameters, where two of them will be related to two values at these opposite points and the third parameter will indicate the exact direction where these two opposite points are located.

[0175] An additional idea here: let's this system will possess some kind of neutrality in some particular cases. And it indeed exists, when the pitches of all wings are equal to some common angle. Let's use this common angle as the first parameter of this referencing system and name it as "Pitch" with a referencing by the first letter "P" from the PGS abbreviation. The next parameter will characterize the level of violation of this neutrality, which is logically connected with a difference in the pitches of the wings at two specific opposite points. Let's reference one of these points as "main" and the other as "opposite", where the word "main" is selected to reflect its impact on the lift force in many operations. And this parameter will be equal to the difference in the pitches between "main" and "opposite". And so, this is the second parameter, which has the name "Gain" and is referenced with the second letter "G". Finally, the remained third parameter will be simply the angular direction of the "main" point. I named the third parameter as "Skew", and I refer to it with the third letter "S". I selected this name, because here exists a logical connection with the "Skew" angle of the aircraft in FIG. **6**, and that aircraft also can utilize the referencing to the PGS-state, although its Skew is fixed.

[0176] Now on the diagram we can see all the referred elements. Here are two Pitch directions, where the wings possess the neutrality with a particular "P" angle. Here is the Gain direction, i.e., Skew with the value "S", where the second parameter "G" can be measured. And finally, at the bottom, an example of such a reference is presented as a three-component vector: PGS=(15;-50;18). Here the values mean in degrees. It can also be written as (15°;-50°;18°). Additionally, the diagram presents a "Phase" parameter definition for a particular wing, which is beyond the scope of the PGS-state itself, but is used to recover an actual pitch for a particular wing after providing the entire PGS-state and this Phase into some routine that calculates the actual pitch using a particular implementation of the steering functionality.

[0177] The wings on the rotor in the selected configuration are in cycloidal motion during the movement of the aircraft. And so, this kind of aircraft is known as cyclorotor aircraft. The history of cyclorotor aircraft has a long trend from the beginning of the twenty century. This trend began at the same time as the trend of helicopters. Finally, the trend of cyclorotors wasn't successful compared to the trend of helicopters. I suppose that a misunderstanding of the capabilities of cyclorotor aircraft mainly caused that. In many cases, there were intentions to build a cyclorotor aircraft with the ability of vertical flight. Adherents of aircraft of this type were lured by the advantage of the movement of the wings in the cyclorotor, relative to the movement of the wings in the helicopter. Indeed, the wings in the cyclorotor move in parallel with the same speed along their entire length compared with the wings of the helicopter, which have a low speed near the center of the rotor. But this advantage is not the main factor for vertical flight. Prior to the end of the nineteen century the moment theory of the actuators was developed, which implies that the area of the actuator is the main factor for the efficiency under the required thrust. A small area of an actuator under a fixed thrust induces a very high inflow, which alters a base flow, creating a high drag. Only an increase in the rotation speed of the actuator, which can slightly increase efficiency, can reduce this drag. However, this cannot alter that inflow at all, as well as the outflow. A presence of this outflow is required by the entire thrust and is reflected in the propulsion efficiency of any kind of actuator. A gliding wing also can be considered as an actuator with a downwash as the outflow. The thrust specific area of a typical cyclorotor aircraft is significantly lower than the thrust specific area of a helicopter of the same scale. The cyclorotor should have its rotation speed much higher than in the case of low inflow. And so, it encounters a number of disadvantages on this way. The main disadvantage here with respect to the helicopter is the direction of centrifugal forces. They always have a radial direction, which is the direction of weakness for the wings of the cyclorotor and the direction of strongness for the wings of the helicopter. Another disadvantage is induced by the first. The centrifugal forces in the helicopter induce an additional rigidness of its wings for the applied aerodynamic forces. This acts as some kind of multiplier coefficient. But for the cyclorotor aircraft, this feature acts as an oscillatory superposition of two forces: centrifugal and aerodynamic. Finally, a cyclorotor aircraft can never have the same level of efficiency for vertical flight as a helicopter. More than, simply creating such a full-size aircraft with any efficiency is a great challenge, also using contemporary advanced materials. This wrong intention was also reflected in the naming of the actuators of such aircraft for use in horizontal flight. They are until now referenced as cycloidal propellers, and the trend is still ongoing.

[0178] Also, I suppose that there was an additional factor that could prohibit the building of cyclorotors for horizontal flight. This is a high value of the rotational moment when the rotor is actuated. This follows from the "flying elevator" concept. The cyclorotor can be considered as a drum of an elevator when winding wire. And the force on the pivot of a wing will be equal to the force on the wire, if the wing is in the forward position and only it provides sustaining. In the real case there are four wings, which provide 90 percent of this sustaining on the forward side. So, the total force in the pivots' radial position will be about half the entire weight of the aircraft. The moment of rotation of the rotor can be represented as the ratio of such a force to the entire weight of the aircraft. I reference it as a particular case of the Moment Ratio (MR) of the entire aircraft when the internal aerodynamic moments of the wings are discarded. Also, this particular case can be referenced as the External Moment Ratio (EMR). This EMR may be too high to actuate the rotor. Indeed, also in the helicopter this problem exists. The helicopter uses a spur gear with a pinion to cope this moment. Also, it uses a high-pressure oil pump to reduce wear in this type of transmission. I resolve this problem in the presented invention in another way: I don't use a power gear transmission at all. Instead this, I use an electric engine with high torque that permitted by its large area of the magnetic air-gaps. And this electric engine is directly connected to the rotor shaft.

[0179] Nevertheless, some people tried to adapt the cyclorotor for horizontal flight. They related a boundary between two kinds of flight to a pair of the operational modes of the rotor. These two kinds of flight are mainly differed by a kind of the cycloid, which their wings follow. The rotor that operates as a propeller with a low airspeed has a low advance ratio relative to the air on infinity, which speed is known as True Aerodynamic Speed (TAS), and a significantly higher advance ratio relative to the airspeed in its vicinity, which can be referenced as Local Aerodynamic Speed (LAS), since here an inflow exists. The advance ratio is simply the ratio of an airflow speed to the linear rotation speed of the wings, which I reference as the winding speed. This ratio is very useful in the realm of propellers. I also use it for characterization the operations of the aircraft that is presented in the invention, but in another form. I use it in the form of the reversed ratio as Winding Ratio (WR), since the presented aircraft can simply glide without a rotation of the rotor at all. In this case, it has the WR equal to zero, instead of

infinity, if I kept the former form of the referencing. Also, it is always referenced relative to LAS. Returning to the mentioned pair of the operational modes of the cycloidal propellers, they were divided into a curtate mode, when the rotors' steering is adapted to the operation with an advance ratio below 1, and into a prolate mode, when the adaptation is targeted on an advance ratio above 1. And this adaptation itself was an intention of a minimizing the powering force reaction normal to the cycloidal path by adjusting angles of attack, which reflects an intention of a minimizing that rotational moment, which I discussed before. For this adaptation, it can be obvious that a wing will perform some oscillating relative to its pivot for the curtate mode in the rotating reference frame of the rotor. Simultaneously, this wing will perform a rotation relative to its pivot, looking at it, from a steady reference frame outside the rotor in this mode. In the prolate mode, there will be opposite picture: the wing will rotate relative to the rotor and will oscillate, looking from the outside. In the latter mode, the rotation of the wings inside the rotor is performed in the opposite direction of the rotation the rotor itself, which can be implemented by using a planetary gear transmission with four gears per wing, where one central gear is common. Such transmissions, which can keep the pitches of all wings equal, were represented in some inventions related to cyclorotor aircraft. And they were accompanied with particular solutions of the steering the wings from the neutral position.

[0180] In the US patent 2,045,233 of Kirsten et al. a cycloidal propeller is described, designed for the prolate operation, and which utilizes a four-gears transmission scheme, where one pair of the meshed gears uses bevel teeth. There, steering of each wing is performed by an additional differential connected to the first of the mentioned bevel gears. These differentials participate in a common movement by levers pivoted on a common eccentric. Also, there exist two handling inputs. One regulates the value of eccentricity, and the second - the direction of the eccentricity. Also, the latter regulation is combined with a regulation of the common pitch by rotating the central gear. Now, from the point of view of the PGS-state, there exist: gain steering using the eccentricity level, a steering of the skew using the direction of the eccentricity, and a steering of the pitch using the combination with skew control. So, there missed a possibility to change the pitch independently of the skew. Nevertheless, the inventors claimed that this is a positive feature, which permits more effective action, having a common control over the center of symmetry and the pitch. Although the inventors only guess in that effective action, it exists indeed, but only for propelling, which may be useful for the runway operations of an SAA. In any case, this solution cannot be adapted for the required aircraft, because the steering elements obstruct the central area of the rotor, disabling to place here a central powering shaft. Also, the separation of these pitch and skew controls in this scheme requires an additional steady base inside, which leads here to exceptional complexity.

[0181] In the US patent 5,100,080 of Servanty a cycloidal rotor for horizontal flight is described, which also utilizes a four-gears transmission scheme. In this rotor, steering of each wing is performed by a rotating hydraulic actuator embedded in a coupling of two intermediate gears of the four-gears transmission scheme. This actuator assures a correct pitch for its wing at any instant, and is managed by a special calculator. Also, there exists mechanics for handling the neutral common pitch. This solution has exceptional flexibility for handling the pitches of particular wings, which is out the scope of the PGS-state. Also, this solution isn't secure and also is dangerous. Indeed, a pitch calculated for a certain instant is correct only in the vicinity of a specific phase. In the case of an outage of the hydraulic pressure or electricity of the calculator, the remained or not assigned pitch will be wrong for another phase, which will drastically change the overall lifting force, leading to an aircraft incident. And so, this example demonstrates an additional advantage of a mechanical steering fitted to limitations of the PGS-state: In the case of a power outage, this steering will be continue operating correctly, since the state simply remains as a mechanical state for any intermediate phase of any wing.

[0182] In the US patent 6,932,296 of Tierney an unmanned aircraft with cycloidal rotor is described, capable to operate in the curtate mode, prolate mode, and with fixed wings using a separate fan as a propeller. It uses a transmission scheme with three gears, which can be considered as a particular case of a four-gears scheme, when all four gears are equal, so the intermediate coupled pair of gears is reduced to one intermediate gear. Also, instead of one central gear there is a set of central gears, one per each wing. These central gears have some elements that allow to switch between the curtate and prolate modes. In the prolate mode, the set of central gears is stationary, and in the curtate mode it rotates. Steering of the wings is performed by moving the entire set of central gears by some XY pair of servos. Also, there exists some case of handling the common pitch by selectively griping the entire set of central gears upon switching to the prolate mode and with the possibility of changing it in the fixed-wings mode. The system of gears keeps the integrity by links pivotally connecting their axes. Also, there is some central shaft to which all inner links are connected, and which follows the rotation of these inner links with some degree of uncertainty. The gears, related to a particular wing, occupy their space in the depth of the rotor, but the links have a common level where they are connected to the central shaft. The rotor is presented for three wings, but the placement of gears and links doesn't allow the use of more than five wings. Above this limit, collisions can occur. Nevertheless, this solution complies with the PGS-state in its prolate operating mode. A notable feature of this unmanned aircraft is the demonstrating of the principal limitation of a cyclorotor aircraft, based on the law of obeying the "propeller rule" of having minimal projections of the lift forces onto the direction of rotation: the aircraft is designed to operate with a high rotation speed upon a low torque, and when the obeying of the mentioned law, upon increasing the speed, leads to the decreased rotation, the propulsion power decreases, so it should use the additional fan for the propelling in the high speed flight, instead of utilizing the lifting power possibility of the primary actuator.

[0183] FIG. **9** represents a kinematic scheme of the rotor used in the preferred embodiment. The scheme is performed in such a way that indicates the actual clearance of neighbored pieces and ensures that no collisions occur. The view should be understood as a transparent projection of the depicted selected internal elements onto the faceplate **112** of the rotor **110**. Any intersections of the selected elements in the scheme mean an overlapping those elements in separate plans. The picture represents the rotor **110** in a neutral pitching with PGS=(5;0;0) relative to the base airflow and with the indicated rotation direction that is appropriate for the particular pitching. The rotor **110** has a faceplate **112** on which some elements are mounted that support the shafts of the wings **111**, those elements and the shafts of the wings aren't pictured on the scheme. The wing **111** has a circular base **113**, which is an integral part of the wing **111**. A bevel gear **114** of a large diameter is mounted on the circular base **113**. A bevel pinion **115** is meshed with the bevel gear **114** and mounted on the shaft **116**. The other end of the shaft **116** has a miter gear **117**, which is meshed with a miter gear **118** of a cluster **120**, which is mounted on the shaft **121**. The other component of the cluster **120** is a pinion **119**, which is meshed with a pitch gear **131** of an earring assembly **130**. The earring assembly **130** has the mentioned pitch gear **131**, fixed on a shaft **132**, a cluster **133**, a groove follower **136**, and a shell **137**, which can hold a number of supporting bearings. The cluster **133** has a steering pinion **134** that is meshed with the pitch gear **131,** and an entry gear **135**. A groove follower **136** is mounted on the cluster **133** and can move inside of a groove ring **123** of a cluster **122**. The cluster **122** also has a central gear **124** that is meshed with the entry gears **135** of all earring assemblies **130**, and an internal gear **125** that is meshed with a pitch pinion **126**. A central powering shaft **127** is fixedly connected to the faceplate **112**.

[0184] The cluster **122** together with the pitch pinion **126** can move in any radial direction up to a certain limit, changing the Gain and Skew of the entire PGS-state. Each shell **137** has a some "window" for the pitch gear **131** of the neighboring earring assembly **130**, preventing collisions during steering. The pitch gear **131** has its name because it always is synchronized in rotation with the related wing **111**. The pitch pinion **126** has its name because its rotation will change the Pitch of the entire PGS-state. The steering pinion **134** has its name because it directly steers the pitch gear **131**. The entry gear **135** has its name because it acts as an entry interface for the entire earring assembly **130**. The pitch gear **131**, the central gear **124**, the entry gear **135** and the steering pinion **134** are the base elements of the four-gears pitch steering scheme.

[0185] FIG. **10** represents the same kinematic scheme as in FIG. **9**, but the rotor **110** is in a high negative gain pitching with PGS=(5;-40;0), which can be used upon gaining altitude. The scheme demonstrates how the pitches of the wings **111** and the positions of the earring assemblies **130** will change upon moving the entire cluster **122** together with the pitch pinion **126** for this pitching. In this high gain pitching there is still sufficient clearance between the earring assemblies **130,** and the applied movement of the entire cluster **122** is far from maximal.

[0186] FIG. **11** represents the same kinematic scheme as in FIG. **9**, but the rotor **110** is in a high positive gain pitching with PGS=(5;40;0), which can be used in recuperative descent. The scheme demonstrates how the pitches of the wings **111** and the positions of the earring assemblies **130** will change upon moving entire cluster **122** together with the pitch pinion **126** for this pitching. The remained clearance here is same as in the scheme of FIG. **10**. Also, the indicated direction of rotation of the entire rotor is opposite, since this pitching is related to recuperative descent.

[0187] It will be very useful to have an end use formula for obtaining the pitch variation of particular wings upon moving the central gear **124** in the four-gears pitch steering scheme. This variation will be a function of the instant distance between the axis of the pitch gear **131** and the axis of the central gear **124**. And this variation will be independent of an orthogonal offset of the central gear **124** from the center of the rotor **110** for this fixed distance. The latter feature may be intuitive, but it isn't obvious. However, it can be proved by the following analysis.

[0188] Let the central gear **124** moves orthogonally from some pitch gear **131**, but their distance will be kept. This movement can be considered as a turn of all four gears participated in the steering, by some angle, with a frozen meshing state. In such a case, the pitch gear **131** will obtain an additional variation, which is equal to the angle of rotation of the system of these four gears. But in this case, the central gear **124** also should obtain the same additional variance as the pitch gear **131** because the meshing state is frozen. But actually, the central gear **124** is fixed from any rotation with the pitch pinion **126** that is irrotational for this movement. And so, the pitch pinion **126** will imply a counteraction that returns this central gear **124** in its original angular position. This reverse rotation of the central gear **124** will break the frozen meshing state of four gears, and the pitch gear **131** will also return to its original angular position, because all pitch gears **131** are synchronized with the central gear **124** in their collective angular movement by the equality ratio.

[0189] Now let's look at FIG. **12** which explains movement all gears relative to some pitch gear **131** upon changing its distance from the central gear **124**. The chart pictures the pitch gear **131** in a horizontal position and upon a zero-Skew pitching of the rotor, but this is not principally for the result that will be obtained. At first, all participating gears have corresponding radii based on their pitch diameters. The pitch gear **131** has a radius r1, the central gear **124** has a radius r2, the entry gear **135** has a radius r3, and the steering pinion **134** has a radius r4. At second, there is a radius of the circle on which the axes of all pitch gears **131** lie. It is designated as R0. At third, a triangle can be constructed with corners based on the axes of the pitch gear **131**, the central gear **124** and the cluster **133**. In this triangle, the axis of the pitch gear **131** is fixed relative to horizontal offset, so, it is designated by the letter O. The axis of the central gear **124** in the neutral position is designated by the letter A, and the axis of the cluster **133** is designated by the letter B for this case. In the case of an offset Δr, last two points will be A1 and B1, respectively. Also, for the triangle OAB, two corner angles for points O and A can be assigned as $\beta 0$ and $\mu 0$, respectively. And for the shift case, they will be designated as $\beta 1$ and $\mu 1$, respectively. Additionally, two meshing points can be considered: between the central gear **124** and the entry gear **135** as the letter C, and between the pitch gear **131** and the steering pinion **134** as the letter D. Also, for the shift case, they will be designated as C1 and D1, respectively. And finally, the pitch variation of the pitch gear **131** upon the shift of the central gear **124** can be designated as δ, and it will be correspond to a reposition of the original meshing point D. The point D will be reposed to two instances. One the instance will lie on the pitch gear **131** and is designated as H1, and the other will lie on the steering pinion **134** and is designated as G1.

[0190] FIG. **13** is a magnified essential portion of FIG. **12** with additional details for deducing the target variation formula. At first, there is presented a reposition of the original meshing point C to two points E1 and F1 laid on the central gear **124** and the entry gear **135**, respectively. Here, E1 is simply the result of the offset the point C by the vector Δr. The changing from the angle β0 to β1 upon the offsetting corresponds to the changing in the related meshing position, and so, the angle of this change is designated as β. Also, an angle μ of the same kind is designated for the other meshing position. And so, the target angle δ can be considered as the sum of the angular change β of the meshing position and a remainder θ that is equal to an additional rotation imposed by the steering pinion **134** itself. The angle θ has a corresponding angle φ on the steering pinion **134**, related to it by a simple gear ratio. This angle φ can be decomposed as the sum of the common change β of the meshing position and an angle γ representing a rotation of the entire cluster **133**. Here, the angle β is secondary pictured as an arc between the points N1 and P1 on the circle of the entry gear **135**, where B1P1 is parallel to the OB and N1 is simply a crossing of OB1 with the circle of the entry gear **135**. Also, the angle γ is pictured on the circle as an arc between the points P1 and Q1, where the latter is a projection of the point G1. The angle γ can be expressed as the sum of an angle η representing a change of the meshing position of the entry gear **135**, and a remainder λ. The angle η is equal to the μ and is pictured as an arc on the circle of the entry gear **135** between the points S1 and C1, where B1S1 is parallel to the AB. The remainder λ is related to the μ by a simple gear ratio. So, now all the components to deducing the target formula exist.

[0191] FIG. **14** represents the entire process of deducing the target formula by grouping the subjects of this deducing. At first, there is one design constraint **S141** for the equality of both of the gear ratios to a certain value K. At second, there are target definitions **S142** for the reposition of the primary meshing point on the pitch gear **131** and for the angle of variation itself. At third, there are two constant definitions **S143** for the base angles in the neutral case. Fourth, there are primary definitions and relations **S144** for a particular position of the pitch gear **131** in the case of shift, including: base angles, a reposition of the primary meshing point on the central gear **124**, and simple equations for variations of those base angles. Fifth, there are secondary definitions **S145**, including: the first remainder and its corresponding angle, the angular variation of the cluster **133**, and the second remainder with the related angular change of the second meshing position. All these five subjects merge together and lead to intermediate relations **S146**, which are resolved by simple algebra to one result relation **S147**. This result is passed to a simplifying **S148** based on the constant sum of angles in a triangle, providing by that the final result **S149**, which states: the pitch variation is equal to the product of inversion of the variation of the apex angle and the sum of unity and the reciprocal of the common gear ratio, where the gear ratio is defined as the ratio of the radius of the central gear **124** to the radius of the entry gear **135**.

[0192] FIG. **15** represents a data flow with definitions for an end-use application of the pitch variation formula for a particular distance of the pitch gear **131** from the central gear **124**. At first, the application routine must be initialized with the values of the constant definitions **S151**. At second, this initialization must be continued by calculating the constant relation **S152**, which is based on the cosine theorem and provides the value of the apex angle in the neutral case. After it, the routine can acquire input of a particular angular position of a wing, which is equal to the angular position of its pitch gear **131**, and calculate an instant distance, using the instant definition **S153**. After this, the routine should substitute the values from all the mentioned subjects into the chain of the instant relations **S154** and calculate the final value of the variation, for the output.

[0193] A particular result of using the pitch variation formula as a plot of the distribution of pitch deviation over all wings' positions of the rotor is shown in FIG. **16**. The result is represented in a wide set of central gear radial offsets for positive and negative gains. The sign of the Δr value is used to display the gain on such a way to be same as the sign of this gain itself. So, its ratio to R0 is used there as a gain parameter, which can be called a linear gain. This result corresponds to the placement of the four gears pictured in FIG. **12**, which I call a normal assembling. But, the kinematic scheme shown in FIG. **9** utilizes another placement variant, which **I** call an inverted assembling. A corresponding result of the distribution of pitch deviation over all positions of the rotor wings for the inverted assembling is shown in FIG. **17**. There, the sign of Δr was changed to be same as the gain sign. This result reflects some advantage of the inverted assembling variant: the main operating modes utilize the negative gain and have heavily loaded wings near the main point, which is near the phase 0.25, so, these wings have a lower pitch deviation upon using the inverted assembling, which provides more exact handling and steering of these wings.

[0194] FIGS. **18**A and **18**B represent features of both normal and inverted assembling, respectively, by a comparative way. In the latter case, the entry gear **135** with the steering pinion **134** is placed in the upper elongation relative to the pitch gear **131** and the central gear **124**, on the side of the zero-Skew direction. Also, the positive direction of the linear gain is referenced on both charts as the black arrow above the Main<—>Opposite indicator for this zero-Skew pitching.

[0195] Of special interest is the behavior of the pitch change in the main and opposite positions when changing the linear gain in its entire range. A result of this kind of calculation is plotted in FIG. **19**.

[0196] Also, it may be interesting the changing of the angular gain itself when changing the linear gain in its entire range. A result of this kind of calculation is plotted in FIG. **20**. This plot also introduces a linear normalized gain, which is equal to the ratio of the linear gain to some maximal linear gain related to a maximal constructive limit in the offset of the central gear, or simply equal to the ratio of the current offset to its limit. The latter definition is pictured in the plot below an alternative scale based on the linear normalized gain. This normalized gain variant is very useful for indicating a gain when using a mechanical indicator, since the mechanics are much simpler and more accurate when measuring linear displacement.

[0197] The diagram in FIG. **21** explains a high-level handling mode, which I call biangular handling. The main idea here: this high-level handling should have a direct relation with angles of attack of the wings at two opposite points in a certain direction. This direction is selected to be pointed by the Skew angle of the PGS-state, and thus it is equal to the gain direction. So, there are two AoAs for the main and opposite points. In aerodynamics AoA is also referred to as angle alpha. And so, I refer to these two angles as the main handling alpha and the opposite handling alpha, and they are reflected in this diagram, which utilizes the same PGS-state as the diagram in FIG. **8**. These two angles are represented for Wing 3 and Wing 8, respectively. The main difference between this handling and the PGS-state is the use of airflow conditions associated with these angles in such a way that these two angles are independent of changes in the parameters of these flow conditions themselves. For example, after providing particular values of the biangular angles to some flight software routine, they will be constant for any change in airspeed and for any change in the winding speed of the rotor. This constant behavior will be ensured by corresponding changes in the P and G components of the PGS-state by using this routine to reflect changes in airspeed and rotor's winding speed. The diagram provides an example of the relationship of the pictured winding speed WS and the true aerodynamic speed TAS of the entire aircraft, which is parallel to the fuselage in this handling mode, with two particular TASs of Wing 3 and Wing 8. The angles of attack relative to these two TAS-vectors imply two related pitches for these two wings. Such positions of the wings and the directions of their chords are depicted in dotted lines on the diagram. And they aren't equal to the actual pitches performed. This differing feature reflects a special correction of the asymmetry of the pitch variation imposed by the gain to the main and opposite points. This correction matters for high gain values and is close to zero for low gain values. Additionally, if exists some remaining error angle between the fuselage and the TAS-vector, this error angle should be in consideration during handling and should be used to correct the resulting PGS-state.

[0198] FIG. **22** represents a plot of the distributions of all related angular components involved in the biangular handling over all positions of the rotor wings of the example of FIG. **21**. At first, there are values of the HANDLING KINEMATIC ALPHA. The word "kinematic" means that the reference flow is simply the vectorial sum of the TAS of the aircraft and the kinematic speed of a particular wing, for its particular phase. This does not include dynamic perturbations in airflow arising from the actual vorticity distribution over the entire rotor. This exclusion means: any handling parameters must be free of all dynamic components containing uncertainty errors, for a steady referencing. And those biangular values are merely kinematic parameters, although some level of uncertainty can still exist upon measuring the TAS. This primary handling distribution is selected so that it is simply linear between the main alpha (MA) and the opposite alpha (OA). At second, there are values of the TAS DIRECTION itself. At third, there are values of the HANDLING PITCH REFLECTED from the first relation for the kinematic alpha referenced at the bottom of the plot. These last values correspond to the pitches depicted in dotted lines in FIG. **21**. Fourth, there are values of the ACTUAL PITCH resulted from the PGS-state. These two kinds of pitch are connected using two match points: MP1, which is shifted from the main direction M of the PGS-state by an angle $\Delta\varphi$, and MP2, which is shifted from the opposite direction O of the PGS-state by the same angle. The formula for the shifting angle is represented in the third equation at the bottom of the plot. It uses the Gain itself and is simply the best approximation for fitting the actual pitch distribution to the desired handling pitch distribution, which I found through numerical experimentation. The flight software routine uses the Gain value from the previous servicing cycle in this equation, since the Gain is also a component of the target result of the fitting these match points. Fifth, there are values of the ACTUAL KINEMATIC ALPHA recovered using the first relation referenced at the bottom of the plot. And sixth, there are values of the ACTUAL ALPHA recovered using the second relation referenced at the bottom of the plot. The second relation uses LAS instead of TAS. To obtain this LAS, the perturbations of the base flow by vorticity were split into the inflow component and the interference distribution component as a result of numerical simulation. And the entire result corrects the TAS to this LAS.

[0199] There is also a simplified variant of the biangular handling mode that ignores airflow conditions, for rare use, which I call biangular pitch handling. FIG. **23** represents a plot of pitch distributions over all positions of the rotor wings in this case, utilizing the same PGS-state as for the biangular alpha handling. The ACTUAL PITCH distribution is depicted together with the values of the HANDLING PITCH, which are also selected so that they are simply linear between the main pitch (PM) and the opposite pitch (PO), as for alpha mode. The matching between two kinds of pitches is performed according to the same algorithm as for alpha mode.

[0200] FIGS. **24**A and **24**B represent diagrams of the particular use of biangular pitch handling in a such named "propelling" mode upon accelerating on the runway and upon a vertical takeoff attempt, respectively. These diagrams depict the relationship between the wings' pitching, the thrust T, the winding speed WS and the airspeed AS. The main feature of this mode is that the P value of the PGS is almost same as the S value and follows its change. Here, the PM and PO values are used for reference only. The thrust force in the second case is still not enough to accomplish its task. Also, a detailed comparative analysis with an equivalent rotor operated in curtate mode indicates a lower thrust than the rotor presented, but it also has a much lower external moment and consumed power. And if enough power for this takeoff will be provided for both kinds of rotors, the rotor with curtate movement will spend much less power with much lower external moment, but will have the winding speed much higher than that of the presented rotor, so too high centrifugal forces will damage it before this condition is met.

[0201] Before continuing to explain the implementation of the preferred embodiment of the invention, it will be useful to explain the correct aerodynamic model for calculating and forecasting the performance of the presented aircraft. This model, executed under a flight dynamics simulation, provides a detailed set of performance values for different flight operations. So, I will start with a short explanation the relevant aerodynamic aspects of such a model.

[0202] The basic aerodynamic aspect of an aircraft with the rotor presented is the choice of some airfoil for the wings of the rotor with obtaining the aerodynamic section coefficients of this airfoil for the relevant range of Reynolds numbers. For any conventional aircraft, it is enough to have only three kinds of such coefficients: of lift CL, of drag CD, and of moment CM, where the last, for much of aircrafts, uses 0.25 of the chord length as its referencing origin point. For the presented rotor, the presence of such CM coefficients isn't enough. At first, I want to use not only a symmetric profile, but also an asymmetric one, which can provide some performance advantage. Such a profile also has the steady moment behavior with respect to 0.25 chord lengths. But its value is too high for steering the wing by gears, comparing with the moment of symmetric airfoil, which is near to zero. Thus, the position of the pivot for this should be optimized by moving it more in the trailing edge direction, as it pictured on the kinematic scheme in FIG. **9**. So, having the CM values for some particular origin point isn't enough, since this optimization can be changed. And so, instead of having a particular CM, it is better to have the coordinates of the center of the entire aerodynamic force, from which the CM for any particular pivot position can be simply calculated. I call such coordinates: airfoil aerodynamic aggregations CFx and CFy for the X and Y coordinates of the center of force, respectively.

[0203] Also, this is still not enough. The wings of the presented rotor operate always in the prolate mode. And at the beginning of the acceleration of the aircraft on the runway, its winding ratio WR is higher than 1. It leads to AoAs of more than 90° for particular wings, but at a lower speed, when the drag is moderate. So, I need the aerodynamic coefficients and aggregations for the entire 360° range of possible AoAs, for enough freedom. Also, the range of airspeed values over all operations is very wide. But Mach number can be ignored for a relatively low-speed aircraft. So, finally, there needs a set of four coefficients and aggregations for the entire 360° range of AoAs in a wide range of Reynolds numbers. Therefore, I prepared such a set of aerodynamic data for the NACA 4410 airfoil in a form friendly for the simulation, using a composition of data from multiple sources, such as: XFOIL paneled simulation, CFD modeling for viscid and inviscid flow, and refactoring the public data of wind tunnel testing. This data has some degree of uncertainty, but this cannot affect the result of the entire simulation at a significant level. Examples of a distribution of the CL, CD, CFx and CFy over the entire 360° angles of attack for the Reynolds number 500,000, which were used in the flight dynamics simulation, are represented as plots in FIGS. **25**A, **25**B, **25**C and **25**D, respectively.

[0204] The next aerodynamic aspect is related to induced drag. For airplanes, it is routine practice to use special formulas to calculate induced drag and the related correction of lift for a given aspect ratio. Such formulas reflect changes in drag and lift created by the influence of the inflow depending on the lift distribution over the wings. But this practice isn't applicable for modeling the powered actuators, like the presented rotor or the rotor of a helicopter, because its modeling implies to know a particular lift and drag of each particular wing of such a rotor. And the simple application of the mentioned formulas to each separate wing isn't correct, due to the mutual influence of the wings. This problem can simply be resolved with the knowledge of the inflow itself. And so, the next aerodynamic aspect for the presented rotor is the calculation of the entire inflow.

[0205] The inflow has a simple relation to the thrust specific area (TSA) of an actuator. From the lifting line theory and from the point of view of the momentum theory of actuators is known: for a monoplane with elliptically loaded wings in the wingspan direction, the TSA is simply an area of the circle based on the wingspan diameter. But the aircraft with the presented rotor doesn't have this elliptical load distribution. Presumably, it has an equal load distribution. This kind of distribution is also often used for monoplane modeling, and it implies a certain coefficient of efficiency that reflects an additional increasing of the induced drag due to a variable distribution of the induced speed, and which is practically above 0.85. But the aircraft with the presented rotor from the glider's point of view isn't a monoplane. For most flight operations, it can be considered as a tetra-plane with an average wings' separation of about 0.05 to 0.07 of its wingspan, or as a bit less-performing triplane with an average wings' separation of about 0.075 to 0.1 of its wingspan. From the work of L. Prandtl "Induced drag of multiplanes", published in NACA TN 182, 1924, one can easily find a coefficient of induced drag of this triplane over an equivalent monoplane. It lies between 0.852 and 0.824 for this referenced range of the wings' separation, respectively. This decrease in induced drag will overlap that increase due to non-elliptical load. So, as a pessimistic appreciation, it can be assumed that the induced drag of the aircraft with the presented rotor is equal to the induced drag of an elliptically loaded equivalent monoplane. And so, going from induced drag to inflow, the TSA of the aircraft with the presented rotor in the case of a gliding will be a circular area based on the wingspan LS, as shown in FIG. **26**. I call this area a downwash specific area (DSA), since it has a direct logical connection to the downwash feature. The impact from the cross-sectional projection of the fuselage **101** will slightly decrease the DSA, but from the other side, it will slightly increase the wings' separation of the equivalent triplane, so I neglected this effect. The aircraft with the rotor presented also exhibits another kind of TSA: this is a propulsion specific area (PSA), which is actualized at the beginning of acceleration on the runway. I selected this area as the sum of the cross-areas of two cylinders based on both rotors **110** with a radius R equal to the distance of the pivot axes of the wings from the center of the rotors, and a length L for each.

[0206] Another parameter that is necessary for calculating the inflow is the thrust specific angle, which is denoted as β. FIG. **27** explains its relationship with thrust and airspeed. The inflow modifies the TAS to the common LAS of the rotor. And this LAS has some angle relative to the thrust vector. It is the β angle. It affects the inflow as follows: when the β is zero, the rotors perform as a pure propeller with TSA equal to PSA, and when the β is 90°, the rotors perform as a pure glider with TSA equal to DSA. In any intermediate case, TSA can be calculated using a simple quadrature formula based on these orthogonal components and angle β. Interestingly, for a helicopter, both areas of the PSA and DSA are equal when the PSA is considered to hover, so the helicopter practically has a constant TSA.

[0207] FIG. **28** represents the data flow and definitions for calculating the inflow. At first, there are constant definitions **S281** for DSA and PSA. At second, there is an input of known values **S282**, including: thrust vector T, TAS vector, previous vector of inflow Vip, air density ρ, chain calculated value of the previous LAS vector (LASp), and β angle. The process continues by calculating the TSA in **S283** using the presented quadrature formula that utilizes DSA, PSA and β. The resulted TSA enters together with the TAS and thrust vectors into the routine **S284** to solve equations based on the desired inflow vector Vi. These equations consist of: an equation for the presumed total flow LAS; a scalar equation reflecting the moment conservation law, and based on the presumed total mass flow and the magnitude of the unknown inflow; and a relation used to restore the entire inflow vector. This routine resolves the first two equations together using Newton's iterative method, and restores the entire inflow vector for output.

[0208] The third aerodynamic aspect is the interference of the rotor wings. Each wing has its own vorticity, which impacts on the base flow of other wings. This changing in the base flow of other wings changes their lift forces. And this changing of lift forces is reflected in a change in that vorticity. And so, there are loops with mutual dependences. The final correct distribution of airflow over the wings permits the correct selection of the aerodynamic coefficients and aggregations to obtain the correct distribution of the forces and moments.

[0209] To model this aspect, I divided each of the N wings into M segments along its chord. It permits to define the elementary influence of all vorticities from all other (foreign) wings on such a segment, as explained in FIG. **29**. The chart depicts the wings of the rotor with a typical distribution of the aerodynamic forces AF, the base flow speed vectors V0 and the actual speed vectors V. These V0 vectors already have the inflow included, and these V vectors are simply the individual LASs of the related wings. Each wing also has its own center of vorticity CV. The wing with the index "k" is a current destined wing. Its m-th segment receives a superposition of induced speeds from the CVs of all other wings, where the wing with the index "l" is a current source wing. The radius-vector from the l-th CV toward the center CS of the m-th segment of the k-th wing is referenced as an h-vector with a combination of indices "kml".

[0210] The FIG. **30** represents a magnified k-th wing from the FIG. **29** and explains how induced speeds "w" from all segments of the wing contribute to the common induced speed. I reference this as a consolidation of the interference induced speed vector, over the entire wing. For this consolidation, I simply use the weighting formula, which is provided below the shape of this wing. The weighting parameter in this formula is the ratio of the area AS of a particular segment "m" to the sum of the distance to the center of aerodynamic force CF for the k-th wing and the chord length equal to 1 upon normalization. All constituents of the consolidation formula are depicted and defined in the chart. And at the bottom of the chart, a simple superposition formula is represented for calculating the induced speed in this segment. On the up, a simple formula provides the result for the k-th V-vector.

[0211] The FIG. **31** explains the calculation of the position of the center of vorticity (CVx;CVy) on the wing depending on the AoA. The center of vorticity itself doesn't actually exist, since the general symmetry of the vorticity distribution is too complicated for that. And so, it is only an approximation. At first, I find the main AoA', which is equal to AoA for the first and fourth quadrants of the angular space and is equal to 180°-|AoA| for others. After that, I find the main CVx' value from the first empirical formula at the bottom of the chart. And the resulted CVx will be equal to the CVx' for the first and fourth quadrants and will be equal to 1-CVx' for others. The CVy is calculated simply as the y-coordinate of the camber-line of the used airfoil for the CVx coordinate. This approximation simply reflects the fact that the vorticity is concentrated in the direction of the corresponding leading edge of the airfoil for high values of AoAs.

[0212] The center of vorticity and counter-parted centers of the segments aren't points. They can be considered as linear segments with wing length L, with presumed flat distribution equal to the vorticity distribution from sources with an equalized load distribution, having the same average load as the actual wing. So there is a need for some specific formula, based on proper integration on both sides for calculating the elementary value of the induced speed. FIG. **32** explains deducing of such a formula. It has in the upper-left corner a 3-d chart that depicts a linear vorticity source and a linear center of the destined segment. Both of these linear elements are oriented in the z-direction. The y-direction is up and the x-direction to the right. The z-coordinate on the sourcing segment is denoted by z', and for the destined segment, simply by z, to separate the different integration variables. Vector-h from FIG. **29** is also represented there. The chart depicts an infinitesimal inducing action of the speed from some subsegment of the sourcing segment to some subsegment of the destined segment. The length of the sourcing subsegment is the spatial differential dz', and the length of the destined - dz. The sourcing subsegment possesses some differential value of aerodynamic force as a vector-dAF oriented perpendicular to this segment, and some value of circulation as a vector-Γ oriented along this segment, where both are induced by the speed vector-V of this segment. These two differential subsegments are connected by an r-vector. On the destined subsegment an induced differential-speed vector-dw exists, which is perpendicular to the r-vector and the destined segment. On the upper-right side of the explanatory chart two base equations are referenced in a common frame. The first is the reversed formulation of the Joukowski theorem for the case of equally loaded wing, which relates the signed scalar circulation Γ with the cross-product of the entire aerodynamic force AF and the vector-V. The second equation in this frame is the Biot-Savart law for induced speed, which relates its differential with the cross-product of the vector-dz' and the vector-r, scaled by this circulation. Below the frame, the Biot-Savart law is expressed, which is reorganized to have the scalar differential dz' on its right side. The frame at the middle-right side of the chart introduces a normalized τ-vector, which is the cross-product of the normalized z-vector and the normalized h-vector, and it is simply the direction of the dw-vector. Also, this frame contains simplified notation for the magnitudes of the h and r vectors as just h and r, an expression for the cross-product of the normalized z-vector and normalized r-vector that utilizes the normalized τ-vector and the ratio of h to r, and an expression for the r as a function of z and z'. The last two expressions are substituted in the equation for the vector-dw from the first line outside of the frame, the result of which is represented in the second line as a function of z. The third line has a simple expression for integrating of the z-functional differential dw over the entire length of the sourcing segment. The forth line expresses the resulting elementary vector-w of the induced speed as a result of averaging the spatial distribution of the induced speed vector over all length of the destined segment. So, after substituting the first integral, there is a double integral expression, which was reduced to a simple algebraic formula for resolving these two integrals, using the tables of integrals. Finally, the frame at the bottom of the chart contains the chained form of this formula, which is more convenient for calculation. At first, there is a 3-d aspect coefficient "a" equal to the ratio of h to L. At second, there is a 3-d factor coefficient K3 expressed from this "a". At third, there is a maximal magnitude w0 of the induced speed, expressed through the entire circulation Γ and the distance h between segments. And fourth, there is a resulted vector-w expressed as the product of w0, K3 and the normalized τ-vector.

[0213] FIG. **33** represents the data flow and definitions for calculating the state of the interference corrected airflow of the entire rotor. To simplify this process, I use unit-based scaling of its constituents for the values of the wing chord, air density, and wing area. But the airspeed is used in absolute units. At first, there are scaled definitions **S331**, where each scaled component has a prime sign ('), including the chord itself, the radius of the rotor, the length of the wings, the distances between the source and destination segments, the aerodynamic force formulation, and the circulation formulation, where the last uses a two-dimensional scalar version of the cross-product. At second, there is an input setup of the known values **S332**, which includes the Reynolds number Re0=c/v, normalized in speed, the common and constant properties of the pivot and segments, and the distributions over the wings for positions, pitches and base flows. And this setup is finalized by calculating the spatial distribution of the centers of segments and by setting the initial distribution of the airspeeds equal to the respective base flows. After this setup, the main cycle **S333** for updating result of each wing begins. It includes calculation of the speed's magnitude, Reynolds number and AoA, Polar querying of aerodynamic coefficients and aggregations, calculation of the scaled aerodynamic force and circulation, calculation of the center of vorticity relative to the chord, and reposition of CF and CV relative to the rotor's origin, which is located in the center of the rotor. After 2N cycles of this updating, the completed result passes to the output. In another case, the updating cycle continues by updating the distribution of the airspeeds themselves, starting with the walkthrough **S334** over the destined wings. This walkthrough begins with the walkthrough **S335** over the segments, which begins with the reset **S336** of the related induced speed to zero and continues with the walkthrough **S337** over the foreign sourcing wings. The last walkthrough performs the incremental update **S338** of the current segment, which includes: calculating the radius-vector from the current CV to the current CS, calculating the direction of the induced speed, calculating the 3-d aspect coefficient, calculating the 3-d factor coefficient, calculation of the maximal magnitude of the induced speed, calculating the induced speed itself and accumulating the induced speed in the current segment. After this, the last walkthrough **S337** continues. After the walkthrough **S337** is finalized, the process returns to continue the walkthrough **S335** for the next segment. After the walkthrough **S335** over the segments is finalized, the process goes to the consolidating **S339** the stream for the current destined wing. This consolidating uses the formulation referenced in FIG. **30** (But here I use the tensorial notation for compactness), which is finalized with updating the airspeed of the current destined wing. The consolidating returns to continuing the walkthrough S**334** over the destined wings. The walkthrough **S334** over the destined wings is finished with the initiation of the next main cycle **S333**.

[0214] The flight dynamics simulation is based on all the aerodynamic aspects mentioned, the basic laws of mechanics and the specific features of the modeled aircraft. Also, this simulation is generally applicable for an aircraft with non-circular actuators, such as the aircraft of FIG. **6**, or for an aircraft without the managed PGS-state, such as a cyclorotor aircraft operating in the curtate mode, if there are known distributions of the wings' positions and their pitches and the correct inflow modeling for the non-circular actuators. The entire simulation process can be considered as a data flow inside of some state of the machine. FIG. **34** represents the data flow inside of such a machine. The process starts as a sequence of cycles with some time step Δt against the background of an arbitrary handling **S340**, including a supervising of the result of the simulation in the background, and includes a chain of updates of different components of the entire state in the order specified on the chart and locked in a closed loop. Each specified update has a name that generally points on an updating of an existed component of the state with the same name. But it is only generally, because some updates may also update others components of the state, as further specified in detail.

[0215] The entire state of modeling of the aircraft is defined in accordance with the chart shown in FIG. **35**. The entire state definition **S350** has nine kinds of data, as it specified in this chart, were all specified kinds are applicable to the entire aircraft, and some of them are also applicable to each wing of the rotor in a particular manner.

[0216] At first, there is a global state **S351**, which doesn't have a common identifier for referencing during the entire update. This state includes: time - t; a location point for the current cycle - LOC, which can also be referenced as a vector; a location point of the same kind, for a cycle before the current cycle - LOCB; a speed vector for the cycle before the current cycle - SPDB; and kinematic viscosity of air - ν. The location components of this kind of data are also applicable to the wings.

[0217] At second, there is a kinematic state **S352**, which is referenced by the identifier CNM. It includes an acceleration vector - ACC and a speed vector - SPD. This kind of data is also applicable to the wings.

[0218] At third, there is a predicted state **S353**, which is referenced by the identifier PDT. It includes: an acceleration vector - ACC; a speed vector - SPD; a point location - LOC; and a winding speed - WS. All components of this state, except the last, are also applicable to the wings.

[0219] Fourth, there is an airflow state **S354**, which is referenced by the identifier AFW. It includes: an angle of attack - AoA; Reynolds number - Re; air density - ρ; a magnitude of the true airspeed vector - TAS; a lift coefficient - CL; a drag coefficient - CD; a moment coefficient - CM; an inflow vector - IFW; and a variation of the angle of attack due to steering the stream by inflow and interference - ΔAoA. This kind of data is mainly applicable for the wings and partially applicable for the entire aircraft.

[0220] Fifth, there is a winding state **S355**, which is referenced by the identifier WND. It includes: a winding acceleration value at the rotor's radius - WA; a related actual winding speed value - WS; a phase of the rotor - PH, which uses the angular position of some zero-wing as an origin; a powering force - PFD, which is directed in one of two possible directions; and a related internal force directed - IFD, which is also applicable for the locked rotor. This kind of data isn't applicable for the wings.

[0221] Sixth, there is a dynamic state **S356**, which is referenced by the identifier DNM. It includes: an aerodynamic force vector - AF; a magnitude of the gravitational acceleration - GR; a vector of the gravitational force - GF; a damper force vector from the undercarriage on the runway - DF; a total force vector - TF; a pitch moment of the entire aircraft induced by the rotor, or a wing's pitch moment - PM; and an internal pitch moment induced by the rotor through its steering mechanics - PMI, which represents the total pitch moment of all wings. All components of this state, except for DF and PMI, are applicable for the wings.

[0222] Seventh, there is a power state **S357**, which is referenced by the identifier PWR. It includes: a consumed power - CPWR; a glide mass - GM; a kinetic energy - KE; and a kinetic energy for the cycle before the current cycle - KEB. The GM and KE components are applicable for the wings.

[0223] Eighth, there is a handling state **S358**, which is referenced by the identifier HND. It includes: an entire PGS-state - PGS; a target winding speed, for the rotor's controller - WST; a mode of the biangular handling - BAM, which has two states, A or P; a value of the main angle of the biangular handling - MA; a value of the opposite angle of the biangular handling - OA; a locking flag - LCF, which has the states On or Off; and a free-wheeling flag - FWF, which also has the states On or Off. This kind of data isn't applicable for the wings.

[0224] And ninth, there is a report state **S359**, which is referenced by the identifier RPT. It has only dimensionless components that allow an invariant analysis of the result of this modeling and the capabilities of a modeled and equivalent aircraft. It has some kind known components, as well as some new ones that will be introduced here or in the details of their updating. This state includes the following components: a cruise ratio - CrR, which is equal to 1 for perfectly balanced power on a cruise; an equivalent lift to drag ratio of the entire aircraft - LDR; an equivalent lift coefficient - CL; an average Reynolds number - <Re>; a normalized magnitude of the inflow - IFWN, where the normalization value will be explained in the details of its updating; a winding ratio - WR; a normalized target winding speed - WSTN; a normalized winding speed - WSN; a moment ratio - MR, which is the pitch moment, normalized by the product of the entire weight of the aircraft and the rotor's radius; an internal moment ratio - IMR, which is the internal pitch moment, normalized by the same way; a thrust ratio - TR, which is the entire thrust normalized by the weight of the aircraft; a thrust angle - TA, which is simply the direction of the thrust, a consumed thrust ratio - CTR (see FIG. **1** for CT), which is the consumed thrust, normalized by the same way as the TR; a normalized acceleration vector - AcN, which uses the current gravitational acceleration for its normalization; a flight path angle - FPA; a normalized TAS magnitude - TASN; a normalized LAS magnitude - LASN; a local gliding angle - LGA, which I introduced before, during the explanation of the splitting of the power of the gravitic thrust; a normalized power lifting speed - PLSN (see FIG. **1** for PLS); a power equalized - PEQ, where the equalizing value will be explained in the details of its updating; a propulsion efficiency - PrE; a "true-gliding" lift to drag ratio - TGLDR, which is the LDR but free from the losses due to the non-ideal propulsion efficiency. This kind of data isn't applicable for the wings.

[0225] The query for altitude conditions **S341** is represented in FIG. **36**A and includes a process **S36A1** having only a call of the entire query based on the standard atmosphere and the y-coordinate of the location, which passes the values of the air density, kinematic viscosity and gravitational acceleration to the respective components of the state.

[0226] The update of the predicted state **S342** is represented in FIG. **36**B. The prediction is based on numerical integration of the current kinematic values at half of the time-step over their related derivatives. It starts by updating **S36B1** the speed, location and winding speed of the entire aircraft in a chain manner, using the current values of the acceleration and speed of the kinematic state to obtain the predicted speed, which is used in obtaining the predicted location. And the same logic is used to obtain the predicted winding speed. Next, there follows a calculation **S36B2** of the angular shift and centripetal acceleration, which is used as a preamble for a walkthrough over all wings. Here, the intermediate variable Shift stores the predicted angular shift of the entire rotor, which is common to all wings, and the intermediate variable ACC0 stores the common centripetal acceleration. Also, the third auxiliary variable Sign stores the actual direction of the winding speed. The mentioned walkthrough, for each wing, consists of updating **S36B3** the acceleration, speed and location. The process begins by obtaining the current speed-direction Dir1 of the current wing using the phase of the rotor and referencing the wing using some function called "GetAbsoluteSpeedDirection". Its name is self- explaining, and the word "Absolute" means that there is a referenced frame that is parallel to the horizon in use, instead of the reference frame parallel to the fuselage. The next call to the simple "Rotate" function provides the predicted direction Dir2 of the speed of this wing using the common predicted Shift value. After that, for each of these two directions of the speed, there is a calculation of the corresponding direction of the related centripetal accelerations ACC1 and ACC2, by rotating the direction of the speed by the right angle in the correct direction, using the auxiliary Sign value. After that, a variation ΔACC of the acceleration vector is calculated by scaling the difference between the directions of the ACC2 and ACC1 by the common value of the centripetal acceleration ACC0. This variation is used to obtain the predicted acceleration of the wing by correcting the acceleration of the kinematic state. Finally, the predicted speed and location of the wing are calculated exactly the same as it was for the entire aircraft. This update ends after updating the last wing.

[0227] The update of the airflow state **S343** is represented in FIG. **36**C and begins by updating **S36C1** the magnitude of the aerodynamic speed using the predicted speed value. The process continues by a walkthrough **S36C2** over all wings, which includes updating **S36C3** the AoA, ρ and gravity, where the last two updates are simply assigning the respective values of the state of the entire aircraft, and where the calculation of the AoA is performed as follows. At first, the angle of the position of the current wing relative to the fuselage is obtained using a self-explaining function "GetPositionAngle", which uses the phase of the rotor and referencing to the wing. At second, the pitch of the wing relative to the fuselage is obtained using a self-explaining function "GetPitch", which uses the current PGS-state and the angle of the wing's position obtained before. At third, an intermediate LAS vector V0 is calculated from the TAS vector of the wing and common inflow. Fourth, there is a correcting of the V0 vector for the case when the obtained pitch of the wing isn't equal to the absolute pitch of the wing relative to the horizon. This is the case when the fuselage follows the stream direction, practically equal to the TAS direction, and is always used in the alpha mode of the biangular handling and very rarely in the other case, so for simplicity I check the "A" flag here. At last, the AoA is calculated using the pitch and the direction of V0 in the common reference frame. After finalizing the walkthrough **S36C2**, the process goes to simulating interference **S36C4** by calling a "SimulateInterference" function, which uses the current kinematic viscosity and a redirection to some callback procedure for setup the initial state of all wings in accordance with the requirements of the "SimulateInterference" functionality, as it was referenced in the explanation of FIG. **31**. A setup callback procedure **S36C5** is called by the "SimulateInterference" function for each wing, providing the corresponding index "i". The "SetupInterference" implementation of this procedure provides the position, pitch and base flow V0, all in the absolute reference frame, as its result, back to the "SimulateInterference" function. After the simulating interference **S36C4** is finalized, the process goes to a walkthrough **S36C6** over all wings, which begins by updating **S36C7** of all end-use components of the current wing using the result of the interference simulation and continues by correcting **S36C8** the ΔAoA value of the current wing for the effect of steering the stream by the inflow, since it was out of the scope of the interference simulation. This update ends after updating the last wing.

[0228] The update of the winding state **S344** is represented in FIG. **36**D and begins by checking **S36D1** for the locked state. The presented logic means: for the case when the locking flag isn't set, the process continues to the next entity of this updating, but in another it can be reset for the case when a non-zero target winding speed is assigned or if the freewheeling flag is set, but in another case the process will go out this updating. After that, the process proceeds to the checking **S36D2** for the lockspeed threshold that is defined using its relation with the acceleration, as referenced there. The logic presented there means: the rotor will be locked in the case when the target winding speed is assigned to zero, the rotor is not in the freewheeling state, and the predicted winding speed less than the lockspeed threshold. In the case when the locking flag will be set to On, the directed powering force will be set to zero, and the process will go out this updating. In the other case, the process proceeds to obtaining **S36D3** the delta acceleration. From the example presented there, it can be understood that the ACC delta acceleration is the acceleration needed to add to the current winding acceleration in order to accelerate the rotation of the rotor with the predicted winding speed to the target winding speed in 0.1 second time. Additionally, a limitation for the magnitude of the ΔACC delta acceleration is calculated and applied here, the value of which is inversely proportional to the inertial abilities of the rotor, as presented in this calculation. After that, the process proceeds to updating **S36D4** of the powering force, which begins by calculating the required directed powering force by adding a force, implied by the delta acceleration ΔACC, to the directed internal force and continues by selecting a limit of the required winding acceleration. In the case of freewheeling, the limit is selected as a very low value, but in the other case, it is selected as 1.4g. So, the magnitude of the directed powering force will be limited below the value related to the acceleration limit, and the process will go out this update.

[0229] The first part **S345A** of the update of the dynamic state is represented in FIG. **36**E and begins by updating **S36E1** the fuselage drag force. It is based on the known values of the FrontArea and WetArea parameters of the fuselage, and the result is stored as the entire aerodynamic force having only the drag component. After that, the process proceeds to updating **S36E2** of the damper force, which begins by calculating two parameters: PushY and SpeedY. The first parameter is the displacement of the undercarriage under the load of the aircraft, which is calculated simply as the difference between the known GroundLevel parameter and the actual altitude. The second parameter is simply equal to the predicted vertical speed of the aircraft. These two parameters are passed to a routine referenced as the "GetDamperForce" function, which calculates the force based on some damping model of a typical undercarriage. This force is zero for a negative PushY parameter when the undercarriage doesn't touch the ground. For the particular case used in the simulation, this force is considered to be vertical, but in the generic case it can have some angle on a sloped ground. After this, the process proceeds to updating **S36E3** the gravitational and total forces, where the latter represents a preliminary balance of all the forces known at this point. After that, the process continues with the remained part **S345B** of this update on the next sheet.

[0230] The remained part **S345B** of the update of the dynamic state is represented in FIG. **36**F and begins by resetting **S36F1** the accumulated forces and moments, which is a preamble of a walkthrough over all wings. The resetting applies to a set of intermediate variables, including accumulators for the aerodynamic force AF, for the non-conservative drag forces NCF, for the internal directed force IFD, for the moment "Moment" and for the internal moment MomentInternal. The mentioned walkthrough begins by updating **S36F2** the forces and pitch moment for the current wing, starting by the calculation the dynamic pressure Q and the related stagnation force QArea, where the latter is used in the followed calculation of the lift and drag components of the aerodynamic force of the wing and its pitch moment, and continues by storing the drag force component in a separate auxiliary vector variable DragForce. This continues with the calculation of the angle of flow LASAngle, using the angle of TAS and the stream steering angle of the current wing. After this, the entire aerodynamic force of the current wing is rotated to be in the correct direction of the LASAngle, followed by the calculation of the gravitational force and total force of the current wing. After that, the current-wing process goes to the accumulating **S36F3** the forces and moments, which begins by accumulating the aerodynamic force and continues with accumulating the projection of the aerodynamic force onto the direction of the rotation speed in the IFD accumulator. Then follows a calculation of the external moment as the cross-product of the wing's position and its total force with accumulating it in the "Moment" accumulator and accumulating the wing's pitch moment in the MomentInternal accumulator. A last accumulated value is the content of the DragForce vector variable, which is rotated to be in the correct direction of the LASAngle and accumulated in the NCF vector accumulator. After finalizing this walkthrough, the process goes to the totalizing **S36F4** the forces, which begins by adding the aerodynamic force vector of the entire aircraft, which has only the drag contribution, to the NCF accumulator, and it is followed by adding the AF vector to the aerodynamic force and total force components of the dynamic state of the entire aircraft. After that, the process goes to updating **S36F5** the thrust reporting, which starts by calculating the LAS vector of the entire aircraft, using the predicted speed and inflow. This value is used to calculate the consumed thrust CTF by refactoring it from the consumed power based on the product of the IFD accumulator and the winding speed. After normalizing by the magnitude of the gravitational force, the result is stored in RPT.CTR. Next, the true thrust force TTF is calculated here by discarding the non-conservative contribution NCF from the entire aerodynamic force. The magnitude of the TTF vector is normalized by the magnitude of the gravitational force and stored in RPT.TR, and the direction of the TTF vector is stored in RPT.TA. After that, the process goes to an updating **S36F6** of the IFD of the winding state. The logic presented there means: if the rotor is locked, set the target IFD to the inversion of the accumulated value, but in the other case, set it to PFD. After this, the process proceeds to calculating **S36F7** the per-wing forces, which means: each wing has the same back projection of a total force during participation in a collective movement. At first, the translation force TF1 is calculated here using the participation coefficient Part of the entire total force, which is equal to the fraction of the wing's mass in the entire mass. At second, the rotation force IFD1 is calculated here as the N-th fraction of the sum of the accumulated IFD and the corresponding value from the winding state. In the case of the locked rotor, the latter will be equal to zero. After this, the process goes to updating **S36F8** the inflow, which is performed by calling a "CalculateInflow" function, which implements the functionality explained in the chart of FIG. **28** using the values of the air density, predicted speed vector, LAS vector and true thrust vector as input. After that, the process proceeds to a walkthrough **S36F9** over all wings, which performs correcting **S36F10** the states of the wings, which at first, includes assigning to the current wing a total force equal to the sum of the translation force TF1 and the projection of the rotation force IFD1 onto the direction of the wing's rotation speed, and at second, it includes correcting of the "Moment" accumulator for the moment value imposed by the actual total force reaction of the wing, which is simply the moment of the inertia force, since a true total force is always opposite to its inertia force. After finalizing the walkthrough **S36F9**, the process goes to the totalizing **S36F11** the moments, where the external and internal moments are summed and stored as the common pitch moment of the aircraft, and the internal moment is stored separately. After this, the process proceeds to updating **S36F12** of the moment reporting, where the moment normalizing value Moment0 is calculated, and the values of both moments are normalized and stored in RPT.MR and RPT.IMR. And so, this update ends.

[0231] The update of the kinematic state **S346** is represented in FIG. **36**G and begins by updating **S36G1** the before state for the location and kinetic energy of the entire aircraft. After this, the process continues with updating **S36G2** the acceleration, location and speed of the entire aircraft, which is based on Newton's second law and the time-step integration of the current kinematic values according to the basic kinematic equations. The process continues with the calculation **S36G3** of kinetic energy for the fuselage using the updated speed value. After that, the process goes to a walkthrough **S36G4** over all wings, which begins by updating **S36G5** the before location, acceleration, location and speed, for the current wing, which is performed in the same manner as for the entire aircraft, and it is continued by the calculating and accumulating **S36G6** kinetic energy for the current wing and the entire aircraft, respectively. After finalizing the walkthrough **S36G4**, the process performs the time update **S36G7** and goes out this update.

[0232] The update of the power state **S347** is represented in FIG. **36**H and begins by checking **S36H1** for the locked state. The presented logic means: for the case when the locking flag is set, ensure that the locking is finalized by resetting the winding speed, acceleration and consumed power, and go out from the main sequence to correcting the handling state **S36H4**, but in another case, continue the main sequence going to the calculation **S36H2** of the power speed. This calculation is performed by measuring the projection of the moving of the first wing from its position in the previous cycle onto the direction of its rotation, as specified in the chart. The projected offset, referenced as DistChange, permits to calculate the PowerSpeed value by dividing by the time-step. After that, the process continues with updating **S36H3** the winding acceleration, speed and consumed power, using the calculated PowerSpeed value, as specified in the chart. After this, the process proceeds to correcting the handling state **S36H4** by calling an "UpdatePGSFromBiangularState" function, which functionality is implemented in accordance with the handling relations explained for the content of FIG. **22**, with accessing the current values of the winding speed and speed vector. And so, this update ends.

[0233] The update of the rotor's phase **S348** is represented in FIG. **36I** and begins by updating the phase and checking its range **S36I1**, where the first is performed by the time-step integrating of the current phase using the actual winding speed and the rotor radius, and the second simply ensures that the phase is in the range from zero to one. After that, the process goes to a walkthrough **S36I2** over all wings, which performs the hard sync **S36I3** of the current wing, which ensures that all its kinematic properties comply with the integrity constraints of the rigid rotor. After finalizing the walkthrough **S36I2**, the process goes out this update.

[0234] The first part of the update of the report state **S349A** is represented in FIG. **36**J and begins by calculating **S36J1** the cruise power. The cruise power is simply a power that needed to perform a cruise flight with a power consumption equal to all current non-conservative power losses. It is calculated by carefully analyzing the power distribution. At first, a GraviticPower value is calculated as the rate of change of the potential gravitational energy using the previous altitude value. At second, a KineticPower value is calculated as the rate of change of the kinetic energy using the previous kinetic energy value. At third, an AccelerationPower value is calculated as the rate of change of the kinetic energy of the center of gravity using the previous speed value. Fourth, an InternalKineticPower value is calculated by discarding the AccelerationPower value from the KineticPower value, and the result reflects the power related to the kinetic energy of rotation. Fifth, an ExternalConsumedPower value is calculated by discarding the value of InternalKineticPower from the total consumed power. And finally, the CruisePower value is calculated by discarding the values of GraviticPower and AccelerationPower from the ExternalConsumedPower value. This calculation can be simplified, but this way better explains the power distribution. After that, the process goes to updating **S36J2** the cruise ratio, LDR, CL and SPDB, which begins by calculating the cruise ratio by dividing the consumed power by the CruisePower value. After this, a SpeedAverage vector is calculated by averaging between the current speed and the previous speed, which is used to calculate the equivalent drag component by dividing the CruisePower value by the magnitude of the SpeedAverage vector. After this, an equivalent lift component is calculated as the projection of the entire aerodynamic force onto the direction perpendicular to the SpeedAverage vector. After this, RPT.LDR is simply calculated as the ratio of these two components, followed by the calculation of RPT.CL using the equivalent lift component, stagnation pressure based on the SpeedAverage magnitude, and total area of the wings. The previous speed vector SPDB is then updated to the current speed value. After that, the process goes to updating **S36J3** the WR, AcN and FPA, which begins by calculating the LAS vector from the current speed and inflow. This value is used to calculate RPT.WR by normalizing the winding speed by the magnitude of the LAS vector. Updating of the RPT.AcN vector and RPT.FPA simply follows after that, as shown here. After that, the process proceeds to preparing **S36J4** for calculating LGA and <Re> by calculating the normalized vector ReactDir that is opposite to the direction of the entire aerodynamic force and means the direction of the inertial vertical. Additionally, this preparing resets the VGDir vector, which is used as an accumulator of the wing's partial impact to the LGA direction, and the RPT.<Re> value, which will also be used for accumulation. After this, the process goes to walkthrough **S36J5** over all wings, which begins by calculating and accumulating **S36J6** the VG (virtual glider) direction as an impact from the current wing. At first, the WingLAS vector is calculated by rotating the predicted speed vector of the wing by its angle of the variation of the angle of attack. At second, its normalized value is assigned to the WinGlideDir vector, and so it points to the direction of the gravitic propulsion for the wing. At third, the WingReact value is calculated as the inverted projection of the aerodynamic force of the wing onto the direction of the common inertial vertical. And finally, the VGDir vector accumulates the WinGlideDir vector weighted in the WingReact value basis. After that, the current-wing process goes to accumulating **S36J7** the <Re>, where the RPT.<Re> accumulates the N-th fraction of the Reynolds number of the current wing, doing the actual averaging. After finalizing the walkthrough **S36J5**, the process goes to updating **S36J8** the LGA, where the direction angle of the VGDir vector is assigned to RPT.LGA. After that, the process continues with the remained part **S349B** of this update on the next sheet.

[0235] The remained part **S349B** of update of the report state is represented in FIG. **36**K and begins by updating **S36K1** the normalized speeds, PrE and TGLDR. At first, the normalizing stagnant pressure Q0 is calculated by dividing the current entire weight by the total area of the wings. At second, the normalizing speed V0 is calculated based on the Q0 and the current air density. At third, the specific refactoring power P0 is calculated based on the V0 and the magnitude of the aerodynamic force. Fourth, all remained values of the report state with the meaning of speed are calculated, except for PLSN, by dividing the related values of other states by the V0, as specified here. Fifth, the propulsion inflow PrInflow is calculated as the projection of the inflow onto the TAS direction. Sixth, the RPT.PrE is calculated as the ratio of the TAS magnitude to its sum with PrInflow in accordance with the Froude formula for an actuator. Seventh, the RPT.PLSN is calculated as the ratio of the ExternalConsumedPower value to P0, scaled by the propulsion efficiency, using the formula for PLS from FIG. **1**. And finally, the true-gliding LDR RPT.TGLDR is calculated by correcting the equivalent LDR value by dividing it by the propulsion efficiency. After that, the process goes to updating **S36K3** the equalized power, which calculates the RPT.PEQ by dividing the consumed power by a specific equalization constant PWR0. This specific constant is defined and calculated in the **S36K2** relations as follows. At first, the equalizing stagnant pressure constant QE is calculated, which is based on the started mass GM0 of the aircraft, the acceleration of gravity GR0 at ground level and the total area of the wings. At second, the equalizing speed constant VE is calculated, using QE and air density ρ0 at ground level. And finally, the specific equalizing power is calculated as the product of GM0, GR0 and VE. After the calculation of the RPT.PEQ, the process goes out this update.

[0236] The self-explaining diagram in FIG. **37** represents simulation constraints grouped by their modalities.

[0237] The simulation result is provided in charts, where each chart is a fixed layout report form and represents all the elements of the HND handling state and RPT report state. Also, it pictures a Rotor State Indicator (RSI). This indicator and its related features are represented in FIG. **38**. The horizontal direction of the indicator is always parallel to the fuselage, but the picture of the horizon inside is inclined by the inverted flight path angle. The wings of the rotor are always pictured in the position in which one of the wings is exactly in the highest position, where the phase is zero, but each of the wings is inclined by the angle of its actual pitch. Also, there are additional three indicators inside and near of its circular border. The thinnest indicator is the TAS direction indicator. The middle thickness indicator is the inflow direction indicator. And the thickest indicator with the curved line along its rim is the LAS direction indicator. The RSI can also be used in the cockpit instrumentation.

[0238] The reporting form depicts all the flags of the handling state in a common field by using the designation of particular flags, as defined in the self-explaining definition chart of FIG. **39**. It also contains additional flags and explains in detail all the flags.

[0239] The simulation was performed for the entire flight from takeoff to landing, including runway operations, and after that the states of particular flight operations were extracted into reports that are presented in the natural flight order. The result is represented in the lettered variants of FIG. **40**. I will comment on the particular values for all flight operations.

[0240] FIG. **40**A represents the result for the "Beginning acceleration on runway" operation where the rotor acts in the "propelling" mode, as reflected in the PS flags, and its winding speed WSN is the highest for all operations. The aircraft still has very low TASN, but LASN is moderate due to the inflow IFWN. However, its winding ratio WR is still greater than unity. The thrust angle TA is small and close to the horizon, also the inflow direction on RSI follows it. The consumed thrust ratio CTR is very high, and PLSN is moderate, which indicates: the aircraft acts as a horizontal lift, moving along its inertial vertical. And the inertia forces are indeed high, as reflected in the high value of horizontal acceleration in AcN. Such an acceleration of 0.3g indicates: the aircraft can perform a short takeoff. This thrust ratio is some higher than this acceleration, because there is also some drag. The moment ratio MR is moderate, but IMR is very low. The propulsion efficiency PrE is low, but the equalized power PEQ only a bit below its maximal value, due to the margin imposed by low TASN. From a glider's point of view, CL is very low, and LDR is zero.

[0241] FIG. **40**B represents the result for the "Before takeoff" operation where the rotor still acts in the "propelling" mode, but TASN is sufficient for takeoff. The rotor's pitching was changed mainly by decreasing the magnitude of the gain in the PGS-state. WSN was also decreased, and the inflow significantly dropped. WR dropped significantly below unity. Also, the CTR dropped. But TR increased, due to representing a significant lift component, which is represented in moderate TA, increased CL and in appearing low LDR with a bit higher TGLDR. The horizontal component of AcN some decreased. The PrE rose significantly, as well as PLSN and the cruise ratio CrR, indicating to a high overpowering for this car-like cruise. Also PEQ is near its maximal value. MR some increased. The aircraft begins elevating on the undercarriage, which is reflected in the low vertical component of AcN.

[0242] FIG. **40**C represents the result for the "After takeoff at 0.5 meters" operation where the rotor acts in the alpha-biangular mode with the “stream following”, which is reflected in the AF flags. The main alpha MA is very high, and the opposite alpha OA is moderate. WSN was increased a bit, as well as WR. CL is high, also LDR increased significantly. TR now is higher than unity, and its angle only 7° below the vertical. IFWN increased due to the increased TR. MR decreased a bit, and IMR changed its sign. Vertical acceleration increased and horizontal dropped. The aircraft already has significant vertical speed, which is reflected in FPA and in the inclined horizon on RSI. The remained horizontal acceleration is accompanied by the moderate negative LGA, and so the gravitic propulsion is already working, which is also reflected in the increased PrE. Although PLSN dropped, it remains high for the vertical lifting. CrR dropped, since the low gliding performance isn't suitable for an optimal cruise. Also PEQ some decreased.

[0243] FIG. **40**D represents the result for the "Getting initial altitude and speed at 12 meters" operation. MA was decreased, but still is high. WSTN was decreased a bit, decreasing the WR. IFWN decreased a bit, but LASN and TASN increased a bit. TR decreased a bit below unity, which is reflected in the small negative vertical acceleration, but the horizontal component of AcN increased a bit. CL decreased below unity, and LDR increased slightly, as well as CrR. PLSN increased a bit, but PEQ and CTR continue to decrease. PrE increased a bit. Vertical speed continued to increase, which is reflected in the FPA. MR decreased, and IMR changed its sign back to negative.

[0244] FIG. **40**E represents the result for the "Getting cruise speed in ascent at 75 meters" operation. MA was dropped to moderate value, as well as OA. Also WSTN was decreased. That is reflected in the significantly decreased magnitude of the negative gain in the PGS-state. LASN and TASN increased moderately, which is also reflected in the decreased WR. The average Reynolds number increased. IFWN continues to decrease. TR is a bit below unity, which is reflected in the small negative vertical acceleration, but the horizontal AcN component rose significantly, as also reflected in the increased negative LGA, which is high for the significantly increased LDR. Also PrE continues to increase, crossing the 99 percent level, and CrR increased more. PLSN decreased insignificantly. CTR continues to decrease due to decreasing the drag, and CL continues to decrease due to increasing the speed. MR increased, and IMR continues to increase in the negative direction. The vertical speed decreased, which is reflected in the decreased FPA.

[0245] FIG. **40**F represents the result for the "Ascending to cruise altitude at 400 meters" operation. MA was reduced to normal value for ascent, as well as OA. The skew is more inclined in the negative direction. WSTN continues being decreased, also the magnitude of the negative gain in the PGS-state was decreased. LASN and TASN increased significantly, which is also reflected in the drastically decreased WR. The average Reynolds number increased to maximal value. IFWN decreased additionally. TR is a bit above unity, which is reflected in the very low positive vertical acceleration, also the horizontal component is near to zero. LGA dropped to its neutral value. LDR increased significantly. PrE continues to increase, also CrR increased to its maximal value, as well as PLSN. CTR decreased more, and CL decreased significantly. MR increased to its maximal value, and IMR increased significantly in the negative direction. The vertical speed increased to its maximal value, which is reflected in the increased FPA. PEQ increased to some below its maximal value.

[0246] FIG. **40**G represents the result for the "Ascending to cruise altitude at 3900 meters" operation. The biangular values and the skew weren't altered, but WSTN was decreased somewhat to

keep a constant value of PEQ. LASN and TASN decreased a bit. WR decreased a bit, also <Re> decreased a bit, partially, due to the increased kinematic viscosity. IFWN increased insignificantly. TR, AcN and LGA are in equilibrium. LDR remains without a change. PrE increased a bit. CrR decreased somewhat, as well as PLSN in accordance with WSN. CTR decreased more, and CL increased a bit. MR decreased a bit, as well as the magnitude of IMR. The vertical speed decreased a bit, which is partially reflected in some decreased FPA.

[0247] FIG. **40**H represents the result for the "Cruise at altitude 4016 meters" operation. MA was decreased to its optimal cruise value, and OA was increased a bit. Also, the inclination of the skew was dropped, and the skew is used for a fine-tuning for the perfect cruise. WSTN was dropped, dropping the PEQ and PLSN. The magnitude of the negative gain was further decreased. CrR indicates the perfect cruise. PrE increased to its maximal value for the positive powering, just about one eighth of a percent below the ideal level. LASN and TASN increased somewhat. WR decreased significantly, and <Re> increased a bit. IFWN decreased a bit. TR, AcN and LGA are in equilibrium. LDR increased to its maximal value, for the powered flight. CTR dropped two times, and CL decreased to its minimal and optimal value. MR decreased, but the negative value of IMR increased, due to the small CL.

[0248] FIG. **40**I represents the result for the "Gliding at altitude 3700 meters" operation. WSTN is zero, and the rotor is locked. MA was decreased to its optimal gliding value, and OA was some increased. The skew is set to zero, also the gain and the pitch are a bit above zero, so all pitches of the wings are almost equal. Nevertheless, the wings are differently loaded, due to interference, which is reflected in the low but significant MR, and so, the external MR will be significantly higher, due to the significant negative value of IMR. All power related values are zero. TAS, LAS and <Re> decreased a bit, but are kept high. IFWN increased insignificantly. TR, AcN and LGA are in equilibrium. LDR increased a bit to its maximal value. CL increased a bit. PrE is insignificantly more than unity, due to the direction of the inflow that is almost perfectly perpendicular to the TAS.

[0249] FIG. **40**J represents the result for the "Recuperative descent at altitude 600 meters" operation. WSTN was set to a high negative value. MA was increased to the high-speed descent value, and OA was significantly decreased, maintaining the MR value above moderate, which is necessary for this operation. The magnitude of the negative IMR decreased somewhat. The gain has high positive value, which is reflected on the RSI, and the skew was decreased a bit. LASN and TASN decreased somewhat, but the <Re> increased, due to the lower altitude. TR, AcN and LGA are in equilibrium. CL increased a bit, and LDR decreased to its value on the ascent. CTR has a moderate negative value. CrR has a high negative value, as well as PLSN and PEQ. So, the power during the recuperation is about two thirds of its value on the ascent, but the vertical speed is much higher, which is reflected in the high negative value of FPA and the horizon tilt on the RSI. PrE is a bit more than unity, since the inflow has some increased projection onto the reverse TAS direction.

[0250] FIG. **40**K represents the result for the "Approaching at altitude 202 meters" operation. It is a low altitude cruise, and so it is slightly different from the high altitude cruise. But some differences exist. They include: somewhat increased WSN and WR, increased value of <Re>, and highest negative value of IMR.

[0251] FIG. **40**L represents the result for the "Enter in descent for landing at 165 meters" operation. This operation is a moderate speed variant of the recuperative descent of FIG. **40**J, and can be characterized by lower MA, higher OA, much higher negative skew, and lesser negative WSTN with lower recuperative power. Also, TASN, LASN and the vertical speed are lower, the last is reflected in the reduced FPA. Also, CL increased somewhat, and LDR is so high as for the cruise, although IFWN increased a bit. AcN has a low negative vertical acceleration.

[0252] FIG. **40**M represents the result for the "Dropping the speed at altitude 82 meters" operation. MA was moderately increased, OA was some increased, and so the gain was increased. Negative WSTN was some reduced. LASN, TASN and <Re> decreased, but WR remains constant. The slope of FPA decreased. MR significantly increased, and the negative IMR value dropped. IFWN increased, as well as CL, but LDR decreased somewhat, due to increasing the drag. TR increased significantly more than unity, which is also reflected in a significant positive vertical acceleration in AcN. The horizontal component of AcN reflects a significant deceleration, which is also accompanied by a significant positive value of LGA. And so, the gravitational force now provides negative propulsion. Also, the projection of the total force onto the flight direction is negative, reflecting the negative propulsion in the negative powering. This is also reflected in TA, which value is greater than the right angle. CrR and PLSN changed insignificantly, and the negative PEQ increased somewhat. During this operation, the aircraft can be considered as a glider flaring up with a high LDR, converting the speed to an altitude with high efficiency, and an elevator that going down converting the gained altitude of the glider to a negative power. And this way, the recuperative deceleration works.

[0253] FIG. **40**N represents the result for the "Dropping the speed at altitude 30 meters" operation. MA was significantly increased, as well as OA. The negative value of WSTN was significantly reduced, but the gain was additionally increased. The negative value of the skew was reduced. LASN, TASN and <Re> decreased more, and WR also decreased. The slope of FPA increased. MR dropped, and IMR changed its sign and stays near to zero. IFWN increased additionally, CL increased more, and the LDR dropped two times. TR is some below unity, which is also reflected in the low negative vertical acceleration in AcN. The negative horizontal component of AcN dropped somewhat, which is reflected in LGA, the related negative slope of which is too low to provide sufficient gravitic thrust for such a low LDR. And so, the deceleration is now performed by the increased aerodynamic drag itself at a relatively low rate. TA switched back to a value less than a right angle. The negative values of CrR, PLSN and PEQ dropped significantly. PrE has its maximal value about unity, due to the combination of the high aerodynamic drag, inflow and remained negative powering.

[0254] FIG. **40**O represents the result for the "Dropping the speed at altitude 20 meters" operation. MA was significantly increased at a rapid rate, and OA was some increased. The negative value of the skew was additionally reduced. WSTN was switched to the positive direction at a rapid rate and has a moderately low value. And this process is still ongoing, as evidenced by the significant difference between the WSTN and WSN values. So, the gain was also switched, having a low negative value. LASN, TASN and <Re> decreased somewhat. WR has a moderate value, in correspondence with WSN. The slope of FPA increased additionally. MR, IMR and IFWN didn't change almost, but MR contains some impact of the moment imposed by the inertia of the rotor. CL continues to increase, and LDR dropped additionally. TR is slowly decreasing, but the vertical component of AcN is a bit positive, since the projection of the aerodynamic drag onto the vertical also participates in the compensation of the entire weight of the aircraft. This high drag is reflected in the additionally dropped LDR. The horizontal component of AcN has a small negative value. The negative value of LGA increased significantly, but the gravitic thrust stays in the old balance with the aerodynamic drag. TA decreased in accordance with the decreased LDR. CTR, CrR, PLSN and PEQ have low positive values. So, the aircraft continues going down after the transition to positive powered mode.

[0255] FIG. **40**P represents the result for the

"Dropping the speed and descent at altitude 6 meters" operation. MA was increased to very high value, which is almost maximal for the operation in the alpha-mode of the biangular handling, and OA was a bit increased. WSTN was significantly increased to a moderate value, so was the value of the negative gain. LASN and TASN continue to decrease at a higher rate, but <Re> decreased insignificantly, due to increasing the speed of rotation, which is also reflected in the highly increased WR. The slope of FPA decreased two times, so the LAS is directed exactly along the inclined horizon. MR increased, but now it is free from the impact of the moment of inertia of the rotor. IMR increased, but has very low value. IFWN increased somewhat, but CL increased more, crossing the level of unity. LDR decreased additionally. TR increased a bit, and the vertical component of AcN increased more. Also, the negative value of its horizontal component increased significantly. CTR, CrR, PLSN and PEQ raised three times, but remain moderately low. PrE decreased a bit, but has the high value due to the high drag itself. The aircraft is in close proximity to the entering to the flight mode with a horizontal fuselage.

[0256] FIG. **40**Q represents the result for the "Dropping the speed and descent at altitude 2 meters" operation. The biangular handling was switched to the pitch-based mode, and the "stream following" was disabled, leading to the horizontal orientation of the fuselage, due to appropriate action of the stabilator. Also, those biangular values of the pitches are mostly used for additional indication, and the gain and WSTN will be the primary handlers until touchdown. And so, the value of the negative gain and the WSTN were moderately increased, accompanied by a very weak decrease of the pitch. MA is a bit below horizontal, and OA is a bit below 45° tilt. Also by looking on RSI, these differences aren't observed, due to that feature of the shifted match points under a high gain in FIG. **23**. WSTN is in the progress of increasing, which is reflected in its significant difference from WSN. LASN and TASN decreased further, but the <Re> decreased a bit. WR continues to increase. MR increased to a moderate value, partially due to the inertia of the rotor. IFWN continues to increase. CL rose significantly, and LDR dropped further. TR increased, crossing the level of unity, but the vertical acceleration in AcN increased more, mostly due to the high projection of the drag force. The last is reflected in the high deceleration in AcN, crossing the level of 0.2g. Also, the gravitic propulsion remains low, which is reflected in the relatively low slopping of LGA. The FPA slope also decreased somewhat. CTR, PLSN and PEQ increased significantly, but stay moderate. CrR increased insignificantly, because the increased drag, and so PrE stays high.

Now, the moderate value of PEQ is maximal for the landing sequence.

[0257] FIG. **40**R represents the result for the "Before touchdown at altitude 0.2 meters" operation. The gain was drastically increased, and WSTN was moderately increased and stays steady. This is also reflected in decreasing the MA and in increasing the OA, as for flaps on an airplane. LASN and TASN decreased further, and the <Re> decreased a bit. MR decreased somewhat, and IMR increased two times, but stays low. IFWN increased somewhat. CL increased significantly, just a bit below the level of two, but LDR increased insignificantly, due to increasing of the drag coefficient, which is reflected in a bit only decreased deceleration in AcN over the decreased speed. Also the slope of LGA decreased additionally. TR decreased a bit, and TA is a bit greater than the right angle, which is reflected in the increased PrE. The FPA slope decreased significantly. CTR increased due to decreasing of speed. PEQ decreased somewhat, and PLSN decreased insignificantly. CrR increased a bit, reflecting a decrease in drag.

[0258] FIG. **40**S represents the result for the "Touchdown" operation. The pitch control of PGS was decreased to keep the vertical descent speed against to be too low, and the negative gain was increased to almost its maximal value. LASN and TASN decreased somewhat, but the <Re> decreased less. WR increased, having a value as maximal for the landing sequence, but even so it remains some below of unity. IFWN increased additionally. CL also increased, crossing the level of two. LDR increased significantly, but stays low. CTR, PLSN and PEQ decreased, due to decreased drag, and so CrR increased, and the horizontal deceleration in AcN decreased. The vertical acceleration in AcN rose drastically up to level 0.25g, reflecting a push from the undercarriage. MR decreased somewhat, and IMR increased somewhat. FPA decreased to almost the horizontal direction. TR decreased a bit, and TA increased a bit. The slope of LGA decreased somewhat, and PrE decreased insignificantly. The runway path should be short since the remained TAS is only 70 percent of the specific stagnation speed.

[0259] FIG. **40**T represents the result for the "Begin aerial braking on runway" operation. The handling was switched to operating in the S-mode when the pitch follows changes of the skew. Additionally, the pitch and the skew were set equal to 35°. The negative gain was dropped to about half its maximal value. Also, the rotor was switched to the freewheeling mode to utilize its freewheel power during deceleration of the rotor. In this mode, the target winding speed is meaningless and can be used only as a hint indication of the minimal winding speed when the freewheeling mode should be switched off. And so, WSTN indicates such a value, having a gray appearance using dithering. WSN, LASN, TASN, WR and <Re> decreased. Since the external moment in the freewheeling mode is zero, the MR dropped to a value of IMR that is very low. TR decreased significantly, and the aircraft continues to descend on the undercarriage, having a low negative FPA. TA increased, as well as PrE. CTR and PLSN decreased, and they aren't equal to zero, since their calculation is based on the external consumed power, which now reflects the power provided by the freewheeling rotor. CL dropped, as well as LDR. AcN exhibits very high deceleration of 0.38g for its horizontal component, mostly from the drag, but it also has a partial impact from the negative gravitic thrust, reflected in the low positive value of LGA. This high deceleration additionally allows the aircraft to make a short landing on the runway.

[0260] FIG. **40**U represents the result for the "Continue aerial braking on runway" operation. The skew and the pitch were increased up to a right angle to maximize the drag. The freewheeling mode was switched off. WSTN is moderately low. LASN and TASN dropped more than in half, and the <Re> dropped less. WR rose, crossing the level of unity. The horizontal deceleration in AcN decreased somewhat, but stays high. TR is low and TA is strongly directed backward. MR is low, and IMR changed its sign to negative and stays low. IFWN and CL dropped more than in half, and the LDR is near to zero. CTR increased due to the dropped TAS, PLSN increased due to the dropped aerodynamic force, and PEQ is low. CrR reflects high drag. The high PrE reflects the opposite direction of the inflow. The aircraft continues to descend on the undercarriage with oscillations, reflected in a small vertical acceleration in AcN.

[0261] FIG. **40**T represents the result for the "Finalizing aerial braking on runway" operation. The skew and the pitch were increased up to a direction above the direction of the inflow that is indicated by TA. And this direction is also close to the TAS opposite direction. LASN and TASN dropped in many times, so WR is very high. IFWN increased to a value much higher than TASN, so the rotor now works in a reversed "propeller mode", and the LAS direction is opposite to TAS. TR and PEQ dropped about two times, but CTR rose two times due to the dropped TAS. PrE increased and has a negative sign due to opposite directions of LAS and TAS, which is also reflected in PLSN. Also, AcN exhibits a very low deceleration. Nevertheless, the current thrust almost sufficient to compensate for losses, which is reflected in CrR that is close to unity. And so, this mode of operation can be used for taxi operations in two directions upon changing the direction of the winding speed. Also the pitching as in FIG. **40**A can be used for these taxi operations.

[0262] From the presented analysis of the result of this simulation, it can be understood that an aircraft with the rotor presented will perform well for all operations. The only problem is the relatively high IMR on the cruise, which can lead to a significant wearing of the steering gears. But this problem can be avoided by using a symmetrical airfoil for the rotor wings. Also, there is another problem that is beyond the scope of this analysis. There are rotor vibrations that should be low enough for a comfortable flight.

[0263] Five components can be selected for the analysis of these vibrations. The first two are the same as I presented for the analysis of the "wired wings" simulations. These are the horizontal and vertical components of the acceleration of the entire aircraft, normalized by gravitational acceleration at the ground level. The third component is the deviation of the external moment ratio EMR or shaft moment ratio. This deviation is calculated as the difference between the instantaneous value and the value averaged over all analyzed samples. The fourth component is the deviation of IMR. And the fifth component is the deviation of WSN. Also, it can be understood that for this analysis only samples are enough that lay in the time range that corresponds to the range of positions between any two neighbor wings or a bit more. This periodic time range is the N-th fraction of the entire rotor phase, and so I refer to the time inside it as a minor phase. Also, I consider that it varies globally from zero to N, instead of from zero to one periodically, as this is better for analysis. And so, I extracted such data from the result of the flight simulation for the cruise flight referenced in FIG. **40**H, and prepared plots for this. These plots are represented in FIGS. **41**A and **41**B, where the FIG. **41**A represents the first three mentioned components, and the FIG. **41**B two remained components, which are exactly synchronized by their common horizontal axes of the minor phase. Also, FIG. **41**A shows a relation for calculating EMR at its bottom for reference.

[0264] The first plot exposes quite low deviations for the vertical acceleration and EMR. In the case of referencing the EMR at the radius of the rotor, both their impacts will be below 0.001g on the amplitude basis. And also, they are in counter phase, so some compensation will exist, since the center of gravity of the aircraft is located some under the forward side of the rotor. And for the horizontal acceleration, these variations are much lower.

[0265] The second plot exposes significantly high deviations for IMR, which have an amplitude of about 0.03g at the radius of the rotor and a spectrum of high harmonics. Also, deviations of WSN, presented here, are low, with an amplitude below 0.000002, or 0.2mm/s if a normalizing speed of 100 m/s is used. Also, they are synchronized with EMR. The vibrations from IMR can be reduced simply by using a symmetrical airfoil. But there is another way. This can be performed by an active vibration reduction system VRS, which poses special patterns of additional current in the coils of the electric engine of the rotor to compensate for the vibrations propagating through the stationary elements of the rotor. These patterns should be synchronized with the minor phase of the rotor. In addition, the low level of these WSN variations provides sufficient margin for this. Also, this VRS will be more simplified if the number of the wings is a common divider of the number of poles of the engine. Also, such a pattern shouldn't follow on straightforward manner from the presented plots, since it depends on the actual mechanics properties of all the tiers of the aircraft near the rotor's vicinity and on particular flight operations. And so, it can only be obtained experimentally or through detailed modeling.

[0266] Another important feature of the flight is the handling the aircraft during a turn. The presented flight simulations are 2-dimensional only. Nevertheless, they permit simply to obtain the result also for a turn. Suppose that the aircraft in a turn has an inside of the turn and an outside of the turn. And so, each side can be modeled separately with some differences in handling for a particular flight operation. After that, only need to compare the differences in the behavior of the acceleration components from two sides and provide the difference in the handlings, accompanied by a related difference in the accelerations. For the case of a well-posed turn, which is usually called a coordinated turn, its introduction begins from a roll inside of the target turn. Such a roll results from the difference in the vertical accelerations between the wings. The roll on an airplane is performed by ailerons, which have an adverse effect on the turn by posing horizontal acceleration in the wrong direction due to the adverse drag distribution. And so, the airplane begins counter rotation in the event that nothing is done. And therefore, to prevent this, two features are used. The main feature is an increasing the pitch by using the elevator, which leads to an increasing the lift and the flight path curvature consequently. And, since the plan of such a curvature is inclined correspondingly with the existed roll, the inertial vertical of the introduced curvature is also inclining, introducing a rotation in the right direction. Also, a correctly performed coordinated turn prevents the airplane from slipping. An additional feature here is the action of the rudder, which enforces the beginning of the rotation. So, finally, the tendency to rotate in any direction will be presented by the difference in the components of horizontal acceleration between the wings. And, if an aircraft during a turn has the same relations in the directions of acceleration of its wings as for a coordinated turn, this will be a coordinated turn, since the correct difference in horizontal accelerations will introduce the same inclining of the inertial vertical, as in the case of the increasing pitch. So, I conducted some experiments during the simulation and found such correct combinations of the desired accelerations between the sides with the related handling.

[0267] The result of this, for various flight operations, is represented as a table in FIG. **42**. There are eight operations that cover the full spectrum of the entire flight. They can be divided into three categories.

[0268] The first is a category of normal turns. I referenced it as normal because it includes the cruise operation itself. For the normal category, the turn is introduced by applying a positive difference in the outside relative to the inside for the MA deviations and the corresponding halved negative difference for the OA deviations. These deviations are presented in separate columns for OA, MA, and related P and G. And, the last column represents the deviations of the accelerations themselves. The normal category includes the first four operations from the low-speed ascending flight up to the cruise. Also, the ratio between the horizontal and vertical components of the induced acceleration varies, so for some operations the roll may be too high relative to the rotation. In this case, additional handling may be required to increase the common lift to enforce the coordinated turn. And after entering a coordinated turn, only the additional control of the increase in lift should be kept, as all airplanes do. But in any case, all variants, listed in the table, avoid the adverse back rotation, featured for the ailerons of an airplane.

[0269] The second category contains only the gliding flight itself, and this is the case of neutral turns. For this case, the horizontal rotation is near to zero. This is enough to perform this rotation by the handling for an additional lift in a coordinated turn, but that can be less effective than in a normal case. And so, a rudder can speed up that turn. For this category, only a small difference in MAs is required to enter in a turn. And the direction of this difference is the same as for the normal category.

[0270] The third category contains all remained operations, and this is the case of inverted turns, since the direction of the handled controls here is opposite to the direction of normal turns. But they have some differences. The first two operations here are the recuperative descents with different levels of the recuperated power. Both the operations use the same magnitudes of the differences applied to MAs and OAs as compared to the normal category. But the operation with higher power has a much higher rate of the horizontal rotation. The third operation is a low altitude part of the landing sequence, where the turns are difficult, due to the risk of slipping during the roll during the introduction the turn. But there is a possibility to perform a flat turn without a roll at all. In this case, the magnitude of the difference between MAs should be two times more than the magnitude of the related handling for OAs.

[0271] Using such differed categories of handling a turn can be problematic for the pilot. But this can be resolved using the flight computer, which interprets the movement of the joystick into corresponding changes in the parameters of the biangular handling and the PGS-state for the rotors on both sides, dependently on the current operational state related with a particular category.

[0272] Another advantage of this handling the turns is a possibility to couple the shafts of both rotors altogether, providing redundancy in the event of a malfunction of the engine or the locking system. Also, the common shaft itself adds an additional rigidness to the inter-rotors base. In the other case, the rotors can use different rotation speeds to accomplish the turn, which is not a good solution, since in pure gliding both rotors must be locked from rotation, and some possibility for turns must be exist.

[0273] For the following description of the preferred embodiment, the accompanied drawings may induce a sensation of to scale representation. However, those drawings may have deviations from such a to scale representation, and certain elements may be exaggerated in scale or pictured with some generalization for the correct and simplified expression their related features.

[0274] Referred now to FIG. **43** there is illustrated an aircraft in accordance with the invention and generally designated by the numeral **100**. In particular, it is an experimental two seat aircraft. The aircraft includes a generally streamlined elongated fuselage **101**, stabilators **102** on each side of the fuselage **101**, rotors **110** on the left side and **110'** on the right side of the fuselage **101**, which kinematic scheme was presented in FIG. **9**, a vertical stabilizer **109a**, as an integral part of the fuselage **101** with a rudder **109**, and also additional components. These components include: an undercarriage bow **283** attached to the fuselage **101**, two undercarriage wheels **284** mounted on each side of the undercarriage bow **283**, a nose supporting fork with damper **287** attached to the fuselage **101** with possibility of rotation around its own axis, a nose wheel **288** mounted on the fork **287**, two parking supports **384** attached to each side of the fuselage **101** with possibility of retracting, two parking wheels **385** mounted in the parking supports **384**, a pitot-static tube (PST) **576** attached to the fuselage **101** on the upper side of its nose, and a stream deviation tube (SDT) **580** attached to the fuselage **101** in the center of its nose. The fuselage **101** has a cabin **103** for the pilot and passenger on its forward side. The cabin **103** can be entered through two doors **104** on each side of the fuselage **101**, and each door **104** has its own window **105**. Also, the fuselage **101** has two rotor's sockets **106** on each side, where the rotors **110** and **110'** are removably mounted, suiting the maintenance or reassembly purposes. These sockets **106** are integral parts of the fuselage **101**, continue inside of the fuselage **101** also, and have generally conical shapes with continuations to engine's fairings **106a**. These engine's fairings **106a** provide an additional space for the electric engines of each rotor **110** and their cooling system, and have air inlets **107** and air outlets **108** for these cooling systems. Each wing **111** of each rotor **110** or **110'** is connected pivotally at its outer end to a respective common end-rotor supporting ring **260**, which provides sufficient rigidness for the entire rotor **110**. The end of each wing **111** has a fairing **170** that provides enough space for a system of pivot's bearings. Also, these fairings **170** act with the end-ring **260** as a distributed wing-fence to alleviate the induced drag. The stabilators **102** are used to maintain the correct orientation of the fuselage **101** during the entire flight by compensating for the moment variations induced by the rotors **110** and **110'**, while the overall moment is mainly compensated by the impact from optimal placement of the center of gravity. The parking supports **384** with the parking wheels **385** are used to service the support of the aft part of the empty aircraft **100** during parking, since the center of gravity may be behind of the undercarriage wheels **284** in this case. Also, there can be a variant of the aircraft **100** without the parking wheels, which has the attaching of the undercarriage bow **283** to the fuselage **101** behind the center of the rotor's socket **106**.

[0275] Referred now to all parts of FIG. **44** and FIG. **56**, the rotor's socket **106** continues inside of the fuselage **101** up to a side force plate **290**, which is an integral part of the fuselage **101**. This force plate **290** has a vertical orientation and begins from the floor of the fuselage in an area shifted forward from the center of the rotor **110**. This shifting leads to the inclination of the parallel rims of the force plate **290**, which continue to up and join in a common semicircular shape coaxial with the axis of the rotor **110**. From the other side, looking at the floor of the fuselage **101** between its joints with the left and right force plates **290**, the rims of these force plates **290** can be considered continued to each other side, since the thickness of the floor in the considering area is increased. Also, the undercarriage bow **283** is placed in the high thickness area, and is inserted and fixed to a special pocket **285**. And so, the presented construction reflects the preferred method of its manufacturing. This is the use overlapping composite materials for the entire fuselage **101** and for some other elements, which is reflected in the diagonal cross hatching for such elements. It can be understood from the presented design that the side force plates **290** are main conductors of the aerodynamic forces from the rotors **110** and **110'** to the fuselage **101** and its content. The side force plate **290** has a socket **293** for an electric engine **300**, as its integral accompanied part, inside the aircraft **100** along the axis of the rotor **110**. This engine socket **293** comprises a drum **294** and a back-ring **295**. Also the socket **293** continues on the part of the force plate **290** toward the axis of the rotor **110** up to the hole for the engine **300**, and is referenced as a setup ring area **290a** in FIGS. **44**A and **44**C.

[0276] A body **301** of the engine **300** is inserted into the socket **293** from the outside, and so this is convenient for maintenance. The body **301** has a setup flange **301a**, which is used to fix the engine **300** to the setup ring area **290a** with screws **632**. After the setup, the engine **300** is included in the chain of the aerodynamic force conduction between the rotor **110** and the force plate **290**. The central powering shaft **127** of the rotor **110** is inserted into a hollow shaft **302** FIGS. **44**B and **44**E of the engine **300** upon inserting the entire rotor **110** into the socket **106**. The central powering shaft **127** is fixed to the hollow shaft **302** by clamping in its fine tolerance collet area **302a** by a clamping nut **310**, utilizing a threaded area **302c** and a clamping cone **302d** of the hollow shaft **302**. Also, this end of the hollow shaft **302** is slotted, as this is necessary for a collet. The hollow shaft **302** has a main radial support from a high load needle bearing **303**, which is placed on the rotor's **110** side of the engine's body **301** in a thick-walled nest. From the other side, the hollow shaft **302** uses the radial and axial support of an engine's rotor **304,** provided by a middle load bearing **309** in an engine's lid **306**. The engine's rotor **304** has a hole corresponding to the shape of the hollow shaft **302** into which this hollow shaft **302** is inserted. Their common interface has a conical segment that provides precise centering. The hollow shaft **302** has a setup flange **302b**, which is used to fix it to the engine's rotor **304** with screws not shown. The other side of the engine's rotor **304** has a radial and axial support from a low load bearing **305**, which is placed coaxially with the needle bearing **303**. This construction provides a possibility to extract the hollow shaft **302** from the engine **300** upon maintenance of the engine, keeping the engine **300** functional. Also, this permits to use a lightweight alloy for the engine's rotor **304** and a high quality steel alloy for the hollow shaft **302**. Also, the rotor's engine **304** has a relatively thin thickness of its medial disc-shaped body with some magnetic related elements located along its perimeter, to create the desired distribution of a rotor's poles **308**. The lid **306** has a centering ring **306a** FIG. **44**D at its periphery, entering inside the engine's body **301** in the vicinity of an engine's stator lamination **307**. The central shafts **127** of the rotors of both sides are coupled together by a common coupling **311**, which has a thickening ring area **311a** at its middle for additional reinforcement. The common coupling **311** has a design of two halves, clamped on each side by two screws not shown. The back-ring **295** of the engine socket **293** is connected to the lid **306** of the engine **300** with screws not shown, and having some sealing, so air cannot leak between the back-ring **295** and the lid **306**. The space between the engine's body **301** and the socket drum **294** is connected to the air inlet **107** via an air separating plate **297** from the bottom and an air sealing plate **298**, see FIG. **56**. The air separating plate **297** is inserted inside of the socket **293** up to the engine's body **301**, so air from the inlet **107** can move only over the plate **297**, around the engine's body **301**, and exit from a window **295a**, which is created in the back-ring **295** under the separating plate **297**. The window **295a** is simultaneously placed inside of an air conduction tube **296**, which is connected to the air outlet **108** at its other end. And so, by this way, air passes through the engine cooling system. Also, the air conduction tube **296** is fixed to the back-ring **295** and to the fuselage **101** near the air outlet **108**, providing additional reinforcement, since the tube **296** is also made of composite material. Additionally, the engine's socket **293** and the fuselage **101** have special holes not shown, which are used for a screwdriver upon fixing the engine **300** with screws **632**, and then sealed.

[0277] The central powering shaft **127** of the rotor **110** represents a rotational tier of the rotor's setup. Also, the rotor **110** has an irrotational tier, which back end is represented by a steady base **154** FIG. **44**B. The steady base **154** is mounted on the engine's body **301** at the ends of mounting supports **168** using washers **169** and nuts **171**. This fraction of the setup is performed from the side of the faceplate **112** of the rotor **110**. So, the faceplate **112** has at least one hole for a tubular wrench holding the nut **171**, since the rotor **110** can be rotated during the setup. This hole or holes must be sealed after the setup, so they aren't shown. The washers **169** are fixed on the steady base **154** from falling in advance.

[0278] Referred now to FIG. **44**C, the wings **111** have fillet areas **111b** on their both sides over the bases **113** to accommodate the high remaining bending forces and to reduce interference from the fuselage proximity. Also, the leading edge of each wing **111** has a transition **111a** over the fillet area, which reflects the used pivot ratio for the airfoil. The limits of the area occupied by the wing during its rotation around its pivot are referenced as **111'** and **111"** for the upward and downward orientations of the leading edge, respectively.

[0279] Referred now to FIGS. **44**A, **44**B, **44**C, **48**A and **48**B, the rotor **110** has the mentioned faceplate **112** that is circular in shape and made of a plate of composite material. The faceplate **112** has ten holes near its perimeter, where wing's sockets **145** are mounted using some screws that are not shown, interleaving with bridges **146**. These wing's sockets **145** are made of lightweight alloy on a lathe and have a cup like shape with additional features. These features, looking from the side and beginning from the direction of the faceplate **112**, are: a centering ring **145e**, for which the main holes of faceplate **112** have complementary grows, a base ring **145a** used for the own mounting and for mounting the bridges **146**, a cone segment **145b**, for which the bridges **146** have complementary rims, and a back-ring **145d**. As an additional feature, there is a window **145c**, which is milled in the floor of this "cup", about the medial level of the back-ring **145d**. This disc-shaped floor in the center goes into a generally cylindrical area with a hole at its center. In this hole a radial needle bearing **183** is placed, which has inside a tail of a tubular flange **179** with a wing's shaft **180**. This shaft **180** protrudes from the center of the wing's base **113**, which has inside of the wing's socket **145** a conical shape following its cylindrical area. The bevel gear **114** is attached to the top of the cone of the base **113**, and has the shaft **180** inside of its center. This attachment is performed by the non-shown screws inside the toothed ring of the bevel gear **114**, which are well suited to transmit significant torque. A primary thrust bearing **181** is placed over the bevel gear **114** under the corresponding ring area of the wing's socket **145,** accommodating the high thrust forces induced from the remained bending moment of the wing **111**, and additionally protects the attachment of the bevel gear **114**. A secondary thrust bearing **182** is placed from the back side of the wing's socket **145** under the flange area of the tubular flange **179**. A nut **185** fixes wing **111** in socket **145**, lying on a washer **184**. A flanged bearing **178** in a hole of the back-ring **145d** supports the shaft **116**, which rotates the bevel pinion **115** fixed on it and meshed with the bevel gear **114**. The bevel pinion **115** occupies window **145c**, so the window **145c** is used for clearance, as well as for setup and maintenance. This setup and maintenance may include installing or extracting the entire wing **111** from the wing's socket **145** on the installed rotor **110.** In this case, a special non-shown window or hatch in the rotor's socket **106** is used to unscrew the nut **185** after positioning the related wing **111** against it. Also, it permits a simplified installation of the entire rotor **110** and transportation of the entire aircraft **100** without the wings **111** mounted on the rotors **110** and **110'**.

[0280] Rotor **110** has a back-ring **147** mounted on the tops of ribs **148** that are mounted on the faceplate **112**, using non-shown screws for both sided of these ribs **148**. The back-ring **147** is placed coaxially with the faceplate **112**, and the ribs **148** are placed in the directions connecting the centers of the wing's sockets **145** and the center of the rotor **110**. The back-ring **147** is also made of composite material and has the same positions of the setup holes for the nuts **185** as the faceplate **112**. Each rib **148** has a flanged bearing **172** inside that supports the other end of the shaft **116** on which the miter gear **117** is fixed. The shaft **116** is locked against axial movement on both sides by locking hubs **173**. Each shaft **121** is supported by a flanged bearing **174** placed inside the faceplate **112** and by a flanged bearing **175** placed inside the back-ring **147**. The cluster **120** is fixed on the shaft **121**, and its miter gear **118** is meshed with the miter gear **117**. The pinion **119** of the cluster **120** is meshed with the pitch gear **131** of the earring assembly **130**, which shaft **132** is supported in flanged bearings **176** and **177** placed inside the faceplate **112** and the back-ring **147**, respectively.

[0281] Referred now to FIGS. **44**B and **45** through **47** the earring assembly **130** has the mentioned shell **137**, which consists of two halves **137a** and **137b** located on the face side and the back side, respectively. These two halves of shell **137** are fixed together by two screws **604**. The half shell **137a** has a bearing **139** FIGS. **44**B, **47**, which supports the hub of the pitch gear **131**. Shaft **132** is inserted into the pitch gear **131** and fixed in this hub. The middle of shaft **132** has a bearing **140** dressed on it and inserted into the half shell **137b** to support this shell. The inner side of bearing **140** has an axial support at a locking hub **138** fixed on shaft **132** outside the half shell **137b**. Shaft **132** has a clearance groove **132a** against collision with the cluster **122** of rotor **110** for high gain values. The other side of the half shell **137b** has a bearing **143** that supports the cluster **133**, inserted from the outside of the half shell **137b**. The entry gear **135** of cluster **133** is remained outside of shell **137**, and the steering pinion **134** of this cluster is meshed with the pitch gear **131**. An adapting flange **141** is dressed on the end of the cluster **133** and is supported in a bearing **142**, which is placed in the half shell **137a**. A closing washer **144** with a screw **603** fixes the cluster **133** from falling out. The groove follower **136** is dressed on the cluster **133** and is fixed by a screw **602** from falling out. The halves of the shell **137** are contacted only at small fixing bases **137c** FIGS. **45**, **46** enough to have holes for screws **604** so that they don't obstruct the pitch gear **131**. From the other side, these fixing bases **137c** are decreased to have a big clearance-window **137d** FIG. **46** against collision with the pitch gear **131** of the neighboring earring assembly.

[0282] Referred now to FIG. **44**B, the central cluster **122** is supported by a radial bearing **151** on a shifting base **149**. Additionally, the cluster **122** is supported by a thrust bearing **152**, which is placed on a closing flange **150**, which is fixed on the shifting base **149**, providing additional fixation of the inner ring of the bearing **151**. The central gear **124** of the cluster **122** is meshed with the entry gears **135** of all the earring assemblies **130**. The groove followers **136** of all the earring assemblies **130** are placed inside the groove ring **123** of the cluster **122**. A flanged hub **153** is fixed on the central powering shaft **127** with some set screws inside a shaft setup ring **153a**, which is thick enough for this. The shifting base **149** has an inside conical profile corresponding to the shape of the setup ring **153a** so as to have the desired clearance during the movement of this shifting base. The flange side of the flanged hub **153** is attached to the faceplate **112**, using screws or rivets not shown. The part of the central powering shaft **127** that protrudes from the flanged hub **153** and enters the corresponding central hole in faceplate **112** is used to center the flanged hub **153** on the faceplate **112** during fixing this flanged hub. A steady flange **155** enters inside the central hole of the steady base **154** and is attached to it by screws not shown. It has a primary bearing **156** inside, supported by the flanged hub **153**. The steady flange **155** also has a secondary bearing **157** inside the other end, which is supported by the central powering shaft **127**. The bearing **157** is axially fixed by a closing hub **158** fixed on the central powering shaft **127**.

[0283] Referred now to FIGS. **44**B, **48**A and **49**, the steady flange **155** has three threaded holes in which three radial rods **159** are screwed in by their threaded areas **159a**, where the central of these rods **159** is oriented at 45 degrees up and back, and the other two rods **159** are perpendicular to the central, spreading in opposite directions. The peripheral ends of the rods **159** are fixed inside clamps **162** mounted on the steady base **154**, using pairs of screws with washers **163**. Each radial rod **159** has either a cross-holes bearing **161** or a cross-holes bearing extended **160** that is dressed on it, where the latter is placed only on the central radial rod **159**. The steady base **154** has three radial clearance dips **154d** FIGS. **48**A, **49** for the movement of each of the bearings **161** or its extended variant **160** in the radial direction along the rods **159** without obstruction. The shifting base **149** has three lateral slots **149b** at its periphery, which correspond in directions to the radial rods **159**, see also FIG. **50**. A tangential rod **165** is placed along each slot **149b** in the direction perpendicular to the corresponding radial rod **159** and fixed by clamps **166** at its ends. These clamps **166** are mounted on the shifting base **149** by using a screw with washer **167** FIG. **50** per each clamp **166**. These tangential rods **165** are inserted into other holes of the respective bearings **161** or **160**. This kind of connectivity between the steady base **154** and the shifting base **149** allows the shifting base **149** to be moved in any direction, but firmly disables any rotation of the shifting base **149**. And so, rotation and moving of the cluster **122** are decomposed. More than, the presented system of rods also provides retention functionality to have the shifting base **149** in a fixed position along the axis of the rotor **110**. The inability to rotate the shifting base **149** can be decomposed into a radial component and a tangential component in terms of tolerances between the rods **159, 165** and the respective holes of the bearings **160** or **161**. The radial component has its own base equal to about of the distance from the center of the distant bearing to the center of the rotor **110**, and it is large. The tangential component has its own base equal to about the length of the hole for the tangential rod **165**, and it is significantly less than the radial. So, the overall inability to rotate may be less than the desired. This problem is resolved by using the cross-holes bearing extended **160**, which has crampons **160a** on the sides. These crampons **160a** expand the tangential base by entering in saddles **164** mounted on the shifting base **149**.

[0284] Referred now to FIG. **44**B and **48**A, a pitch flanged bracket **187** is mounted on the shifting base **149** in a hole opened to the inside space of the shifting base **149** and is fixed by screws not shown. A primary bearing **188** of the pitch flanged bracket **187** supports a pitch steering shaft **186**. The other end of the pitch steering shaft **186** is supported by a secondary bearing **189**. The pitch pinion **126** is fixed on the pitch steering shaft **186** and is meshed with the internal gear **125** of the central cluster **122**. The shifting base **149** has a hole opened to the outside, which provides clearance for the pitch pinion **126**. A pitch worm gear **190** is fixed on the other end of the pitch steering shaft **186**. The shape of the internal perimeter **149a** of the shifting base **149** is correspondent to the outer shape of the steady flange **155** with a clearance enough for the unobstructed movement during its shifting. Their shapes are generally circular, but have a flat segment near the vicinity of mounting the pitch flanged bracket **187**. The steady base **154** has a hole **154a**, which provides sufficient clearance to move the pitch flanged bracket **187** during the movement of the shifting base **149** and allows the use a screwdriver during mounting the pitch flanged bracket **187**. The upper side of the pitch flanged bracket **187** has a worm support bracket **187a** FIG. **48**A, the inner end of which has a flanged bearing **193** inside its hole, and the outer end has a flanged bearing **194** inside the other hole. These flanged bearings support an inner shaft **195a** of a telescopic universal joint assembly **195**. A pitch worm **191** is dressed on the inner shaft **195a** inside the worm support bracket **187a** and is meshed with the pitch worm gear **190**. A locking hub **192** fixes the inner shaft **195a** from axial movement.

[0285] The telescopic universal joint assembly **195** consists of an inner universal joint **195b**, an outer universal joint **195d** and a meshed spline-pair **195c** between them. The inner shaft **195a** belongs to the inner universal joint **195b**. An outer shaft **195e** belongs to the outer universal joint **195d** and is supported by two flanged bearings **197** inserted into a common hole of a pitch bracket **196**, which is mounted on the steady base **154** by screws not shown. A locking hub **198** fixes the outer shaft **195e** from axial movement. The steady base **154** has a clearance recess **154b** near the vicinity of the inner universal joint **195b**, which is sufficient to move and rotate this universal joint. Another clearance recess **154c** is located near, in the vicinity of spline-pair **195c** between the sides of the pitch bracket **196**, and it is less deep, but sufficient for transverse movement of the inner spline-pair segment. The outer shaft **195e** is one of the interfaces of a steering tier of the setup of the rotor **110**.

[0286] The steering of the gain and the skew is incorporated in a common Gain-Skew-node **200** or simply a GS-node, which is referenced in FIG. **44**B without details. Its detailed construction can be understood by looking at FIGS. **48**A and **51** through **53**. The GS-node **200** can be divided into two logical domains: a GS-variator **210** FIGS. **48**A, **51** and **52**, and a Skew-to-Gain-compensator **240** FIGS. **48**A, **52** and **53** or simply a SG-compensator. A circular mounting base **201a** of a flange **201** of the GS-variator **210** is used as a setup interface of the entire GS-node **200**, since the flange **201** is inserted into a corresponding hole **154e** of the steady base **154** opened to the outside, lying on it, and is fixed here with screws that are not shown. The axial direction from this interface to the shifting base **149** will be referenced as bottom and opposite as the upper direction.

[0287] The flange **201** is used for assembly in its interior at the bottom direction the main components of the GS-variator **210**. An intermediate ring **202** FIG. **51** is mounted inside the flange **201** and is fixed to it by the non-shown screws inserted from the outside of the flange **201**. This fixation of the intermediate ring **202** is an operation that finalizes the assembling of the content of the flange **201**. The intermediate ring **202** fixes an outer bearing **208** and an inner bearing **212**, and is placed between them. A retaining ring **204** is supported by the outer bearing **208** in the radial and bottom axial directions, and is attached to a skew worm gear **203** by screws **205**, using a mounting groove **203a** of the gear **203** to center it. The central hole of the skew worm gear **203** has a flanged bearing **211** inside that supports a gain steering shaft **209** in the radial and bottom axial directions. A gain gear **213** is fixed on the gain steering shaft **209,** and its hub is inserted into the inner bearing **212**, obtaining the secondary radial and upper axial supports. The last upper axial support also extends to the skew worm gear **203**. The skew worm gear **203** has a circular recess in the center in which the gain gear **213** can rotate freely. Also, the skew worm gear **203** has another, rectangular, recess in which a toothed rack **207** is placed and can be moved, slipping on its surfaces from the bottom and opposite to teeth. The toothed rack **207** is meshed with the gain gear **213** and is connected with a steering lead **206**, which is inserted into a rectangular hole of the skew worm gear **213** from the bottom and fixed with screws not shown. The steering lead **206** has a slipping ledge **206a**, which slips over the bottom surface of the skew worm gear **203**, completing the vertical support of the toothed rack **207** and its own. Also, the steering lead has a steering pin **206b** that enters inside a flanged bearing **199** placed in a hole on the periphery of the shifting base **149**. A gain worm gear **214** is fixed on the gain steering shaft **209**. The flange **201** has two G-worm supports **201b**. Flanged bearings **218** and **219** are inserted into the inner and outer supports **201b**, respectively, and support a gain inner shaft **216**, on which a gain worm **215** is fixed, meshed with the gain worm gear **214**. A locking hub **217** fixes the gain inner shaft **216** from axial movement.

[0288] A skew bracket **220** is mounted on the mounting base **201a** of the flange **201** on the side opposite to the gain worm **215** and is fixed with screws that are not shown. A skew steering shaft **221** is supported in the skew bracket **220** by the flanged bearing **224** at its end and by a bearing **225** at its entry. A skew worm **222** is fixed on the skew steering shaft **221** and is meshed with the skew worm gear **203**, occupying a sectorial cylindrical space milled inside the flange **201** for that. A spacer **223** is dressed on the shaft **221** and is used to propagate the secondary axial support from the bearing **225** fixed inside the skew bracket **220** by the non-shown set screws. The skew steering shaft **221** has a tail **221a**, on which a gear **226** is fixed. A skew outer shaft **228** is placed in an appropriate position and is supported by the flanged bearings **230** and **231** at its end and entry, respectively, which are inserted into the skew bracket **220**. A gear **227** is fixed on the skew outer shaft **228** and is meshed with the equal gear **226**. A spacer **229** is dressed on the skew outer shaft **228** and is used for secondary axial support of this shaft. The skew outer shaft **228** is another of the interfaces of the steering tier of the setup of the rotor **110**.

[0289] The GS-variator **210** permits to have a desired gain for any particular skew by placing the steering pin **206b** in the desired shifted position. For this placement of the steering pin **206b**, appropriate rotations of the gain inner shaft **216** and the skew steering shaft **221** are necessary. But the GS-variator **210** has a principal drawback for use: the desired position of the steering pin isn't decomposable to gain and skew values on the worm shafts of the variator, since there is an induced gain that depends on the skew, through its mechanics. Indeed, let's consider that the gain has fixed and the skew is changing. So, in order for the gain to remain unchanged, the gain worm gear **214** must be rotated at the same angular speed as the skew worm gear **203**. But, it is fixed by the gain worm **215** and induces an adverse movement of the toothed rack **207**. So, in order to have decomposable mechanics, the GS-variator **210** must be accompanied by a compensator, which will rotate the gain inner shaft **216** at the speed exactly needed for rotating the gain worm gear **214** at the same angular speed as the speed of the skew worm gear **203**. This task can be accomplished explicitly, when the gain inner shaft **216** and the skew outer shaft **228** are under computer control or sophisticated control. But doing this task implicitly through pure mechanics has a significant advantage, especially in the event of an electricity outage. And so, it accomplished by the SG-compensator **240**.

[0290] When handling the presented aircraft in biangular mode, for example, by changing the main angle, the rate of change of the gain is approximately two times the rate of change of the pitch. And so, this ratio is optimal for most operations and should be reflected in the mechanics by default. This leads to the need for an additional reducer for the gain for its desired fine handling, optimally aligned with the fine handling of the pitch. The main feature of this reducer is the presence of coaxial alignment of the outer and inner shafts, so it should have two pairs of gears with the same sum of gear teeth in each pair. And, in particular, these two pairs of gears are selected to be equal. Such a reducer is composed together with the SG-compensator **240**. This composition means: inserting the differential of the SG-compensator **240** between two equal stages of said reducer.

[0291] The elements of the SG-compensator **240** with the reducer of the gain are distributed on a gain bracket **232** FIGS. **48**A, **52** and **53**, which has a complex shape, is mounted on the mounting base **201a** of the flange **201** and fixed by the non-shown screws. The outer end of the gain inner shaft **216** has an additional support in a flanged bearing **233** inserted into the gain bracket **232**. A flanged bearing **257** shares a common hole with the flanged bearing **233** and supports the inner end of a gain outer shaft **255**, which entry is supported by a flanged bearing **258**, inserted into another hole of the gain bracket **232**. An outer reduction pinion **254** is fixed on the gain outer shaft **255**. A spacer **256** is dressed on the gain outer shaft **255** and is used for secondary axial support of this shaft. An inner reduction gear **234** is fixed on the gain inner shaft **216** and is meshed with an inner reduction pinion **235**, which is fixed on the a tail **238a** of an adapter **238**, providing to it the full rotation support together with flanged bearings **236** and **237** inserted into the end and entry holes of the gain bracket **232** for the tail **238a**, respectively. The inner reduction gear **234** consumes too much space in the direction toward the engine **300**, so the engine's body **301** has a clearance slot **301b** FIG. **44**B, in which the inner reduction gear **234** partially enters. An inner miter gear **239** is fixed in the adapter **238**. An outer reduction gear **247** supported on its hub by a bearing **248** FIG. **53**, inserted into the gain bracket **232,** and is meshed with the outer reduction pinion **254**. An outer miter gear **246** is fixed in the hub of the outer reduction gear **247**. An adapting ring **252** is inserted into a large hole of the gain bracket **232** and accommodates a flanged bearing **253**, which supports a compensating shaft **250**. Said large hole is created during drilling of the hole for the bearing **248** and is also used for setup. The flanged bearing **249** is inserted into the central hole of the outer reduction gear **247** and supports a tail **250a** of the compensating shaft **250**. A compensating gear **251** is fixed on the compensating shaft **250**, completing its axial support. The tail **250a** enters the central holes of an outer and inner miter gears **246** and **239** and can freely rotate inside these holes. A transverse shaft **242** has a rectangular body at its center and freely rotated intermediate miter gears **241** dressed on its ends, which are axially supported and fixed by washers **243** and E-rings **244**. The transverse shaft **242** with the intermediate miter gears **241** is being placed relative the inner and outer miter gears **239** and **246** in the meshing position to create a differential before installing the compensating shaft **250**. After this, the tail **250a** is inserted into the outer miter gear **246**, a central hole of the transverse shaft **242** and the inner miter gear **239**. After this, the tail **250a** is fixed in the central hole of the transverse shaft **242** by a set screw **245**, creating a spider of the completed differential. A compensating pinion **608** is fixed on the tail **221a** of the skew steering shaft **221**, which has an additional support in a flanged bearing **609** inserted into the gain bracket **232**. An intermediate gear **605** is meshed with the compensating pinion **608** and the compensating gear **251**, and is fixed on an intermediate shaft **606**, supported by a pair of flanged bearings **607**, inserted into the gain bracket **232**. The gain outer shaft **255** is last of the interfaces of the steering tier of the setup of the rotor **110**.

[0292] The presented SG-compensator **240** permits to compose the gain and skew values from the gain outer shaft **255** and the skew outer shaft **228**, respectively, to the gain and skew state of the rotor, but imply a strict mode of operation. This strict mode means: any non-rotating shaft either the gain outer shaft **255** or the skew outer shaft **228** must be in a hold on or locked state when the other rotates. Indeed, the differential of the SG-compensator imply mutual propagation of rotation from the gain shaft to the skew shaft and vice versa. The mechanical friction will diminish this effect, but nevertheless it will exist. Practically, this problem can be resolved upon using the electromechanical control of these shafts by servos of the gain and skew, which automatically compensate for any adverse deviation of the angular position of the respective shafts. But for the case of the pure mechanical handling, some mechanical elements must exist to lock the idle control shafts.

[0293] Referred to FIGS. **43**, **54** and **55**, the end-rotor support ring **260** has a flat surface from the side of the wings **111** and has a streamlined surface from the outer side with a bell-shaped profile. It is made of composite material and has equidistant holes related to the corresponding wings. Inside these holes are elements for connecting with wings **111**. Adapter flanges **262** are partially inserted into the holes of the support ring **260** and are fixed by screws **267** over their outer rings. A radial needle bearing **266** is inserted into each adapter flange **262** from the side of the support ring **260**. A tubular flange **263** is inserted into the radial needle bearing **266** from the side of the support ring **260**, and has a secondary thrust bearing **265** between its own flange and the adapter flange **262**. A washer **268** is placed next to the tubular flange **263**. The end-wing fairing **170** has a flat end-wing base **170b** FIG. **55**. And from this direction, it has an interior space used for its rotational mating with the adapter flange **262,** where a primary thrust bearing **264** is placed next to the adapting flange **262**. A bolt **261** is inserted from the outside, through the hole of the support ring **260**, into the washer **268**, the tubular flange **263** and the fairing **170**, where it is screwed into a corresponding threaded hole. Two set screws **269** fix the bolt **261** against unscrewing, using setup holes **170a** on both sides of the fairing **170**. A seal **270** from plastic closes the outer holes of the support ring **260** and is fixed by two screws **271** FIG. **55**. After this connection, a thin gap remains between the flat side of the support ring **260** and the end-wing base **170b** with the possibility of free rotation of the entire wing **111** supported against the free-end bend.

[0294] Referred to FIGS. **44**C and **56**, all three interfaces of the steering tier of the rotor setup: the outer shaft **195e** for the pitch from the FIG. **48**A, the gain outer shaft **255** and the skew outer shaft **228** are connected to related coupled shafts **274** of a PGS gearbox **280** by PGS couplings **259**. The PGS gearbox **280** is placed between the rotor socket **106** and the side force plate **290,** and its body **273** is fixed to the side force plate **290** by the non-shown screws. The rotor socket **106** has three windows **272**, which can be crossed by the PGS couplings **259**. During the rotor setup, the couplings **259** are dressed on the shafts **274** and lay loosely on PGS gearbox **280**. After the other tiers are secured, these couplings **259** are moved up and fixed on both sides on the respective shafts. Windows **292a**, **292b** and **292c** in the side force plate **290** are used for this operation for the pitch, gain and skew, respectively. The coupled shafts **274** of PGS gearbox **280** are supported by pairs of flanged bearings **275** on outside and inside the body **273** and are axially secured by locking hubs **276**. Vertical miter gears **281'** are mounted inside the PGS gearbox at the ends of the coupled shafts **274** in different vertical positions. Horizontal miter gears **281"** are meshed with the vertical miter gears **281'** and fixed on primary shafts **277**, **278** and **279** for the pitch, gain and skew, respectively. Each of these primary shafts is supported by a pair of flanged bearings **282** FIG. **44**C and has a non-shown locking hub too. Also, these primary shafts are tubular to be lightweight. The horizontal miter gear **281"** can be placed on its shaft on either side of the vertical miter gear **281'**. This permits to adjust the correct direction of rotation of any primary shaft on both sides of the aircraft **100**. Also, the construction of the right side rotor **110'** is exactly symmetrical to the left side rotor **110**, except for worms used for the PGS steering. On both rotors, they can be right-handed since the PGS gearbox makes it easy to adjust steering directions to control end use. Also, the construction of the SG-compensator is invariant for chirality of the worms, since it uses two worms in the compensating loop. They only need to have the same chirality. The body **273** of PGS gearbox **280** is open in the direction of the side force plate **290**, which has maintenance windows **291a**, **291b** and **291c** for the pitch, gain and skew, respectively. Separated sheets or a common sheet can close all the setup and maintenance windows after the respective operation.

[0295] Referred to FIGS. **44**F, **56** and **60**, secondary shafts **360**, **361** and **362** for the pitch, gain and skew are respectively connected to their respective primary shafts **277**, **278** and **279** by using universal joints **367** FIG. **56**. Also, the primary shafts near these joints have adapter tubes **277a**, **278a** and **279a** for the pitch, gain and skew, respectively, which are used to adapt the total length of both the primaries and secondary shafts. Those secondary shafts are referenced for the right side of the aircraft **100** as **360'**, **361'** and **362'** for the pitch, gain and skew, respectively. All the secondary shafts go towards a cockpit **440** FIG. **44**F. The right side secondary shafts are more inclined in the horizontal direction and utilize some holes or windows in the right side force plate **290**.

[0296] Referred to FIGS. **44**E and **56**, the elements of a locker **312** of the rotor **110** mounted on the engine **300**. The entire locker **312** is kind of a band brake, which is used on some bicycles, but adapted to have a precise control. A locker's drum **313** is mounted on the setup flange **302b** of the hollow shaft **302** using screws not shown. A locker's band **314** with a frictional lining **315** goes along the perimeter of the drum **313** at a certain distance when the locker **312** is in the unlocked state. Looking additionally at FIG. **57**, one end of the band **314** is dressed on an axle on the base **327**, which is mounted on the engine's lid **306** with screws **328**. Also, the end of the band **314** is fixed on the axle **327** with a washer **329** and a screw **330** from falling out. The other end of the band **314** is pivotally fixed on the end of a pull lever **317**, sharing a common pulling axle **316**. The pull lever **317** is fixed to its shaft **319** by a nut with washer **320** and can rotate together with the shaft **319** relative to its base **318** FIG. **56**, which is mounted on the engine's lid **306** with screws not shown. The other end of the pull lever **317** has an axle **323** inserted from the engine's side into the corresponding hole. A groove follower **324** is dressed on the axle **323** from another side of the lever **327** between two washers **325** FIG. **57** and is fixed together with the axle **323** by a screw **326** from falling out. A locker's main bracket **331** is mounted on the engine's lid **306** and fixed by four screws **332**. A locker's screw **335** is fixed on an outer locking shaft **336**, which is supported by a flanged bearing **337**, inserted in the lower side of the locker's main bracket **331**, and by two flanged bearings **338**, inserted in the upper side of the locker's main bracket **331**. A threaded lead **334** can move in the vertical direction during rotation of the locker's screw **335** inside it. A guide rod **333** is fixed on the locker's main bracket **331** parallel to the locker's screw **335** and is inserted into the corresponding hole of the threaded lead **334**, additionally aligning it during its movement. The threaded lead **334** has a slot or groove in which the groove follower **324** of the pull lever **317** is placed, and can be moved in the horizontal direction. Also, the threaded lead **334** has a thin slot from the direction of the pull lever **317**, in which the remained area of the end of the pull lever **317** that more than the diameter of the groove follower **324** can move freely for clearance or for an additional aligning of the pull lever **317**. A spring **321** FIG. **44**E constantly pushes the pull lever **317** upward to remove the backlash, and has a push support at the other end with a screw **322** that is screwed into the base **318**. It can be understood from the presented construction that rotation of the outer locking shaft **336** permits precision control of the lock state of the rotor **110**. A locking hub **339** is fixed on the outer locking shaft **336** over the top of the upper flanged bearing **338**, providing additional axial support. A miter gear **340** is fixed on the upper end of the outer locking shaft **336** and is oriented to down. It is used to link with the right side rotor's locker, and on the right side, it is placed in opposite bottom place, instead of the locking hub **339**.

[0297] Referred to FIGS. **44**E and **57**, a locker's link bracket **341** is mounted on the engine's lid **306** and is fixed by two screws with washers **342**. A side linking shaft **344** is supported by two flanged bearings **345** in the locker's link bracket **341**. A miter gear **343** is fixed on the inner end of the side linking shaft **344** and is meshed with the miter gear **340**. A locking hub **346** completes the axial support of the side linking shaft **344**. A locker link coupling **347** connects the side linking shaft **344** with a central linking shaft **348**, which is used for easy setup of the entire locker link.

[0298] Referred to FIGS. **44**F and **56**, a lock gears bracket **350** is mounted on the floor of the fuselage **101** using screws not shown. The end of the outer locking shaft **336** enters to the lock gears bracket **350** from top and is supported by a flanged bearing **351**. A miter gear **352** is fixed on the end of the outer locking shaft **336** and is meshed with a miter gear **353**, which is fixed on a primary lock shaft **354**. The primary lock shaft **354** is supported in two non-designated flanged bearings inside the lock gear bracket **350** and has an additional axial support by a locking hub **356** FIG. **56**, fixed on it. Also, the primary lock shaft **354** significantly protrudes to the back, permitting to place the miter gear **353** on the opposite side to adjust the rotation of the lock shaft **354** in the correct direction upon changing it on the control side.

[0299] Referred to FIGS. **44**F and **60**, a secondary lock shaft **357** is connected to the primary lock shaft **354** by a universal joint **367**, like as similar connections for the PGS controls. On the way towards the cockpit **440**, the secondary lock shaft **357** passes through a hole **299a** in a stand **299** of the pilot seat **289**.

[0300] Referred to FIG. **59**, a stabilator worm gear **376** resides inside the fuselage **101** under the vertical stabilizer **109a** and is fixed on a stabilator pivot shaft **375**, which connects two stabilators **102** together. A stabilator worm bracket **377** is mounted on an aft support **382** and a forward support **383** on the floor of the fuselage **101** parallel to the floor under the stabilator worm gear **376**. A stabilator steering shaft **378** is supported at its end by a flanged bearing **381** inserted into the stabilator worm bracket **377**. The entry of the stabilator steering shaft **378** is supported by a non-shown bearing inside the stabilator worm bracket **377**. A stabilator worm **379** is fixed on the stabilator steering shaft **378** and meshed with the stabilator worm gear **376**. A spacer **380** is dressed on the stabilator steering shaft **378**, completing its axial fixation. A primary stabilator pitch shaft **373** is connected to the stabilator steering shaft **378** by a universal joint **374**, having near it an adapter tube **373a**. Additionally to the presented construction, the stabilator worm bracket **377** can be extended to accept an additional support from the stabilator pivot shaft **375** to prevent changing the axial distance between the stabilator worm gear **376** and the stabilator worm **379** under deformation of the fuselage, induced by the forces from the stabilators. In this case, rubber washers should be inserted between the stabilator worm bracket **377** and both supports **382** and **383**.

[0301] Referred to FIG. **56**, a stabilator pitch (SP) conducting bracket **368** is mounted on the floor of the fuselage **101** near of the aft vicinity of the floor horizontal segment and a bit shifted toward the left side of the fuselage **101** from its centerline. An SP conducting connector **369** is supported by two non-designated flanged bearings inside the SP conducting bracket **368** and is axially secured by a locking hub **370** fixed on its tail **369a**. A universal joint **372** is connected to the primary stabilator pitch shaft **373** from one side and is inserted into the SP conducting connector **369** from the other side, where it is fixed. A universal joint **371** connects the tail **369a** of the SP conducting connector **369** to a secondary stabilator pitch shaft **358**, which passes towards the cockpit **440**, see FIG. **44**F also.

[0302] The parking support **384** is placed on each side of the presented aircraft and occupies the interior space near the aft vicinity of the rotor's socket **106** outside the inner level in the axial direction of the engine **300**. It can be retracted or put out upon respective rotation of a retracting screw **389**, which is screwed inside a related threaded complement placed inside the parking support **384** made from a high diameter tube of a lightweight alloy. The lower end **384a** of the parking support **384** is slotted and is rounded, and permits to insert into this slot the parking wheel **385** freely rotated on an axle **386**. A keying rib **387** is fixedly attached to the aft side of the parking support **384**, and prevents the rotation due to a corresponding slot in a guide **388**, in which the parking support **384** can slippery move that is fixed to the fuselage **101**. A heel **390** is fixed on the upper side of the fuselage **101**, permits a free rotation of the retracting screw **389** in it and secures the retracting screw **389** from falling out. A retracting gear **391** is fixed on the non-threaded segment of the retracting screw **389** and is meshed with a retracting pinion **392** of a retract servo **393**. A parking hatch **394** can be opened by the parking wheel **385** itself when the parking support **384** is lowering, and its shape exactly corresponds to the shape of the opened window, allowing a level of sealing enough for pressurizing. This ability is permitted by the related level of the pivot system of the hatch **394**, which is detailed in FIG. **58**. An outer and inner side segmented saddles **398** and **398'** are respectively mounted on the fuselage **101** and each has inside a segmented pivot **401**, which is fixed to the related side of the parking hatch **394** and can rotationally move inside the interior of this saddle. These segmented pivots **401** are additionally secured by related radial washers **402** with screws **403**, which are inserted into slots **398a** and are screwed into these segmented pivots **401**. A lever **400** is mounted on the hatch **394** and is used for retracting the hatch **394** by a spring **397**, pivotally connected to an axle **399** at the end of the lever **400**. The other end of the spring **397** is pivotally fixed on a support **396** mounted on the fuselage **101**. The shape and position of the outer end of the retracting hatch **394** optimally corresponds to the tubular shape of the parking support **384** and to the toroidal shape of the parking wheel **385**, for that retracting operation. This begins with slipping the end of the parking hatch **394** over the forward-outer side of the parking support **384** and smoothly moves to the forward outer side of the parking wheel **385**. At this point, the parking wheel **385** begins to rotate, instead of the problematic slipping, until the entire wheel **385** will over the hatch **394**, and so the entire retracting is performed without obstructions. An electromechanical latch **395** is mounted inside the fuselage **101**, near the aft vicinity of the parking hatch **394**, and secures the closed state of the parking hatch **394**.

[0303] Referred to FIG. **56**, the main part of accumulators **437** FIG. **76** of aircraft **100** is placed on two racks **404** FIG. **56** and **404'** FIG. **76** on each side of the aircraft **100**. The accumulators **437** are fixed on shelves **405**, but they aren't shown, due to the target of presenting other elements of the aircraft’s interior. Additionally, the aircraft **100** has a place for accumulators in its forward compartment along the forward walls. FIG. **44**F provides an example of it for nose side accumulators **349**. This position of the accumulators permits to shift the center of gravity to forward, which is desirable, since it will decrease the moment compensating force provided by the stabilators **102** operating in a partial downwash. Additionally, each accumulator rack can be moved in flight or before that in the longitudinal direction. This allows to alleviate the moment changing due to the variability of the aircraft's load that can shift the required operating range for the stabilators beyond the allowable limits during takeoff or during the cruise. Also, this can be used as assistance for the stabilators to optimize performance.

[0304] Referred to FIG. **56**, the accumulator rack **404** is placed on two saddles **406** that are placed relative the axis of the rotor **110** in a position that allows the rack **404** to be very close to the elements of the rotor's locker **312** without obstruction while sliding on the saddles **406**. The saddles **406** are mounted on aft supports **407** and forward supports **408**, which are fixed to the fuselage **101**. A bottom sliding plate **409** is fixed to the rack **404** and secures it from falling out from the saddles **406**. A threaded rib **416** is mounted on the forward end of the bottom sliding plate **409**. A screw **410** can move the rack **404** while rotates. A forward support **411** for the screw **410** is mounted between the pair of the forward supports **408** and is fixed to them using screws **417**. An aft support **412** for the screw **410** is attached to the inclined floor of the fuselage **101**. A rack moving gear **413** is fixed on the screw **410** near the aft support **412** and is meshed with a rack moving pinion **414** of a rack moving servo **415**, mounted on the floor of the fuselage **101**. A rack position encoder **418** is rotatably connected at its entry to the shaft of the screw **410** protruded from the forward side of the forward support **411** and is mounted on the bottom side of one or both saddles **410**.

[0305] The presented implementation of the movable rack **404** for accumulators **437**, it can be optionally modified to have only three shelves **405** in the vertical direction, lowering the center of gravity, but be two times longer, since this is permitted by the clearance in the presented implementation. In this case, it can be 40 percent thinner in the axial direction, increasing the cargo space between the rotors. Also, the longitudinal movement can be increased to better alleviate the moment issue.

[0306] Referred to FIG. **44**F, a nose wheel node **286** is mounted on the forward floor of the fuselage **101**, and the nose support fork with damper **287** FIG. **43** is connected to it. A sensors port **363** is mounted inside the nose of the fuselage, having the PST **576** and the SDT **580** is connected to it from the outside, see FIG. **43**. A pitot pressure hose **364**, a static pressure hose **364'**, an upward pressure hose **365** and a downward pressure hose **365'** are connected to the sensors port **363** and pass toward the cockpit **440**. Also, the sensors port **363** has a socket in its center to which a pair of electrical wires **366** for the anti-icing heaters of the PST and SDT from the cockpit **440** is connected.

[0307] Referred to FIG. **60**, all secondary control shafts: **360**, **361**, **362**, **360'**, **361'**, **362'**, **357** and **358** are connected to diverters: **419**, **420**, **421**, **419'**, **420'**, **421'**, **422** and **423**, respectively. Here, each diverter, for example the left gain diverter **420**, is a box having inside a pair of meshed miter gears on shafts supported by related bearings, which has outside an horizontal universal joint **420a** and a vertical universal joint **420b**. So, the secondary shaft of the left gain **361** is connected to the horizontal universal joint **420a**, and the vertical universal joint **420b** is used for linking to an upper universal joint **435** mounted on an exit shaft **512** FIG. **66** of the respective trimmer of the cockpit **440**. And so, linking shafts **430**, **431**, **432**, **430'**, **431'**, **432'**, **433** and **434** connect the diverters **419**, **420**, **421**, **419'**, **420'**, **421'**, **422** and **423** to the related upper universal joints **435**, respectively. The inner shaft of each horizontal universal joint passes through its diverter and is rotatably connected to a related encoder mounted on the diverter or fuselage. So, the diverters **419**, **420**, **421**, **419'**, **420'**, **421'**, **422** and **423** are rotatably connected to the encoders **424**, **425**, **426**, **424'**, **425'**, **426'**, **427** and **428**, respectively. A left pedal **429** and a right pedal **429'** are placed under the cockpit **440** and are connected by respective wires **359** and **359'** to the rudder **109** FIG. **43**, see also FIG. **44**F. Some non-shown pulleys are used to conduct the wires **359** and **359'**. The connectivity and use of the rudder pedals **429** and **429'** are the same as for a conventional airplane.

[0308] Referred to FIG. **61**, the cockpit **440** has two main domains: an indicator panel **441**, which has generally a vertical orientation, and a control panel **442**, which is tilted by about 45 degrees. A display **445** of a central computer **600** FIG. **76** is placed on the indicator panel **441** under an anti-glare guard **446** and is inclined on a pivot toward this guard **446** at some angle. A CP-switch **447** is placed on the indicator panel **441** and is used to manage the power state of the components of the Control Panel **442**. An EC-switch **448** is placed on the indicator panel **441** and is used to manage the power state of an Engine Controller **597** FIG. **76**. A WSA-indicator **449** is placed on the indicator panel **441** and is used to indicate of the actual winding speed of the rotors **110** and **110'** by the engine controller **597**. An RPM-indicator **450** is placed on the indicator panel **441** and is used to indicate of the RPM of the rotors **110** and **110'** by the engine controller **597**. An MR-indicator **451** is placed on the indicator panel **441** and is used to indicate of the Moment Ratio (external) on the common powering shaft **127** FIG. **76** by the engine controller **597**, with uses some preset value of the entire weight of the aircraft **100** as the value of the MR normalization.

[0309] A CM-switch **452** is placed on the control panel **442** and is used to enable the Computer Management over all trimmers of the control panel **442**. An SF-switch **453** is placed on the control panel **442** and is used to enable the automatic Stream Following mode by using the operation of the stabilators **102** FIG. **76** from the side of a stabilator controller **579** FIG. **76**.

[0310] The control panel **442** contains a number of trimmers, which are used for control and indication of the controllable mechanical features of the aircraft **100**. These features include: the each side PGS-state, the target winding speed (WST) of the rotors, the stabilator pitch (SP) and the lock state of the rotors. These trimmers are mounted under the control panel **442** and are closed by a cover **443** along the sides of the control panel **442** and their bottoms, together with the other elements of the control panel **442**, see FIG. **66** also. The trimmers for the PGS-state are placed symmetrically for the pilot. The Pitch-trimmers **454** and **454'** are placed on the inner lower part of the left and right sides, respectively. The Skew-trimmers **456** and **456'** are placed on the inner upper part of the left and right sides, respectively. The Gain-trimmers **459** and **459'** are placed on the outer, middle part of the height of the left and right sides, respectively. The meaning of this placement for the Gain-trimmers is to reflect the maximal impact of the gain change on the turns operations. The WST-trimmer **462** is placed on the right side under the WSA-indicator **449**. The SP-trimmer **464** is placed at a middle height of the right side above the SF-switch **453**, which turning on inserts the SP-trimmer **464** into the automatic controlled loop. Also, here is a Stream Deviation Indicator (SDI) **468**, under the SP-trimmer **464**, which can assist in the case of a manual handling of the SP-trimmer **464** or can be used to indicate the efficiency of the automatic controlled loop. A Lock-trimmer **466** is placed on the remained bottom medial right side. The manual handling of each trimmer is allowed by a retractable handle **490**, which can directly rotate the face side of the trimmer, see FIG. **66** also. Exactly the same rotation of the face side of each trimmer with its handle **490** is performed in case of non-manual handling. So, the face side of each trimmer is located under the face level of the control panel **442**, including also the handle **490**. This resolves a possible obstruction problem for the pilot, since the self-rotating of the handle **490** over the level of the control panel **442** can be dangerous.

[0311] The handling value of each trimmer can be changed by using a pair of buttons close to it, where the lower button is used to decrease this value with some speed, and the upper button is used to increase it with the same speed. The buttons **455** and **455'** change the values of the pitch-trimmers **454** and **454'**, respectively. The buttons **457** and **457'** change the values of the skew-trimmers **456** and **456'**, respectively. The buttons **460** and **460'** change values of the gain-trimmers **459** and **459'**, respectively. The buttons **463**, **465** and **467** change values of the WST-trimmer **462**, SP-trimmer **464** and lock-trimmer **466**, respectively. The orientation of the buttons for changing the pitch and gain isn't vertical. Their inclinations reflect the impact of the related feature on the turns operations during the normal turn mode, which includes the cruise, see the explanation to FIG. **42**. This impact is moderate for the pitch and high for the gain. Also, the directions of these inclinations reflect the normal turn mode. For example, the inclination of the left gain buttons hints: "press the leftmost button of the left gain to turn to left". Also, this turn action should be accompanied by pressing the opposite button of the other side gain, pointing for this example to "the leftmost of the right gain" button.

[0312] The gain and skew trimmers must have abilities for the strict handling, as it was mentioned upon describing the SG-compensator **240**. So they have special locking knobs on their upper outer sides. The locking knobs **458** and **458'** belong to the skew-trimmers **456** and **456'**, respectively. The locking knobs **461** and **461'** belong to the gain-trimmers **459** and **459'**, respectively. In the case of the computer-managed handling, the impact of these locking knobs is irrelevant. But, in the case of the manual handling, the locking knob of each required to be locked trimmer should be rotated to a locking position, which is indicated by the letter "L" near a tick of the exact position. And, in case of non-manual handling without the computer management, any locking knob should be in the locking position, it will be unlocked automatically. Also, each locking knob fixes its normal or locking position with some force, but it doesn't fix its intermediate position.

[0313] A joystick pad **444** is mounted some below the upper level of the control panel **442** on its concave support **444a**, which corresponds to the central concave rim of the control panel **442**. It has a joystick **477** mounted in its center and other controls, see FIG. **62** also. Pairs of the buttons of common controls are placed in forward of the joystick **477**. These pairs are: a common pitch **472**, a common gain **473** and a common skew **474**. Here, the upper buttons increase the related value for both rotors, and the lower buttons decrease it. An HS-button **475** is placed between the pairs of the common pitch and common skew buttons. When the button is pressed, the both side trimmers of the pitch and skew will be operated with a High Speed of change if appropriate change commands are presented. This high-speed feature is required during the beginning and finalizing the aerial braking on the runway, when the pitch and the skew are drastically changed simultaneously, see FIG. **40**T and FIG. **40**U. An S->P-switch **476** is placed on the right side wall of the pad **444**. It enables for the pitch-trimmers to follow with the same speed and direction after the changes of the skew-trimmers, so only the common skew buttons **474** can be used. This feature services all runway operations, and also was referenced as a "propelling" mode; see FIGS. **24**A, **39** and **40**A.

[0314] The buttons for side based differential operations are placed on respective sides of the central symmetry line of the control panel **442**. These differential buttons for the pitch are P-buttons **469** and **469'** for the left and right side, respectively. Similar buttons for the gain are G-buttons **470** and **470'**. And, for the skew, these are S-buttons **471** and **471'**. Pressing of each of these buttons will decrease the related value on the side where the button was pressed, and increase the related value on the other side. The decreasing was selected, because decreased values for the pitch and gain are required for the inner side of the normal mode turn. The P-buttons and the G-buttons service the turns operations in a more convenient way than the paired buttons of the trimmers. And, the S-buttons are placed here for completeness. All these buttons reflect their "decreasing" action by having a shape with a narrowed end below. Additionally, the P-buttons and the G-buttons have a side-pointing shift of the lower end and an increased high those reflect their impact on the turns ability.

[0315] Prior to this point, all described handling buttons were designed for operation without using the computer-managed handling, i.e. the CM-switch **452** should be in the "OFF" position for that. In this mode, only a simple electromechanical logic is used for their respective variations. This provides an additional level of redundancy, in addition to the computer-managed handling. And, the manual handling of the trimmers is the third, lowest level of redundancy. This architecture was selected, because the presented aircraft is experimental, and all tiers of its entire handling pipeline must be researched and optimized. But, for the end user aircraft, some redundancy levels can be simplified or eliminated, leaving a more simplified aircraft handling interface, like as the only components of the computer-managed handling.

[0316] Elements of the computer-managed handling are placed directly under the display **445** and additionally include the joystick **477** with a capture button **478** FIG. **62** on its top. This capture button **478** is used to enable the joystick **477** and store its initial position with the initial values of controlled features as a reference point for handling further deviations of the joystick **477** from this initial position. And so, the handling of the presented aircraft with the joystick is generally variational, which permits to accommodate very wide operative ranges of handling features, maintaining a high variation accuracy for particular operations, for the pilot friendly convenient handling. For a simplest use of this handling, computer can sophisticatedly interpret the spatial motion of the joystick for the spatial and kinematic evolution of the aircraft. Also, the kinds of such interpretation can be flexible parameterized and selected on demand of the pilot for the different operations.

[0317] A pad of the common handling **479** is placed in the center under the display **445** and has four pairs of buttons, where the upper buttons increase respective values and the lower buttons decrease them. Here, S-buttons manage the skew, O-buttons manage the opposite value of the biangular control, M-buttons manage the main value of the biangular control and G-buttons manage the difference between the main and opposite values of the biangular control, the variations of which at low gain in the pitch-mode of the biangular control are very close to the variations of the gain of the PGS-state. So, this parameter can be considered as a high-level gain or biangular gain, and the G-button is placed between the O-button and the M-button to reflect its differential nature. All these SOGM-buttons manage the respective parameters for the rotors on both sides simultaneously, which is reflected in the word "common" in the name of the pad **479**.

[0318] A pad of the in turn handling **480** is placed on the right side from the pad of the common handling **479**. It has in its center a C-letter inside of a G-letter. The G-letter is connected by diagonal lines to the buttons in four corners of the pad **480**. These corner buttons are used to manage biangular gain, similar to the G-buttons **470** and **470'**. Here, the bottom corner buttons decrease the biangular gain value for the side where this button was pressed and simultaneously increase this value for the opposite side. These bottom corner buttons are used in the normal mode of the turns operations. The variation of the biangular gain for turns on the cruise operation can be simply deduced looking at the table in FIG. **42**. It has the same sign as the variation of the gain of the PGS-state and is a bit higher. And so, the logic for turns that use biangular gain is the same as for low-level gain. This is also reflected in the down directed arrow signs pictured on the lower corner buttons. The upper corner buttons are used in the case of inverted mode of turns, which is applicable for much of operations during descent of the presented aircraft. Some kind of a high-level pitch can be defined for the biangular mode, like as it was introduced for the high-level gain. It will be simply an average value of the opposite and main angle. But, I don't use the word "pitch" for this parameter. It is better to use the word "collective" for each side rotor, like it is used for the rotor of a helicopter, since the word has more universal meaning for both modes of biangular handling, like as the word "gain". So, the C-letter in the center of the pad **480** hints to the word "collective", like the G-letter hints to the word "gain". The buttons on the center of the side of the pad **480** are used to decrease the collective angle of the rotor on the side where the button was pressed and to increase on the opposite side, and it is reflected in the down directed signs of arrow pictured on them. This is OK for the normal mode of turns, but for the inverted mode, other buttons are required here for the intuitive handling, similar to the upper corner buttons used for gain. Such buttons can be added to each respective side of the pad **480**, but there is another way for this intuitive handling. Instead of looking for the opposite direction buttons, which yet require some switch in thinking, better is to begin thinking about the normal mode of turns as be managed by inside turn controls, and about the inverted mode of turns as be managed by outside turn controls. So, the buttons on the lower corner and the center of the side of the pad **480** from the out turn side can be used to initiate such a turn. The center upper button on the pad **480** increases the collective angles for both rotors simultaneously, and it can be used to assist in a coordinated turn, reducing inner slip in the turn when entering the turn. Similarly, the center bottom button on the pad **480** decreases the collective angles for both rotors simultaneously, and it can be used to assist in a coordinated turn, balancing against having an outer slip and to exit a turn. These two vertical buttons of the pad **480** can also be used without a connection with a turn. They can be considered as a complement to the four common handling pairs of buttons of the pad **479** as the fifth pair of C-buttons for the common handling of collective angles.

[0319] WS-buttons **481** are simply a computer processing equivalent of the pair of WST buttons, which is placed in a more convenient place. An L-button **482** is simply a button for a lock command. Without this button, the lock of the rotors will be performed when two conditions will be met altogether. The first condition is the presence of the WST equal to zero (with some error range, of course). The second condition is the presence of the magnitude of the actual winding speed (WSA) below some threshold; see **S36D2** in FIG. **36**D. And, the L-button **482** only sends a command to reset the WST value with a speed of the natural rotation of the servo of the WST-trimmer **462**. This finite speed of rotation of the WST-trimmer additionally prevents to perform a too fast lock, which can induce a very high moment on the rotors shaft **127** and on related elements. Also, the use of the WS-buttons **481** is subject to this WST change rate limitation.

[0320] An extended command pad **483** is used to select particular commands by the pilot. They can include particular customizations of the control buttons and joystick for particular flight operations, any switches for display's **445** representations or any other commands. Also, the display **445** can be touch-sensitive.

[0321] The indicator panel **441** has also standard instruments, which can assist the information on the display **445** or can be used independently, especially as standby instruments. These instruments currently selected as: an Attitude Indicator (AI) **484**, an AirSpeed Indicator (ASI) **485**, an altimeter **486**, a compass **487**, a Turn and Slip Indicator (TSI) **488** and a Vertical Speed Indicator (VSI) **489**. The indicated speed (IAS) of the airspeed indicator **485** will be proportional to the LASN, which only subtly varies during normal flight over a wide range of the operating altitudes, see FIGS. **40**F through **40**K. And so, the airspeed indicator **485** well suits for the standby instrument to control the presented aircraft.

[0322] Designing trimmers for control of the presented aircraft isn't a simple task, since there is requirement to handle values in a wide dynamic range, controlling them with a high precision. More than, they are bidirectional and can change their signs. The internal construction of these trimmers is mainly originated from the design of the placement of their scales.

[0323] Referred to FIG. **63**, each trimmer, for example the pitch-trimmer **454**, has a handle **490** that passes through a ring **508** retaining a glass and a primary rotating can **491** on which this ring **508** is fixed. The primary rotating can **491** can be rotated over its center axis altogether with the retaining ring **508** and a glass lid **530**, see FIG. **66** also. The primary rotating can **491** can also be referenced as a handling can. It has a continuation inside as a rotating fine scale **491a**. The fine scale **491a** has 5 degrees range on its full turn, tics distance of 0.1 degrees and labeled tics distance of 0.5 degrees. Also, all labels on the fine scale have a negative sign, including a zero value, which means that the scale is used only for negative pitch values. The positive direction of rotation for all trimmers is counter clockwise with the origin on the right, which is known as the mathematical convention for angular reference. For this direction, for positive pitch values, the rotating fine scale is used only as an arrow. The wedged frame around the "-0" value represents the position of this arrow. It coincides with the position of the center of the handle **490**. The arrow of the rotating fine scale **491a** points to a neighbor steady fine scale **492**, which is placed inside the rotating fine scale **491a**. The steady fine scale **492** is equal to the rotating fine scale **491a**, but has only positive values and the horizontal orientation of all labels. Also, the arrow sign near the "0" value indicates the arrow position, which is used to read values from the rotating fine scale **491a** in the case of a negative pitch. The rotating fine scale **491a** has a center orientation of all labels, so each its label will be in the horizontal orientation against of the arrow of the steady fine scale **492**. A rotating intermediate scale **493** is placed inside the steady fine scale **492**. It has 60 degrees of its full turn and services the negative pitch and has a positive arrow, similarly as that does the rotating fine scale **491a**. A steady shield **494** is placed inside the rotating intermediate scale **493**. A steady intermediate scale **494b** is located along outer perimeter of the steady shield **494** and is equal to the rotating intermediate scale **493**, except for the sign of the labels and their orientation, similarly as this exists on the steady fine scale **492**. Also, its labels are much larger than for the rotating intermediate scale **493** and are the largest of all scales. A general scale **494a** is located around the inner side (hole) of the steady shield **494**. It has a dynamic range from -180 degrees to 180 degrees and occupies the entire circle. And so, this trimmer can be considered limitless, although practically this feature is not used and has a meaning only for some taxi operations. A generic rotating arrow shield **495** is placed inside the steady shield **494** and has a large arrow, which points to the actual value of pitch in the general scale **494a**. This generic rotating arrow shield **495** is in use for all PGS trimmers and the WST-trimmer **462**. The steady shield **494** has an identifier of the kind of this trimmer as a big letter "P" placed between the zero values of the general scale **494a** and the steady intermediate scale **494b**, which means: "Pitch". And so, this trimmer can also be referenced as a P-trimmer. Also, the steady shield **494** has a designation of the unit in which the values of the pitch-trimmer **454** are measured, as a degree-sign "°" in its center up.

[0324] The skew-trimmer **456** is equal to the pitch-trimmer **454**, except for its steady shield **494'**, which has an identifier as a big letter "S", which means: "Skew". And so, this trimmer can also be referenced as an S-trimmer.

[0325] The gain-trimmer **459** generally has a similar design as the P-trimmer, but differs in particular scales and has an additional features. The main difference between this trimmer is the unit of values. Instead of degrees, which are non-linearly mapped to the linear rotation space, the trimmer uses the normalized linear gain, see FIG. **20**, which magnitude has a maximal value of 1.0. And so, the percent units are used for this trimmer, which is indicated by the sign "%" on a steady shield of gain **498**. A general scale of gain **498a** has a dynamic range from -100% to 100%, and it occupies only about two thirds of the half turn in each direction. A steady intermediate scale of gain **498b** has a full turn range of 50%, as well as a rotating intermediate scale of gain **497** has the same. A rotating fine scale of gain **491b** has a tics distance 0.1%, labeled tics distance 1% and range of full turn of 10%, as well as a steady fine scale of gain **496** has the same. Windows **498c** and **498d** in the steady shield of gain **498** indicate values of the pitch deviation in the main and opposite directions, respectively, see FIG. **19** also. Reading values from these windows is performed by thin arrows against their centers, which is accompanied by degree signs "°" and arrows to the respective directions. Here, the degree sign means: these windows perform a non-linear mapping from the linear rotation space to the degrees deviation space, and the entire gain can be calculated as the difference between the main and opposite value. The windows of this type, such as **498c** and **498d**, are known in cockpit instrumentation as "Kollsman windows". They are used in altimeters to indicate atmospheric pressure. A main pitch deviation scale **500a** that is shown inside the window **498c**, and an opposite pitch deviation scale **500b** that is shown inside the window **498d** are located on a rotating flange **500**, on which the generic rotating arrow shield **495** is mounted. This composed element is shown on the upper-right from the scale placement of the gain trimmer **459**, see also FIG. **68**. Optionally, there can be a variant of the gain-trimmer, where only one such window exists to indicate the entire gain. The steady shield of gain **498** has an identifier as a big letter "G", which means: "Gain". And so, this trimmer can also be referenced as a G-trimmer.

[0326] The WST-trimmer **462** has a similar design as the P-trimmer, but differs in particular scales. The main difference between this trimmer is the unit of values. Instead of degrees it uses the "meters per second", which is indicated as "m/s" on a steady shield of WST **502**. Also, it has an identifier as letters "WS" with a letter "T" under them, which means: "Winding Speed Target". A general scale of WST **502a** has a dynamic range from -20m/s to 40m/s, and it doesn't occupy the full turn. A steady intermediate scale of WST **502b** has a full turn range of 20m/s, as well as a rotating intermediate scale of WST **501** has the same. A rotating fine scale of WST **491c** has a tics distance 0.02m/s, labeled tics distance 0.2m/s and range of full turn of 2m/s, as well as a steady fine scale of WST **499** has the same.

[0327] The SP-trimmer **464** has a design significantly differed from the P-trimmer. It has exactly the same rotating fine scale **491a** as for the P-trimmer, as well as a steady fine scale **503b** with the corresponding placement from that trimmer. But, the steady fine scale **503b** isn't isolated. It is located along the outer perimeter of a steady shield of SP **503**, which has a much larger diameter than the steady shield of pitch **494**. And so, the intermediate scale is missing in the SP-trimmer **464**. A general scale of SP **503a** is located along the inner perimeter of the steady shield of SP **503**. It has a dynamic range from -30° to 30° and it doesn't occupy the full turn. The identifier of this trimmer is located above the left side of the steady shield **503** as letters "SP", which means: "Stabilator Pitch". A rotating arrow shield of SP **504** is placed inside the steady shield **503** and has a large arrow, which points to the actual value of SP in the general scale **503a**. A rotating shield **505** of the stabilator actual position is placed inside the rotating arrow shield of SP **504**. It has an image of airfoil painted on it, so this "airfoil" has exactly the same natural angle relative to the horizontal level of the indicator, as it has the stabilator **102** relative to the fuselage **101**.

[0328] The lock-trimmer **466** looks as a simplified version of the SP-trimmer. Its rotating arrow shield **507** has the same size as the rotating arrow shield of SP **504**, but it doesn't have a hole inside. Also, its rotating fine scale **491d** is wider than for the other trimmers, consuming the reduced width of a steady shield of lock **506**, which has on its left side a trimmer identifier as a letter "L", which means: "Lock". And so, this trimmer can also be referenced as an L-trimmer. The unit of values for the L-trimmer is percent, which is reflected by the "%" sign above the identifier letter "L". Here, the zero value corresponds to the state, when the bands **314** of the lockers **312** touch by their frictional linings **315** the related drums **313**, see FIG. **44**E. A general scale of lock **506a** has a dynamic range from -20% to 100% and it doesn't occupy the full turn. The rotating fine scale of lock **491d** has a tics distance 1%, labeled tics distance 2% and range of full turn of 20%, as well as a steady fine scale of lock **506b** has the same.

[0329] The stream deviation indicator **468** FIG. **64** is simply an airspeed indicator modified to have the ability of bi-directional indication. Its arrow **627** is repositioned to the left side to the zero position, and its scale doesn't have a unit of indication. A set of symmetrical tics is placed from the zero position up to 90 degrees up and down. Here, the upper direction means: "stream goes more from the upper direction in respect of fuselage". And for normal operation, its arrow **627** should be close to the zero position. It has an identifier "SDI" under the axis of the arrow **627**.

[0330] Although the scales of all trimmers and SDI were presented as black on a white background, they should actually be luminous on a black background, as is usual for other instruments in the cockpit.

[0331] Before proceeding to the description of the internal construction of the trimmers, let's look at the placement of their underneath transmissions, which have some common elements. Their placement views are taken from the face direction and are represented in FIGS. **65**A through **65**D. The PGS trimmers on each side are combined in a common PGS trimmer block **510** FIG. **65**A. This combination permits a more compact placement of the trimmers on the control panel **442**. The PGS trimmer block **510** has a case **509** made of a lightweight alloy and fixed to the control panel **442** with screws not shown, which are located on the middles of the bridging areas of each pair of the adjacent trimmers toward the outside. Each trimmer has its own primary shaft **511**, which enters into its interior. Each trimmer composition with its underneath transmission has a related exit shaft **512**, which exits toward its controlled element. In the current design for all trimmers, except for the S-trimmers **456** and **456'**, the primary shaft **511** is simultaneously the exit shaft **512**, but that can be changed under particular circumstances. The exit shaft **512** of any trimmer has an exit gear **513**, fixed on it, which accepts movement from an intermediate gear **515**, meshed with it. Servos **518** provide electromechanical movement for all trimmers except the WST-trimmer **462**. The controlled element of that trimmer is only a WST encoder **436** FIG. **65**B, mounted under the WST-trimmer **462** and requiring only low power for its rotation. So, a mini-servo **520** is used for the WST-trimmer **462**. The servo **518** or the mini-servo **520** for all trimmers, except for the S-trimmers **456** and **456'**, has a servo gear **514** fixed on its shaft and meshed with the intermediate gear **515**. Each S-trimmer **456** or **456'** has on the shaft of its servo **518** a much smaller servo pinion **517,** instead of the servo gear **514**. An external primary pinion **516** is fixed on the primary shaft **511** of each S-trimmer **456** or **456'** and is meshed with the exit gear **513**. This difference in the transmissions of the S-trimmer **456** reflects the need for equal angular speed of changing the pitch and skew for both power-tiers of this movement: from servos or from manual handling of the trimmers. Trimmer's locking brackets **556** FIG. **65**A are mounted on the bottom outer sides of the S-trimmers **456** and **456'** and G-trimmers **459** and **459'**, see FIG. **67** also. Locking knob's brackets **564** are mounted above the trimmer's locking brackets **556** under the control panel **442** and have handles **566** above the face level of the control panel **442**, which vicinity is referenced in representing the skew locking knobs **458** and **458'** and gain locking knobs **461** and **461'**. Each individual trimmer is represented in FIGS. **65**B through **65**D has a case **519** made of a lightweight alloy and is attached to the control panel **442** with screws not shown, which are located above the non-shown extensions on the periphery of the case **519**.

[0332] The trimmers have some common elements in their constructions. Let's look at the construction of the P-trimmer **454** FIG. **66** as a reference point for other trimmers. The servo **518** is mounted on a bottom **509a** of the case **509** of the PGS trimmers block at some distance using supports **522**. The intermediate gear **515** is supported by two flanged bearings **524**, which are placed on the axle **523** and are fixed together by screw **525** to the bottom **509a** of the case **509**. The servo gear **514** is fixed on a shaft **521** of the servo **518** and is meshed with the intermediate gear **515**. The primary shaft **511** is supported by two flanged bearings **535** inserted into the bottom **509a** of the case **509**. A primary pinion **534** is mounted on the inside end of the primary shaft **511** and provides it with one-way axial support. The exit gear **513** is fixed on the primary shaft **511**, meshes with the intermediate gear **515** and completes the axial support of the primary shaft **511**. The upper universal joint **435** is fixed on the outer end of the primary shaft **511**, which acts here as the exit shafts **512** and consumes a corresponding hole in the cover **443** made of plastic. The other end of the upper universal joint is fixed on the linking shaft **430**. The glass lid **530** lies inside a corresponding socket of the primary rotating can **491** on a rubber ring **529** and is secured by the retaining ring **508**. The handle **490** is inserted through holes in the retaining ring **508** and the primary rotating can **491** into a non-obstructed space between the walls of the case **509** and the primary rotating can **491**. A tube **526** is dressed on a tail **490a** of the handle **490**, can freely rotate on it and is secured with a washer **527** and a screw **528** from falling out. When the handler **490** is pulled out, the tube **526** retains it by some friction forces inside of the corresponding hole of the primary rotating can **491**, which also allows the handle **490** not to rotate in the pilot's fingers. Also, the washer **527** prevents detaching the handle **490** from the trimmer.

[0333] A central axle **509b** is located in the center of the bottom **509a** as its integral part. The primary rotating can **491** is supported by two bearings **531** dressed on the central axle **509b** and separated from each other on their insides by a spacer ring **532**. Also, one of the bearings **531** is inserted from the inside of the primary rotating can **491**, and the other is inserted from its outside, so they are separated on their outsides by a small inner ring area of the rotating can **491**, which axial thickness is equal to the height of the spacer ring **532**. A two-stages central axle **536** is screwed into a central hole of the central axle **509b** and provides an axial support for both bearings **531** and the primary rotating can **491** in the upper direction by using its flanged side laid on the inner ring of the upper bearing **531**. A primary central gear **533**, is dressed on the tail of the primary rotating can **491**, fixed to the bottom of this can and meshed with the primary pinion **534**. So, the rotation of the primary rotated can **491** will be transmitted to the primary shaft **511** and vice versa.

[0334] A flanged primary central pinion **537**, from plastic, is dressed on the central axle **536** and is fixed on the bottom of the primary rotating can **491**, utilizing its wide flange for this fixation. The outer rim of its flange also provides its centering on the bottom of the primary rotating can **491**, by entering to a corresponding circular recess. This centering permits to have some clearance between the central hole of the flanged primary central pinion **537** and the central axle **536**, so they aren't in touch, preventing a friction and permitting to make the flanged primary central pinion **537** also from non-plastic material, to increase durability. A secondary gear **538**, from plastic, is fixed on a secondary shaft **539**, which is inserted into a corresponding hole in the bottom of a primary steady can **540** from the outside. A secondary pinion **543**, from plastic, is fixed on the secondary shaft **539**, securing it from falling out together with the secondary gear **538**. The primary steady can **540** is mounted on the first stage of the central axle **536** between two primary nuts **541**. Each primary nut **541** has some low-height centering ring, which permits precise centering the primary steady can **540**, the central hole of which corresponds to the ring. Positioning of the secondary gear **538** below the lower primary nut **541** is problematic for the setup of the primary steady can **540**, since the lower primary nut **541** requires to be placed in the first order, before than the primary steady can **540** will be laid on it. This operation is limited by a deficiency in the clearance between the secondary gear **538** and the primary rotating can **491** or between its central hole and the central axle **536** for some other trimmers. So, the primary nuts **541** should have features, resolving this problem. One of these features for that may be a standard hexagonal shape of the lower primary nut **541**. So, the flat segment of the hex will provide an increased clearance for the positioning of the secondary gear **538,** and the corners of the hex will provide enough abilities to clamp the primary steady can **540**. The presence of only one flat or concave segment for the lower primary nut **541**, instead of entire hex, can optimize this variant. Another feature can be used in the primary nut **541** with a round shape: here should be some keying holes around the interior of its centering ring. These holes can be used together with a corresponding tubular setup key to screw the lower primary nut **541** after its simultaneous positioning with the primary steady can **540**. The secondary gear **538** is meshed with the flanged primary central pinion **537** after the setup of the primary steady can **540**. The steady fine scale **492** is fixed on top of the primary steady can **540**. A primary washer **542**, from plastic, is dressed on the central axle **536** and lies on the upper primary nut **541**. A cluster **545,** from plastic, has a secondary central gear and pinion and is attached outside to the bottom of a secondary rotating can **544** after being centered in the corresponding hole by its centering ring and protrudes the pinion component inside the secondary rotating can **544**. The cluster **545** with the secondary rotating can **544** is dressed on the central axle **536** and lies on the primary washer **542**, and also has the possibility of free rotation utilizing the low friction between the plastic of its body and the central axle **536**. A tertiary gear **546**, from plastic, is fixed on a tertiary shaft **547**, which is inserted into a corresponding hole in the bottom of a secondary steady can **548** from the outside. A tertiary pinion **551**, from plastic, is fixed on the tertiary shaft **547**, securing it from falling out together with the tertiary gear **546**. The secondary steady can **548** is mounted on the second stage of the central axle **536** between two secondary nuts **549**, which are similar to the primary nuts **541**, but have a reduced size. Also, the problem of positioning the tertiary gear **546** below the lower secondary nut **549** can be resolved in a similar way as for the first stage. Additionally, another possibility exists for that: the secondary rotating can **544** can have some clearance window for the tertiary gear **546**, since the can **544** isn't sealed. The pinion component of the cluster **545** has a thin tubular continuation at the top, which provides an axial support in the upper direction for the cluster **545**. The tertiary gear **546** is meshed with the pinion component of the cluster **545** after the setup of the secondary steady can **548**. A secondary washer **550**, from plastic, is dressed on the central axle **536** and lies on the upper secondary nut **549**. A tertiary central gear **552**, from plastic, is mounted under the bottom of a rotating flange **553** after centering in the corresponding hole by its centering ring. The tertiary central gear **552** with the rotating flange **553** is dressed on the central axle **536** and lies on the secondary washer **550**, and also has the possibility of free rotation utilizing the low friction between the plastic of its body and the central axle **536**. A screw with washer **554** fixes the tertiary central gear **552** in the upper direction on the two-stage central axle **536**, resides in a corresponding hole in the rotating flange **553** and leaves a thin gap over the flange of the tertiary central gear **552** for its free rotation. The rotating intermediate scale **493** is fixed on top of the secondary rotating can **544**. The steady shield of pitch **494** is fixed on top of the secondary steady can **548**. The generic rotating arrow shield **495** is fixed on top of the rotating flange **553**.

[0335] Referred to FIG. **67**, the construction of the S-trimmer **456** is almost the same as that of the P-trimmer **454** and differs only in the steady shield of skew **494'** and the presence of additional elements for locking. The S-trimmer **456** uses a lockable variant of the primary rotating can **491'**, which has at the bottom a skirt **491z** for locking. Locking needles **555** are screwed into the skirt **491z** from outside, using their threaded ends, and are equidistantly distributed outwardly with their sharp ends. The number of these needles **555** is equal to the number of ticks on the rotating fine scale **491a** FIG. **63**, which corresponds to 0.1° of skew for the locking precision. A locking wedge **557** performs the actual locking when it enters into a window **509c** upon the force of a spring **559**, which is dressed on the tail **557a** of this wedge and has a back support on the flange of a solenoid **558**. The window **509c** partially continues on the bottom **509a** of the case **509** of the PGS trimmers block. The solenoid **558** is mounted inside the trimmer locking bracket **556** and can pull the ferromagnetic tail **557a** of the locking wedge **557** into the interior upon powering. A rigid wire **560** is mechanically connected to the tail **557a** inside the solenoid **558** and passes outward through some hole in the mounting wall of the locking bracket **556** for the solenoid **558**. The rigid wire **560** has a hooked opposite end on which a soft string **561** is tied. A pulley **563** freely rotates on an axle **562** fixed in the locking bracket **556**, and guides the soft string **561** toward the skew locking knob **458**.

[0336] The bracket **564** of the skew locking knob **458** is mounted under the control panel **442**, to which it is fixed by screws not shown. A shaft **565** of the locking knob enters into an opened to top corresponding hole of the bracket **564**, nesting in the lower part of this bracket, where it can rotate freely, while having axial support in the downward direction. The upper part of said hole has an increased diameter, so a clearance exists between the shaft **565** and this hole of the bracket **564**, enough to place here the soft string **561**, which is guided to this direction through a hole **564a** by a pulley **571**, which freely rotates on an axle **570** fixed in the bracket **564**. The pulley **571** and the hole **564a** in the bracket **564** are positioned to guide the soft string **561** to the shaft **565** tangentially. Also, any sharp edges of the hole **564a** are removed, against damaging the soft string **561**. The shaft **565** has a threaded hole in bottom into which a screw **567** is screwed through a bottom hole of the bracket **564**. A spacer ring **568** is dressed on the screw **567** and can rotate freely in the bottom hole of the bracket **564**, as well as the screw **567** can rotate freely together with it and with the shaft **565**, providing axial support for the shaft **565** in the upper direction. Some free space remains above the screw **567** inside the shaft **565**, in which the soft string **561** enters through a corresponding hole and has a knot inside that fixes it. A spacer ring **569** is dressed on the shaft **565** and enters inside the bracket **564**, consuming the clearance above the soft string **561** and lies on a thin circular step inside the clearance hole. A snapping ball **572** enters into the bracket **564** from a corresponding hole and is continuously pushed in by a spring **573** the other end of which is supported by a screw **574** into the bracket **564**. Some hole exists in the spacer ring **569**, in which the snapping ball **572** can enter, providing an initial fixation of the spacer ring **569** against rotation. Also, the spacer ring **569** has a final fixation upon mounting the entire skew locking knob **458** under the control panel **442**, which clamps it along its flange. The shaft **565** has two coned nests **565**a in which the snapping ball **572** enters for the normal and locking position of the skew locking knob **458**. The handle **566** is fixed on the shaft **565** after mounting the entire skew locking knob **458.**

[0337] When the skew locking knob **458** is in the normal position, the soft string **561** is maximally wound onto the shaft **565**, and the locking wedge **557** is out of the trimmer space, permitting the free rotation of the primary rotating can **491'**. The shaft **565** is retained in this position by the snapping ball **572** against the increased force of the spring **559**. When the skew locking knob **458** is in the locking position, the soft string **561** is maximally unwound from the shaft **565**, so the remained rotation moment on the shaft **565** is zeroed. If the solenoid **558** isn't powered for this case, the locking wedge **557** enters the trimmer space between a nearest pair of the needles **555** and disables the rotation of the primary rotating can **491'**. But, if the solenoid **558** will be powered for the latter case, the locking wedge **557** will be out of the trimmer space, permitting the free rotation of the primary rotating can **491'**, so a loose-hanging loop of the soft string **561'** will be created. Having this loose-hanging loop isn't a well-secured solution. More than, the unwinding force of the soft string **561** will be missed at all in the case of actuating the knob **458** toward the locking position when the solenoid **558** is powered, which will lead to jamming of the soft string **561**. Thus, between the pulleys **563** and **571**, an intermediate pulley pulled by a low-force spring should be placed to solve this problem. This additional pulley isn't shown for simplicity. The solenoid **558** is powered each time when the servo of its trimmer is powered. Sometimes this can be performed with high frequency. So, it is better to use the knob **458** in the normal position for the non-manual handling to prevent the soft thread **561** from wearing out.

[0338] Referred to FIG. **68**, the construction of the G-trimmer **459** inside of the case **509** of the PGS trimmers block is almost same as for the S-trimmer **459**. It also uses the variant of the primary rotating can **491'** with locking abilities, but it utilizes the rotating fine scale of gain **491b**. A Gain exclusive variant **543'** of the secondary pinion with an increased diameter is used instead of the basic **543** variant. A Gain exclusive variant **545'** of the cluster **545**, having a reduced diameter of its gear component, is used instead of the basic variant. A Gain exclusive variant **544'** of the secondary rotating can **544**, having a reduced diameter of its flange interfaced with the cluster **545'**, is used instead of the basic variant. The Gain exclusive variant **500** of the rotating flange **553**, having additional scales **500a** and **500b** FIG. **63**, is used instead of the basic variant. The steady fine scale of gain **496** is used instead of the steady fine scale of pitch **492**. The rotating intermediate scale of gain **497** is fixed on top of the secondary rotating can **544'**. The steady shield of gain **498** is used instead of the steady shield of skew **494'**.

[0339] Referred to FIG. **69**, the construction of the WST-trimmer **462** inside of the trimmer case **519** is almost the same as for the P-trimmer **454**. It utilizes the rotating fine scale of WST **491c**. A WST exclusive variant **537'** of the primary central pinion **537**, having a bit reduced diameter, is used instead of the basic variant. A WST exclusive variant **538'** of the secondary gear **538**, having a bit reduced diameter, is used instead of the basic variant. A WST exclusive variant **543"** of the secondary pinion **543**, having a bit increased diameter, is used instead of the basic variant. A WST exclusive variant **545"** of the cluster **545**, having a reduced diameter of its gear component and an increased diameter of its pinion component, is used instead of the basic variant. A WST exclusive variant **546'** of the tertiary gear **546**, having a reduced diameter, is used instead of the basic variant. A WST exclusive variant **551'** of the tertiary pinion **551**, having a reduced diameter, is used instead of the basic variant. A WST-and-SP shared variant **552'** of the tertiary central gear **552**, having some-reduced diameter, is used instead of the basic variant. A WST exclusive variant **540'** of the primary steady can **540**, having some-decreased radial position of the hole for the secondary shaft **539**, is used instead of the basic variant. A WST exclusive variant **548'** of the secondary steady can **548**, having some-decreased radial position of the hole for the tertiary shaft **547**, is used instead of the basic variant. The steady fine scale of WST **499** is fixed on top of the primary steady can **540'**. The rotating intermediate scale of WST **501** is used instead of the rotating intermediate scale of pitch **493**. The steady shield of WST **502** is fixed on top of the secondary steady can **548'**.

[0340] Referred to FIG. **70**, the construction of the SP-trimmer **464** inside of the trimmer case **519** retains some similarity with the P-trimmer **454**, including the use of the same rotating fine scale **491a**. An SP-and-Lock shared variant **537"** of the flanged primary central pinion **537**, having a bit reduced diameter, is used instead of the basic variant. An SP-and-Lock shared variant **538"** of the secondary gear **538**, having a bit reduced diameter, is used instead of the basic variant. An SP-and-Lock shared variant **543'''** of the secondary pinion **543**, having some-reduced diameter, is used instead of the basic variant. An SP exclusive variant **545'''** of the cluster **545**, having a bit reduced diameter of its gear component and an increased diameter of its pinion component, is used instead of the basic variant. An SP exclusive variant **546"** of the tertiary gear **546**, having a reduced diameter, is used instead of the basic variant. An SP exclusive variant **551"** of the tertiary pinion **551**, having a reduced diameter, is used instead of the basic variant. A WST-and-SP shared variant **552'** of the tertiary central gear **552**, having some-reduced diameter, is used instead of the basic variant. An SP exclusive variant **540"** of the primary steady can **540**, having a decreased radial position of the hole for the secondary shaft **539**, is used instead of the basic variant. An SP exclusive variant **544"** of the secondary rotating can **544**, having an increased diameter of the central hole and a reduced overall height, is used instead of the basic variant. An SP exclusive variant **548"** of the secondary steady can **548**, having a decreased radial position of the hole for the tertiary shaft **547** and a significantly reduced height due to missing of a flange for mounting a scale, is used instead of the basic variant. An SP exclusive variant **553'** of the rotating flange **553**, getting the shape of a ring with a thickened wall and having the rotating shield **505** of the stabilator actual position fixed on it, is used instead of the basic variant. The rotating arrow shield of SP **504** has a large flange lowered and directed radially outward, which is used to mount this shield on top of the secondary rotating can **544"**. The steady shield of SP **503** is fixed on top of the primary steady can **540"** and hides the mounting flange of the rotating arrow shield of SP **504**.

[0341] Referred to FIG. **71**, the construction of the L-trimmer **466** inside of the trimmer case **519** also has some similarity with the P-trimmer **454**. It utilizes the rotating fine scale of lock **491d**. The main difference here is the use of a one-stage central axle **536'** instead of the basic two-stages central axle **536**. An SP-and-Lock shared variant **537"** of the flanged primary central pinion **537**, having a bit reduced diameter, is used instead of the basic variant. An SP-and-Lock shared variant **538"** of the secondary gear **538**, having a bit reduced diameter, is used instead of the basic variant. An SP-and-Lock shared variant **543'''** of the secondary pinion **543**, having some-reduced diameter, is used instead of the basic variant. An exclusive central gear **575**, having a diameter equal to the diameter of the gear component of the cluster **545'''** that is used in the SP-trimmer, is used instead of the basic cluster **545**. A Lock exclusive variant **540'''** of the primary steady can **54**0, having a decreased radial position of the hole for the secondary shaft **539** and a reduced diameter, is used instead of the basic variant. The long hub of the secondary central gear **575** enters into the corresponding hole of the inner hub of an exclusive secondary rotating can **544'''** for centering before attaching. The screw with washer **554** fixes the exclusive secondary rotated can **544'''** in the upper direction on the one-stage central axle **536'**, leaving a thin gap over the inner hub of the exclusive secondary rotating can **544'''** for its free rotation. The steady shield of lock **506** is fixed on top of the exclusive primary steady can **540'''**. The rotating arrow shield of lock **507** is fixed on top of the exclusive secondary rotating can **544'''**.

[0342] Referred to FIGS. **72** and **73**, the SDT has a consoled base **581** as its support. This consoled base **581** is an elongated tube with a conical transition at its forward end to a reduced diameter. A tubular case **582** is clamped between a forward flange **583** and a back diverting flange **585** by two long bolts **588** going through holes **585b** FIG. **75**, which are screwed into the forward flange **583** and also pass through corresponding holes in a collector **584** placed over the back diverting flange **585**, and having a vertical alignment. The tubular case **582** protrudes from the inside of the consoled base to the outside through the hole at the end of said conical transition, which diameter corresponds to the outer diameter of the tubular case **582**. The back diverting flange **585** also has a conical segment in its shape, which corresponds to the inner conical segment of the conical transition of the consoled base **581**. The collector **584** is attached to the consoled base **581** inside its interior with screws **589**. A moisture collector **586** with its sealing lid **587** is placed inside the tubular case **582** in its middle, and having a generally cylindrical shape with a diameter corresponding to the inside diameter of the tubular case **582** and two holes **586b** FIG. **74** used for conducting the bolts **588**.

[0343] The forward flange **583** has a generally cylindrical shape with a diameter equal to the outside diameter of the tubular case **582** and is inserted a bit into the tubular case **582**, using some centering flange at its base. Also, the same kind of the centering flange on the back diverting flange **585** is used at the other end of the tubular case **582**. Two equal slopes **583a** are milled on the forward side of the forward flange **583**, where the one looks to up and the other looks to down, each having about 40 degrees from the horizontal plane. Two equal entry channels **583b** are drilled in the centers of the slopes **583a** perpendicular to their surfaces. Two equal horizontal channels **583d** are drilled in the base of the forward flange **583** and have a symmetrical horizontal arrangement. Two equal diverting channels **583c** are drilled from the cylindrical surface of the forward flange **583** to its interior, lying in its cross-section plane and connecting the horizontal channels **583d** with the respective entry channels **583b**. So, the upper entry channel **583b** has a connection with the right (from the pilot position) horizontal channel **583d**, and the lower entry channel **583b** has a connection with the left horizontal channel **583d**. Two seals **583e** seal the outer ends of the respective diverting channels **583c** from the environment, repairing the original cylindrical shape of the forward flange **583**. A forward tube **590** of the upward pressure and a forward tube **590'** of the downward pressure connect the horizontal channels **583d** of the forward flange to forward entry holes **586a** FIG. **74** of the moisture collector **586**, lie on the right and left sides, respectively, and enter into output sockets **583f** of the forward flange **583** and forward entry sockets **586f** of the moisture collector **586** by their ends. A backward tube **591** of the upward pressure and a backward tube **591'** of the downward pressure **591'** connect backward entry holes **586a** of the moisture collector **586** to entry holes **585a** FIG. **75** of the back diverting flange **585**, lie on the right and left sides, respectively, and enter into backward entry sockets **586f** of the moisture collector **586** and entry sockets **585e** of the back diverting flange **585** by their ends.

[0344] A forward heater **593** has a generally tubular shape and is placed inside the tubular case **582**, wrapping the bolts **588** and the forward pressure tubes **590** and **590'**. A backward heater **594** has a generally tubular shape and is placed inside the tubular case **582**, wrapping the bolts **588** and the backward pressure tubes **591** and **591'**. Isolated electrical wires **595** connect the forward heater **593** to the backward heater **594** and exit from the collector **584**, passing through holes **586c** in the moisture collector **586** and **585c** in the back diverting flange **585**, see FIGS. **74** and **75**. These heaters **593** and **594** provide anti-icing ability for SDT operating.

[0345] Referred to FIGS. **73** and **74**, the moisture collector **586** has two equal internal cavities **586d** in a horizontal arrangement, which are separated at their bottoms by a thin wall **586e** in the vicinity of which moisture will collect. These internal cavities **586d** are manufactured by milling. A sealing lid **587** is in the form of a tube segment and seals both cavities, using some waterproof adhesive or a sealant before inserting it with the moisture collector **586** into the tubular case **582**. Also, some small leakage is permissible, since the pressures in both cavities **586d** are continuously pumped by big entry holes **586a**. Small drain holes **596** are drilled in the sealing lid **587** and the tubular case **582** on each side from the separating wall **586e** of the moisture collector **586**. A small pressure leak through the drain holes **596** corresponds to an equal environmental pressure near their vicinity due to symmetry in the placement of the drain holes **596** and the cavities **586d**. So, the symmetric sensitivity in the vertical direction of the entire SDT wouldn't be jeopardized by this implementation of the moisture collecting.

[0346] Referred to FIGS. **73** and **75**, the back diverting flange **585** has two equal diverting channels **585d**, which restore the original up-down positions for pressure exit sites and increase the separation base between them. The collector **584** has two equal output tubes **592** and **592'**, which are brazed inside of vertically arranged holes in the collector **584**, placed correspondingly to the arrangement of the exit sites of the diverting channels **585d**, providing the upward and downward output pressures, respectively.

[0347] Referred to FIG. **76**, the in-flight management of the presented aircraft can be resumed and considered as follows.

[0348] The left rotor **110** and the right rotor **110'** share the common powering shaft **127**, to which also the left electric engine **300** and the right electric engine **300'** are connected. The separate power circuits **438** and **438'** provide required currents in the coils of the electric engines **300** and **300'**, respectively, have a common management from the engine controller **597** and consuming power from the accumulators **437** placed on the left and right accumulator racks **404** and **404'**, respectively. A control panel **439** of these racks manages their longitudinal position, having a feedback from the left and right encoders **418** and **418'**, respectively, mechanically connected to these racks, and reports their positional state to the central computer **600**. The WST-trimmer **462** mechanically manages the WST-encoder **436**, which defines the related target winding speed for the engine controller **597**. The engine controller **597** uses the value of the target winding speed to provide instant managing signals to the power circuits **438** and **438'**, and has from them a feedback about the instant phase state and the power consuming by the engines **300** and **300'**, which is also reported, after conversions to respective forms, to the WSA indicator **449**, MR indicator **451**, RPM indicator **450** and to the central computer **600**.

[0349] The output pressures from the SDT **580** are propagated by the pressure hoses **365** and **365'** to the SDI **468** and to pressure electric sensors **578** and **578'** for the upward and downward pressures, respectively. The stabilator controller

579 uses the values of the upward and downward pressures from the electric sensors **578** and **578'** as a feedback to determine a remained error in the orientation of the fuselage **101** of the aircraft **100** and after application some low-pass filter generates a respective command (if need) to actuate the SP-trimmer **464** by its servo, where this command passes through the control panel's logics **598**. The movement of the SP-trimmer **464** during this actuating transmits to the stabilators **102**, correcting the position of the fuselage **101**. Also, the movement of the SP-trimmer **464** transmits to the SP-encoder **428**, which reports its value to the central computer **600**. The bidirectional connection between the stabilator controller **579** and the central computer **600** permits to apply a more sophisticated management to the stabilator controller **579** from the side of the central computer **600** upon reusing the propagated values of pressures from the electric sensors **578** and **578'**. Also, this connection permits to pass the value of the SP-encoder **428** to the stabilator controller **579** as a feedback to prevent it from operating outside the operating margins of the stabilators **102**. Additionally, the movement of the accumulator racks **404** and **404'** using the control panel of racks **439** can alter any such operations that use the SP-trimmer **464**.

[0350] The L-trimmer **466** mechanically manages the lock state of both rotors **110** and **110'**, simultaneously, and is mechanically connected to the lock-encoder **427**, which reports its value to the central computer **600**, which can manage the L-trimmer by generating respective commands to actuate the servo of this trimmer, where these commands pass through the control panel's logics **598**.

[0351] The PGS-trimmers **454**, **459** and **456** mechanically manage the PGS-state of the left rotor **110** and are mechanically connected to the PGS-encoders **424**, **425** and **426**, respectively, which report their values to the central computer **600**. Also, the same task can be performed by the right side PGS-trimmers **454'**, **459'** and **456'** with the PGS-encoders **424'**, **425'** and **426'**, respectively, for the right rotor **110'**. The central computer **600** can manage both sides PGS-trimmers by generating respective commands to actuate their servos, where these commands pass through the control panel's logics **598**.

[0352] The output pressures from PST **576** are propagated by the pressure hoses **364** and **364'** to pressure electric sensors **577** and **577'** for the pitot and static pressures, respectively. Also, the static pressure propagates to the ASI **485**, VSI **489** and altimeter **486**, while the pitot pressure to the ASI **485** only, as in a conventional airplane.

[0353] The central computer **600** uses the values from the electric sensors **577** and **577'** and the value from the outside temperature sensor, not shown, to restore the horizontal and vertical components of the TAS and the flight altitude value. Additionally, it can use the signal from a GPS receiver **599** and the output from the Inertial Navigation System (INS) **601** to do that more correctly. The corrected value of the TAS vector can be used to calculate the error of the "stream following" state managed by the stabilator controller **579** for its sophisticated correction. The TAS magnitude together with the actual winding speed is used to calculate the correct PGS-states for the desired biangular values of each rotor **110** or **110'**, see **S36H4** in FIG. **36**H and FIG. **22**. The joystick **477** is connected to the central computer **600** and can moderate the biangular values of each rotor **110** or **110'** in the variational manner, performing the actual handling of the presented aircraft **100**, and this can be done by the computer buttons also. The actual biangular values of each rotor **110** or **110'** can be reflected on the display **445** in the numerical or graphical forms, also sharing their representation with another kind of information, such as navigation, for example. Also, the RSI of FIG. **38** can be presented on the display **445** for each rotor **110** or **110'** or for their average state in the presence of an actual inflow vector calculated in accordance with the data flow in FIG. **28**. More than, after a small number of trying flights, corrected actual parameters of particular aircraft can be refactored, such as actual coefficients of drag for the fuselage for some range of speeds. So, using such information, the central computer can execute the entire simulation for a particular aircraft in accordance with FIG. **34** in real time to predict a behavior of the aircraft in advance. For this case, the presented simulation should be completed by a tier related to the stabilators **102** and the induced longitudinal moments. Also, the simulation can be divided into two components related to each rotor **110** and **110'** and linked by a composed 3-d movement, to also predict the behavior of the aircraft during turns.

[0354] The control panel's switches **598** can disable the management of the trimmers by the central computer **600** and (or) stabilator controller **579** in the event of their malfunction or of any other circumstances. In this case, the trimmers can be managed by using the control panel's buttons **598,** and the pilot can use the standby instruments instead of the malfunctioned computer.

[0355] Also, in the event of an electricity outage, all trimmers can be managed manually when the pilot uses special tables to handle the aircraft directly through the PGS-states of their rotors **110** and **110'** for particular flight operations.

[0356] In the event of a malfunction of one of the power circuits **438** or **438'** or one of the engines **300** or **300'**, the aircraft may continue to fly on the related component of the remaining side, having a limitation in power.

[0357] In the event of malfunction of both of the power circuits **438** and **438'** or both of the engines **300** and **300'** or in the event of limitation of the remaining energy in the accumulators **437**, the aircraft can glide, having the rotors **110** and **110'** in the locked state. When this event occurs instantaneously upon a power outage, both rotors **110** and **110'** continue to rotate due to inertia, and so this is subject for a pilot mistake. Instinctively, the pilot wants to lock the rotors, since the moment induced by the engines and the linking the external moment of the rotors with the composed sum of the moments from the center of gravity and the stabilators **102** is vanished, so the aircraft begins promptly to rotate down by its nose, which can significantly shift the pitch of the fuselage **101** from its "stream following" position before the rotors will be locked for gliding. But, a too prompted locking in this case will be dangerous too, since the inertial force moment has a non-favorable direction, additionally lowering the nose of the aircraft. So, finally, the locking of the rotors should be performed no faster than 0.3-0.5 seconds after the power outage with instantaneous switching the gain to zero and the pitch to 5°, having the P-mode of the biangular handling. This time is enough to brake the rotors by their external moment before they begin to rotate back. Also, for this time, the stabilator controller **579** moves the stabilators **102** to a position that decreasing the adverse nose rotation, and the preset pitch of 5° will alleviate the issue of the decreased lift from the accumulated nose lowering angle. When such an event occurs during a recuperative descent, the inertial force moment of the rotors is in a favorable direction for braking. But also in this case, the locking of the rotors should begin only after switching the gain to -10° and the pitch to 3°, having the P-mode of the biangular handling. This action will promptly switch the sign of the external moment of the rotors, converting their kinetic energy to the external energy of the entire aircraft, braking the rotors in a time about 0.4 seconds. After this, the gain should be set to zero after stopping the rotors to restore the normal external moment. Only after that, the rotors can be locked. An actuating the lockers before the rotors approach low rotation may result in the application of too high external moment to the fuselage **101** and damage to the frictional linings **315** FIG. **44**E. Doing this entire task upon a total power outage, when also the servos of the trimmers are out of power, can be performed directly by using the handles of the G-and-P-trimmers with an additionally handling of the SP-trimmer **464**, trying to keep the SDI **468** pointed to zero.

[0358] Additionally, the in-flight management can be extended upon including an active VRS to depress the remained vibrations from the variations of the steering moment, see explanations for FIGS. **41**A and **41**B. The VRS applies compensating patterns of currents to the coils of both engines **300** and **300'** by a pattern generator connected to both power circuits **438** and **438'**. The pattern generator plays a particular active pattern, which is scaled in time using a minor phase signal. Particularly, the minor phase signal can be synchronized with the phase powering of these engines **300** an **300'** for a particular number of poles in the rotors of these engines. In another case a separated minor phase sensor extracts this minor phase signal from the rotors **100** and **100'**. The central computer **600** can manage this pattern generator through loading this active pattern from a pattern store, dependently on a particular flight operation or a load state. Also, this pattern generator can be implemented as a part of the engine controller **597**, especially in the case of synchronizing the minor phase signal with the phase powering of the engines.

[0359] The presented aircraft can be used with an enlarged wingspan to have a higher aspect ratio, and therefore the performance reflected in the LDR. But, that cannot be performed straightforwardly, simply by installing more longer wings **111** on the rotor **110**, since they wouldn't possess the enough rigidness against the loads from the aerodynamic and centrifugal forces. So, there needs some intermediate ring for that.

[0360] An option of using the presented rotor **110** with an intermediate ring in its middle is represented in FIG. **77**. In this option, instead of each one wing **111**, two wings are used: the inner wing **611** and the outer wing **613**. These wings **611** and **613** have generally the same length. Also, the inner end of the inner wing **611** is equal to the inner end of the original wing **111**, and the outer end of the outer wing **613** is equal to the outer end of the original wing **111**. The outer end of the inner wing **611** has an intermediate fairing **612**, which provides enough space for elements of its linking with the inner end of the outer wing **613** and has an outer shape equal to the outer shape of the end-wing fairing **170** of the original wing **111**. The inner end of the outer wing **613** has intermediate fairing **614**, which is symmetrically equal to the intermediate fairing **612** of the inner wing **611**. An intermediate ring **610** has flat surfaces on both sides. It is made of composite material and has equidistant holes related to the corresponding wings. A radial needle bearing **617** is inserted into each such a hole of the intermediate ring **610**. Adapter flanges **616** are dressed on the radial needle bearing **617** on each side. The intermediate fairings **612** and **614** of the respective wings have flat intermediate bases adjusted to the respective sides of the intermediate ring **610**. And from these directions, they have interior spaces used for their rotational mating with the adapter flanges **616**, with thrust bearings **618** lying on these adapter flanges **616**. A link shaft **615** is inserted into the radial needle bearing **617**, thrust bearings **618**, adapter flanges **616** and into two respective intermediate fairings **612** and **614**, where it is screwed into corresponding threaded holes by its threaded tails **615a** and **615b**, respectively. The tail **615a** has a right handed thread, and the tail **615b** has a left handed thread. Two set screws **619** on each side of the intermediate ring **610** fix the shaft **615** against unscrewing, using setup holes **612a** and **614a** on both sides of the intermediate fairings **612** and **614**, respectively. During the setup of the intermediate ring **610** and the outer wings **613**, those set screws **619** can be periodically screwed and unscrewed on respective sides to switch between the screwing of the shaft **615** or the outer wings **613** relative to the stationary inner wings **611**. So, for this operation, the outer wing **613** acts as some handle, and only one from two set screws **619** can be used for this kind of switching. And, the operation will be completed when the overall gap of the bearings will be optimal, having a free rotation without a backlash with coinciding of the trailing edges of the inner wing **611** and the outer wing **613**. After this, all four set screws should be fixed. The high diameter of the shaft **615** with using these set screws **619** permits to transmit enough high torque from the inner wing **611** to the outer wing **613**. This kind of assembly of the intermediate ring **610** together with the outer wings **613** on the inner wings **611** permits their fast installation after the first setup. Indeed, in the case of a disassembling, only from one side these set screws **619** can be unscrewed. So, for the next installation, each outer wing **613** will be screwed together with its constantly assigned inner wing **611**, simply by its rotating, until their trailing edges will be coincided without a visible backlash in their linking. Also, the presented rotor **110** may be extended to use more than one intermediate ring **610**.

[0361] Using the intermediate ring **610** at the end of the rotor **110** permits to install winglets on it that are not supported at their ends. These winglets can well withstand the bending forces, having a short length. An option of this is represented in FIG. **78**A. Here, the inner wings **611** are supported by the installed intermediate ring **610** on their intermediate fairings **612** and may have a full length or be linked from components. Short winglets **628** are installed after the intermediate ring **610** on their intermediate fairings **614** and have wing fences **629**. These wing fences **629** decrease the induced drag by delaying generation of the end wings vortices, similarly the wing fences in a conventional airplane. FIG. **79**B represents another example of this option. Here, swept winglet **630** is used, which also has the wing fence **629**. But, this winglet is swept to the forward. Such a winglet has a significantly shifted to the forward the center of force relative its pivot, and so this induces a significant positive moment. This moment provides an advantage in the cruise flight, where exists a significant negative moment on the entire wing. So, the forwardly swept winglet **630** will partially compensate for the negative moment, leaving the steering moments for the wings below a moderate level. The optimal level of this kind compensating is about 70 percent, since more high moments from the winglets **630** will create too high positive steering moments during runway operations.

[0362] The presented aircraft can be used with the wings **111** based on a symmetrical airfoil, such as NACA 0010, which has a close to zero moment coefficient CM over a wide range of angles of attack when it is used with a pivot position of about 0.25 of the chord length. Using this airfoil allows to have low steering moments for all positions of the wings for main operations, which is especially important for the high speed cruise, where the rotors **110** have the greatest IMR, see FIG. **40**H. Reducing the steering moments leads to greatly reducing of a possible wearing of the steering gears and has an additional advantage when the rotor **110** is used with the optional intermediate ring **610**, highly decreasing the transmitting rotation moment from the inner wing **611** to the outer wing **613**. Also, an additional advantage of using a symmetric profile is: a significantly reduced level of vibrations existing in another case, see FIG. **41**B. Another advantage of using a symmetric profile is having absolutely equal wings **111** for the left and right rotors instead of only symmetrically equal wings.

[0363] An option of using the presented rotor **110** with the wings **111**, based on a symmetric airfoil, is represented in FIG. **79** which pictures the base portion of the wing **111** detached from the rotor having only the bevel gear **114** and the wing's shaft **180** on the base **113**. The position of the shaft **180** corresponds to 0.25 of the chord length of the wing **111**, but the base **113** has not changed. The straight part of the wing **111** is shifted toward its trailing edge to have the desired pivot position. This shift some changed the shape of the leading edge transition **111a** at the wing's fillet **111b** and introduced a trailing edge transition **111c** from the base **113** to somewhat protruded now the trailing edge of the wing **111**.

[0364] Upon transition to a higher-scale of size, the presented aircraft can reach high subsonic speed on a cruise. This ability is permitted by the low winding speed of the wings **111** of the rotor **110** relative to the speed of the cruise and the speed of sound. For this variant, the wings **111** can utilize a supercritical airfoil to increase the cruise speed. Such wings **111** based on the supercritical airfoil can be installed on the rotor **110** with the original alignment of the wing trailing edge relative to the rim of the wing's base **113** FIG. **44**C, since this kind of airfoil has a more rearwardly displaced center of the aerodynamic force. Also, its pivot position can be optimized for the cruise by reducing the diameter of the wing's base **113** by shifting the leading edge of the wing **111** forward. Additionally, the wings with a supercritical airfoil can be used with the forwardly swept winglets **630** FIG. **78**B, to have low steering moments. Another advantage of the wings with a supercritical airfoil for use in rotor **110** is the increased average thickness of the wings in their section, which increases their rigidness.

[0365] Using of the presented aircraft powered by the accumulators only doesn't permit long-distance flights, due to the limitations of contemporary accumulators. That may be enhanced in the future, but these days, long-distance flights of an aircraft with moderate performance can only be performed using combustion engines. The presented aircraft permits to have a hybrid power solution, where a combustion engine is used only for generating electricity to charge the accumulators of the aircraft and (or) to power the electric engines of the united rotors, with keeping ability of the recuperative descent and deceleration.

[0366] A modified variant of the presented aircraft accommodated to use the combustion engine is represented in FIG. **80**. A combustion engine **620** with an electric generator **621** is placed in the aft compartment of the fuselage **101** of the aircraft **100** and is enveloped by an air-conducting envelope **623**, which is used for: cooling the combustion engine **620**, provide it with oxygen from the air, and for conducting the exhaust of the combustion engine **620** toward an air outlet **623a** on the tail edge of the fuselage **101**. A fairing with air inlet **622** is used as a lobby for the air-conducting envelope **623** and is spanned between the rotor's sockets **106**, including in its interior the air outlets **108** of the cooling systems of the electric engines **300**. For this kind of airflow connectivity, a minor air cooling stream **625** enters in the air inlets **107**, passes around the electric engines **300** inside of their sockets **293** and continues moving through the air conduction tubes **296** to the air outlets **108**, where it merges with an air cooling mainstream **624** that enters from the forward to the fairing with air inlet **622**. The electric generator **621** has generally a cylindrical shape with a short length, and the air conducting envelope **623** is sealed around it, which allows maintenance for the electric generator **621** with respect to its powering connectivity to the accumulators **437** placed on the racks **404**, and (or) to the engines **300** without removing the air-conducting envelope **623**. Maintenance of the combustion engine **620** can be performed after opening some hatches in the fuselage

101 and the air-conducting envelope **623** above it. Fuel tanks aren't shown here and can be placed under the area of the accumulator racks **404** and (or) in other free spaces.

What is claimed is:

1. A rotor for powered flight with managed PGS-state comprising:

a principal rotational element with generally round shape and generally flat surface face side having a central axis perpendicular to said face side;

a set of equal wings equidistantly mounted on the periphery of said principal rotational element and extended outside from said face side parallel to said central axis at a fixed distance from that axis, wherein each wing has ability of rotation around axis thereof located in a respective pivot position relative to the chord of this wing and parallel to said central axis;

a principal irrotational element rotatably mounted on said principal rotational element with respect to said central axis at a fixed distance therefrom, the principal irrotational element is used as a reference base for steering said wings in accordance with managed PGS-state;

a central cluster comprising, placed coaxially each to the other, a central gear and a circular groove, the central cluster has a common axis of said elements thereof parallel to said central axis and is mounted on said principal irrotational element together with means for steering said central gear in angular, radial and azimuthal directions relative to said principal irrotational element, where each respective freedom of this steering is mapped to managing the pitch, gain or skew component of said PGS-state, respectively; and

a set of steering elements for each of said wings including a pitch gear having angular position of its axis generally directed toward axis of the corresponding wing from direction of said central axis, a steering pinion meshed with said pitch gear, an entry gear that is meshed with said central gear of said central cluster and shares common axis with said steering pinion joined to it into a respective steering cluster, having ratio of its own teeth' number to number of teeth of said central gear equal to ratio of teeth' number of said steering pinion to number of teeth of said pitch gear, a groove follower inserted into said circular groove of said central cluster and sharing common axis with said entry gear and included in said steering cluster, means for keeping a fixed distance between the axes of said steering cluster and said pitch gear, and a transmission between said pitch gear to the corresponding wing, providing a unitary angular relation between said pitch gear and the pitch of the corresponding wing.

2. The rotor set forth in claim **1** wherein said rotor has features and elements comprising:

a faceplate of circular shape representing said principal rotational element, providing a mounting basement for said wings;

a central powering shaft placed on said central axis;

a flanged hub fixed on the end of said central powering shaft, having a flange side fixed to the back side of said faceplate;

a back-ring coaxially mounted on the back side of said faceplate at a fixed distance therefrom, imposing axial position of said central cluster between the axial positions of this back-ring and said faceplate;

a steady base with flange representing said principal irrotational element mounted on said central powering shaft at a fixed distance from said back-ring with freedom of rotation in respect of said central powering shaft;

a circular base of each of said wings as its integral element entered into a corresponding hole in said faceplate, having a face side generally on same level with the face level of said faceplate, the circular base has a fillet interface on each side of its wing and a smooth transition of the leading edge of its wing to its rim;

a shaft for each said pitch gear on which this pitch gear is fixed, the shaft is rotatably mounted on its ends between said faceplate and said back-ring; and

a shell for each said pitch gear, which represents said means for keeping a fixed distance between the axes of said steering cluster and said pitch gear, the shell is rotatably mounted on said shaft of this pitch gear and provides full rotation support for the corresponding steering cluster, becoming with all said elements of content thereof an earring assembly.

3. The rotor set forth in claim **2** wherein each said transmission between related pitch gear and the corresponding wing comprises:

a bevel gear with substantially high diameter fixedly mounted on said circular base of the corresponding wing;

a bevel pinion meshed with said bevel gear;

a shaft-mounted cluster of joined together a miter gear and a pinion that is meshed with said corresponding pitch gear, where ratio of teeth' number of said pitch gear to number of teeth of the pinion is equal to ratio of teeth' number of said bevel gear to number of teeth of said bevel pinion, and which shaft is rotatably mounted on its ends between said faceplate and said back-ring;

a separate miter gear meshed with the miter gear of said shaft-mounted cluster; and

a transmission shaft at the ends of which said separate miter gear and said bevel pinion are fixed.

4. The rotor set forth in claim **3** wherein a set of equal ribs, the number of which is equal to the number of said wings, is used as a distributed separating support of said back-ring on said faceplate, which ribs are equidistantly placed around the outer rim of said back-ring, providing also rotation support for said transmission shafts from the sides of said separate miter gears.

5. The rotor set forth in claim **3** wherein a set of equal wing sockets of cup-like shape, the number of which equal to the number of said wings, is mounted on periphery of said faceplate and is used to support rotation of said wings and to support rotation of said transmission shafts from the sides of said bevel pinions.

6. The rotor set forth in claim **3** wherein a set of screws is used to fix each said bevel gear to the corresponding circular base of its wing, which screws are placed around the periphery of the inner tooth region of this bevel gear.

7. The rotor set forth in claim **5** wherein a wing owned shaft for each of said wings is mounted inside this wing and protrudes from the center of the corresponding circular base in the direction opposite to the wing, servicing as the pivot axis of the wing, and wherein each of said wing sockets has a set of parts assigned thereto and related to support and installation of the corresponding wing, comprising:

a primary thrust bearing placed between the bottom of this wing socket and the periphery of the inner tooth region of the corresponding bevel gear;

a radial needle bearing placed inside a central hole of this wing socket;

a tubular flange dressed on said wing owned shaft, having a tubular part inside said radial needle bearing and a flanged part outside of this wing socket;

a secondary thrust bearing placed outside between the bottom of this wing socket and the flanged part of said tubular flange; and

a nut screwed from outside on a threaded end of said wing owned shaft over the flange part of said tubular flange.

8. The rotor set forth in claim **5** wherein a set of bridges is used for connecting pairs of adjacent wing sockets, where each said bridge is a segment of a plate having mating rims complementing the external shape of the respective wing sockets on the mating surface, and oriented parallel to said faceplate upon mounting this bridge on the respective wing sockets.

9. The rotor set forth in claim **2** wherein said central cluster has its own body joined coaxially with said central gear, a shifting base is mounted on said steady base as an interface between said central cluster and means for steering it in radial and azimuthal directions with respect to said steady base, and wherein means of angular steering of said central cluster are mounted on said shifting base.

10. The rotor set forth in claim **9** wherein an interface of management PGS-state is provided and represented by elements comprising:

a pitch outer shaft, which rotation is used to change the pitch of said rotor;

a gain outer shaft, which rotation is used to change the gain of said rotor in linear form; and

a skew outer shaft, which rotation is used to change the skew of said rotor or skew and gain at the same time.

11. The rotor set forth in claim **9** wherein said central cluster includes an internal gear coaxially fixed thereon, and said rotor includes:

a pitch flanged bracket mounted on said shifting base on a flange side thereof upon inserting through a corresponding hole of said steady base and having a worm support bracket as other side thereof;

a pitch steering shaft mounted inside said pitch flanged bracket with freedom of rotation;

a pitch pinion fixed on the inner end of said pitch steering shaft and meshed with said internal gear;

a pitch worm gear fixed on the outer end of said pitch steering shaft;

a telescopic universal joint, which outer shaft is mounted on said steady base with freedom of rotation and is used as a pitch outer shaft, and which inner shaft is mounted with freedom of rotation on said worm support bracket; and

a pitch worm fixed on said inner shaft of said telescopic universal joint and meshed with said pitch worm gear.

12. The rotor set forth in claim **9** wherein a rotation support of said central cluster on said shifting base is provided by a system comprising:

a radial bearing placed between said shifting base and said central cluster;

a closing flange coaxially mounted on said shifting base from the side of said faceplate; and

a thrust bearing placed between said central cluster and said closing flange.

13. The rotor set forth in claim **9** wherein angular fixation in a fixed axial position for said shifting base relative to said steady base is provided by a retaining system comprising:

a set of three radial rods, where each of its rods is mounted with its inner end on said flange of said steady base with a radial orientation relative to said central axis between said steady base and said shifting base and fixed with its outer end on said steady base, where two of said radial rods are oriented exactly in opposite directions, and the third such rod is oriented at right angles to both others, becoming a central radial rod;

a set of three tangential rods, where each of its rods is mounted with its ends on said shifting base with orientation at a right angle its axis to the axis of the corresponding radial rod; and

a set of three cross-holes bearings, where each of its bearings has in its cross-holes said respective radial and tangential rods, which are inserted there with the possibility of free axial movement.

14. The rotor set forth in claim **13** wherein all said tangential rods are located between said shifting base and said central cluster, and said shifting base has three side-slots that provide clearance for said respective cross-holes bearings.

15. The rotor set forth in claim **13** wherein at least one of said cross-hole bearings has two crampons as symmetrical extensions along the direction of the corresponding tangential rod, and said crampons are inserted into two respective saddles mounted on said shifting base, expanding the retaining base of this cross-hole bearing.

16. The rotor set forth in claim **10** wherein said means of steering of said shifting base in radial and azimuthal directions are represented by a Gain-Skew-node (GS-node), which is mounted on said steady base upon inserting kernel part thereof, referenced as GS-variator, into a corresponding hole of said steady base, said GS-variator provides a direct steering interface to said shifting base and comprises:

a flange, which has generally circular shape and is mounted on said steady base by a mounting base thereof, which axial direction relative to said shifting base from said steady base is referenced as bottom direction;

a skew worm gear coaxially mounted inside and under said flange at a fixed distance with freedom of rotation;

a toothed rack mounted on said skew worm gear with tangential orientation of its toothed side at a fixed distance from the axis of said skew worm gear with freedom of movement along said tangential orientation;

a gain steering shaft coaxially mounted with freedom of rotation on said flange;

a gain gear fixed on said gain steering shaft and meshed with said toothed rack;

a steering lead fixed on said toothed rack, having a round steering pin inserted into a corresponding hole of said shifting base with a rotation support, where said steering pin is coaxial with the axis of said skew worm gear for the neutral gain state;

a gain worm gear fixed on said gain steering shaft in the upper outside position from said flange;

a gain inner shaft mounted with freedom of rotation on said flange, which acts as said gain outer shaft when the simultaneous change in skew and gain using said skew outer shaft is permissible;

a gain worm fixed on said gain inner shaft and meshed with said gain worm gear;

a skew steering shaft mounted with freedom of rotation on said flange, which acts as said skew outer shaft when the axis location of said skew outer shaft between said steady base and said shifting base is permissible; and

a skew worm fixed on said skew steering shaft and meshed with said skew worm gear.

17. The rotor set forth in claim **16** wherein said GS-variator for compactness in the axial direction has features and elements comprising:

a rectangular recess on the upper side of said skew worm gear, in which said toothed rack is moveable sliding along its own lower and opposite-to-teeth surfaces;

a hole in the area of said rectangular recess, in which said steering lead is inserted from the lower side of said skew worm gear and fixed to said toothed rack, having a slipping ledge that slides along the lower surface of said skew worm gear, providing a support for said toothed rack and for self in the axial direction;

a circular recess on the upper side of said skew worm gear into which said gain gear is inserted having correct vertical alignment with said toothed rack;

a retaining ring mounted coaxially on said skew worm gear, the retaining ring has a protrusion inside its perimeter on its upper rim;

a flanged bearing inserted coaxially into a central hole of said skew worm gear from above, the flanged bearing provides radial and bottom axial supports for said gain steering shaft relative to said skew worm gear and is laid under said gain gear;

an intermediate ring mounted coaxially inside said flange of said GS-variator, the intermediate ring has two protrusions apart its perimeter on its lower rim;

an outer bearing placed between said retaining ring and said intermediate ring providing radial and bottom axial supports for said skew worm gear using said protrusions of both such said rings; and

an inner bearing placed between said intermediate ring and a hub of said gain gear, completing radial and axial supports for said gain

steering shaft and said skew worm gear.

18. The rotor set forth in claim **16** wherein said GS-variator permits simplified manufacturing and also convenient placement of said skew outer shaft of said interface of management PGS-state, having elements comprising:

a skew outer shaft, which represents said skew outer shaft of said interface of management PGS-state;

a skew bracket mounted over said mounting base of said flange of GS-variator, having a flat-sector shape of a mounting interface with inner radius corresponding to related outer radius of said flange, the skew bracket provides a rotation support for said skew steering shaft at its inner end and on the entry side, so manufacturing of said flange without such a support function allows the use of turning operations, and additionally the skew bracket provides rotation support for said skew outer shaft at its inner end and at the other entry side, placing its axis above said steady base and in parallel orientation to the axes of said gain inner shaft and said skew steering shaft; and

two meshed gears, where one of these two gears is fixed on said skew steering shaft outside said skew bracket and the other gear is fixed on said skew outer shaft near its inner end inside said skew bracket.

19. The rotor set forth in claim **16** wherein said GS-node has a SG-compensator, which allows to completely decompose the gain and skew components of entire PGS-state, by transmitting the rotation of said skew steering shaft to said gain inner shaft using appropriate gear means and means of differential transmission, where the rotation transmitted to said gain steering shaft provides a movement of said toothed rack, compensating the adverse respective movement induced by the rotation of said skew worm gear, and where other side of said means of differential transmission accepts rotation from said gain outer shaft of said interface of management PGS-state.

20. The rotor set forth in claim **19** wherein said SG-compensator compositionally includes a gain-handling reducer for aligning rotational speeds of said gain outer shaft and said pitch outer shaft of said interface of management PGS-state toward changing variations of the corresponding components of the PGS-state with an optimal ratio for the main flight operations, the reducer has two stages with coaxial placement of said gain outer shaft and said gain inner shaft where said means of differential transmission are placed between these two stages, and with such composition said SG-compensator comprises:

a gain bracket mounted over said mounting base of said flange of said GS-variator, having a flat-sector shape of a mounting interface with inner radius corresponding to related outer radius of said flange, the gain bracket rotatably supports all parallel shafts of entire SG-compensator, the outer end of said gain inner shaft and the outer end of said skew steering shaft;

a gain outer shaft, which represents said gain outer shaft of said interface of management PGS-state, the gain outer shaft is supported by said gain bracket at a its inner end and at its other entry side coaxially with said gain inner shaft;

an outer reduction pinion fixed on said gain outer shaft inside said gain bracket;

an outer reduction gear meshed with said outer reduction pinion, having a rotation support around its hub in the radial and inner axial directions by a bearing inserted into said gain bracket from outside;

an outer miter gear fixed in said hub of said outer reduction gear;

an inner miter gear;

an adapter, which has a rotation support at its tail from said gain bracket and provides fixation for said inner miter gear, supporting the latter coaxially with said outer miter gear;

an inner reduction pinion fixed on said tail of said adapter;

an inner reduction gear meshed with said inner reduction pinion and fixed on said gain inner shaft;

a transverse shaft, which has a rectangular section in its center with a cross-hole to its axis and a threaded hole in the perpendicular direction;

two intermediate miter gears placed with freedom of rotation at the respective ends of said transverse shaft and with support in outer axial directions, these miter gears are meshed with said outer and inner miter gears in the differential's position;

a flanged bearing inserted into a central hole of said outer reduction gear from outside;

a compensating shaft inserted into said flanged bearing up to limit of its tail, the compensating shaft also has a rotation support at its outer end in said gain bracket, completing the rotation support of said outer reduction gear, and its tail is also inserted into said cross-hole of said transverse shaft and into central holes of said outer and inner miter gears;

a set screw screwed into said threaded hole of said transverse shaft, fixing said compensating shaft inside said transverse shaft and creating a spider of the completed differential;

a compensating gear fixed on said compensating shaft;

a compensating pinion fixed on said skew steering shaft; and

an intermediate gear mounted with freedom of rotation on said gain bracket and meshed with said compensating gear and said compensating pinion.

21. The rotor set forth in claim **1** wherein an end-rotor support ring is installed at the ends of said wings with freedom of rotation of each of said wings at its connection with said end-rotor support ring, using features and elements comprising:

a convex cross-sectional shape of said end-rotor support ring in the outer axial direction, which provides sufficient volume to accommodate other elements inside said end-rotor support ring and remains favorable for airflow;

a flat inner side in the axial direction of said end-rotor support ring;

a substantially big and flat end-wing base of each of said wings, which permits to have a tight interface with said flat inner side of said end-rotor support ring;

an end-wing fairing of each of said wings, which provides sufficient volume to accommodate other elements inside thereof and has favorable for airflow the cross-sections between its transition from airfoil section of its wing to said flat end-wing base together with having enlarged chords of its own airfoil sections in the direction of its leading edge;

plurality of equal step-holes equidistantly spaced along a center-line of said end-rotor support ring in an amount equal to the number of said wings having generally three stepping stages, where the stage with the highest diameter is located on said flat inner side of said end-rotor support ring;

a tubular flange inserted by its flanged side into the middle stage of each of said step-holes;

a secondary thrust bearing lying on the wing's side of each of said tubular flanges;

a radial needle bearing dressed on a tubular part of each of said tubular flanges after said secondary thrust bearing;

an adapter flange lying over each of said secondary thrust bearings upon entering by its centering ring into the outer stage of the respective step-hole and fixed to said end-rotor support ring by screws around its perimeter, having said radial needle bearing inside its central hole without possibility of falling out, closing that bearing by a part of its body;

a step-hole located at said flat end-wing base of each of said wings coaxially with the pivot axis of its wing, having generally three stepping stages, where the stage with the smallest diameter has on continuation thereof a threaded finalizing inside its wing;

a primary thrust bearing with a diameter higher than said secondary thrust bearing, lying in the middle stage of said step-hole of each of said wings after said corresponding adapter flange, where the latter enters in the outer stage of said step-hole of the corresponding wing by the area of said screws of its fixation and provides additional radial aligning of this bearing by a protruded part of its body;

a bolt inserted from the outside of each of said step-holes of said end-rotor support ring into said tubular flange and screwed into said threaded finalizing inside of the corresponding wing, having its head in the inside of the step-hole within the smallest diameter stage, the bolt has freedom of rotation inside said end-rotor support ring with said tubular flange altogether;

two set screws fixing each said bolt against unscrewing, using respective setup holes on both sides of the corresponding end-wing fairing; and

a seal inserted into an outside remainder of each of said step-holes of said end-rotor support ring, which seals its content from the environment, having its external surface corresponding to the surface of said end-rotor support ring.

22. The rotor set forth in claim **1** wherein, to increase rigidness thereof, at least one intermediate ring is installed in midst of said wings with freedom of rotation of each of said wings at its intersection with said intermediate ring with the possibility of transmitting torque between an inward and outward adjacent linked components of each of said wings, using features and elements comprising:

two flat sides in axial direction of said intermediate ring;

a substantially big and flat intermediate base of each of the linked components of each of said intersected wings, which permits to have a tight interface with said flat sides of said intermediate ring;

an intermediate wing fairing of each of the linked components of each of said intersected wings, which provides sufficient volume to accommodate other elements inside thereof and has favorable for airflow the cross-section between its transition from airfoil section of its linked component to said flat intermediate base together with having enlarged chords of its own airfoil sections in the direction of its leading edge;

plurality of equal holes equidistantly spaced around the center of said intermediate ring in an amount equal to the number of said wings;

a radial needle bearing inserted into each said hole of said intermediate ring and protruding slightly on both sides of said intermediate ring;

an adapter flange placed on each side of each said hole of said intermediate ring and centered on the corresponding end of said protruding respective radial needle bearing, the adapter flange has a part of its body, which prevents from going out the said respective radial needle bearing;

a step-hole located at said flat intermediate base of each of the linked components of each of said intersected wings coaxially with the pivot axis of its linked component, having generally three stages of the stepping, where the stage with the smallest diameter has on continuation thereof a threaded finalizing inside its linked component;

a thrust bearing lying in the outer stage of said step-hole of each of the linked components of each of said intersected wings after said corresponding adapter flange, where the latter provides additional radial aligning of this bearing by a protruded part of its body;

a link shaft having a central part with substantially big diameter, which enters in each of said radial needle bearings and in the middle stages of both said step-holes of said intermediate bases of corresponding linked components, and has also two symmetrical tails of smaller diameter with threaded ends, which are screwed into said threaded finalizings of the respective step-holes, having complementary right-left handing of its said threaded ends for fine regulation of a backlash between said intermediate ring and both corresponding linked components; and

two set screws fixing each side of each of said link shafts for transmitting torque, using respective setup holes on both sides of the corresponding intermediate wing fairing, these set screws also allow to use one of the linked components as a handle for fine regulation of said backlash upon alternated screwing-unscrewing of said set screws on the respective sides of said link shaft.

23. The rotor set forth in claim **22** wherein winglets are installed as the outermost linked components of said wings intersected with said at least one intermediate ring and having a wing fence at their own ends.

24. The rotor set forth in claim **22** wherein winglets are installed as the outermost linked components of said wings intersected with said at least one intermediate ring and having a longitudinal sweeping in the direction of their own leading edges, to partially compensate for the negative moments of rotation of the said wings in high speed flights performed with said rotor.

25. The rotor set forth in claim **2** wherein a cross-section of each of said wings utilizes a symmetrical airfoil having substantially low moment coefficient on 0.25 of its chord, which position is used as said pivot position, and wherein each of said wings has its trailing edge substantially protruded from the rim of said circular base of this wing, thereby preventing too large a diameter of said circular base.

26. The rotor set forth in claim **1** wherein a cross-section of each of said wings utilizes a supercritical airfoil.

27. A rotary wing aircraft generally based on the concept of performing a powered flight by performing a work against gravity using a gliding wing as a steady support, namely the "flying elevator" concept, the aircraft comprises:

a fuselage having generally streamlined elongated shape;

engine means installed on said fuselage, the operation of the engine means represents said work performing against gravity of said "flying elevator" concept;

energy supply means installed on said fuselage and connected to said engine means;

two rotors for powered flight with managed PGS-state mounted apart and transverse on the left and right sides of said fuselage, where each of said two rotors comprises:

a principal rotational element with generally round shape and generally flat surface face side having a central axis perpendicular to said face side;

a set of equal wings equidistantly mounted on the periphery of said principal rotational element and extended outside from said face side parallel to said central axis at a fixed distance from that axis, wherein each wing has ability of rotation around axis thereof located in a respective pivot position relative to the chord of this wing and parallel to said central axis;

a principal irrotational element rotatably mounted on said principal rotational element with respect to said central axis at a fixed distance therefrom, the principal irrotational element is used as a reference base for steering said wings in accordance with managed PGS-state;

a central gear having an axis parallel to said central axis, the central gear is mounted on said principal irrotational element together with means for steering said central gear in angular, radial and azimuthal directions relative to said principal irrotational element, where each respective freedom of this steering is mapped to managing the pitch, gain or skew component of said PGS-state, respectively;

a set of steering elements for each of said wings including a pitch gear having angular position of its axis generally directed toward axis of the corresponding wing from direction of said central axis, a steering pinion meshed with said pitch gear, an entry gear that is meshed with said central gear and shares common axis with said steering pinion joined to it into a respective steering cluster, having ratio of its own teeth' number to number of teeth of said central gear equal to ratio of teeth' number of said steering pinion to number of teeth of said pitch gear, means for keeping a fixed distance between the axes of said steering cluster and said pitch gear, and a transmission between said pitch gear to the corresponding wing, providing a unitary angular relation between said pitch gear and the pitch of the corresponding wing; and

means for keeping a fixed distance between the axes of said steering clusters and the axis of said central gear;

where said principal rotational element of each of said two rotors is drivingly connected to said engine means and said principal irrotational element of each of said two rotors is stationary with respect to said fuselage, the wings of said rotors represent generally the said gliding wing of said “flying elevator” concept, providing for said aircraft the desired horizontal acceleration induced by the sum of gravitic propulsions of said wings gliding relative to respective local airstreams, and also providing the desired vertically acceleration induced by the balance between the entire gravity force and respective aerodynamic forces, having respective angles of attack distributed in a manner providing the said respective aerodynamic forces to being dominated on the forward wings that have a high vertical speed, which the said concept of "flying elevator" requires, and operating that way during applying respective PGS-states to the said two rotors;

two stabilators pivotally mounted apart on the left and right sides of aft of said fuselage, with ability to control the pitch of said fuselage on background the variable external moment ratio (EMR) induced generally by the said highly loaded forward wings of said two rotors; and

locking means used to lock said two rotors against rotation when said aircraft glides.

28. The aircraft set forth in claim **27** wherein each of said two rotors has an interface of management PGS-state, represented by elements comprising:

a pitch outer shaft, which rotation is used to change the pitch of this rotor;

a gain outer shaft, which rotation is used to change the gain of this rotor in linear form;

and

a skew outer shaft, which rotation is used to change the skew of this rotor or skew and gain at the same time;

and wherein a servo and an encoder for each of said outer shafts are rotatably connected to the corresponding shaft and used to control the corresponding component of the respective PGS-state, respectively.

29. The aircraft set forth in claim **28** wherein pitch control of said two stabilators and switching of said locking means between locked and unlocked states are performed by rotation of two respective primary shafts, respectively, having a servo and an encoder for each such primary shaft, rotatably connected to each such shaft, and wherein the aircraft further comprising: an attitude sensor system, an airstream sensor system and a stabilator controller, where the stabilator controller manages the pitch of said stabilators by actuating the servo related to them to maintain a desired pitch of said fuselage relative to the ground using said attitude sensor system, or for holding said fuselage pointed to the direction of airstream using said airstream sensor system (i.e. "Stream Following" operating mode), depending on the actual flight operation.

30. The aircraft set forth in claim **29** wherein said engine means comprise two electric engines drivingly connected to said principal rotational elements of said two rotors, respectively, and wherein said energy supply means include electric sources connected to two power circuits, which are connected correspondingly to these two electric engines.

31. The aircraft set forth in claim **30** wherein said electric engines, said power circuits and said electric sources are operating in a mode of recuperation of the mechanical power provided by said two rotors, conducting the power from said electric engines toward said electric sources.

32. The aircraft set forth in claim **30** wherein each of said two rotors has on said central axis thereof a central powering shaft fixedly connected with said principal rotational element of this rotor, and said central powering shafts are drivingly connected to the respective electric engines.

33. The aircraft set forth in claim **32** wherein said central powering shafts of both rotors are fixedly connected with each other becoming a common central powering shaft and said two power circuits have a common control.

34. The aircraft set forth in claim **33** further comprising:

an encoder, which is used as a primary source for defining a target winding speed for said both rotors;

a servo, which manages the encoder; and

an engine controller, which accepts values from the encoder and manages said two power circuits for reflecting the desired target winding speed of said both rotors toward an actual winding speed of them, having a feedback thereabout, and for keeping moment of rotation induced by the acceleration of said both rotors and by aerodynamic forces on wings thereof inside limits of prescribed constraints.

35. The aircraft set forth in claim **32** wherein each of said two electric engines has generally disk-like shape with a large diameter equal to about half the diameter of the corresponding rotor, allowing to have high torque, and with small thickness, allowing to have low weight, and their own rotors are directly coupled with said powering shafts of the respective rotors, respectively.

36. The aircraft set forth in claim **35** wherein said fuselage has two rotors' sockets with generally conical shape and with a diameter generally about 40 percent higher than the height of said fuselage in their vicinity and with the alignment of their outer bases with adjacent levels of said fuselage, in which said two respective rotors are inserted from outside of said fuselage up to beginning of the wings of said two rotors, these rotors' sockets act as fairings for said two rotors while also providing additional rigidness for said fuselage, and wherein said fuselage has in its shape intermediate interfaces along intersections of its streamlined part with these rotors' sockets to smooth these intersections.

37. The aircraft set forth in claim **36** wherein said fuselage has in inside thereof on each lateral side a force plate that extends from the floor of said fuselage to the upper limits of said fuselage and has a large hole coaxial with the corresponding rotor, and the vicinity of the hole is integrally connected with the inner base of said conical shape of the corresponding rotor's socket providing additional rigidness for said fuselage, and wherein said two electric engines are respectively inserted into said holes from outside of said fuselage and fixed around the perimeter of said holes, having setup flanges around bodies thereof for this fixation, and which bodies also provide respective mounting locations for said principal irrotational elements of the respective rotors.

38. The aircraft set forth in claim **37** wherein said fuselage has respective sockets for said two electric engines, and each such engine's socket comprises:

a socket's drum, which is a ring integrally connected to the inner side of said corresponding force plate in a coaxial arrangement with said hole of the force plate, having: a diameter moderately higher than the diameter of the corresponding electric engine, small thickness and the same axial length with the axial length of the protruding electric engine part above said force plate;

a socket's back-ring, which has: an outer diameter equal to the outer diameter of said socket's drum, small thickness and an inner diameter that is slightly smaller than the diameter of said electric engine, the socket's back-ring is integrally connected to said socket's drum along its entire perimeter and generally seals the entire air volume between said socket's drum and the electric engine upon additional fixation of the inner flange of the electric engine thereto; and

a remainder of said corresponding force plate, created in inside upon integration of said socket's drum with this force plate;

and wherein said fuselage has a cooling system for each of said two electric engines, based on said engine's socket, comprising:

an entry-airflow window of said engine's socket created in the upper-forward quadrant of said socket's drum;

an air inlet located at an engine's fairing over forward streamlined part of said fuselage near an interface thereof with said engine's fairing, and having a shape substantially matching the horizontal projection of said entry-airflow window onto said engine's fairing;

an air separating plate placed generally horizontally from the bottom of said entry- airflow window to the cylindrical surface of the corresponding electric engine, generally close to its tangent, and also extending in the forward direction to the bottom of said air inlet and having a width equal to the distance between the corresponding force plate and said socket's back-ring, not allowing cold air to go down directly;

an air sealing plate placed generally horizontally from the top of said air inlet to the top of said entry-airflow window, having a width equal to said air separating plate, conducting cool air directly to said entry-airflow window together with the extending of said air separating plate;

an exit-airflow window of said engine's socket, created in the upper-forward quadrant of said socket's back-ring under said air separating plate, allowing warm air to escape from said engine's socket after it is turned around said electric engine;

an air outlet located at the backward streamlined part of said fuselage near the interface thereof with said engine's fairing after aft limit of said force plate, but more inner than the said air inlet; and

an air conducting tube placed inside said fuselage in a direction generally parallel to the ceiling of said fuselage and close to said ceiling in the direction of the aft of said fuselage, the air conducting tube is generally rectangular in any of its cross sections fixedly connected to said socket's back-ring along the perimeter of said exit-airflow window and is fixedly connected to said fuselage around the perimeter of said air outlet, conducting warm air and increasing the rigidness of said fuselage.

39. The aircraft set forth in claim **35** wherein said central powering shaft of each of said two rotors passes coaxially through a rotor of the corresponding electric engine and is fixed therein with possibility of detaching.

40. The aircraft set forth in claim **39** wherein each of said two electric engines has a hollow shaft as part of its own rotor, mounted coaxially on a remained part of this rotor, having a tubular part inserted into a corresponding hole in said remained part from inside direction of said fuselage, having a flanged part referenced as setup flange fixed to said remained part, the hollow shaft has a continuation of the tubular part at other side of said setup flange, providing said fixation for said central powering shaft inserted into a central hole thereof, and also this hollow shaft is made of high modulus alloy, which allows the use of light alloy for said remained part.

41. The aircraft set forth in claim **40** wherein each said hollow shaft has a collet clamp used for said fixation of said central powering shaft of the corresponding rotor comprising:

a fine tolerance clamping area with a thread on said continuation of tubular part, with a clamping cone at its end and with several slits around this end; and

a clamping nut, which is screwed onto the thread of said fine tolerance clamping area and has an inner cone corresponding to said clamping cone.

42. The aircraft set forth in claim **40** wherein each of said two electric engines has elements in interior thereof related to accepting of external forces, comprising:

a high load needle bearing, which is placed inside the electric engine body and provides radial support for the end of said hollow shaft at its entry side for said central powering shaft;

a lid closing interior of the electric engine from the inside of said fuselage, having a central hole with a diameter slightly larger than the outer diameter of said setup flange of said hollow shaft;

a middle load bearing, which is placed inside said lid and has an inner diameter generally equal to the diameter of the central hole of said lid, the middle load bearing provides radial and inner axial supports for said remained part of the rotor of the electric engine; and

a low load bearing, which is placed inside the electric engine body, overlapping in axial position said high load needle bearing, the low load bearing provides radial and outer axial supports for said remained part of the rotor of the electric engine.

43. The aircraft set forth in claim **40** wherein said locking means on side of each of said two rotors have a locker comprising:

a drum, which is fixed on said setup flange of said hollow shaft of the corresponding electric engine;

a band brake, which includes a band with a frictional lining inside, corresponding to said drum and pivotally fixed at one end thereof on the electric engine, and a pulling lever pivotally connected to the other end of said band at one end thereof, having a groove follower at the other end and pivotally mounted on the electric engine;

a main bracket fixed on the electric engine;

an outer locking shaft, which has a rotation support on said main bracket;

a screw, which is fixed on said outer locking shaft within said main bracket;

a guide rod, which is fixedly mounted on said main bracket, having an axis parallel to the axis of said screw; and

a threaded lead, in which said screw is screwed and which has an additional hole accepting said guide rod, the threaded lead has an open groove in direction perpendicular of axis of said screw into which said groove follower of said pulling lever of said band brake is inserted, providing precise control of said band brake.

44. The aircraft set forth in claim **43** wherein said locker is selected on one side as the main one and its outer locking shaft is rotatably connected to one of said primary shafts, which is used to switch said locking means between locked and unlocked states, and wherein said locker is selected on the opposite side as the dependent other and its outer locking shaft is rotatably connected to said outer locking shaft of said main locker by using two pairs of meshed miter gears.

45. The aircraft set forth in claim **37** wherein for each of said two rotors a PGS gearbox exists and placed near the floor of said fuselage, between said corresponding rotor's socket and said corresponding force plate, comprising:

a body, which is fixed to the corresponding force plate;

three coupled shafts for all said components of said PGS-state of the corresponding rotor, each of these coupled shafts has a rotation support in the body and is oriented vertically;

three primary shafts for all said components of the PGS-state, each of these primary shafts has a rotation support in the body and is oriented horizontally; and

three pairs of meshed miter gears, which are fixed on said respective coupled and primary shafts, rotatably connecting such coupled and primary shafts, respectively;

and wherein elements and features accompany said PGS gearbox, comprising:

three PGS couplings, which connect all said outer shafts of said interface of management PGS-state of the corresponding rotor with respective coupled shafts of said PGS gearbox, respectively;

three windows in the rotor's socket for all said outer shafts, in which said outer shafts enter freely and respectively upon axial movement of the rotor in time of setup, and in which said PGS couplings rotate freely; and

three windows in the force plate, which are aligned with said three windows of the rotor's socket respectively, these windows are used to assist in mounting of said PGS couplings upon setup of the rotor.

46. The aircraft set forth in claim **27** wherein the pitch control of said two stabilators has elements comprising:

a common pivot shaft connecting said two stabilators to each other;

a worm gear fixed on said common pivot shaft;

a worm bracket mounted on said fuselage, the worm bracket has an extension for accepting additional support from said common pivot shaft, ensuring a fixed distance from said common pivot shaft;

a steering shaft, which has a rotation support in said worm bracket;

a worm fixed on said steering shaft and meshed with said worm gear;

a primary stabilator pitch shaft, which is used as a handling interface for the pitch control of said two stabilators; and

a universal joint, which rotatably connects said steering shaft with said primary stabilator pitch shaft.

47. The aircraft set forth in claim **29** wherein said airstream sensor system comprises:

a Stream Deviation Tube (SDT) mounted on the nose of said fuselage, the SDT reflects a deviation of the airstream from its horizontal plane as a difference in a pair of pressures at its respective pneumatic outputs, where one of such outputs represents upward pressure and the other represents downward pressure; and

a pair of electric sensors respectively connected to said pair of pneumatic outputs of said SDT, the sensors convert the corresponding pressures into electrical signals used as the output signals of said airstream sensor system.

48. The aircraft set forth in claim **34** wherein a central computer has interfaces for management all said servos and encoders directly or indirectly on behalf of the respective controllers.

49. The aircraft set forth in claim **34** wherein two racks are placed inside said fuselage near to said two electric engines, respectively, these racks have said electric sources fixed on their shelves and are movable along said fuselage to adjust the center of gravity of said aircraft depending on load variation and for additional assistance to said stabilator controller.

50. The aircraft set forth in claim **48** wherein said airstream sensor system is capable of measuring true aerodynamic speed (TAS), and when said stabilator controller operates in said "Stream Following" mode, said central computer interprets handling commands expressed as biangular values for respective handling rotors into respective PGS-states, using the measured TAS value from the airstream sensor system and said actual winding speed of said both rotors from said engine controller.

51. The aircraft set forth in claim **36** wherein said energy supply means include a power plant based on a combustion engine with an electricity generator installed inside the aft compartment of said fuselage, with associated elements comprising:

a fairing with an air inlet, which is spanned between said two rotor's sockets above the ceil of said fuselage and continues in the aft direction; and

an air-conducting envelope, which accepts air through its entry hole located inside said fairing with an air inlet, directs air toward said combustion engine for cooling and breathing, and conducts exhaust of said combustion engine and hot air toward a trailing edge of said fuselage, the air-conducting envelope wraps said combusting engine, generally having said electricity generator outside thereof, and has an air outlet at the trailing edge of said fuselage.

52. The aircraft set forth in claim **50** wherein said fuselage has a cabin with a cockpit that has handling elements comprising:

a display of said central computer;

a joystick connected to said central computer, which is used as the primary handler on the pilot side, providing commands based on variations of the biangular values for the respective handling rotors upon interpretation its movements by said central computer, assuming intuitive and convenient characteristics of such movements;

a lock command button, which sends a command to said central computer to actuate said encoder corresponding to said engine controller toward the position corresponding to zero of said target winding speed of said both rotors;

a pair of buttons for increasing-decreasing the target winding speed by actuating said encoder corresponding to said engine controller in the respective directions; and

a versatile command pad from buttons, which is used for customization of handling said aircraft and for management said central computer;

and wherein said central computer automatically locks said both rotors with zero target winding speed if the magnitude of said actual winding speed is below a prescribed threshold value.

53. The aircraft set forth in claim **52** wherein said cockpit further has handling elements reflected in commands of said central computer, comprising:

a handling control capture button on said joystick, which is used to enable movements commands from said joystick with initial remembering of its absolute position and states of biangular handling or PGS-states of said two rotors depending on particular flight operations;

a pad of common handling of skew, opposite angle, biangular gain and the main angle of both rotors at the same time, having a pair of increasing-decreasing buttons for each of such handling parameters; and

a pad of in turn handling, which based on the differential handling of mixed biangular gains and the collective angles of said two rotors, the pad has buttons related to the biangular gain in the corners of its quad, and buttons associated with the collective angle on the sides of its quad, here the bottom corners buttons decrease the biangular gain for the same side rotor with same increase on the opposite side, and the upper corners buttons perform the opposite action, here, also, the center sides buttons decrease the collective angle for the same side rotor with same increase on the opposite side, and the vertical center buttons act as a complement for the buttons of said pad of common handling, providing an additional pair of buttons for common handling of collective angles.

54. The aircraft set forth in claim **53** wherein said skew outer shaft of each of said two rotors is used only to change the skew, and wherein a set of trimmers rotatably and respectively connected to said all respective servos and encoders of the handling components to enable manual handling of such respective components by mechanical means in the interior of each such a trimmer with high accuracy is included comprising:

two P-trimmers, which manage the pitches of the PGS-states of the respective rotors, each P-trimmer has a general scale with a range from -180° to 180°, which occupies full circle, and has a tics distance on a highest precision scale in order of 0.1°;

two G-trimmers, which manage the gains of the PGS-states of the respective rotors, each G-trimmer operates over the linear normalized gain, having a general scale with a range from -100% to 100%, and has a tics distance on a highest precision scale in order of 0.1%, also each G-trimmer has an overall indication of the gain or indications of pitch deviations at the main and opposite points on the skew direction;

two S-trimmers, which manage the skews of the PGS-states of the respective rotors, each S-trimmer has a placement of its scales equal to the placement of any of said P-trimmers;

a WST-trimmer, which manages said target winding speed of said engine controller, the WST-trimmer has a general scale with a positive segment about two times longer than the negative segment, and has a tics distance on a highest precision scale no worse than 0.1m/s;

an SP-trimmer, which manages the pitch of said two stabilators, the SP-trimmer has a general scale with a range about from -30° to 30°, and has a tics distance on a highest precision scale in order of 0.1°, also the SP-trimmer has an indication of an actual position of said two stabilators by a pictogram of section of a typical airfoil; and

an L-trimmer, which manages the lock state of said locking means, the L-trimmer has a general scale with a range about from -20% to 100%, where 0% reflects state when said locking means begins actual braking of said two rotors, and full range thereof reflects full excursion of braking elements of said locking means.

55. The aircraft set forth in claim **54** wherein said trimmers are placed on said cockpit together with accompanied elements comprising:

a pair of increasing-decreasing buttons for each said trimmer, which are used to electromechanically change the value of the corresponding handling component by actuating the corresponding servo, these buttons are placed near the corresponding trimmer (trimmer-buttons);

four locking knobs (L-knobs), which are placed only near the S-trimmers and G-trimmers as an outer interface of their internal locking systems and are used for locking the respective trimmers during the manual handling against possible mutually induced rotations of said outer shafts of rotors for the skew and gain components, these locking knobs are handled manually by turning between a locking and non-locking positions and said respective internal locking systems are under automatic unlocking in case of non-manual handling;

three pairs of increasing-decreasing buttons for changing the pitch, gain and skew respectively and simultaneously for said both rotors electromechanically by actuating the respective servos (pairs of common P- G- S- buttons);

a high speed button (HS-button) used for enabling high speed actuation for servos of pitch and skew, which action is applicable during runway operations;

a pitch follows skew switch (S->P-switch) used for enabling said P-trimmers to follow said S-trimmers with same speed and direction after respective changes of said S-trimmers during pressing any button from said pair of common S-buttons, which action is applicable during runway operations;

two sets of differential P- G- S- buttons, which are placed apart on respective sides related to said two rotors and are used to decrease the pitch, gain or skew, respectively, for the same side rotor with the increase on the opposite side, electromechanically by actuating the respective servos;

a Stream Deviation Indicator (SDI), which is connected to said airstream sensor system and reports a deviation of the airstream relative to horizontal plane of said aircraft, the SDI is used as feedback upon the manual handling of said SP-trimmer and to indicate the efficiency of the automatic controlled loop of said stabilator controller;

a WSA-indicator, which is connected to said engine controller and reports said actual winding speed of said two rotors;

an RPM-indicator, which is connected to said engine controller and reports the actual RPM of said two rotors;

an MR-indicator, which is connected to said engine controller and reports said variable EMR on said common central powering shaft of said rotors, which value is normalized to a particular total weight of said aircraft;

an SF-switch, which is used for turning on said "Stream Following" operating mode of said stabilator controller;

an EC-switch, which is used for managing the power status of said engine controller; and

a CM-switch, which is used for turning on the management over all trimmers from the side of said central computer.

56. The aircraft set forth in claim **55** wherein said cockpit has an indicator panel oriented generally vertically, which is used to accommodate standard standby instruments of an airplane with the following said elements of said cockpit: the display, EC-switch, WSA-indicator, RPM-indicator and MR-indicator, and wherein said cockpit has also a control panel, sloped generally on 45 degrees and placed under the indicator panel as its continuation, having all said remained elements of said cockpit with placement, shaping and features comprising:

all elements of the computer management based on buttons are placed just below said display, having said pad of common handling in the center from said display and in the center from the pilot;

said joystick is placed on a pad, which is hanged on a concave support from the center of said control panel just below said pad of common handling;

said two sets of differential P- G- S- buttons are placed on said control panel on the respective sides from said concave support, having said P-buttons in the inner-most positions and said G-buttons in the outer-bottom positions, and all these buttons have bottom arrowed shapes for a hint of their decreasing effect, where the P- and G- buttons additionally have an outward offset in the shapes of their bottom-arrowed ends for a hint of their turn effect;

said pairs of common P- G- S- buttons and said HS-button are placed on said pad of joystick forward from said joystick, having said P-buttons in the center and said HS-button between the pairs of the P- and S- buttons for a hint of scope of effect of said HS-button;

said S->P-switch is placed on a rim of said pad of joystick near said pair of common S-buttons for a hint of the accompanied control used with this activated S->P-switch;

said two sets of P- G- S- trimmers are placed on said control panel on the respective sides from position of said display in the corners of triangles, having the P-trimmers in the inner-bottom positions and the G-trimmers in the outer-middle positions for a hint of maximal impact of the latter trimmers on the flight turn operations;

said trimmer-buttons for P- G- S- trimmers are placed generally in the inner-bottom positions from the respective trimmers, having their decreasing buttons at bottom with a different inclinations from vertical with the lower buttons on outside, which hints at the different impact of respective components on the flight turn operations, as well as on the normal turn side, so the trimmer-buttons for G-trimmers have maximal inclinations and such buttons for S-trimmers are upright;

said L-knobs are placed generally in the upper-outer positions from the respective trimmers, minimizing an effect of possible obstruction from there;

said WST-trimmer is placed in the upper-outer position from the pilot on the inner-most side of said control panel under said WSA-indicator from said indicator panel, having said trimmer-

buttons in the upper-inner position;

said SP-trimmer is placed under said WST-trimmer, having said trimmer-buttons in the bottom-inner position;

said SDI is placed under said SP-trimmer, alluding to its feedback control;

said SF-switch is placed in the upper-inner position from said SDI, hinting at the possibility of linking the stabilator's pitch managed by said stabilator controller to the remaining deviation on the SDI;

said L-trimmer is placed at bottom of the inner-most side of said control panel under said G-trimmer, having the trimmer-buttons in the upper-inner position; and

said CM-switch is placed at top of the inner-most side of said control panel over said G-trimmer and are oriented horizontally, having the enabling direction pointed to said display for a hint of the enabling state of the computer management.

57. The aircraft set forth in claim **54** wherein said P- G- S- trimmers for each respective rotor share a common case with an equilateral triangular placement for compactness.

58. The aircraft set forth in claim **52** wherein said fuselage has a vertical stabilizer with a rudder, and said cockpit has two pedals for steering said rudder with an appropriate connectivity.

59. The aircraft set forth in claim **36** wherein said fuselage has two parking wheels that are rotatably mounted on two respective retractable parking supports resided on lateral sides of said fuselage and occupying the interior space near aft vicinity of said rotor's sockets, these parking supports are oriented and retracting generally in the vertical direction, made of light alloy tube, and each of such parking supports has accompanied features and elements comprising:

a slotted end having a slot for the corresponding parking wheel in the center plane of the end of this parking support and rounded with a radius equal to about half of its remaining lateral length;

an axle on which the corresponding parking wheel is mounted inside said slotted end, which is fixed on the sides of said slotted end;

a guide mounted on said fuselage, having a vertical hole for this parking support, retaining it in the transverse directions and allowing it to slip vertically;

a keying rib mounted along the rear side of this parking support and entered in a corresponding slot of said guide, preventing rotation of this parking support;

a retracting screw aligned with the axis of this parking support;

a threaded complement mounted inside this parking support, having said retracting screw screwed inside thereof;

a heel fixed on the upper side of said fuselage, providing a rotation support for said retracting screw;

a servo with gear means rotatably connected with said retracting screw; and

a parking hatch pivotally mounted on said fuselage with the possibility of opening outside upon a pushing force of the corresponding parking wheel and with the retracting back by a spring.

60. The aircraft set forth in claim **33** wherein an active vibration reduction system (VRS) is included to partially decrease vibrations induced generally by the remaining variations of an overall steering moment of the wings of said two rotors over time of changing the minor phase of rotation of these rotors, the system comprises:

a minor phase sensor, which provides a synchronization signal of the minor phase of these rotors upon detecting occurrences of crossing a zero-phase point by any wing of these rotors;

a pattern store, which stores compensating patterns related to respective flight operations and respective load states; and

a pattern generator, which is connected to said minor phase sensor and to said pattern store, and plays an active pattern from it, synchronized and time-scaled with said synchronization signal of the minor phase from said minor phase sensor, the pattern generator passes an output pattern signal to said two power circuits for obtaining the desired level of representation of such a signal in the currents of coils of said two electric engines.

61. A trimmer for high-precision control and indication of bidirectional values of a steering of a handled element through a rotation transmission, comprising:

a case having generally cylindrical shape, closed only from bottom and having outside on its other end fixtures for attaching said trimmer under a corresponding hole of a control panel of a cockpit;

a primary shaft having a rotation support in the bottom of said case when entering from the outside and used to transmit a rotation state to said handled element or to return it back;

a primary rotating can mounted coaxially inside said case with a rotation support on the bottom thereof, the primary rotating can has a handling ring around its face side;

a primary rotating scale having the shape of a ring, mounted coaxially inside said handling ring of said primary rotating can or is an integral part thereof, the primary rotating scale has tics and radially oriented labels with the highest precision that serve the negative values of said steering, and their zero label is used as an arrow for positive values, by having a frame in the form of an arrow;

a handle mounted on said handling ring of said primary rotating can, having a face level below the face level of said case, and being retractable up over the level of said control panel, having a rotation support in this retracted state, the handle is used for manual handling of said trimmer by fingers;

at least one ring-shaped steady scale or shield mounted coaxially on said case, each having a face level that is the same as for said primary rotating scale, where the innermost steady shield has a scale along its outer perimeter and a general scale along its inner perimeter, which exposes a full range of values for said trimmer, and where each steady scale or said outer scale of each shield serves the positive values of said steering, and the scale for the outermost such scale or shield has the same placement of tics and horizontally oriented labels as for said primary rotating scale, using the reading against said arrow from said primary rotating scale, and in another case an intermediate rotating scale is assumed in an outer neighborhood with the similar placement rules as for said primary rotating scale, and the zero value of said steady scale or of the outer scale of said shield serves as an arrow for the corresponding rotating scale for the negative values of said steering;

at least one rotating scale or shield with the shape of a ring or circle, mounted coaxially on said case with a rotation support, each having a face level that is the same as for said primary rotating scale, where any rotating scale serves as said assumed corresponding intermediate rotating scale for the negative values, and where the outermost rotating shield is placed inside said innermost steady shield and depicts an arrow that points to the respective values of said general scale;

a set of gear means, where each member thereof transmits rotation from a respective said outer rotating scale or shield, including said primary rotating scale, to a corresponding next said inner rotating scale or shield with desired reducing, serving all said rotating elements; and

gear means of the primary stage, which transmit rotation of said primary rotating can to said primary shaft and vice versa.

62. The trimmer set forth in claim **61** wherein said steady and rotating scales or shields and said set of gear means are accommodated for an intermediate level of indication by including elements comprising:

a primary steady scale placed inside said primary rotating scale;

an intermediate rotating scale, placed inside said primary steady scale;

a steady shield placed inside said intermediate rotating scale, having an intermediate steady scale along its outer perimeter;

a central rotating arrow shield placed inside said steady shield;

gear means of the secondary stage, connecting said primary rotating can and said intermediate rotating scale; and

gear means of the tertiary stage, connecting said intermediate rotating scale and said central rotating arrow shield.

63. The trimmer set forth in claim **61** wherein a functionality for mapping of low-precision alternative values exists with features and elements comprising:

at least one window in said innermost steady shield with a thin arrow or a line on the outside for reading an indication inside it; and

at least one mapping shield with the shape of a ring, coaxially joined with said outermost rotating shield, having a face level below said innermost steady shield and having an alternative sectorial scale, partially observed from the respective said window in this steady shield.

64. The trimmer set forth in claim **63** wherein two windows for two respective variants of said alternative values exist in said innermost steady shield within different radial positions and non-overlapped angular segments thereof, and two respective alternative scales are placed on said mapping shield, respectively.

65. The trimmer set forth in claim **61** wherein said steady and rotating scales or shields and said set of gear means are accommodated for having an indication of the actual position of said handled element by including elements comprising:

a steady shield placed inside said primary rotating scale, having a primary steady scale along its outer perimeter;

a rotating arrow shield placed inside said steady shield;

a central rotating shield of the actual position, placed inside said rotating arrow shield, the central rotating shield of the actual position has a pictogram of said handled element, the angular position of which is equal to the angular position of said handled element relative to a common base;

gear means of the secondary stage connecting said primary rotating can and said rotating arrow shield; and

gear means of the tertiary stage connecting said rotating arrow shield and said central rotating shield of the actual position.

66. The trimmer set forth in claim **61** wherein said rotation support of said primary rotating can has elements and features comprising:

a central axle of the case being an integral part of said case and protruding from said bottom thereof toward the interior thereof in a coaxial position, the central axle of the case has a threaded hole on its axis;

a spacer ring;

two bearings dressed on said central axle of the case, separated by said spacer ring that is dressed on said central axle of the case, the bottom bearing has an axial support at its inner ring at said bottom of said case, and the upper bearing has its upper level equal to the upper level of said central axle of the case;

a tail of the primary rotating can being an integral part of said primary rotating can as a continuation from its bottom toward the down, the tail has a central hole with a small inner ring area inside, which separates the outer rings of said two bearings inserted into this hole; and

a long central axle screwed into said threaded hole of said central axle of the case and having a flange that rests on top of said central axle of the case, providing an upper axial support for the inner ring of said upper bearing;

and wherein said gear means of the primary stage comprises:

a primary central gear fixedly mounted on said tail of the primary rotating can; and

a primary pinion fixedly mounted on said primary shaft and meshed with said primary central gear.

67. The trimmer set forth in claim **61** wherein a rotating arrow shield is placed inside said innermost steady shield together with gear means of the secondary stage connecting said primary rotating can and said rotating arrow shield, and all such shields inside said primary rotating can have support elements comprising:

a long central axle mounted coaxially on said case and protruding in interior of said primary rotating can, the axle has a threaded segment in its middle, a tail above the threaded segment and a coaxial threaded hole on top;

a primary steady can that is coaxially mounted on said threaded segment of said long central axle by clamping a bottom of this can between two nuts, the primary steady can has a thickened area on its rim, which is used for mounting said steady shield;

a secondary rotating can that is coaxially mounted on said tail of said long central axle with a rotation support, the secondary rotating can has a thickened area on its rim, which is used for mounting said central rotating arrow shield;

and

a screw with a washer screwed into said threaded hole of said long central axle, providing the upper axial support for said secondary rotating can;

and wherein said gear means of the secondary stage have elements comprising:

a flanged primary central pinion dressed on said long central axle and attached to the bottom of said primary rotating can, utilizing its flange for this fixation, the flanged primary central pinion does not touch said long central axle by its own central hole;

a secondary shaft crossing a bottom of said primary steady can, having rotation support therein;

a secondary gear fixed on the lower end of said secondary shaft and meshed with said flanged primary central pinion;

a secondary pinion fixed on the upper end of said secondary shaft; and

a secondary central gear mounted coaxially on the bottom of said secondary rotating can and meshed with said secondary pinion.

68. The trimmer set forth in claim **67** wherein all the gears of said gear means of the secondary stage are made of plastic, having accompanied features and elements comprising:

low friction hubs of said secondary gear and said secondary pinion, which provide axial support of said secondary shaft;

a low friction central hole of said secondary central gear, which provides radial support for said secondary rotating can; and

a low friction plastic washer placed between the upper nut of said two nuts and said secondary central gear for the lower axial support of said secondary rotating can, the plastic washer can be manufactured as an integral part of said secondary central gear.

69. The trimmer set forth in claim **62** wherein said scales and shields inside of said primary rotated can have support elements comprising:

a long central axle mounted coaxially on said case and protruding in interior of said primary rotated can, the axle has a primary threaded segment in its middle, a tail above the primary threaded segment, a secondary threaded segment in the middle of the tail, a short tail after the secondary threaded segment and a coaxial threaded hole on top;

a primary steady can that is coaxially mounted on said primary threaded segment of said long central axle by clamping a bottom of this can between two primary nuts, the primary steady can has a thickened area on its rim, which is used for mounting said primary steady scale;

a secondary rotating can that is coaxially mounted on said tail of said long central axle with a rotation support, the secondary rotating can has a thickened area on its rim, which is used for mounting said intermediate rotating scale;

a secondary steady can that is coaxially mounted on said secondary threaded segment of said long central axle by clamping a bottom of this can between two secondary nuts, the secondary steady can has a thickened area on its rim, which is used for mounting said steady shield;

a rotating flange mounted coaxially on said short tail of said long central axle with a rotation support, the rotating flange is used for mounting said rotating arrow shield; and

a screw with a washer screwed into said threaded hole of said long central axle, providing the upper axial support for said rotating flange, these screw with washer are located inside a corresponding hole of said rotated flange;

and wherein said gear means of the secondary and tertiary stages have respective elements comprising:

a flanged primary central pinion dressed on said long central axle and attached to the bottom of said primary rotating can, utilizing its flange for this fixation, the flanged primary central pinion does not touch said long central axle by its own central hole;

a secondary shaft crossing the bottom of said primary steady can, having rotation support therein;

a secondary gear fixed on the lower end of said secondary shaft and meshed with said flanged primary central pinion;

a secondary pinion fixed on the upper end of said secondary shaft;

a cluster of secondary central gear and pinion attached coaxially from the outside to the bottom of said secondary rotating can, having its pinion inside the interior of said secondary rotating can, and having its central gear meshed with said secondary pinion;

a tertiary shaft crossing the bottom of said secondary steady can, having rotation support therein;

a tertiary gear fixed on the lower end of said tertiary shaft and meshed with the pinion element of said cluster of secondary central gear and pinion;

a tertiary pinion fixed on the upper end of said tertiary shaft; and

a tertiary central gear attached coaxially to the bottom of said rotating flange and meshed with said tertiary pinion.

70. The trimmer set forth in claim **69** wherein all the gears of said gear means of the secondary and tertiary stages are made of plastic, having accompanied features and elements comprising:

low friction hubs of said secondary gear and said secondary pinion, which provide axial support of said secondary shaft;

a low friction central hole of said cluster of secondary central gear and pinion, which provides radial support for said secondary rotating can;

a low friction plastic washer placed between the upper nut of said two primary nuts and said cluster of secondary central gear and pinion for the lower axial support of said secondary rotating can, the plastic washer can be manufactured as an integral part of said cluster of secondary central gear and pinion;

low friction hubs of said tertiary gear and said tertiary pinion, which provide axial support of said tertiary shaft;

a low friction central hole of said tertiary central gear, which provides radial support for said rotated flange;

a low friction plastic washer placed between the upper nut of said two secondary nuts and said tertiary central gear for the lower axial support of said rotating flange, the plastic washer can be manufactured as an integral part of said tertiary central gear.

71. The trimmer set forth in claim **61** wherein the interior of said primary rotating can is sealed using features and elements comprising:

a nest inside said handling rim of said primary rotating can above a face level of said primary rotating scale;

a rubber ring placed on the bottom of said nest along its periphery;

a glass lid inserted into said nest and lying on said rubber ring; and

a ring retaining said glass lid, fixed on the top of said handling rim of said primary rotating can, this ring has a hole corresponding to said handle.

72. The trimmer set forth in claim **61** wherein said handle and said primary rotating can have features and elements comprising:

a head at the top of said handle, having a substantially increased diameter;

a hole in said handling rim of said primary rotating can into which said handle is inserted from above and rests on said head with the possibility of pulling by fingers;

a tail as a continuation of said handle below the lower level of said handling rim;

a threaded hole on the axis of said tail from the bottom;

a tube dressed on said tail with the possibility of free rotation, the tube has an outside diameter matched to the diameter of said hole of said handling rim to retain the tube against rotating and to retain said handle against falling down in the retracted up position; and

a screw with a washer screwed into said threaded hole of said tail, where the outer diameter of the washer is substantially higher than the diameter of said hole of said handling rim to retain said handle inside said trimmer and to support said tube against falling out.

73. The trimmer set forth in claim **61** wherein a locking system is included with said trimmer, with a locking knob on said control panel, and this locking system also has features and elements comprising:

locking needles equidistantly mounted on said primary rotating can or on a continuation thereof, around perimeter thereof, and outward from the center thereof in a non-obstructed area of said case;

a window on the periphery of said case, aligned with the level of said locking needles;

a locking bracket mounted on the periphery of said case, having an interface of the interior thereof with said window;

a solenoid mounted inside said locking bracket with its axis directed toward said window;

a locking wedge having magnetic tail inserted into said solenoid, the locking wedge can enter said window with positioning between a pair of adjacent locking needles, performing actual locking, also it can be pulled out said window when the power applies to said solenoid;

a spring dressed on said tail of said locking wedge having a back support on a flange of said solenoid, the spring pushes said locking wedge toward its locking position;

a rigid wire connected to the end of said tail of said locking wedge and passing through a hole in the mounting place of said solenoid in said locking bracket;

a soft string attached to the end of said rigid wire, the soft string unlocks said trimmer when the other end of this string is pulled;

a pulley mounted on said locking bracket with the possibility of free rotation, the pulley guides said soft string in the direction of said locking knob;

a bracket of said locking knob mounted under said control panel near said trimmer;

a pulley of said locking knob mounted on said bracket of said locking knob with the possibility of free rotation, the pulley receives the other end of said soft string from the side of said locking bracket;

a shaft of said locking knob mounted with a rotation support inside said bracket of said locking knob and having a tail protruding above a face level of said control panel passing through a corresponding hole, the opposite end of said soft string is attached to a middle segment of this shaft, the shaft pulls said soft string with its own rotation, and said soft string is wound on said middle segment in a clearance area around this wound soft string;

a shaft snapping system placed inside said bracket of said locking knob and providing a snapping with some force of said shaft in two angular positions associated with the locking and non-locking states of said locking knob; and

a handle of said locking knob fixed on a tail of said shaft and having a pointer that indicates the actual lock state of said locking knob.

74. The trimmer set forth in claim **61** wherein a servo is mounted outside on said bottom of said case, the servo provides rotation of said primary shaft and the said steering of said handled element by using gear means mounted on said bottom of said case.

75. A Stream Deviation Tube (SDT) for detecting airstream deviations from the symmetry plane of this tube in the direction of its pitch and in the form of two pressures, the SDT assumes its use by installing on the forward of a fuselage of an aircraft to detect deviations of said fuselage from a “stream following” position, and the SDT comprises:

a consoled base, which is used to position the forward end of said SDT at a desired distance from said fuselage, the consoled base has a generally tubular shape with a conical transition to a small diameter at its forward end;

a tubular case mounted at the forward end of said consoled base and having an outside diameter corresponding to said conical transition of said consoled base;

a forward flange mounted on the forward end of said tubular case and having an outside diameter equal to the outside diameter of said tubular case, the forward flange has a symmetrical shape when viewed in the lateral direction, with two equal slopes at angle of about 40 degrees from its symmetry plane in the pitch direction, having an entry channel on the center of each of said slopes with a continuation to a corresponding output socket at a mounting base of said forward flange;

two pressure output tubes, which are mounted inside said consoled base and provide upward and downward pressures at their outputs; and

a system of pressure conduction, which conducts pressures from said output sockets of said forward flange to the said respective pressure output tubes, respectively.

76. The SDT set forth in claim **75** wherein said tubular case has a transverse support by inserting into a corresponding hole in said conical narrowing of said consoled base, and said system of pressure conduction and entire mechanical connectivity have features and elements comprising:

a collector having a circular flanged shape and mounted inside said consoled base at a rearward vicinity of said conical transition, the collector has the two said pressure output tubes brazed inside its two corresponding holes, and the collector also has two other holes for its own fixation;

a backward flange mounted inside said consoled base at a middle vicinity of said conical transition between said collector and said tubular case and inserted into said tubular case by a short own centering area, the backward flange has two holes, the forward sides of which have entry sockets, and the backward sides have a respective connectivity to the said holes of collector for pressure output tubes, providing pressure transfer from the short base between said entry sockets to an enlarged base between said pressure output tubes, and also has two other holes for its own fixation, which coincide with the respective said fixation holes of said collector;

a centering area created on said mounting base of said forward flange, which is inserted into the forward end of said tubular case, providing transverse support for said forward flange;

two threaded holes at said centering area of said forward flange, axially corresponding to the said two respective fixation holes of said collector;

two tubes for upward pressure and downward pressure inserted into the respective said output and entry sockets between said forward flange and said backward flange; and

two long bolts inserted from backward of said collector into the respective said fixation holes of said collector and of said backward flange, these bolts are screwed into the respective said threaded holes of said forward flange, providing fixation for said forward flange, said tubular case, said backward flange and said two tubes for both pressures.

77. The SDT set forth in claim **76** wherein said two bolts and their respective holes are arranged in a vertical plane, said output sockets of forward flange and said entry sockets of backward flange are arranged in a horizontal plane, each of said two tubes for pressures is divided into two parts with a gap between them in the middle, and an anti-icing and moisture eliminating system is included with features and elements comprising:

a moisture collector placed in said gap between the forward and backward pairs of said divided pressure tubes, which are inserted into its corresponding entry sockets, respectively, the moisture collector has generally cylindrical shape with a diameter equal to the inner diameter of said tubular case with two mounting holes for said two long bolts, and also has two internal laterally-symmetrical cavities in its middle, which are opened to the bottom and lateral directions, having a separation by a thick wall with the bottom mounting hole inside and by a thin wall under it, where moisture is collected, and said cavities are connected by respective holes to said entry sockets of said moisture collector on both sides;

a sealing lid having a tube segment shape, complementing the perimeter of the middle section of said moisture collector to a completed circle and sealing said both cavities of said moisture collector by using a sealant, having an interface with said thin wall of said moisture collector, in the vicinity of which two drain holes with a symmetrical arrangement are created for the respective said two cavities;

two drain holes created in the bottom of said tubular case, coinciding with said two drain holes of said sealing lid; and

two electric heaters placed inside said tubular case on each side of said moisture collector, wrapping by their tubular bodies the forward and backward pairs of said divided pressure tubes and the said two long bolts, these two heaters are complemented with two electrical wires passing through said collector and have a desired electrical connectivity between them and said two electrical wires using corresponding holes created in said moisture collector, said backward flange and said collector.

78. The SDT set forth in claim **77** wherein the pressure connectivity in said forward flange and said backward flange has features and elements comprising:

two horizontal channels of the forward flange going from said respective output sockets inside the body of said forward flange to about the middle of the thickness of the body;

two diverting channels of the forward flange drilled from the cylindrical surface of said forward flange to its interior, lying in a cross-section plane thereof and connecting said two horizontal channels with said respective entry channels, also having an inclination to the horizontal plane of about 45 degrees;

two seals of the diverting channels sealing the outer-ends of said respective diverting channels from the environment, restoring the original cylindrical shape of said forward flange; and

two diverting channels of the backward flange created on the back side of said backward flange, having 90-degrees sectors for restoring the sites of pressure exit to the originating up-down positions, providing vertical alignment for said two pressure output tubes with a convenient direct geometric relationship between said two entry channels of said forward flange and said two pressure output tubes.

79. A system of methods of operation and handling of an aircraft having two sets of equal wings placed apart on the sides of a fuselage of the said aircraft and involved in collective movement along a fixed loop relative to the central plane of said aircraft with a common and changeable winding speed of said wings along said loop with variable steering of the pitches of said wings for different phases along said loop, and where, for a ground based reference frame, the magnitude of variations of the said steering of pitches does not exceed 90 degrees, but the collective steered pitch of all said wings can have any arbitrary value in the range from -180 degrees to 180 degrees, and also where said aircraft is accommodated for normal operations by means for maintaining a controlled pitch of said fuselage, upon having the value of the overall driving force used for said collective movement of said wings, lying in the range between 15 and 85 percent of the entire weight of said aircraft generally, the system comprises methods of:

on the runway acceleration, comprising the steps of:

setting a distribution of the pitches of said wings along said loop, which has a high angle of attack relative to the sum of said winding speed, the anticipated ground speed and the anticipated inflow related to the anticipated thrust about 40 percent of the entire weight of the said aircraft, for a phase of the forward wings those dominate in said thrust, has at least a moderate negative angle of attack for a phase of the backward wings, and also has intermediate pitches between these two phase points;

establishing a high positive winding speed, where the positive direction is defined as the direction when the upper wings move forward, and keeping said distribution of pitches in accordance with the change in ground speed, having an acceleration of about 0.3g with a desired margin; and

progressively decreasing said positive winding speed upon increasing of ground speed with a corresponding change of said distribution of pitches toward a gradual increase in the vertical thrust component, while maintaining high acceleration and having the consumed power close to the maximal value designed for said aircraft;

flight handling, comprising the steps of:

establishing said fuselage in the direction of the flight path of said aircraft or with some other controlled angle in the case of proximity to the ground, and continuing to retain the state of said fuselage, against changing the pitch moment of said aircraft, induced by said variable driving force, using said means for maintaining a controlled pitch of said fuselage;

setting a distribution of the pitches of said wings along said loop generally in accordance with the "flying elevator" concept and the forward dominating wings, i.e. having the angles of attack inducing a high load on the loop's segment tied to the wings with a high vertical speed and placed more forward, and correspondingly, having the angles of attack inducing a low load on the loop's segment tied to the wings with a high vertical speed and placed more backward;

adjusting said distribution of the pitches of said wings to provide a desired horizontal acceleration of said aircraft induced by the sum of gravitic propulsions of all said wings gliding relative to respective local airstreams;

adjusting the value and direction of said winding speed to provide a desired vertical movement of said aircraft, while maintaining said distribution of the pitches of said wings for a desired state of acceleration of said aircraft; and

differentially adjusting said distribution of the pitches of said wings of the respective sets to control the roll and yaw of said aircraft;

and on the runway deceleration, comprising the steps of:

progressively increasing the collective pitch of all said wings, while maintaining the vertical thrust component below the entire weight of said aircraft, providing a deceleration of about 0.4g with a desired margin; and

maintaining a positive winding speed for having maximized deceleration after crossing by the collective pitch of all said wings the value of 90 degrees and after a significant decrease in the speed of said aircraft.

80. The system of methods as recited in claim **79** wherein said means for maintaining a controlled pitch of said fuselage include two stabilators placed apart on the sides of aft of said fuselage, which are used to compensate for changes in the pitch moment of said aircraft by changing their pitch.

81. The system of methods as recited in claim **79** wherein said means for maintaining a controlled pitch of said fuselage include means for moving portions of the content of said fuselage, providing a desired offset of the center of gravity of said aircraft, which are used to compensate for changes in the pitch moment of said aircraft by shifting the center of gravity in longitudinal direction.

82. The system of methods as recited in claim **79** wherein said loop has circular form by using two

rotors with managed PGS-state that are constructed in accordance with the four-gears pitch steering scheme, and said variable percentage of said overall driving force is mapped to the external moment ratio (EMR) with the same range, and wherein the common handling of said rotors for said on the runway acceleration method comprises the steps of:

setting high negative gain about -65 degrees;

setting the pitch and skew almost the same and slightly below zero and beginning to use the skew control for control the pitch; and

progressively decreasing of the magnitude of said negative gain upon increasing ground speed and decreasing said winding speed, and doing it with a simultaneous and progressive approaching of said small negative values of the skew and pitch toward zero for increasing the vertical component of the thrust;

and also wherein the common handling of said rotors for said on the runway deceleration method comprises the steps of:

permitting for said two rotors to enter in a deceleration of their rotation, but without dropping said winding speed below the level of about one third of the specific stagnation speed of said aircraft, where said specific stagnation speed is defined as the speed whose stagnation on the pitot-tube creates a pressure equal to the specific load of said wings of said two rotors;

dropping the magnitude of high negative gain to a moderate value of about -40 degrees;

setting the skew equal to the current value of the pitch and beginning to use the skew control for control the pitch with common values;

progressively increasing the skew and pitch up to the value 90 degrees; and

increasing the skew and pitch to around 120 degrees to maximize remaining deceleration after a significant drop in ground speed.

83. The system of methods as recited in claim **82** wherein said aircraft has a pitch-based biangular handling (P-mode) for each of said two rotors, and wherein said P-mode biangular handling is related to the corresponding PGS-state by rules comprising:

handling of the skew in this handling mode is same as the skew handling upon the direct management of the PGS-state;

the handling consists from a handling two formal pitch values located apart on the skew direction line and belonging to an idealized PGS-control that has a linear distribution of pitches between two respective phase points of said two formal pitch values, and where the value at the direction of the skew is referred to as the main one and the other - as the opposite;

the actual PGS-state is mapped from a set of the selected skew value and two biangular values by refactoring the PGS-state for a pair of match-points, where each match-point is some known value of entire pitch distribution, which exists in some known angular position of the phase space;

the known angular positions of said match-points are simply the two opposite directions on said skew direction line shifted by some known phase shift;

the known values of said match-points are simply linear interpolations between said biangular values for the respective known angular positions; and

the value of said known phase shift is the product of some fixed empirical value and the square root of the normalized magnitude of the gain with the sign of inverted sign of the gain, where a maximal constructive limited value of the gain is used for said normalization.

84. The system of methods as recited in claim **83** wherein said fixed empirical value for said phase shift is about 24 degrees.

85. The system of methods as recited in claim **83** wherein said aircraft has an angle-of-attack-based biangular handling (A-mode) for each of said two rotors, which is used in conjunction with the establishing of said fuselage in the direction of the flight path of said aircraft with some remaining error, and wherein said angle of attack is referenced as alpha, and said A-mode biangular handling is related to the corresponding PGS-state by rules comprising:

an error angle value is considered and calculated as a difference between the orientation of said fuselage and the direction of the true airspeed (TAS) vector;

the actual skew value is equal to a required handling skew value minus said error angle value;

the handling consists from a handling two formal alpha values located apart on the skew direction line and belonging to an idealized distribution of alphas, which has a linear distribution of the alphas between two respective phase points of said two formal alpha values, and where the value at the direction of the skew is referred to as the main one and the other - as the opposite;

the actual PGS-state is mapped from a set of the actual corrected skew and two biangular values by refactoring the PGS-state for a pair of match-points, where each match-point is some known value of entire pitch distribution, which exists in some known angular position of the phase space;

the known angular positions of said match-points are calculated exactly by same rules as for said match-points of said P-mode biangular handling; and

the known value of said each match-point is the sum of the related alpha from the function of said linear distribution for the known angular position of the match-point, with the angle of the direction of the TAS of a wing in the known angular position, where this TAS is calculated as the vectorial sum of the winding speed vector of the wing and the TAS vector of said aircraft, mapped to the reference frame of said fuselage.

86. The system of methods as recited in claim **85** wherein the common handling of said two rotors for said flight handling method comprises the steps of:

enabling said A-mode biangular handling;

ensuring said main value of the biangular handling is higher than the said opposite value of the biangular handling;

setting the skew value near to zero;

adjusting said main value of the biangular handling to a desired airspeed and horizontal acceleration at a particular vertical speed;

adjusting said opposite value of the biangular handling to a desired airspeed, performance and EMR;

adjusting the value and direction of said winding speed to have a desired vertical movement of said aircraft, while maintaining said values of biangular handling for a desired state of acceleration of said aircraft; and

adjusting the skew value to optimize performance, said EMR and the flight path angle of said aircraft.

87. The system of methods as recited in claim **86** wherein the differential handling of said rotors for said flight handling method for the case of entering in a turn upon said A-mode biangular handling has three categories, comprising respectively the steps of:

for ascending flight and cruise: setting a positive difference between the main values of the biangular handling of the respective rotors at the outer and inner sides of the turn, and setting about half of it a negative difference between the opposite values of the biangular handling of the respective rotors at the outer and inner sides of the turn;

for gliding with optimal speed: setting a positive difference between the main values of the biangular handling of the respective rotors at the outer and inner sides of the turn; and

for descending flight: setting a negative difference between the main values of the biangular handling of the respective rotors at the outer and inner sides of the turn, and setting about same a positive difference between the opposite values of the biangular handling of the respective rotors at the outer and inner sides of the turn, where the latter value being decreased by half when approaching a very high common main value of the biangular handling.

88. The system of methods as recited in claim **86** wherein said flight handling method for the case of a high powering recuperative descent at high speed comprises the steps of:

setting the skew about -5 degrees for said both rotors;

progressively increasing the common main value of the biangular handling to about 10 degrees higher than the zero-lift alpha for the airfoil used on the wings of said rotors;

progressively decreasing the common opposite value of the biangular handling to about 3 degrees higher than the said zero-lift alpha upon said increasing of the common main value; and

progressively and simultaneously with the change in the biangular values, changing said winding speed to a high negative value of about -40 percent of the said specific stagnation speed, having a recuperating power of about two thirds of the maximal consuming power and a flight-path angle of about -13 degrees in the final state.

89. The system of methods as recited in claim **86** wherein said flight handling method for the case of a middle powering recuperative deceleration in descent at middle speed comprises the steps of:

setting the skew about -15 degrees for said both rotors;

progressively increasing the common main value of the biangular handling to about 14 degrees higher than the zero-lift alpha for the airfoil used on the wings of said rotors;

progressively decreasing the common opposite value of the biangular handling to about 6 degrees higher than the said zero-lift alpha upon said increasing of the common main value; and

progressively and simultaneously with the change in the biangular values, changing said winding speed to a high negative value of about -25 percent of the said specific stagnation speed, having a recuperating power of about 40 percent of the maximal consuming power, a horizontal deceleration of about 0.1g and a flight-path angle of about -6 degrees in the final state.

90. A computer memory based method for modeling flight an aircraft having two sets of equal wings belonging to two respective actuators placed apart on the sides of a fuselage of said aircraft and involved in collective movement along a fixed loop relative to the central plane of said aircraft with a common and changeable winding speed of said wings along said loop with variable steering of the pitches of said wings for different phases along said loop, and where said two actuators can be locked from moving said wings along said loop, and also said two actuators are considered in this method as being operated as one actuator with a common state, the method is composed of operational tiers, a memory state and a processing executed as a sequence of cycles with some time-step against the background of an arbitrary handling and supervising, with modifying said memory state to reflect the actual modeling the flight in an order of sequential rules of this method, and with performing calls of said tiers on demand from these rules, wherein said tiers are used for modeling particular aspects of the relationship of said aircraft to flight for the respective particular conditions and comprises:

a tier of the ambience aspect, which is used to model the ambient conditions affecting said aircraft, in particular air conditions and gravity, depending on the flight altitude;

a tier of the wings' placement aspect, which is used to model a distribution of positions, speed directions and pitches for particular wings of said two actuators, having a relative reference frame located at the common origin of said two actuators in the central plane of said aircraft and oriented along said fuselage, the tier depends on said phase, a particular steering state of said actuators and on direction of said winding speed, where the positive direction is defined as the direction when the upper wings move forward, the tier also provides at its output absolute positions and speed directions of the respective wings relative to the ground, using a known pitch angle of said fuselage;

a tier of the airfoil aspect, which provides access to a respective datum of the coefficients and aggregations of the section of the airfoil that is used in said wings for a broad range of Reynolds numbers and for the full range of angles of attack of 360 degrees or their sub-range sufficient for said modeling;

a tier of the inflow aspect, which is used to model the inflow for end use, depending on a thrust vector, overall true airspeed (TAS) vector, air density and outdated local airspeed (LAS) vector;

a tier of the aspect of the wings' interference, which is used to model a state of airspeeds for all said wings, induced by the vorticity distribution between said wings, depending on the kinematic viscosity and a provided state based on the wings, including base flow LAS vectors, absolute pitches and positions, the tier provides the end use state of LAS vectors; and

a tier of the aspect of interaction with the ground, which is used to model a force induced by an undercarriage of said fuselage, depending on the position and speed of displacement of the undercarriage relative to said fuselage;

and wherein said sequential rules are grouped into a set of updates and queries, for convenient organizing and referencing to said rules, comprising:

a query air density, kinematic viscosity and magnitude of gravitational acceleration as the altitude conditions from said tier of the ambience aspect, using a vector of the current location of said aircraft;

an update of a predicted state, comprising the steps of:

updating a predicted speed, location and winding speed of said aircraft by performing numerical integration of the respective current values at half of said time-step, using an acceleration vector, the predicted speed vector and a winding acceleration of the entire aircraft as the respective derivatives; and

updating a predicted speed and location of each of said wings by performing numerical integration of its respective current values at half of said time-step, using an acceleration vector and the predicted speed vector of this wing as the respective derivatives;

an update of an airflow state, comprising the steps of:

updating a magnitude of the airspeed of said aircraft by the magnitude of the corresponding predicted speed vector;

updating an angle of attack of each of said wings as the angular difference between a pitch and a LAS vector, where the pitch is provided from said tier of the wings' placement aspect, and the LAS vector is calculated as the correction the current speed vector of this wing on an inflow vector with additional restoring to the fuselage reference frame, using the fuselage pitch angle;

simulating of interference that performs a call of said tier of the aspect of the wings' interference by providing all said required information for it, restoring said absolute pitches from the respective angles of attack; and

updating an airflow state of each of said wings by the corresponding result of the interference simulation, including angle of attack, airspeed magnitude, Reynolds number, lift, drag and moment coefficients, and a variation of the angle of attack due to steering the stream by the interference and inflow;

an update of a winding state, comprising the steps of:

checking a locked state reflected in a locking flag, and if it is set and a target winding speed is zero, exiting from said update the winding state, but in another case, resetting the locking flag and continuing;

checking a predefined lock-speed threshold, and if the magnitude of the predicted winding speed is below the threshold, setting said locking flag, setting a directed powering force to zero and exiting from said update the winding state, but in another case, continuing;

obtaining a needed delta acceleration depending on the difference between said target winding speed and said predicted winding speed and said winding acceleration, and with applying a limitation based on the ratio of the total mass of said aircraft to the mass of all said wings; and

updating said directed powering force by the sum of a directed internal force and the product of said calculated delta acceleration and the mass of all said wings, with applying a limitation based on a predefined maximal magnitude of such force;

an update of a dynamic state, comprising the steps of:

updating a fuselage drag force by building an aerodynamic force vector oriented opposite said predicted speed vector with magnitude based on a front area and a wet area of said fuselage, the said magnitude of airspeed and said air density;

updating a damper force by building a damper force vector oriented generally in the upper direction and with magnitude based on a displacement of the undercarriage under a load of said aircraft and on the vertical component of said predicted speed vector, and obtained from the said tier of the aspect of interaction with the ground, providing to it these two parameters;

updating a gravity force and a total force by building a gravity force vector with magnitude based on a current mass of said aircraft and on the said magnitude of gravitational acceleration, and by building a total force vector with preliminary content from said vectors of aerodynamic force, of damper force and of gravity force;

preparing intermediate accumulators of forces and moments, by assigning and resetting variables for the accumulation aerodynamic forces, non-conservative forces, directed internal forces, external moments and internal moments induced on the wings;

entering in walkthrough over all said wings;

updating the forces and pitch moment of the current wing by building an aerodynamic force vector with a drag component aligned in the LAS direction based on the predicted TAS angle and the said variation of the angle of attack, where the drag and lift components of this vector are derived from said respective coefficients, airspeed magnitude and wing's area, also by calculating the pitch moment from said coefficient of moment, airspeed magnitude, wing's area and wing's chord, also by building a gravity force vector using wing's mass and said magnitude of gravitational acceleration, and also by building a total force vector from said vectors of aerodynamic and gravity force;

accumulating the forces and moments of the current wing by accumulating said aerodynamic force vector, also by querying an absolute speed's direction and an absolute position of the current wing from said tier of the wings' placement aspect, also by accumulating the directed internal force obtained as scalar projection of said aerodynamic force vector onto the speed's direction, also by accumulating an external moment obtained as cross-product of the wing's position and said total force vector, also by accumulating said pitch moment in said accumulator of the internal moments, also by building a drag-only version of said aerodynamic force vector, and also by accumulating the drag-only vector in said accumulator of non-conservative forces;

exiting from said walkthrough over all said wings;

totalizing the forces by adding said aerodynamic force vector to said accumulator of non-conservative forces, and by adding said accumulator of the aerodynamic forces to said aerodynamic force vector and to the said total force vector with preliminary content;

updating a thrust reporting by calculating a LAS vector as the sum of said predicted airspeed vector and said inflow vector, also by refactoring a consumed thrust force from said accumulator of the directed internal forces, said actual winding speed and the LAS vector magnitude, also by normalizing the consumed thrust force on the magnitude of said gravity force to obtain a consumed thrust ratio (CTR), also by calculating a true thrust force from said aerodynamic force vector upon subtracting the vector of said accumulator of non-conservative forces, also by normalizing the magnitude of the true thrust force on the magnitude of said gravity force to obtain a true thrust ratio (TR), and also by obtaining a thrust angle (TA) as the angle of said true thrust force;

updating said directed internal force if said locking flag is set by assigning an inverted value of said accumulator of directed internal forces to the said directed internal force, but in another case, assigning the last acquired value of said directed powering force;

calculating average forces per any of said wings by calculating a partial translation force as a mass-proportional part of said total force vector, and by calculating a partial directed internal force as a member-proportional part of the sum of said accumulator of directed internal forces and said directed internal force;

updating said inflow vector by calling said tier of the inflow aspect with passing thereto the said air density value, said predicted speed vector, said LAS vector and said true thrust force vector;

entering in walkthrough over all said wings;

correcting particular states for a contribution of the current wing by querying the absolute speed's direction and the absolute position of the current wing from said tier of the wings' placement aspect, also by calculating the said total force of this wing as a superposition of said partial translation force and the projection of said partial directed internal force onto said wing's speed's direction, and also by subtracting the cross-product of said wing's position and said total force from said accumulator of the external moments;

exiting from said walkthrough over all said wings; and

totalizing moments by storing the sum of values of said accumulator of the external moments and said accumulator of the internal moments as a pitch moment of said aircraft, and by storing the value of said accumulator of the internal moments as an internal pitch moment of said aircraft;

an update of a kinematic state, comprising the steps of:

updating the states of a previous location and a previous kinetic energy by the respective values of said current location vector and a kinetic energy of the current state;

updating the vectors of the acceleration, current location and current speed by calculating said acceleration vector as a ratio of said total force vector to the said current mass, and also by using time-step integration of said current location and current speed vectors according to the basic kinematic equations;

calculating a kinetic energy of said fuselage by using the magnitude of the said current speed vector and the mass of said fuselage, and storing this energy in a total variable;

entering in walkthrough over all said wings;

updating a previous location vector of the current wing by its current location vector;

updating the vectors of the acceleration, current location and current speed of the current wing by calculating its acceleration vector as a ratio of its total force vector to its mass, and by using time-step integration of its current location and current speed vectors according to the basic kinematic equations;

calculating kinetic energy of the current wing by using the magnitude of its current speed and its mass, and accumulating this energy in the said respective total variable;

exiting from said walkthrough over all said wings; and

updating a time variable of said processing by incrementing it by said time-step;

an update of a power state, comprising the steps of:

checking the locked state of said locking flag, and if it is set, ensuring the locking is finalized by resetting the values of said actual winding speed, said winding acceleration and a consumed power, continuing by exit from said update the power state, but in another case continuing;

calculating a power speed by building a localized vector of changing position of any one wing by subtracting its localized previous position from its localized current position, also by querying an absolute speed's direction vector of this wing from said tier of the wings' placement aspect, and also by dividing the scalar projection of this localized vector onto this speed's direction vector by said time-step;

updating said winding acceleration, said winding speed and said consumed power by assigning to said winding acceleration the result of dividing the changing of said actual winding speed on said time-step, also by assigning to said actual winding speed the said power speed, and also by assigning to said consumed power the product of said directed powering force and said actual winding speed; and

updating said current mass of said aircraft, related to a fuel consumption rate with respect to said consumed power, if it is applicable;

an update of said phase of said actuators, comprising the steps of:

updating said phase and checking its range by adding to current phase a ratio of the product of said actual winding speed and said time-step to the length of said loop, and also by normalizing this result in a case of overranging; and

doing a hard sync for each of said wings by querying an absolute speed's direction vector and an absolute position vector of this wing from said tier of the wings' placement aspect, also by setting to its current location vector the superposition of this position vector and the said current location vector of the entire aircraft, also by setting to its current speed vector the superposition of this speed's direction vector scaled by said actual winding speed and of the said current speed vector of the entire aircraft, and also by setting to its acceleration vector the superposition of this speed's direction vector scaled by said winding acceleration and of the said acceleration vector of the entire aircraft;

and an update of a report state, comprising the steps of:

calculating a cruise power by calculating a gravitic power, using a change of the vertical component of said vector of the current location relative to the same component of said previous location vector, also by calculating a kinetic power, using a change of said kinetic energy from said previous kinetic energy, also by calculating an acceleration power, using a change of the square of said vector of the current speed from the square of said previous speed vector, also by calculating an internal kinetic power as the difference between said kinetic power and said acceleration power, also by calculating an external consumed power as the difference between the said consumed power and said internal kinetic power, and also by obtaining the cruise power as the loss power remained after subtraction said gravitic power and said acceleration power from said external consumed power;

updating a cruise ratio by dividing said consumed power by said cruise power;

updating an equivalent lift to drag ratio (LDR) and a lift coefficient (CL) by calculating an average speed vector between said current speed vector and said previous speed vector, also by calculating an equivalent drag as a ratio of said cruise power to the magnitude of said average speed vector, also by calculating an equivalent lift as a scalar projection of said aerodynamic force vector onto a direction orthogonal to said average speed vector, also by obtaining the equivalent LDR as the ratio of said equivalent lift to said equivalent drag, also by calculating a stagnation pressure based on said average speed and said air density, and also by obtaining the CL as the ratio of said equivalent lift to the product of said stagnation pressure and the total area of said wings;

updating said previous speed vector by the said current speed vector;

updating a winding ratio (WR), a normalized acceleration and a flight path angle (FPA) by calculating a LAS vector from said current speed vector and said inflow vector, also by obtaining the WR as the ratio of said actual winding speed to the magnitude of the LAS vector, also by obtaining the normalized acceleration vector as the ratio of said acceleration vector to said gravitational acceleration, and also by obtaining the FPA as the angle of said current speed vector; and

updating a propulsion efficiency (PrE), a power lifting speed (PLS) and a true gliding lift to drag ratio (TGLDR) by calculating a propulsion inflow as a scalar projection of said inflow vector onto the direction of said current speed vector, also by obtaining the PrE as the ratio of the magnitude of said current speed vector to its sum with said propulsion inflow, also by obtaining the PLS as the ratio of said external consumed power scaled by said PrE to the magnitude of said aerodynamic force vector, and also by obtaining the TGLDR as the ratio of said LDR to the said PrE.

91. The method as recited in claim **90** wherein said update of the report state of said sequential rules includes an obtaining of a local glide angle (LGA) of the embedded virtual glider, comprising the steps of:

preparing the calculation of said LGA by obtaining a common direction of the inertial vertical of said entire aircraft as a normalized vector in the inverted direction of said aerodynamic force vector, and also by initializing an accumulating vector of the LGA direction by a zero vector;

entering in walkthrough over all said wings;

obtaining a LAS vector of the current wing by rotating said predicted speed vector of this wing by its angle of the said variation of the angle of attack;

obtaining a LAS direction vector of the current wing as a normalized vector of this LAS vector;

obtaining a weighting value for the said LAS direction as an inverted dot-product of said common direction vector and said aerodynamic force vector of the current wing;

accumulating said LAS direction vector scaled by said weighting value in said accumulating vector of the LGA direction;

exiting from said walkthrough over all said wings; and

updating an LGA value by the angle of said accumulating vector of the LGA direction.

92. The method as recited in claim **90** wherein said tier of the aspect of the wings' interference uses a set of general rules for modeling said interference upon its own processing, comprising:

said processing uses only one from said two actuators for consideration;

said processing has generally a sequence of equal main cycles with a number of about 2N, where N is the number of wings of this actuator;

said processing considers the cross-section of each wing of this actuator being split on M segments along the chord of its airfoil section, having a known area and center, where said center is calculated as the center of gravity of its segment;

said processing builds in each of said main cycles a draft distribution of LAS vectors over said N wings, by merging a draft distribution of modeled induced speed vectors with the known base distribution of LAS vectors;

said processing sequentially accesses in each of said main cycles each destination wing to calculate its induced speed vector during a destination cycle;

said processing sequentially accesses in the said destination cycle each said segment of said destination wing to calculate its induced speed vector during a segment cycle;

said processing sequentially accesses in the said segment cycle each of others wings for calculating and accumulating a partial induced speed vector from this source wing during a source cycle;

said processing considers for the calculation of said partial induced speed vector a vorticity source located at some center of vorticity (CV) as an approximation of an entire vorticity distribution around said source wing, depending on the angle of attack of this wing;

said processing considers for the calculation of said partial induced speed vector a vorticity destination located at said center of said segment;

said processing calculates said partial induced speed vector basically in accordance with the Biot-Savart law, having a signed magnitude equal to the scalar projection of a circulation onto the direction of a z-axis, divided by the double-length of a circle with a radius equal to the length of the radius-vector from said vorticity source to said vorticity destination and directed along the cross-product of the normalized vector on the z-axis and the normalized vector on said radius-vector, considering the z-axis is oriented along any wing from said fuselage to the outward, and considering the circulation is calculated in accordance with the

Joukowski theorem as the cross-product of the aerodynamic force vector of said source wing and the normalized vector of the direction of LAS of this wing divided by air density, length of this wing and magnitude of the LAS;

said processing further corrects said partial induced speed vector by scaling using a 3-d factor coefficient, which is calculated by subtracting a 3-d aspect coefficient from the square root of the sum of unity and the square of the 3-d aspect coefficient, where the 3-d aspect coefficient is a ratio of said length of said radius-vector to the length of the wings;

said processing calculates said induced speed vector of said destination wing by a consolidation algorithm, which is a weighted average over all said segments of this wing, having a weighting coefficient equal to the ratio of said area of a current segment to the sum of the chord length and the distance from said center of the current segment to a some focusing point on said airfoil section or at vicinity thereof;

said processing uses a center of aerodynamic force (CF) as said focusing point, depending on the angle of attack and the Reynolds number of said destination wing, in a form of pair of coordinates (CFx and CFy) relative to the leading edge of said airfoil;

said processing calculates in each of said main cycles respective angles of attack and Reynolds numbers for all said N wings and queries said tier of the airfoil aspect for getting respective coefficients of the lift and drag and said values of CFx and CFy as aggregations; and

said processing uses a known pivot position of the wings relative to the leading edge of said airfoil, the pitches of the respective wings and their positions as pivot coordinates for doing all desired transformation of the positions of all geometrical features that is used for said interference modeling.

93. The method as recited in claim **92** wherein said center of vorticity (CV) is approximated by empirical sequential rules comprising:

scale the geometry of said airfoil for having its chord length equal to unity, if this length differs from unity;

for a given angle of attack (AoA) obtain its magnitude |AoA|;

assign to a main angle of attack AoA' the value of said AoA if the |AoA| isn't higher than 90°, but in another case, assign to the AoA' the value of 180°-|AoA|;

calculate a main x-component of said CV relative to the leading edge of said airfoil along its chord (CVx') as half of $(1-(\sin(|AoA'|))^{0.07})$;

assign to an x-component of said CV relative to the leading edge of said airfoil along its chord (CVx) the said CVx' if the |AoA| isn't higher than 90°, but in another case, assign to the CVx the value of 1-CVx';

calculate a y-component of said CV relative to the chord of said airfoil in the upper direction (CVy) as a value on the camber-line of said airfoil for said particular CVx; and

rescale said CVx and CVy back to the original scaling of said airfoil geometry, if it is applicable.

94. The method as recited in claim **92** wherein said tier of the aspect of the wings' interference uses a partially dimensionless scaling to simplify and speed up the processing of said tier , the scaling is defined by rules comprising:

use said LAS vectors in their original form;

use a scaled chord length of said airfoil c' equal to unity instead of the original chord c;

use any geometrical one-dimensional feature of the processing divided by the length of the original chord instead of the original feature;

use any geometrical two-dimensional feature of the processing divided by the square of the length of the original chord instead of the original feature;

use a scaled aerodynamic force vector AF' instead of said original aerodynamic force vector AF and defined as a vector built on the respective lift and drag coefficients in accordance to an original transform relative to the direction of said LAS vector of the considered wing and multiplied by half of the square of this LAS vector; and

use a scaled circulation value instead said original circulation value and defined as a cross-product of said scaled aerodynamic force vector AF' and a normalized vector along the direction of the LAS vector and divided by the magnitude of said LAS vector using the two-dimensional scalar version of said cross-product.

95. The method as recited in claim **94** wherein said processing of the tier of the aspect of the wings' interference comprises the steps of:

entering into a basic initialization;

acquiring the actual chord length of the wings and the used airfoil section with a unit length of its chord;

acquiring the known pivot position on the said airfoil section;

acquiring the actual length of the wings with scaling it in said chord length;

splitting said airfoil section on said M segments and calculating the area of each segment ASm and the center of each segment CSm as the center of gravity;

acquiring the actual number of said wings N and

establishing a storage of per wing states;
exiting from said basic initialization;
receiving a call on demand of the simulation and acquiring a kinematic viscosity and a distribution of the pivot positions, pitches and base LAS vectors over said wings;
normalizing the distribution of the pivot positions by scaling each position in said chord length;
calculating an actual position of a center of segment CSim for each of N wings depending on the corresponding position and pitch of this wing;
initializing the resulting distribution of the LAS vectors by the respective values of said distribution of the base LAS vectors;
entering into said main cycle of said processing with resetting a counter of the main cycles;
entering in walkthrough over all wings;
calculating the LAS vector magnitude and the Reynolds number of the current wing, using said kinematic viscosity and said actual chord length;
calculating the angle of attack of the current wing by subtracting the corresponding LAS direction angle from the pitch of this wing;
querying said tier of the airfoil aspect for the respective coefficients and aggregations for the current wing, providing to this tier said angle of attack and said Reynolds number;
calculating said scaled aerodynamic force vector for the current wing, using the related lift and drag coefficients and said LAS vector;
calculating said scaled circulation value for the current wing, using said scaled aerodynamic force vector and said LAS vector;
calculating said center of vorticity of the current wing in the airfoil's reference frame, using said angle of attack of this wing;
calculating the actual position of said center of force of the current wing by reposition the center force coordinates from the obtained aggregations, using the actual pivot position and pitch of the wing and said pivot position on the said airfoil section;
calculating the actual position of said center of vorticity of the current wing by reposition said center of vorticity in the airfoil's reference frame, using the actual pivot position and pitch of this wing and said pivot position on the said airfoil section;
exiting from the said walkthrough over all wings;
updating said counter of main cycles and exiting from said processing for the case of reaching the desired number of said main cycles, but in another case continuing;
entering in walkthrough over all destination wings;
entering in walkthrough over all segments of the current destination wing;
resetting the induced speed vector of the current segment of the current destination wing;
entering in walkthrough over all source wings, excluding the current destination wing;
calculating said radius-vector from said center of vorticity of the current source wing to said center of the current segment of the current destination wing;
calculating the direction vector of said partial induced speed vector using the direction of said radius-vector;
calculating said 3-d aspect using the magnitude of said radius-vector and said scaled length of the wings;
calculating said 3-d factor using said 3-d aspect;
calculating said signed magnitude of said partial induced speed vector using said scaled circulation value of the current source wing and the magnitude of said radius-vector;
building said partial induced speed vector using said signed magnitude, said 3-d factor and said direction vector thereof;
accumulating said partial induced speed vector in said induced speed vector of the current segment of the current destination wing;
exiting from the said walkthrough over source wings;
exiting from the said walkthrough over all segments of the current destination wing;
calculating an array of weighting coefficients for all segments of the current destination wing, using respective distances of said centers of segments from said center of force of the current destination wing and said respective areas of segments;
calculating the consolidated induced speed vector of current destination wing from the induced speed vectors of all segments of this wing, using said array of weighting coefficients;
updating said LAS vector of the current destination wing by the superposition of the corresponding base LAS vector and said consolidated induced speed vector;
exiting from the said walkthrough over all destination wings; and
entering into next main cycle of said processing.

96. The method as recited in claim **90** wherein said loop has a circular form due to using two rotors as said two respective actuators, where each of said two rotors has a radius R from a central axis thereof to the pivot axis of any of its wings, and wherein said tier of the inflow aspect uses a set of general rules for modeling said inflow upon its own processing, comprising:

said processing considers the resulting inflow vector is oriented in the opposite direction of a known thrust vector, for which said true thrust force serves;

said processing considers the magnitude of said thrust vector is equal to the product of a duplicated air density, a thrust specific area (TSA) of said aircraft, a magnitude of a LAS vector and a magnitude of said inflow vector, where said LAS vector should be equal to the sum of a known TAS vector and said inflow vector, implying a non-linear equation for resolving;

said processing uses the Newton's method or another method for resolving said non-linear equation under a low number of iterations;

said processing considers said TSA depends on a downwash specific area (DSA), a propulsion specific area (PSA) and a thrust specific angle β between said thrust vector and said LAS vector by a quadrature formula implying said TSA is equal to the square root of the sum of squares of DSA*sin(β) and PSA*cos(β);

said processing considers said DSA is generally equal to a circle area with a diameter based on the total wingspan of said aircraft;

said processing considers said PSA is generally equal to 4*L*R, where the L is a common length of any wing of any of said two rotors; and

said processing uses said outdated known LAS vector to calculate said thrust specific angle β.

97. The method as recited in claim **96** wherein each of said two rotors is constructed in accordance with the four-gears pitch steering scheme, having a central gear with an omnidirectional controlled offset from said central axis of this rotor and with a controlled angular position, a pitch gear for each of said wings synchronized with pitch of this wing, and a steering cluster for this pitch gear, having a steering pinion meshed with said pitch gear and an entry gear meshed with said central gear, and wherein said tier of the wings' placement aspect uses the managed PGS-state as said particular steering state, and uses a set of general rules, for modeling the distribution of the pitches of particular wings upon its own processing, comprising:

said processing considers that axes of said pitch gears are placed on a common circle around said central axis of the rotor with radius R0;

said processing considers that said pitch gear has a radius r1, said central gear has a radius r2, said entry gear has a radius r3 and said steering pinion has a radius r4;

said processing considers that the gear ratio of r1 to r4 equal to the ratio of r2 to r3 and equal to some constant K;

said processing considers that a triangle build on the axis of said pitch gear, axis of said central gear and axis of said steering cluster has two short sides with the lengths r14=r1+r4 and

r23=r2+r3 from the side of the pitch gear and from the side of the central gear, respectively;

said processing considers that a constant S1 is equal to the double product of r14 and r23;

said processing considers that a constant S2 is equal to the sum of the squares of r14 and r23;

said processing considers, by using cosine theorem, that a constant angle ω0 is equal to the arccosine of the ratio of the difference of S2 and the square of R0 to S1;

said processing considers the distance between the axis of said pitch gear and the axis of said central gear as a variable r;

said processing considers, by using cosine theorem, that a variable angle ω1 is equal to the arccosine of the ratio of the difference of S2 and the square of r to S1;

said processing considers that a variable ω = ω1- ω0;

said processing considers the pitch deviation of a particular wing to which a particular pitch gear having a certain r belongs, as a variable δ = -ω*(1+1/K);

said processing considers that the angular direction from said central axis of the rotor toward any particular wing is equal to the angular direction toward the corresponding pitch gear of this wing, unless otherwise specified;

said processing considers that a direction of the skew reflects the skew-angle specified by the S-component of said PGS-state in the counter direction of said positive direction of said winding speed, beginning from the forward-most position relative to said fuselage;

said processing considers that said r in the said direction of the skew has an extremum with a value r';

said processing considers that a variable Δr is equal to R0-r' for the case of a normal assembling of said four-gears pitch steering scheme, and considers it is equal to r'-R0 for the other case of an inverted assembling, where the inverted assembling is defined as having said steering cluster in an upper elongation relative to said pitch gear located in the zero-value direction of the skew;

said processing considers a maximal magnitude of said Δr as a constant Δrmax;

said processing considers a difference between said pitch deviation in the direction of the skew and in the opposite direction as the G-component or the gain of said managed PGS-state and can pass it back on a request of the callers of this tier;

said processing considers that the given angular position of a particular wing uses same direction and origin as the skew-angle;

said processing considers a ratio of said Δr to the said Δrmax as a linear normalized gain Gn that is accompanied the said managed PGS-state for direct changing said gain; and

said processing considers that said pitch of a particular wing is equal to said pitch deviation δ summed with the P-component of said managed PGS-state.

98. The method as recited in claim **97** wherein said processing of said tier of the wings' placement aspect, for a case of querying the pitch for a given angular position of a particular wing, comprises the steps of:

calculating a relative angular position by subtracting said S-component of said managed PGS-state from said given angular position;

building a vector of the position of the axis of said central gear using said Gn accompanied said managed PGS-state, said Δrmax and the skew-angle;

inverting the sign of said vector of the position of the axis of said central gear if said inverted assembling is specified;

building a vector of the position of the axis of said pitch gear using said constant R0 and said given angular position;

building a distance vector by subtraction said vector of the position of the axis of said central gear from said vector of the position of the axis of said pitch gear;

obtaining said distance r as the magnitude of said distance vector;

calculating said ω1 using said distance r and said constants S1 and S2;

calculating said ω using said ω1 and said constant ω0;

calculating said pitch deviation δ using said ω value and said constant K;

inverting the sign of said pitch deviation δ if said inverted assembling is specified; and

providing the result as the sum of said pitch deviation and said P-component of said managed PGS-state.

99. The method as recited in claim **96** wherein said second step of said predicted state update of said sequential rules implements an advanced prediction updating comprising the steps of:

calculating an angular shift and a centripetal acceleration by obtaining the angular shift upon dividing the product of the inverted half of said time-step and said actual winding speed by the said radius R of the rotor, also by obtaining a sign of the centripetal acceleration as the sign of said actual winding speed, and also by obtaining a magnitude of said centripetal acceleration as the square of said winding speed divided by said R;

entering in walkthrough over all said wings;

obtaining a direction vector of the current speed of the current wing from said tier of the wings' placement aspect;

obtaining a direction vector of the predicted speed of the current wing by rotating said direction vector of the current speed by the said angular shift;

obtaining a direction vector of the current centripetal acceleration by rotating said direction vector of the current speed by the product of 90 degrees and the said sign of the centripetal acceleration;

obtaining a direction vector of the predicted centripetal acceleration by rotating said direction vector of the predicted speed by the product of 90 degrees and the said sign of the centripetal acceleration;

obtaining a variation of the acceleration vector by subtracting said direction vector of the current centripetal acceleration from said direction vector of the predicted centripetal acceleration with scaling by said magnitude of said centripetal acceleration;

updating a predicted acceleration vector of the current wing by the sum of the said variation of the acceleration vector and the current acceleration vector of this wing;

updating said predicted speed vector of the current wing by the sum of the said predicted acceleration vector scaled by the half of said time-step and said current speed vector of this wing;

updating said predicted location vector of the current wing by the sum of the said predicted speed vector scaled by the half of said time-step and said current location vector of this wing; and

exiting from said walkthrough over all said wings.

100. The method as recited in claim **96** wherein said update of a dynamic state of said sequential rules further includes an updating on the end thereof, comprising the steps of:

calculating a value of moment normalizing by multiplying the said current mass of said aircraft, said gravitational acceleration and said radius R of the rotor;

updating a moment ratio by dividing said pitch moment of said aircraft by said value of moment normalizing; and

updating an internal moment ratio by dividing said internal pitch moment of said aircraft by said value of moment normalizing.

101. The method as recited in claim **90** wherein said arbitrary handling updates by its own action a set of two handling angles of attack in two generally opposite and specified directions to reflect such kind of handling based on this set, namely the biangular handling, in said modeling, and wherein a tier of the handling interpretation is included and provides a mapping of said parameters of said biangular handling to said particular steering state of said actuators, using said current speed vector of said aircraft and said actual winding speed to match to said two prescribed angles of attack during a call of this tier of the handling interpretation at a step placed at the end of said update of a power state of said sequential rules.

102. A system for cruise flight generally based on the concept of performing a powered flight by performing a work against gravity using a gliding wing as a steady support, namely the "flying elevator" concept, the system comprises:

a fuselage having generally streamlined elongated shape;

at least one transversely symmetrical wing or a lightweight glider with control elements, having abilities for remote control of pitch, roll and yaw thereof at glide with a payload suspended under it, generally with a wide range of a load force induced by said payload, the wing has mass generally in significant order less than said fuselage with its content;

a wire for each of said wings connecting this wing with said fuselage, having a connection position with this wing at a central chord thereof, generally;

a wire winding system per each said wire, having this wire wound on a drum and means for powering the drum for rotation with a controlled winding speed in both directions and for locking the drum against the rotation, the wire winding system is installed on said fuselage, generally near of its center of gravity;

means for attitude control of said fuselage at least for its pitch and yaw to direct said fuselage in the airstream direction, these means are placed on said fuselage;

means for remote control of each of said wings from the side of said fuselage, these means are placed on said fuselage, with a respective connectivity with said control elements of the respective wings; and

a cruise control system with ability for managing at least said winding systems and said means for remote control of each of said wings upon applying periodical and adaptive patterns of an actuation said systems and means, generally in accordance with handling rules comprising:

any wing involved in a winding-in movement relative to said fuselage should have a pitch implying, together with its true airspeed (TAS) vector, generally high load from the side of its wire, if other handling rules don't override that;

any wing involved in a winding-out movement relative to said fuselage should have a pitch implying, together with its TAS vector, generally low load from the side of its wire, if other handling rules don't override that;

any winding system should switch its actuation direction or locking its drum upon encountering a respective limit of a prescribed range of lengths of the free wire outside said respective drum, if other handling rules don't override that;

any winding system should provide the load force on the respective wire below a prescribed operational limit;

any winding system should prevent a forceless state of the respective wire by a respective winding-in actuation;

any winding system should operate in a prescribed range of lengths of the free wire outside said respective drum, if other handling rules don't override that;

any elongation of any of said wings relative to another said wing should be reflected in a respective policy of proximity of said members of this elongation;

any elongation of any of said wings relative to said fuselage should be reflected in a respective policy of proximity of said members of this elongation;

any winding system shouldn't imply the load force of the respective wire for accelerating or decelerating the respective wing outside prescribed limits of the TAS of this wing;

the overall force from all of said wings and the gravity force shouldn't imply vertical and horizontal accelerations of said fuselage outside prescribed limits;

said system for cruise flight should have a TAS magnitude of its center of gravity between prescribed limits; and

said system for cruise flight should have a TAS magnitude of its center of gravity near to a desired handled value, if other handling rules don't override that.

103. The system as recited in claim **102** wherein each of said wings is handled by varying a position of its connection point with the respective wire, and wherein said control elements reflected in a central node of this wing, which is used simultaneously to connect said wire, and has elements comprising:

two longitudinal pathways fixed on this wing along said central chord on some equal distance from this chord, having some window between them;

a caret mounted between said two longitudinal pathways and movable on the said pathways in the longitudinal direction;

two transverse pathways placed on the forward and rearward side of said caret or substituting said sides thereof, having some window between them;

two movable supports mounted on said two transverse pathways, respectively, for moving on said pathways in the transverse direction;

a common frame pivotally mounted on said two movable supports, having its common pivot axis oriented in the longitudinal direction and constraining a fixed distance between said two movable supports;

a central shaft mounted between two sides of said common frame in transverse direction, having its axis crossed with the said common pivot axis of said common frame;

a link pivotally mounted on said central shaft by its upper end inside said common frame;

a C-shape earring pivotally mounted on a bottom end of said link and connected with the end of said wire;

a transverse screw goes through a corresponding threaded hole in one of said two movable supports along the respective transverse pathway;

a transverse servo rotatably connected to said transverse screw and placed on one side of said caret;

a longitudinal screw goes through a threaded hole in a corresponding element on a side of said caret, along the respective longitudinal pathway; and

a longitudinal servo rotatably connected to said longitudinal screw and placed on this wing.

104. The system as recited in claim **103**, having two of said wings, and wherein one of said two wings is always placed above the other wing, having its wire passing freely through said central node of said other wing, using a pulley assembly inside said common frame of this central node as a substitution of said link to conduct this wire, comprising:

two equal cheeks, where each of said cheeks has three holes in the vertical direction with a symmetrical placement relative to the central hole of these holes, and this central hole is used for said pivotal mounting of this pulley assembly on the said central shaft, having an additional longitudinal offset, for the better securing of said wire of the upper wing, in the opposite direction to the direction of entry of this wire into said pulley;

an upper shaft, which is mounted between the upper ends of said two cheeks;

a bottom shaft, which is mounted between the bottom ends of said two cheeks and is used for mounting said C-shape earring; and

three pulleys respectively dressed on the said upper, central and bottom shafts with the possibility of free rotation, and having said wire of the upper wing conducted between them.

105. The system as recited in claim **102**, having only one of said wings referenced as a wired wing,

and wherein said fuselage includes two symmetrical wings mounted apart on its sides, symmetrically, with a respective roll control and also either with a possibility of a shared pitch control of said wing with said fuselage or with a possibility of an independent pitch control, and in any case said pitch control is reflected in the further handling rules of said cruise control system, comprising:

for a case if said wired wing is involved in a winding-in movement relative to said fuselage, the said fuselage's wings should have a pitch implying, together with its TAS vector, generally low sustain support, if other handling rules don't override that; and

for a case if said wired wing involved in a winding-out movement relative to said fuselage, the said fuselage’s wings should have a pitch implying, together with its TAS vector, generally high sustain support, if other handling rules don't override that.

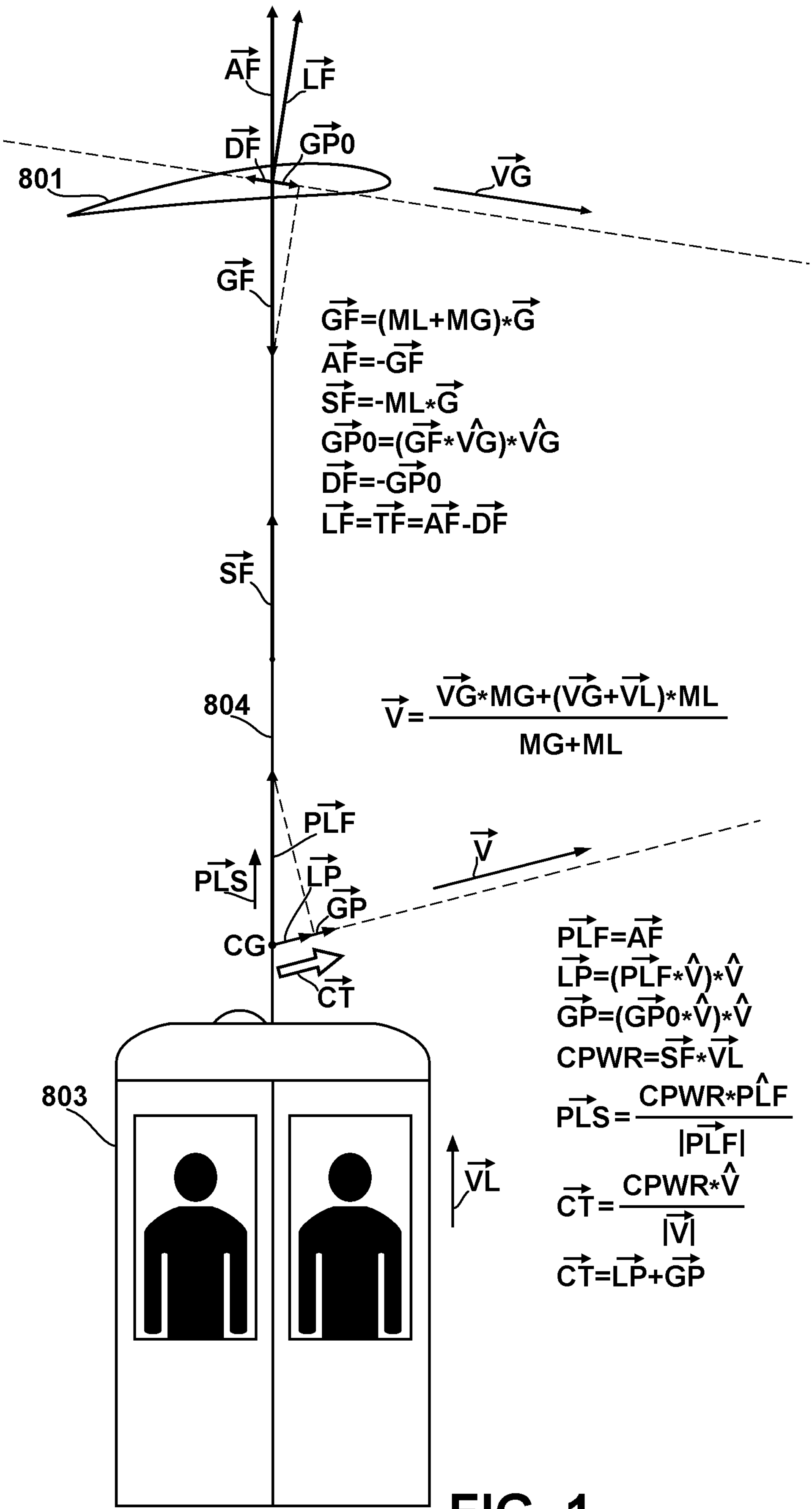
AF
LF
DF
GP0
801
VG
GF
GF=(ML+MG)*G
AF=-GF
SF=-ML*G
GP0=(GF*VG)*VG
DF=-GP0
LF=TF=AF-DF
SF
804
V = (VG*MG+(VG+VL)*ML) / (MG+ML)
PLF
V
PLS
LP
GP
CG
CT
PLF=AF
LP=(PLF*V)*V
GP=(GP0*V)*V
CPWR=SF*VL
PLS = CPWR*PLF / |PLF|
CT = CPWR*V / |V|
CT=LP+GP
803
VL

FIG. 1

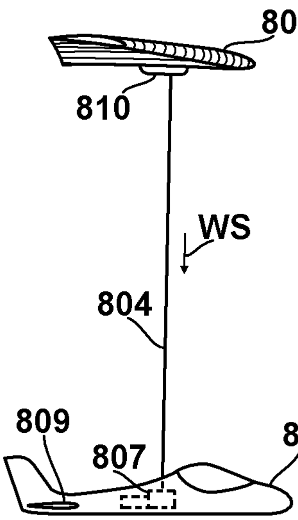

FIG. 2A

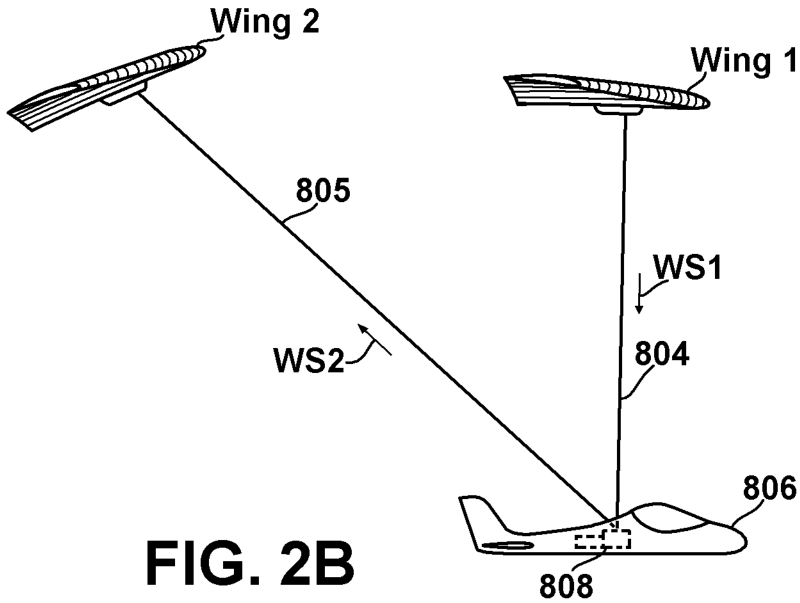

FIG. 2B

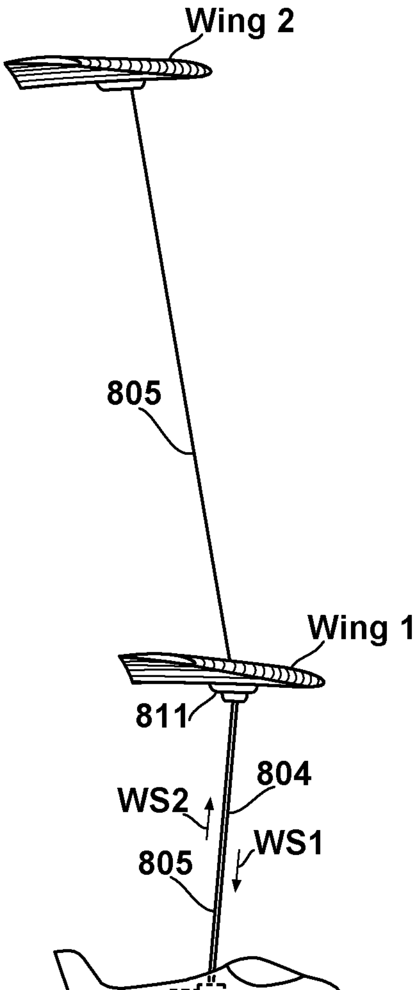

FIG. 2C

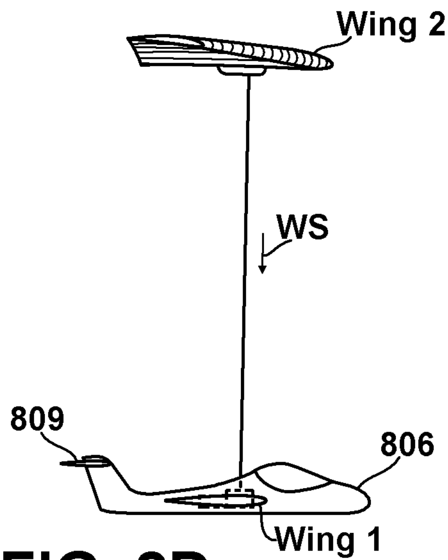

FIG. 2D

811

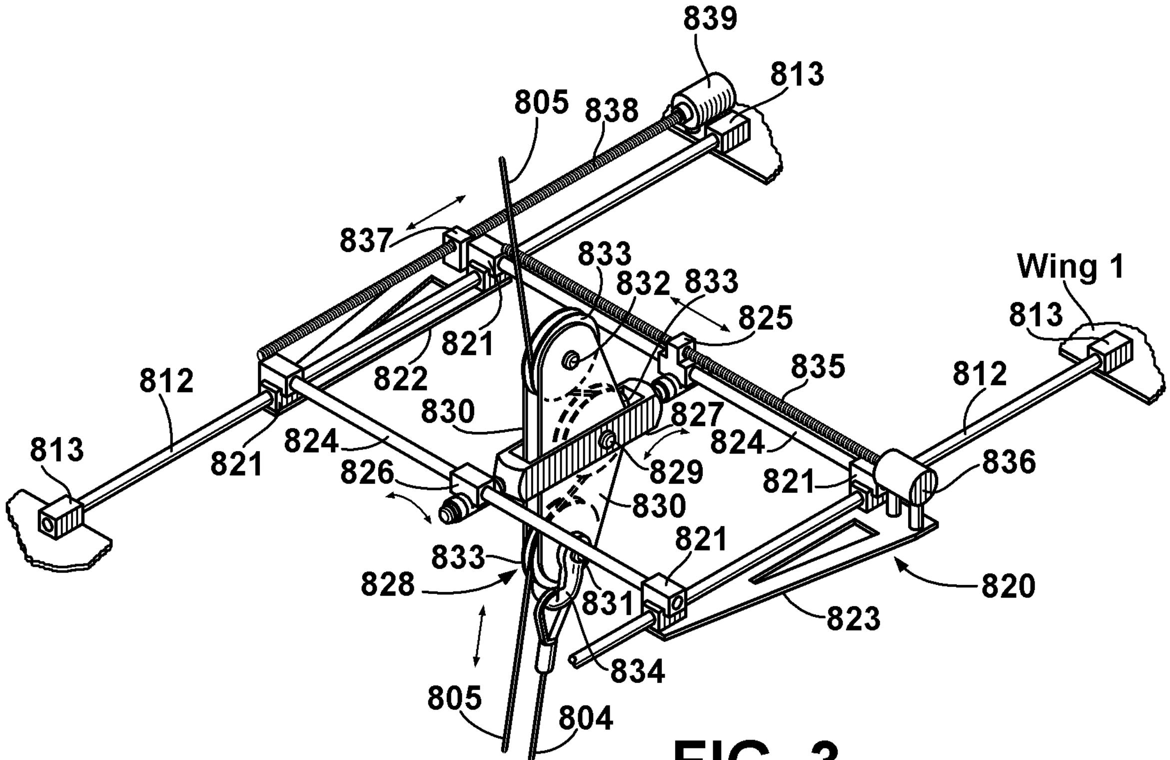

FIG. 3

Common constraints used in wired wing(s) simulations:

Entire and wings:
WingsMass/TotalMass=0.1
Winding Force Limitation Ratio(WFLR)=
WFL/(TotalMass*g)=1.4, where:
WFL - Winding force limitation;
g - gravity acceleration.
Wing airfoil: NACA 4410
Wing Aspect Ratio (AR)=20

Fuselage:
FrontArea/WingArea=0.094
WetArea/WingArea=0.527

Timing:
Time discretization - 0.001s
Result sampling - 0.1s

Wire:
Material: Braided UHMPE
CrossSectionArea/WingArea=0.00000025
ShortestUnwindedLength/Wingspan=1

FIG. 4

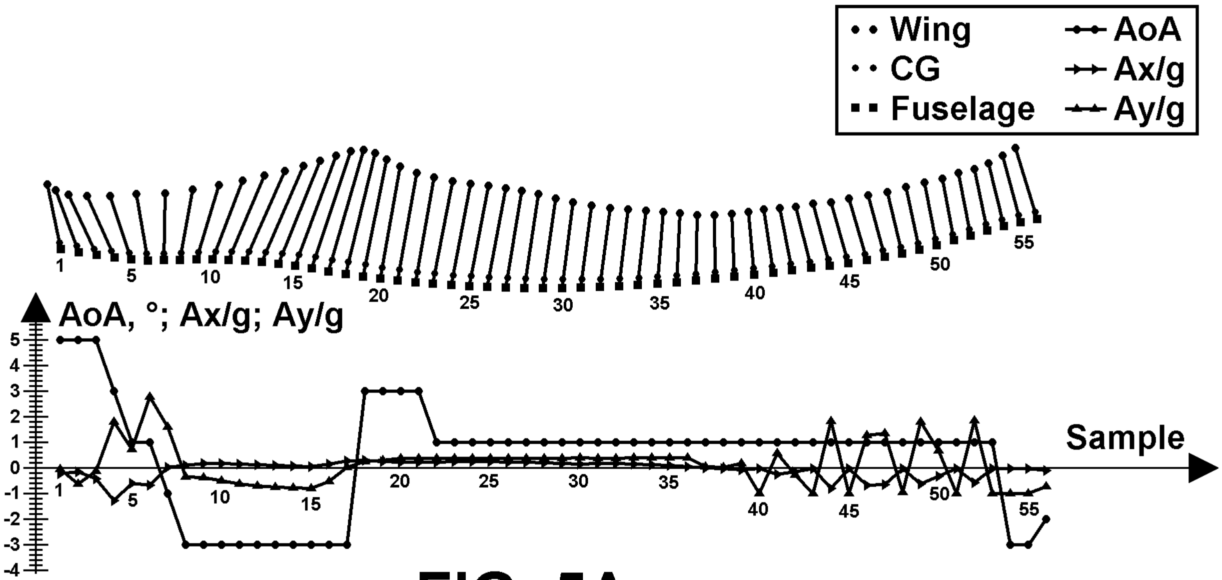
Wing
CG
Fuselage
AoA
Ax/g
Ay/g
AoA, °; Ax/g; Ay/g
Sample

FIG. 5A

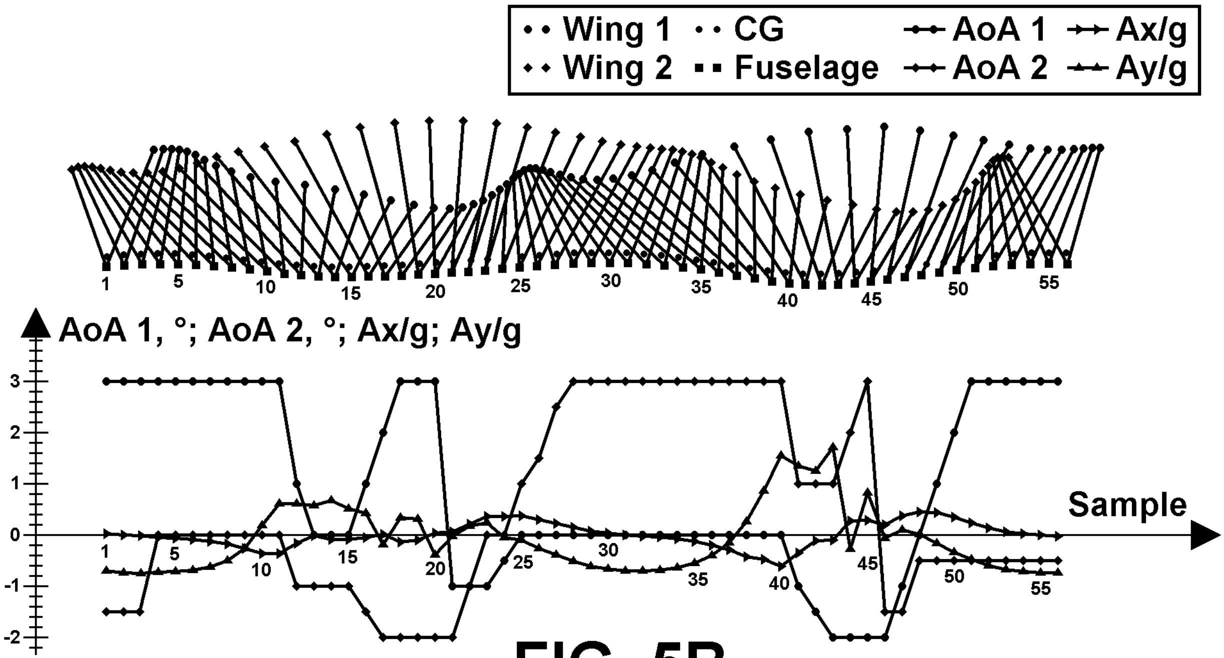
Wing 1
Wing 2
CG
Fuselage
AoA 1
AoA 2
Ax/g
Ay/g
AoA 1, °; AoA 2, °; Ax/g; Ay/g
Sample

FIG. 5B

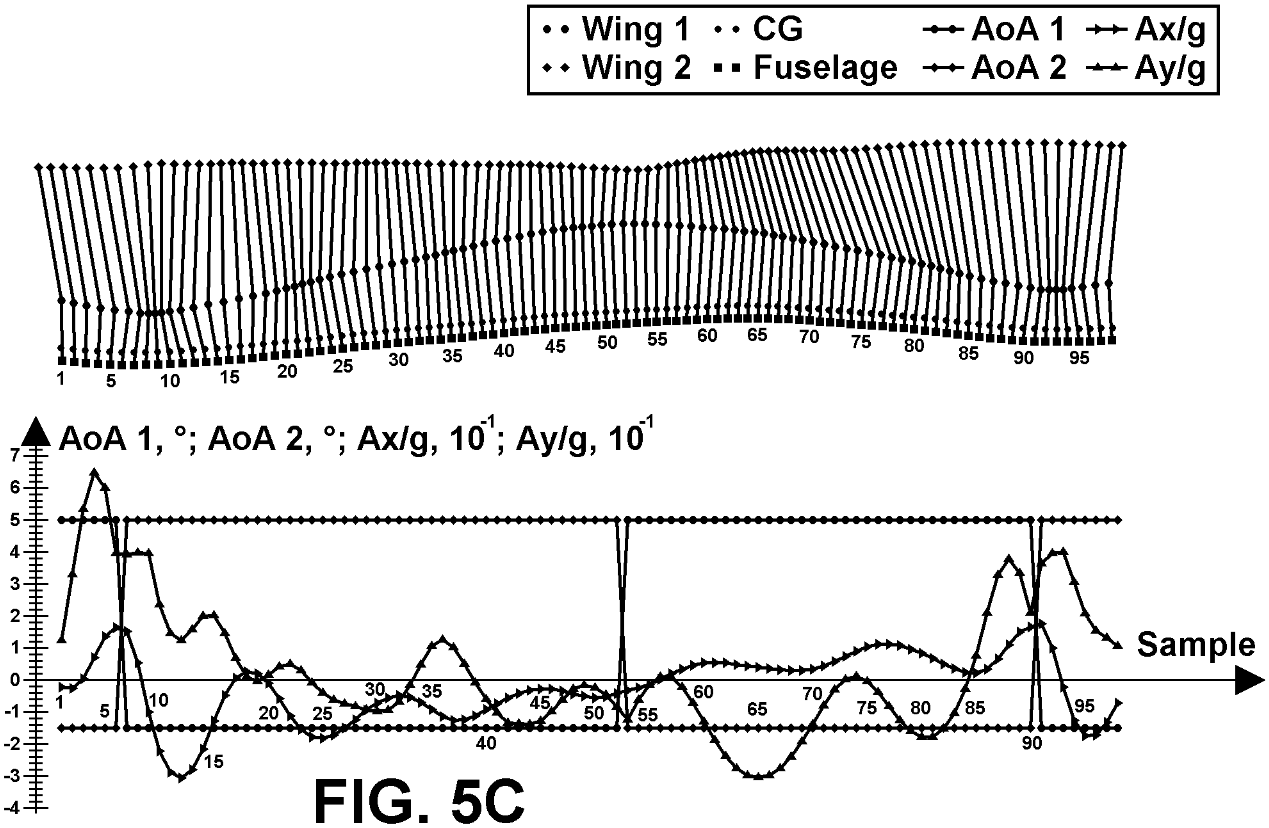
Wing 1
CG
AoA 1
Ax/g
Wing 2
Fuselage
AoA 2
Ay/g
AoA 1, °; AoA 2, °; Ax/g, 10^-1; Ay/g, 10^-1
Sample

FIG. 5C

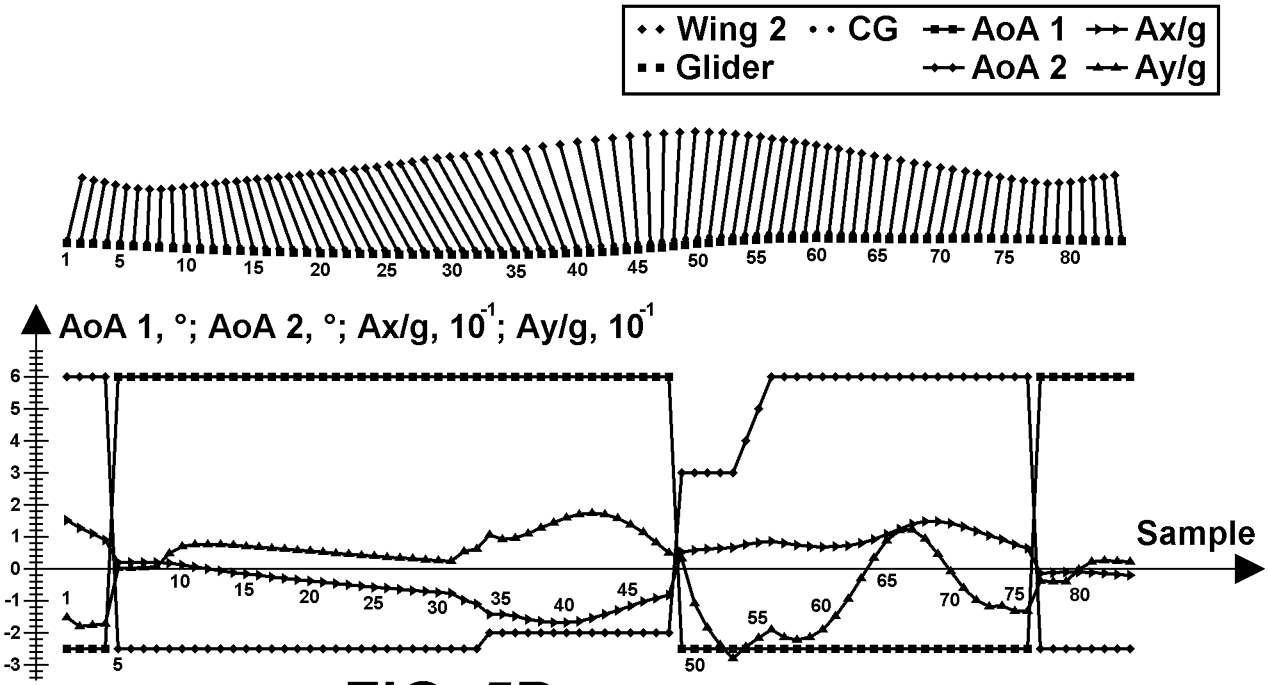
Wing 2
CG
AoA 1
Ax/g
Glider
AoA 2
Ay/g
AoA 1, °; AoA 2, °; Ax/g, 10^-1; Ay/g, 10^-1
Sample

FIG. 5D

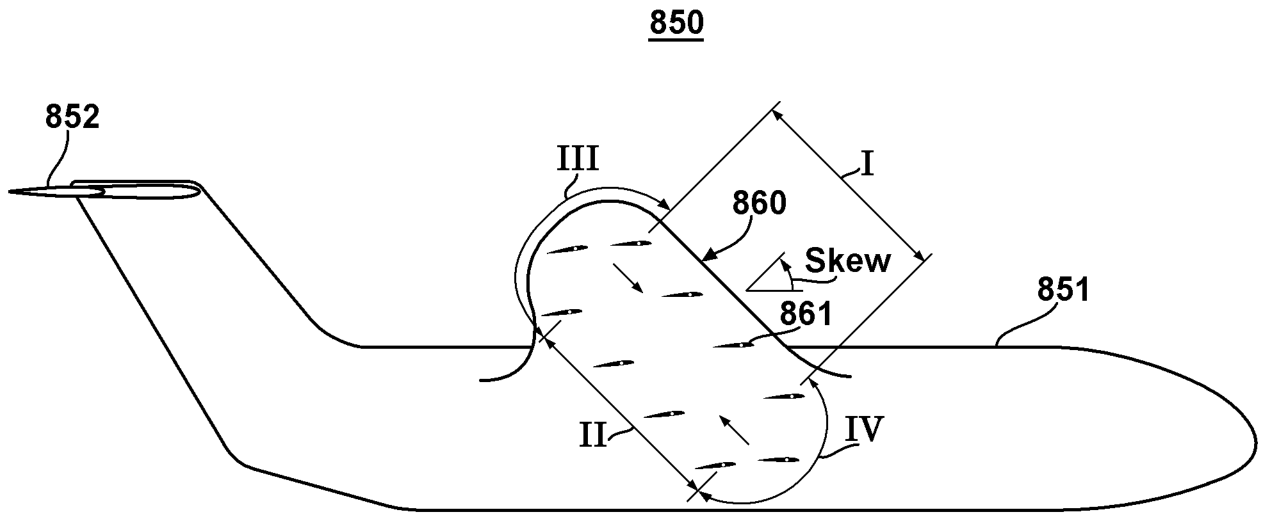
850
852
III
I
860
Skew
851
861
II
IV

FIG. 6

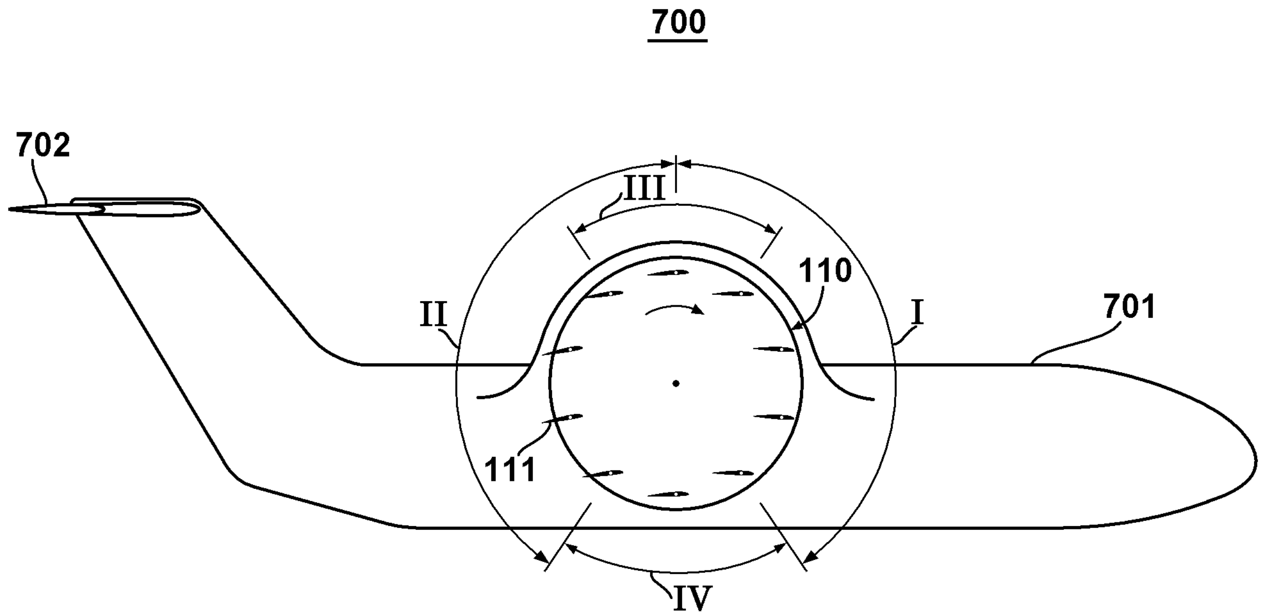
700
702
III
110
II
I
701
111
IV

FIG. 7

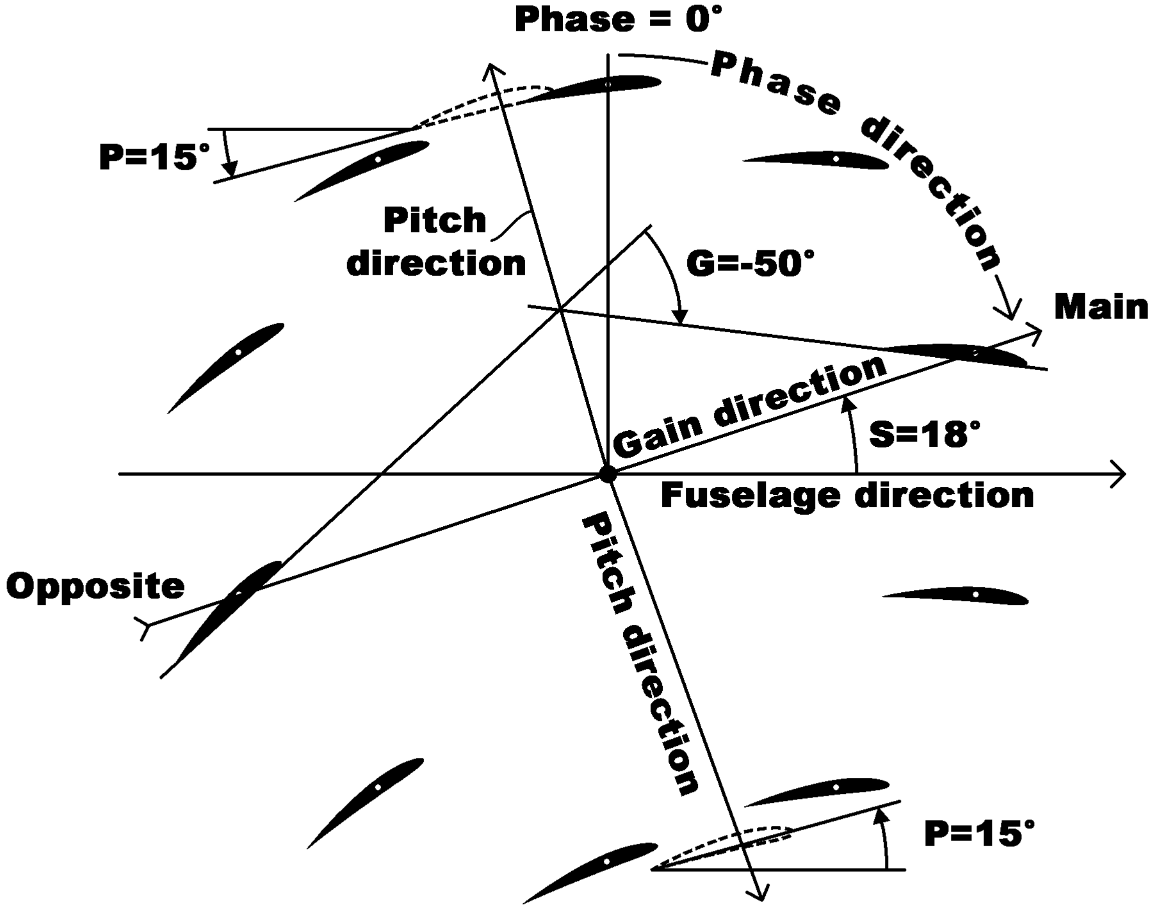
Phase = 0°
Phase direction
P=15°
Pitch direction
G=-50°
Main
Gain direction
S=18°
Fuselage direction
Opposite
Pitch direction
P=15°
PGS=(15;-50;18)

FIG. 8

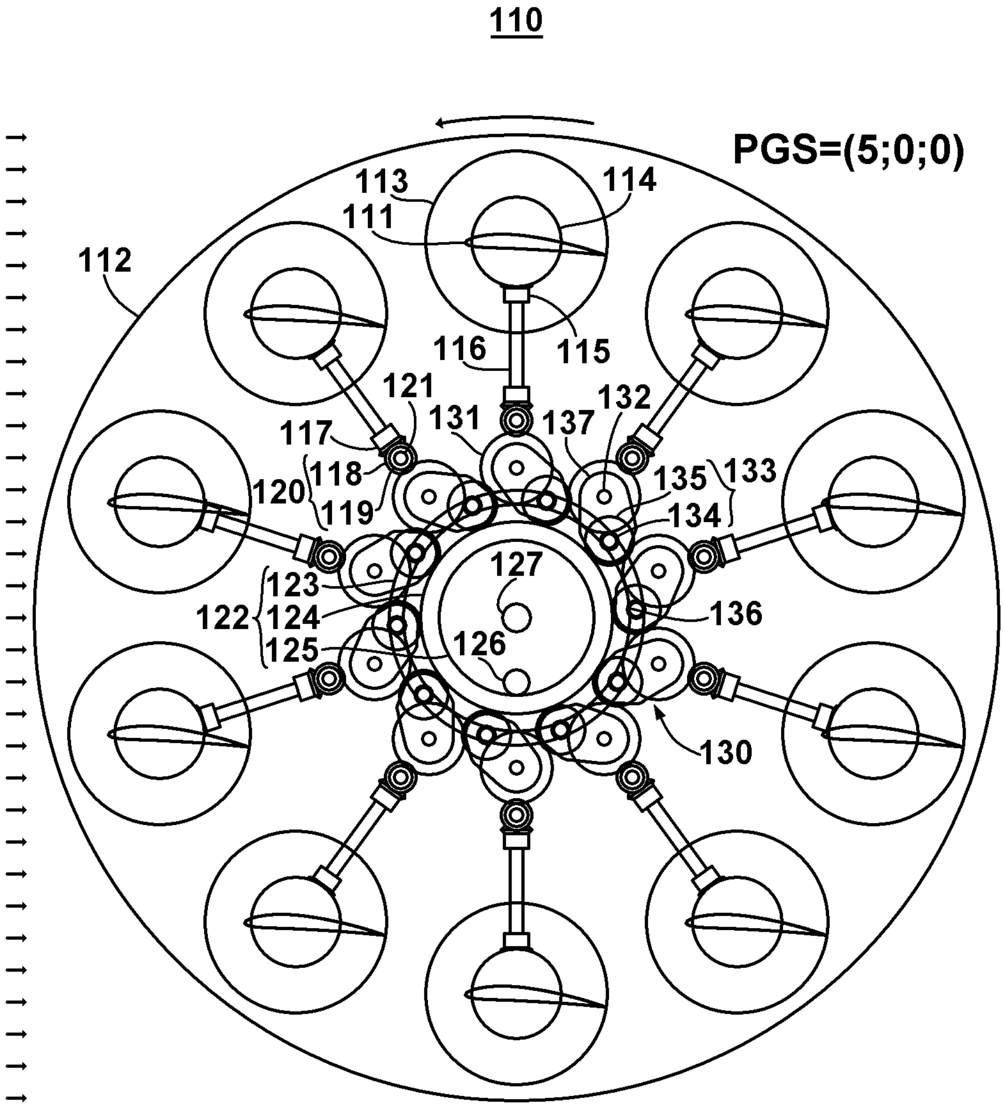
110
PGS=(5;0;0)
113
114
111
112
116
115
121
132
131
137
117
118
135
133
120
119
134
127
123
122
124
136
125
126
130

FIG. 9

110

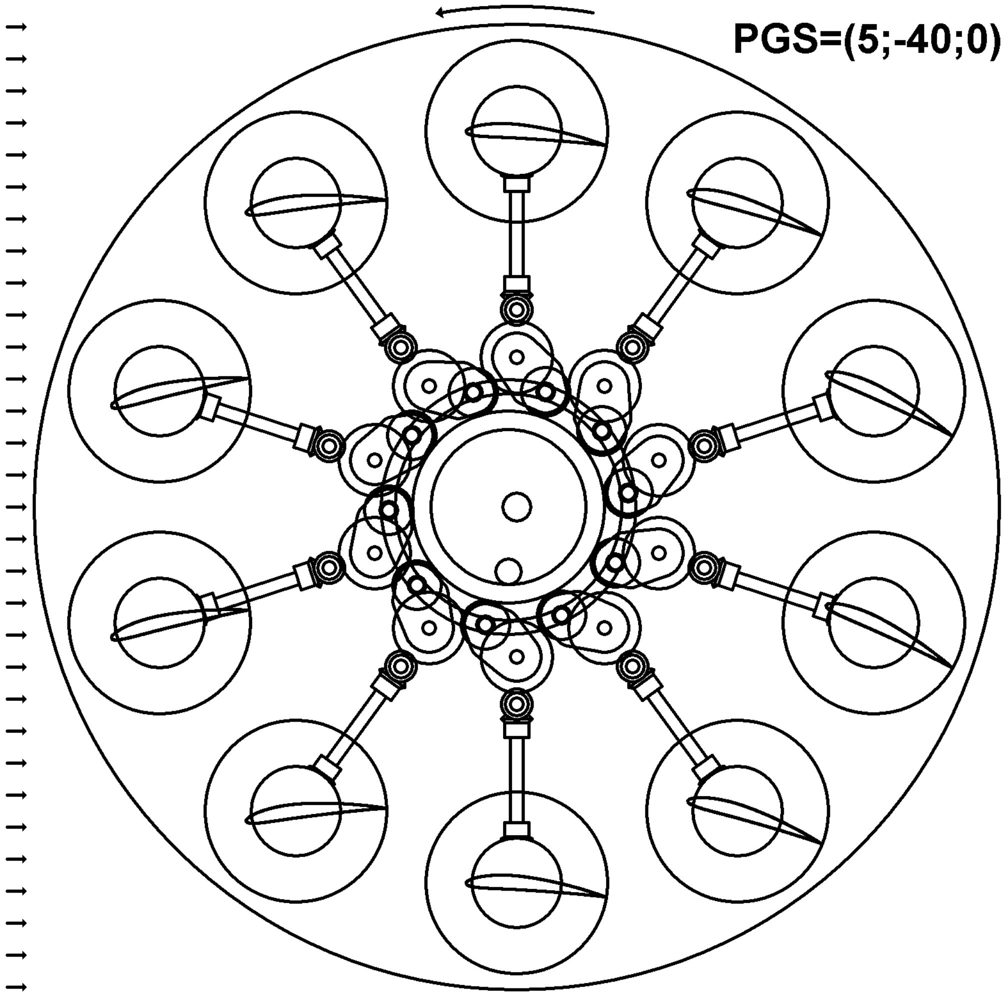

FIG. 10

110

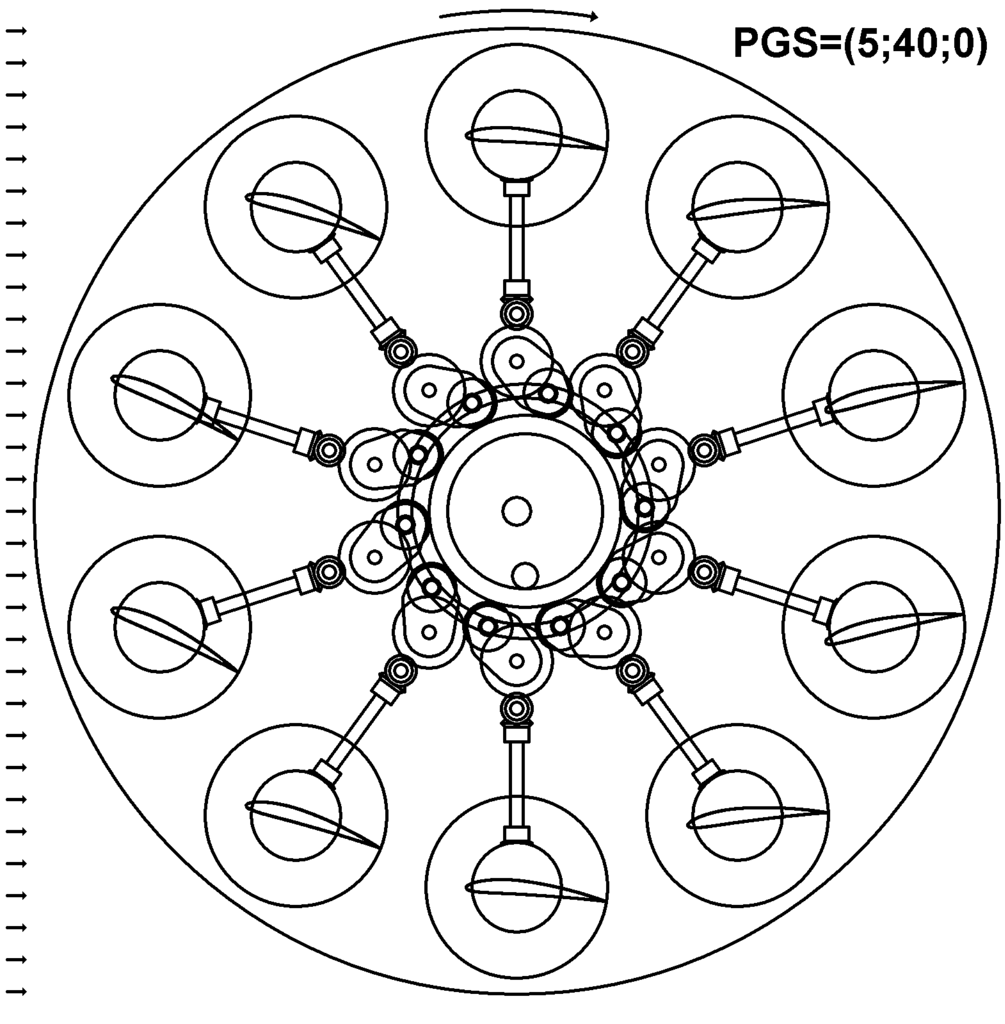

FIG. 11

FIG. 12

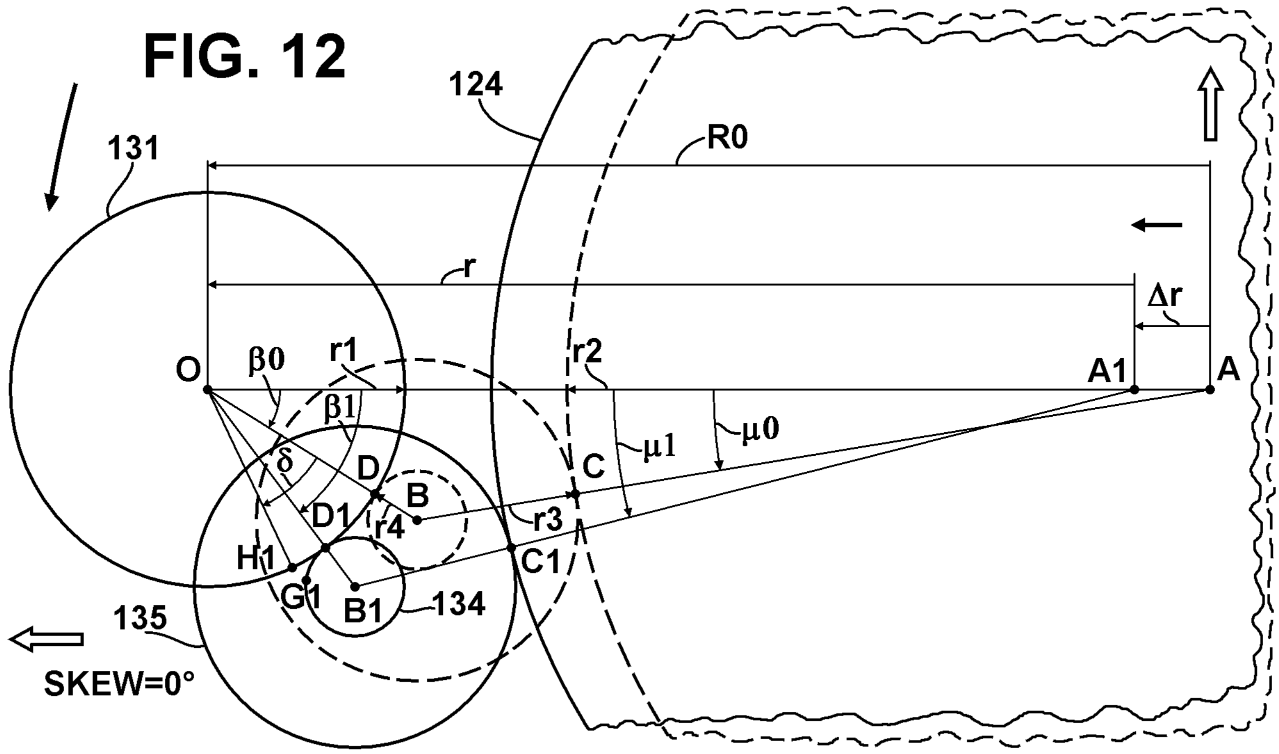
124
131
R0
r
Δr
O
β0
r1
r2
A1
A
β1
δ
D
C
μ1
μ0
B
D1
r4
r3
H1
C1
G1
B1
134
135
SKEW=0°

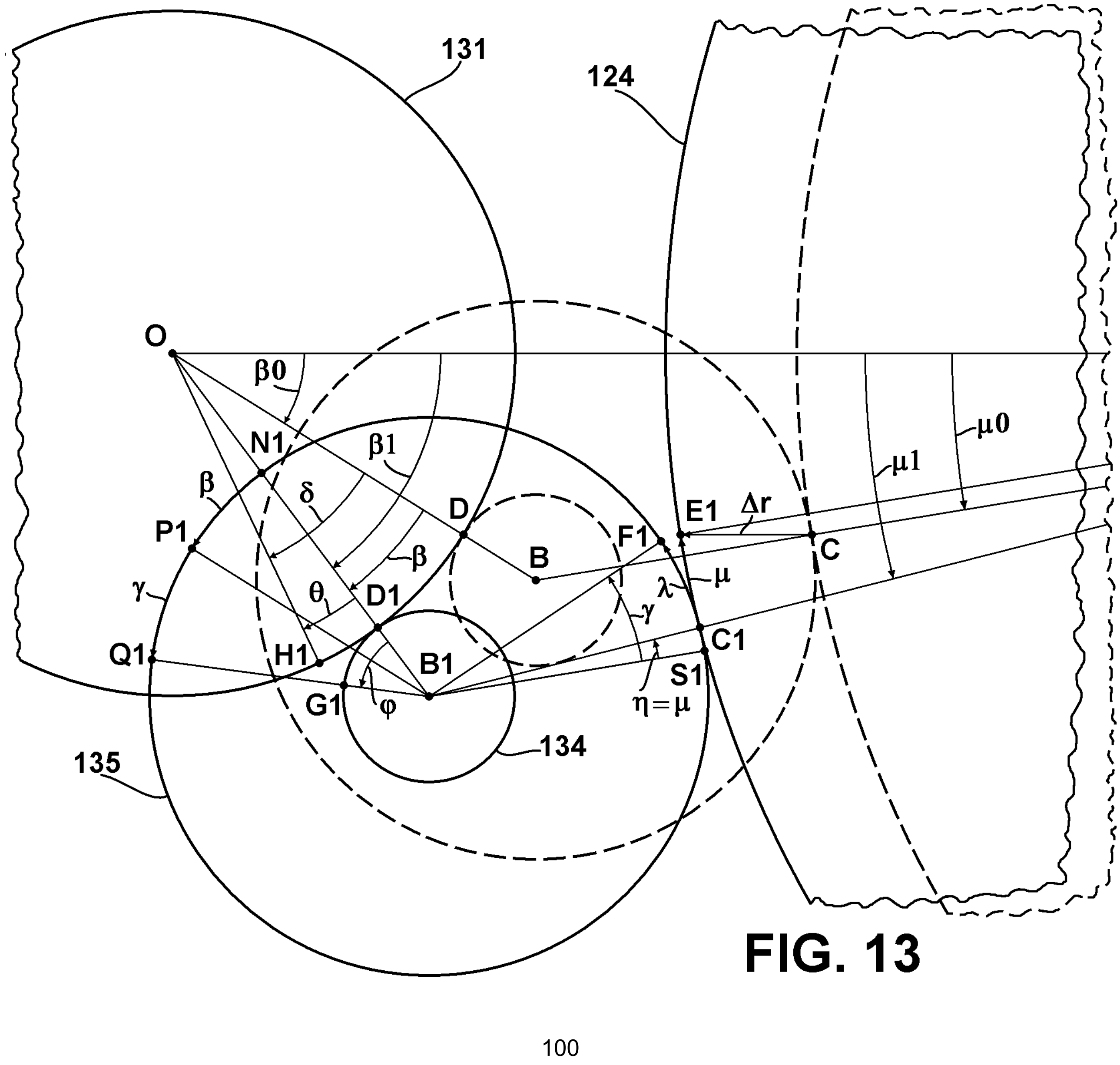
131
124
O
β0
μ0
N1
β1
μ1
β
δ
D
E1
Δr
P1
F1
C
B
β
γ
μ
θ
D1
γ
λ
C1
Q1
H1
B1
S1
G1
φ
η=μ
134
135

FIG. 13

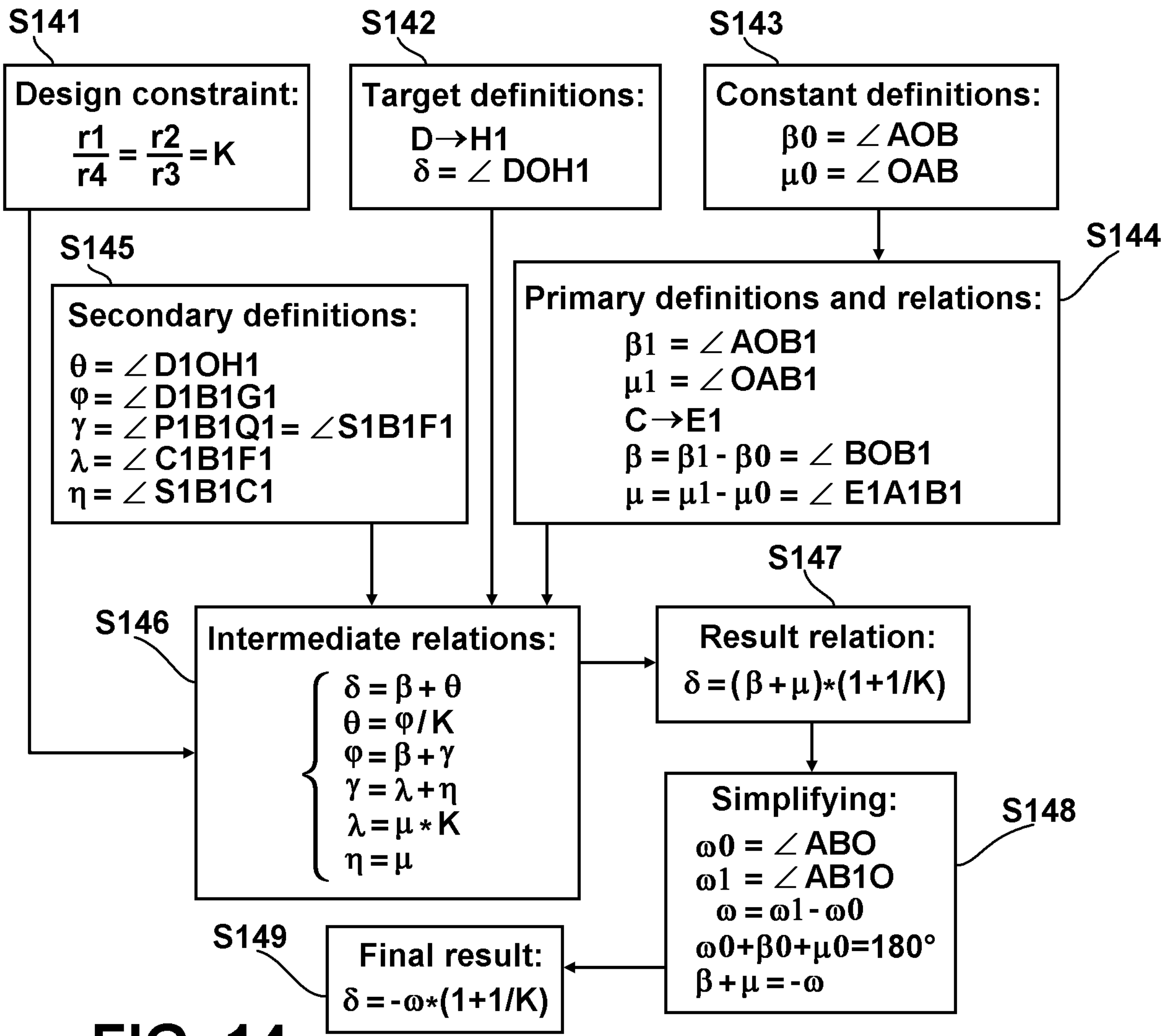
S141
Design constraint:
r1/r4 = r2/r3 = K
S142
Target definitions:
D→H1
δ = ∠ DOH1
S143
Constant definitions:
β0 = ∠ AOB
μ0 = ∠ OAB
S144
Primary definitions and relations:
β1 = ∠ AOB1
μ1 = ∠ OAB1
C→E1
β = β1 - β0 = ∠ BOB1
μ = μ1 - μ0 = ∠ E1A1B1
S145
Secondary definitions:
θ = ∠ D1OH1
φ = ∠ D1B1G1
γ = ∠ P1B1Q1 = ∠ S1B1F1
λ = ∠ C1B1F1
η = ∠ S1B1C1
S146
Intermediate relations:
δ = β + θ
θ = φ / K
φ = β + γ
γ = λ + η
λ = μ * K
η = μ
S147
Result relation:
δ = (β + μ)*(1+1/K)
S148
Simplifying:
ω0 = ∠ ABO
ω1 = ∠ AB1O
ω = ω1 - ω0
ω0+β0+μ0=180°
β + μ = -ω
S149
Final result:
δ = -ω*(1+1/K)

FIG. 14

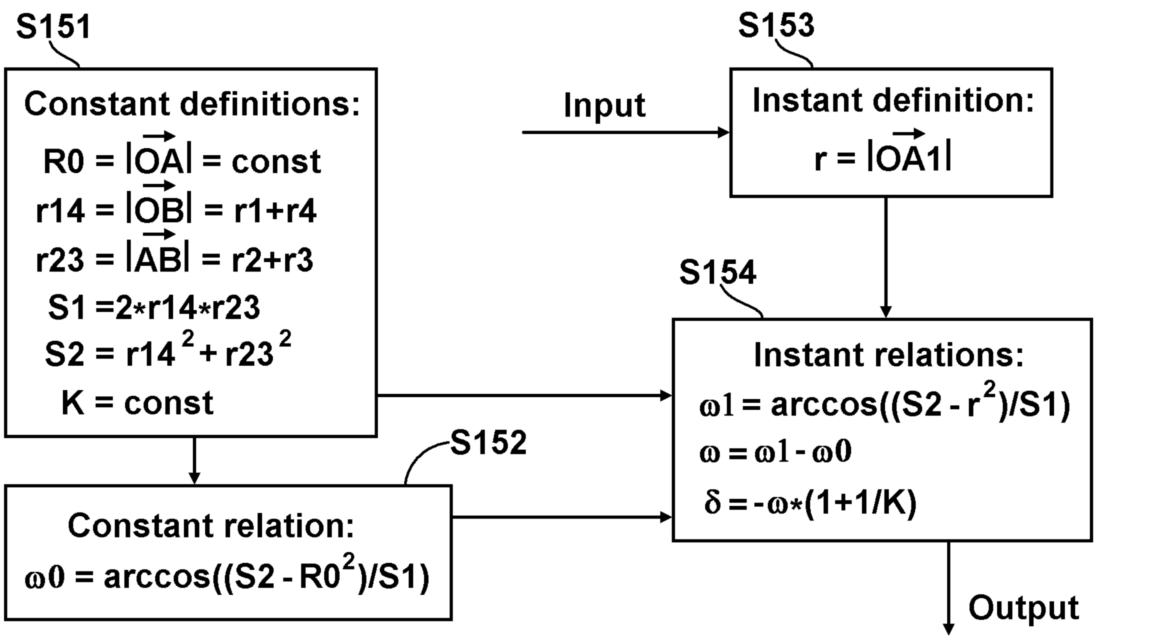
S151
Constant definitions:
R0 = |OA| = const
r14 = |OB| = r1+r4
r23 = |AB| = r2+r3
S1 = 2*r14*r23
S2 = r14² + r23²
K = const
S152
Constant relation:
ω0 = arccos((S2 - R0²)/S1)
Input
S153
Instant definition:
r = |OA1|
S154
Instant relations:
ω1 = arccos((S2 - r²)/S1)
ω = ω1 - ω0
δ = -ω*(1+1/K)
Output

FIG. 15

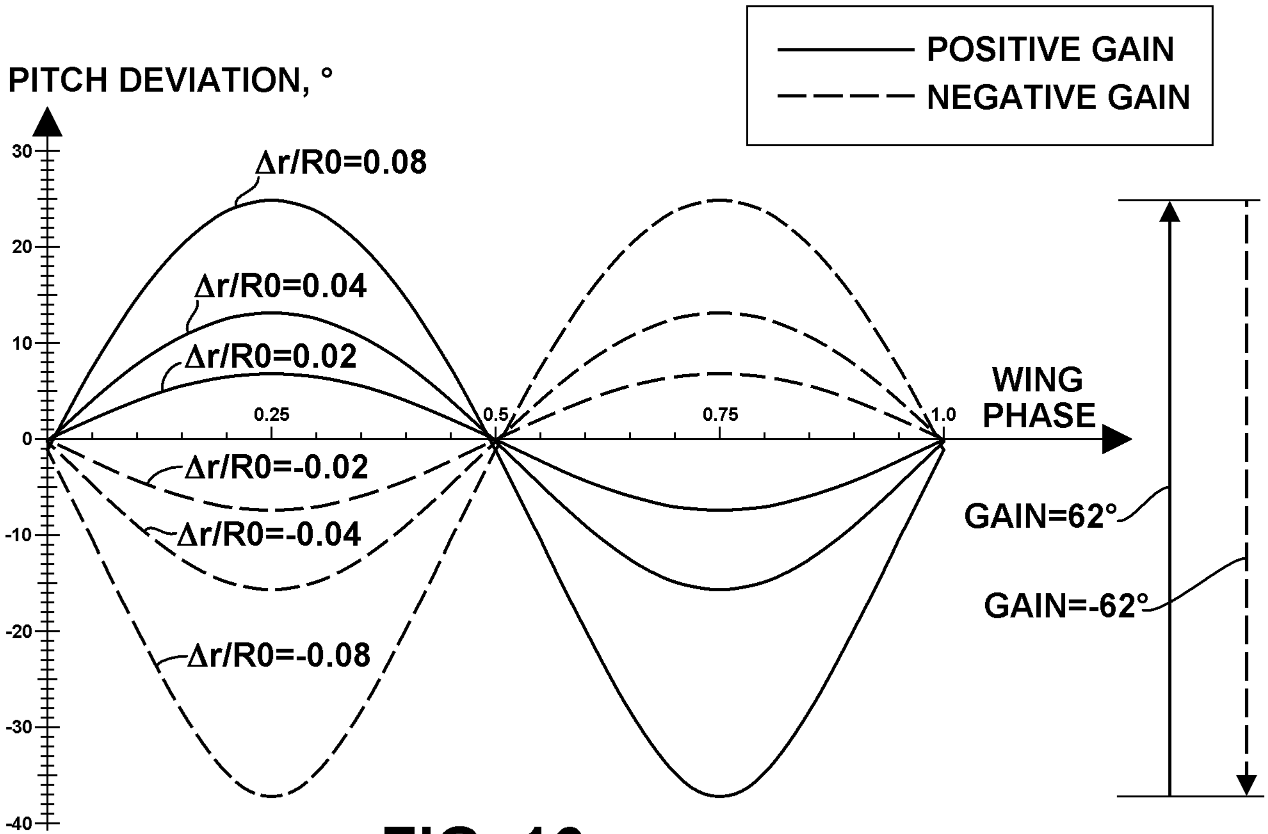
POSITIVE GAIN
NEGATIVE GAIN
PITCH DEVIATION, °
Δr/R0=0.08
Δr/R0=0.04
Δr/R0=0.02
Δr/R0=-0.02
Δr/R0=-0.04
Δr/R0=-0.08
WING PHASE
0.25
0.5
0.75
1.0
30
20
10
0
-10
-20
-30
-40
GAIN=62°
GAIN=-62°

FIG. 16

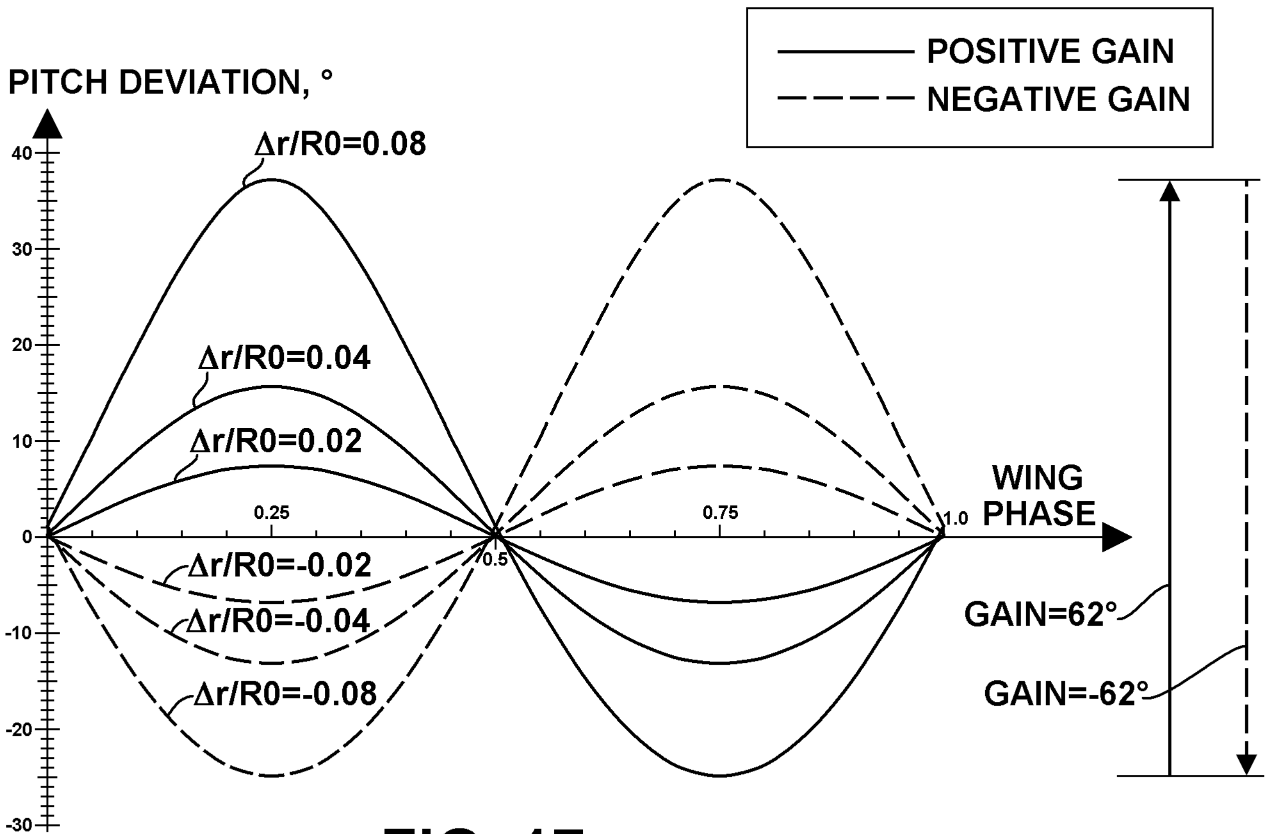
POSITIVE GAIN
NEGATIVE GAIN
PITCH DEVIATION, °
Δr/R0=0.08
Δr/R0=0.04
Δr/R0=0.02
Δr/R0=-0.02
Δr/R0=-0.04
Δr/R0=-0.08
WING PHASE
0.25
0.5
0.75
1.0
40
30
20
10
0
-10
-20
-30
GAIN=62°
GAIN=-62°

FIG. 17

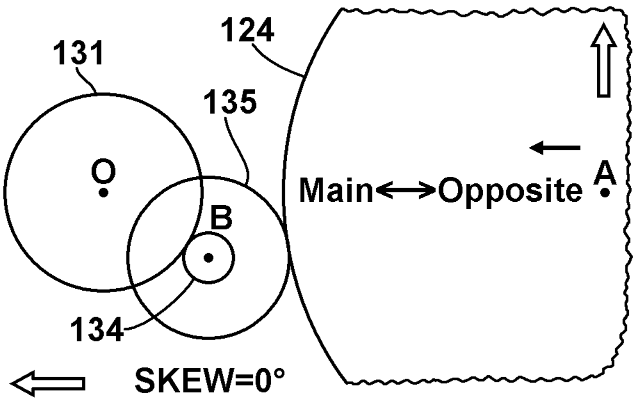

FIG. 18A

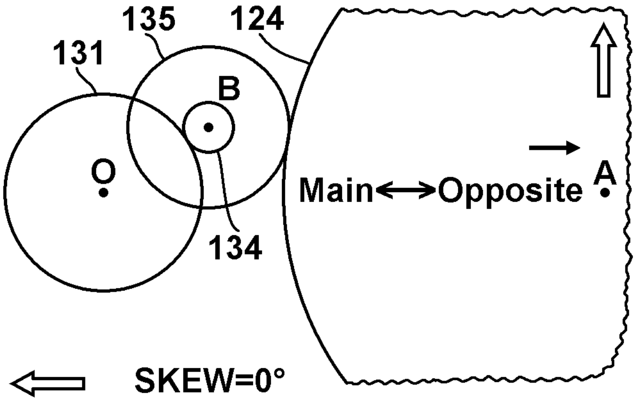

FIG. 18B

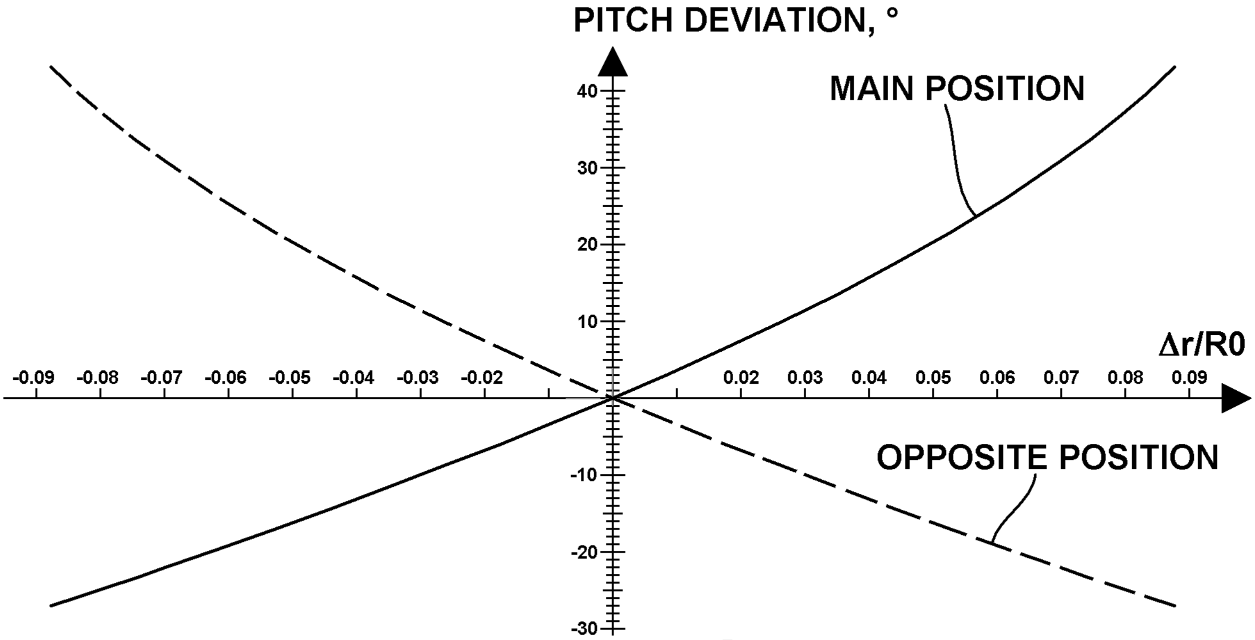

FIG. 19

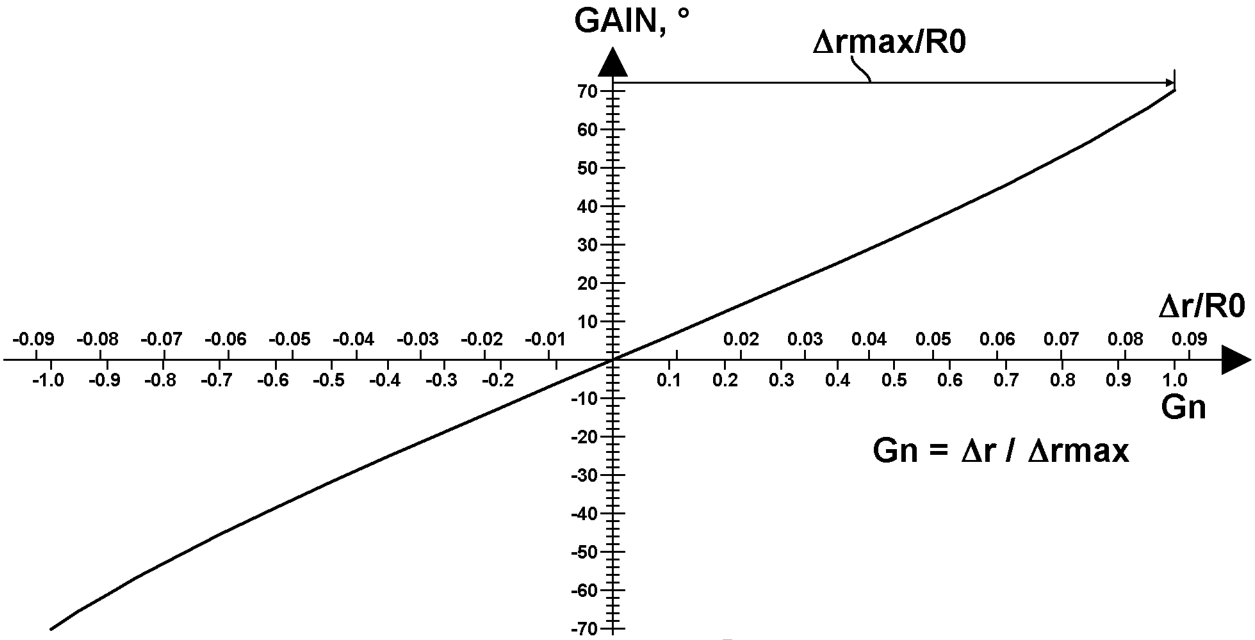

FIG. 20

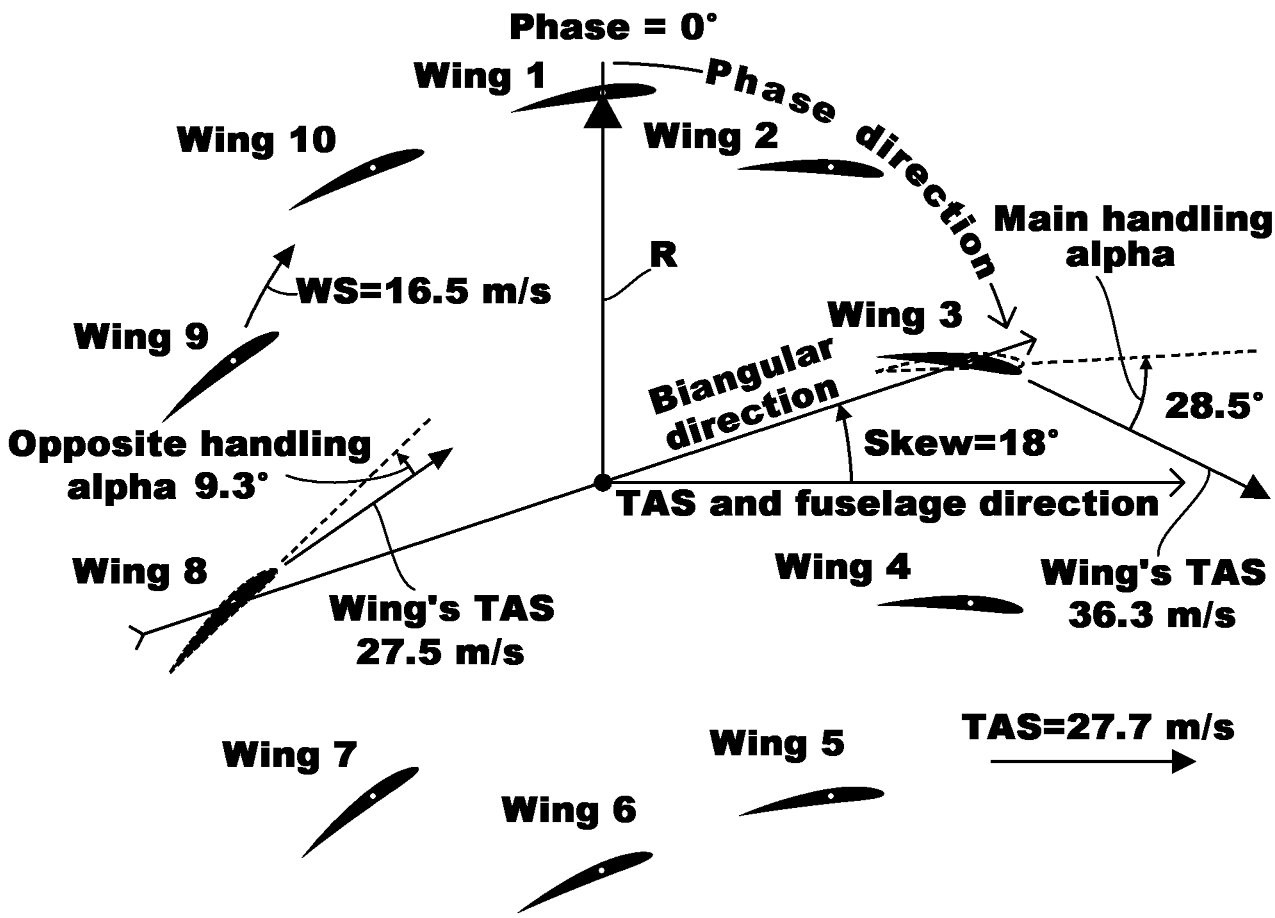
Phase = 0°
Wing 1
Phase direction
Wing 10
Wing 2
Main handling alpha
R
WS=16.5 m/s
Wing 3
Wing 9
Biangular direction
28.5°
Opposite handling alpha 9.3°
Skew=18°
TAS and fuselage direction
Wing 8
Wing 4
Wing's TAS 36.3 m/s
Wing's TAS 27.5 m/s
TAS=27.7 m/s
Wing 7
Wing 5
Wing 6

FIG. 21

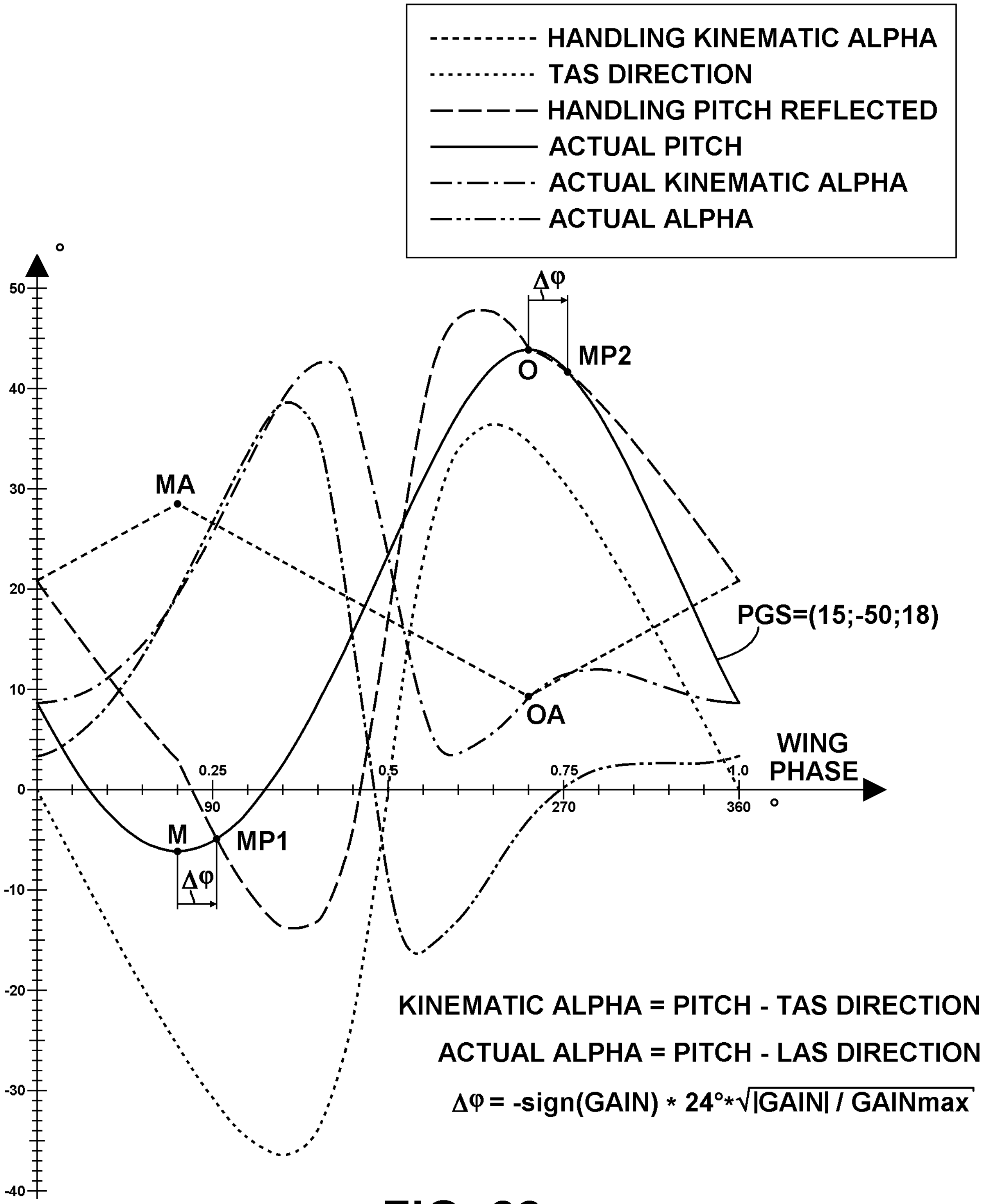
HANDLING KINEMATIC ALPHA
TAS DIRECTION
HANDLING PITCH REFLECTED
ACTUAL PITCH
ACTUAL KINEMATIC ALPHA
ACTUAL ALPHA
°
50
40
30
20
10
0
-10
-20
-30
-40
Δφ
O
MP2
MA
PGS=(15;-50;18)
OA
WING
PHASE
0.25
0.5
0.75
1.0
90
270
360
°
M
MP1
Δφ
KINEMATIC ALPHA = PITCH - TAS DIRECTION
ACTUAL ALPHA = PITCH - LAS DIRECTION
Δφ = -sign(GAIN) * 24°*√|GAIN| / GAINmax

FIG. 22

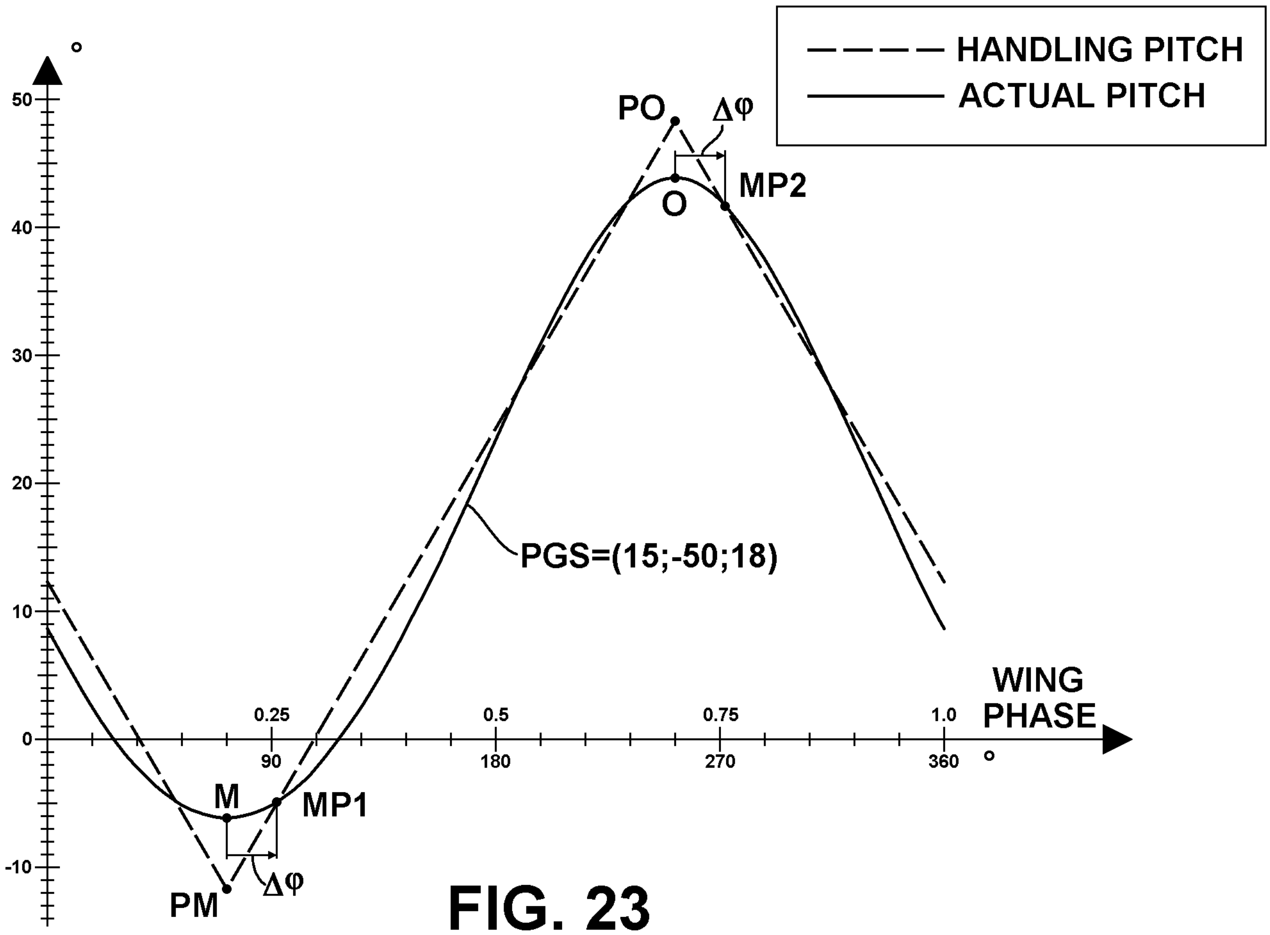

FIG. 23

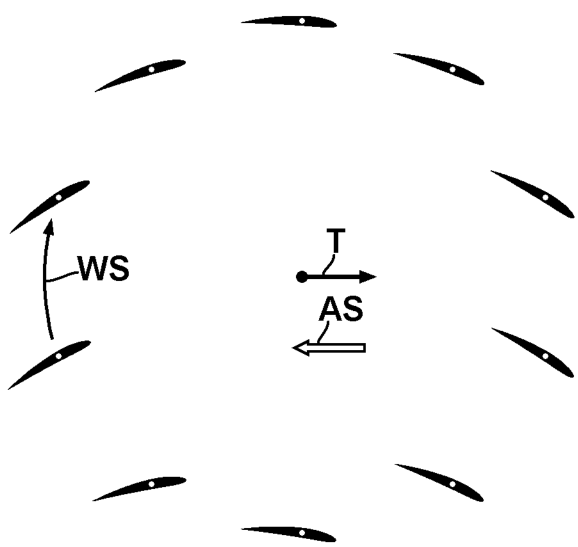

PM=-40° PO=40° Skew=-5°
PGS=(-5.6;-66.1;-5)

FIG.24A

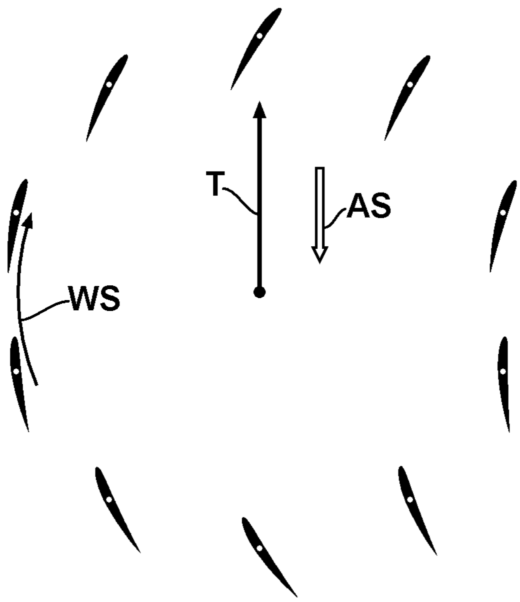

PM=50° PO=130° Skew=85°
PGS=(84.4;-66.1;85)

FIG. 24B

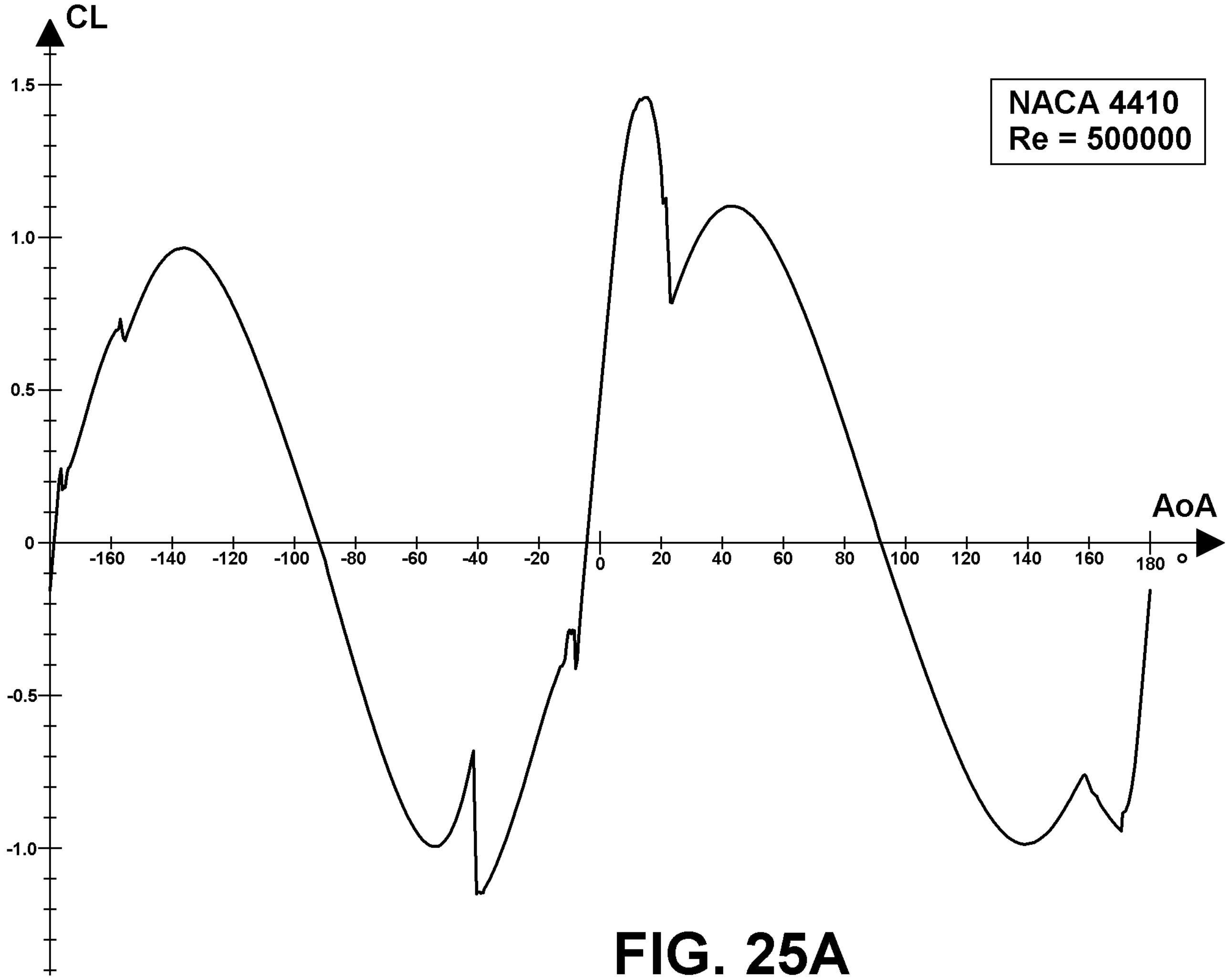

FIG. 25A

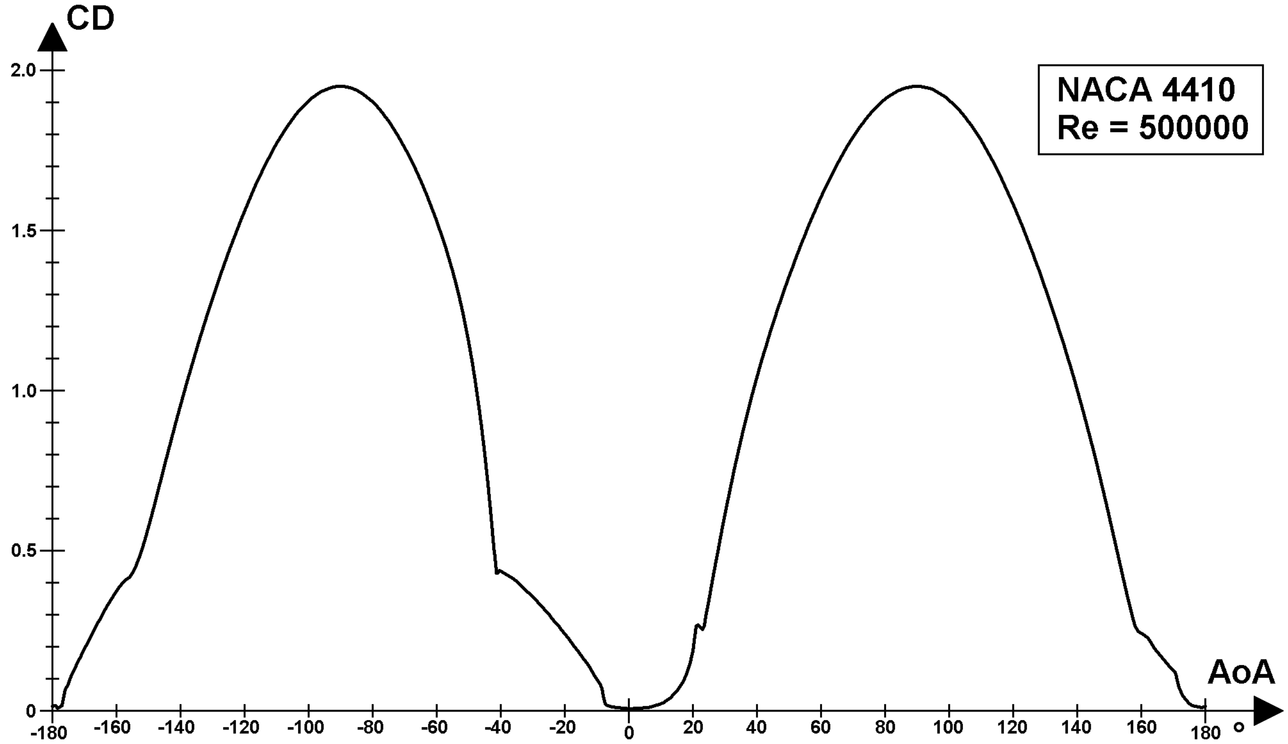

FIG. 25B

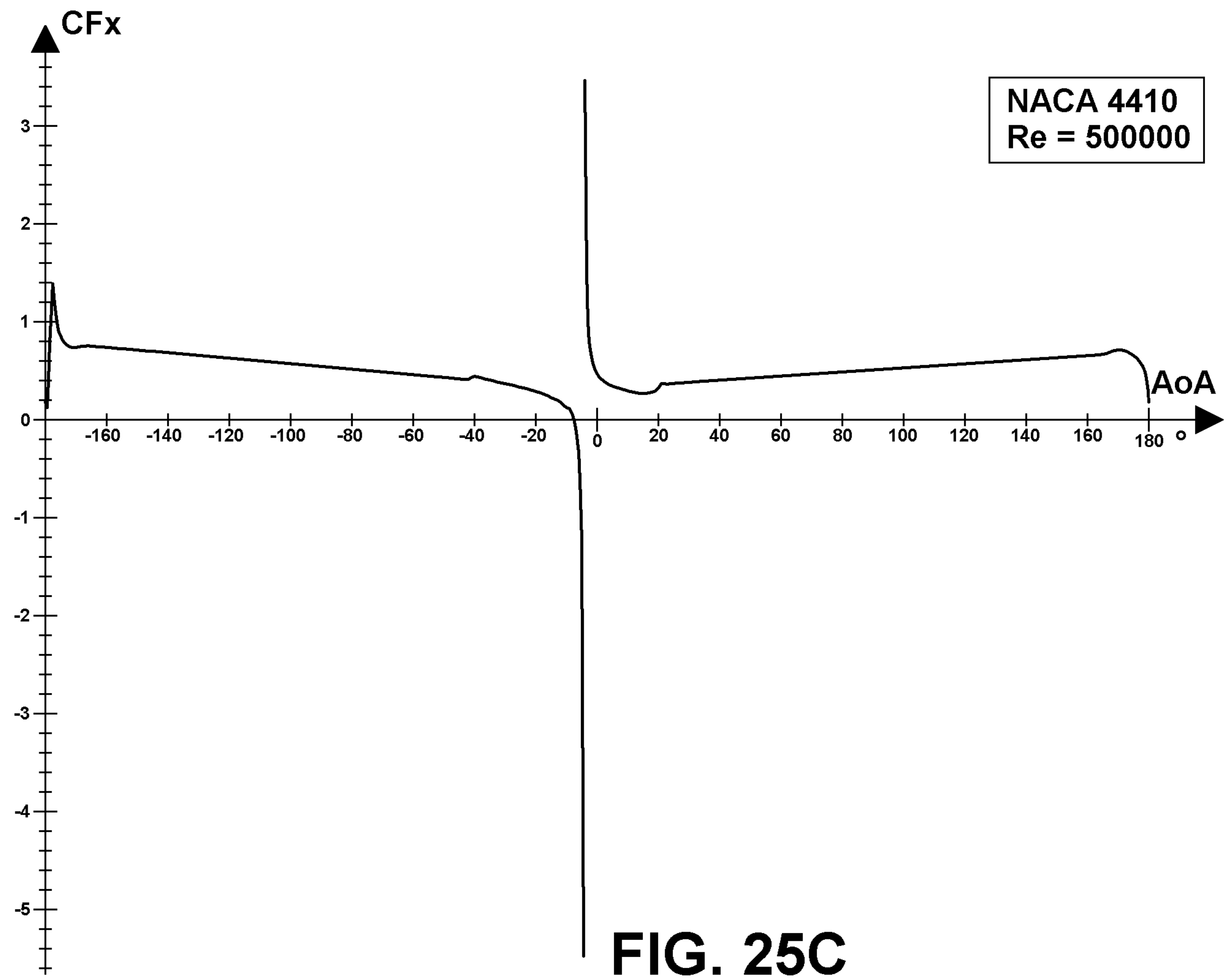

FIG. 25C

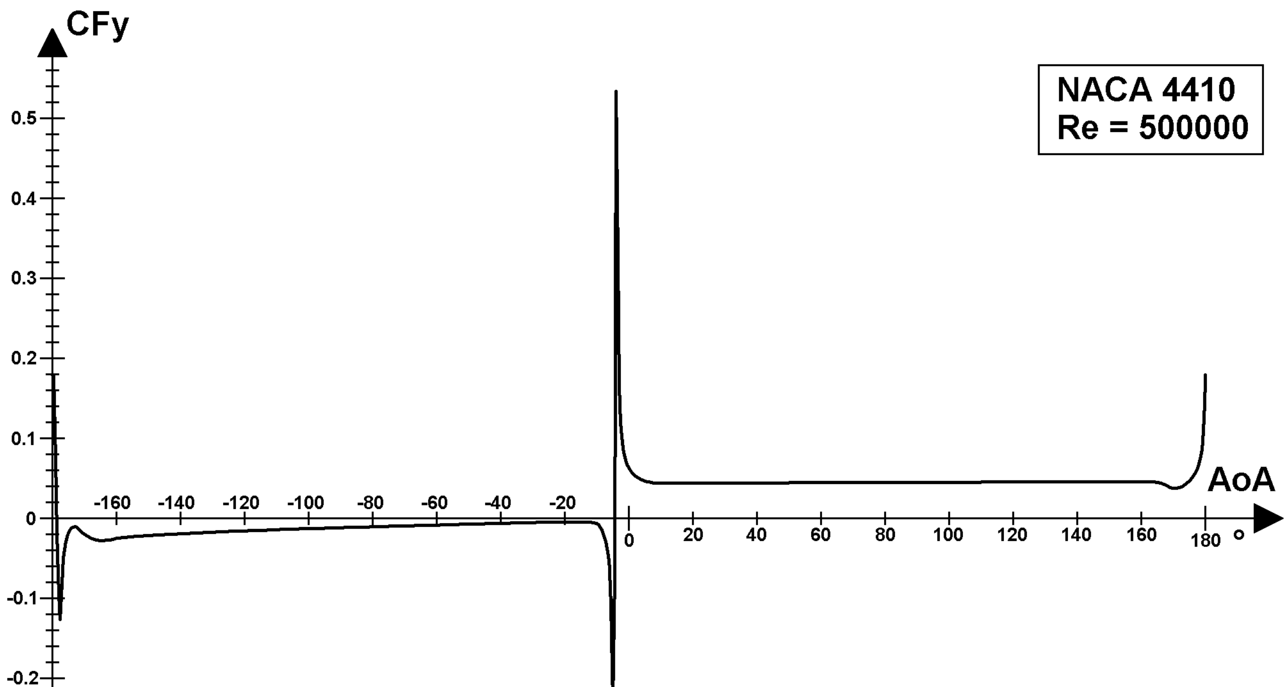

FIG. 25D

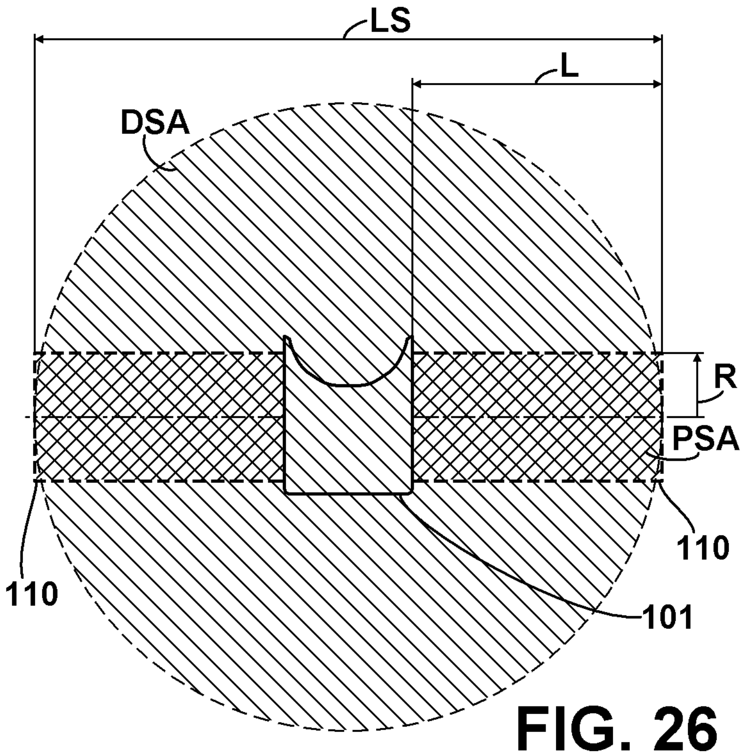

FIG. 26

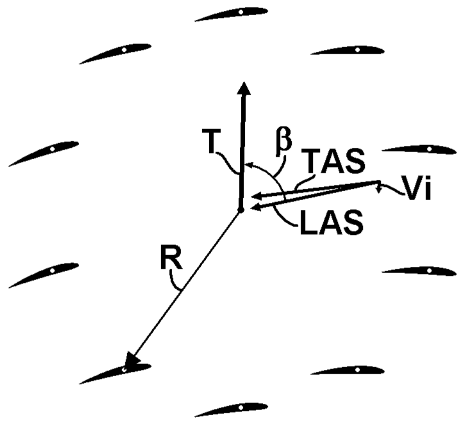

FIG. 27

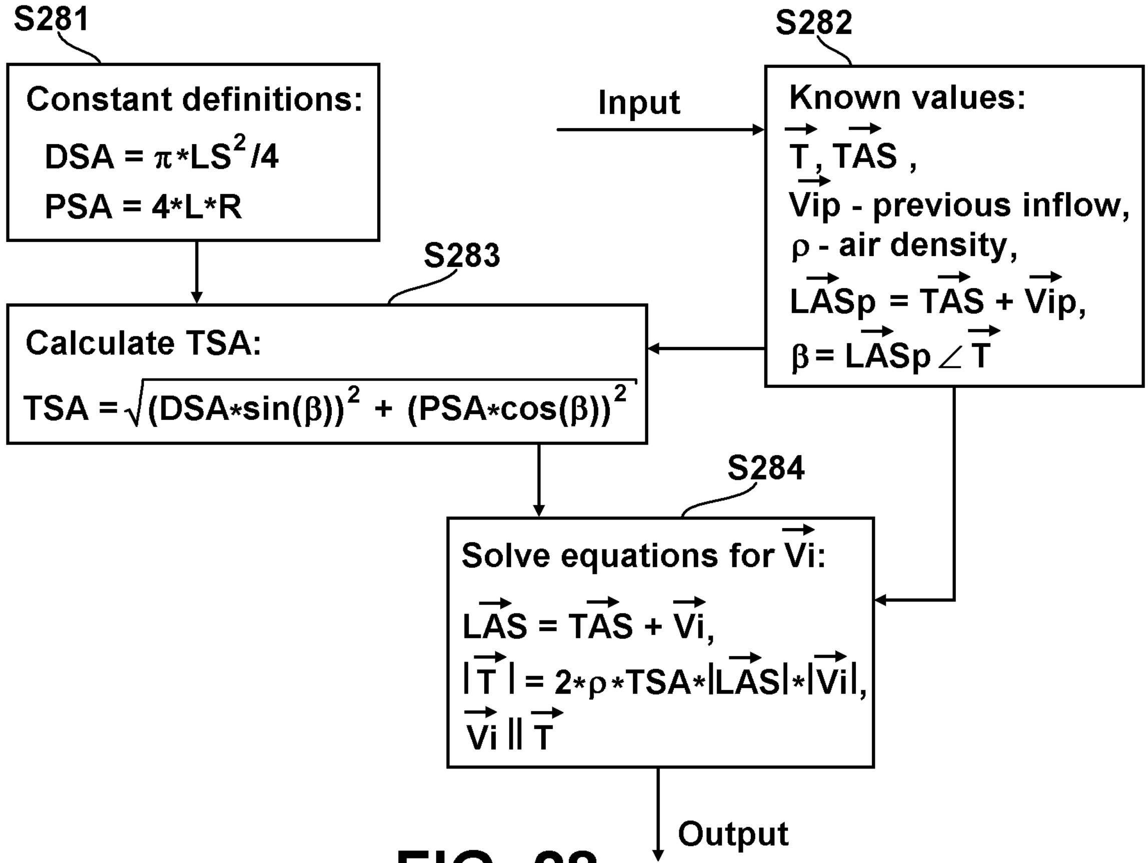

FIG. 28

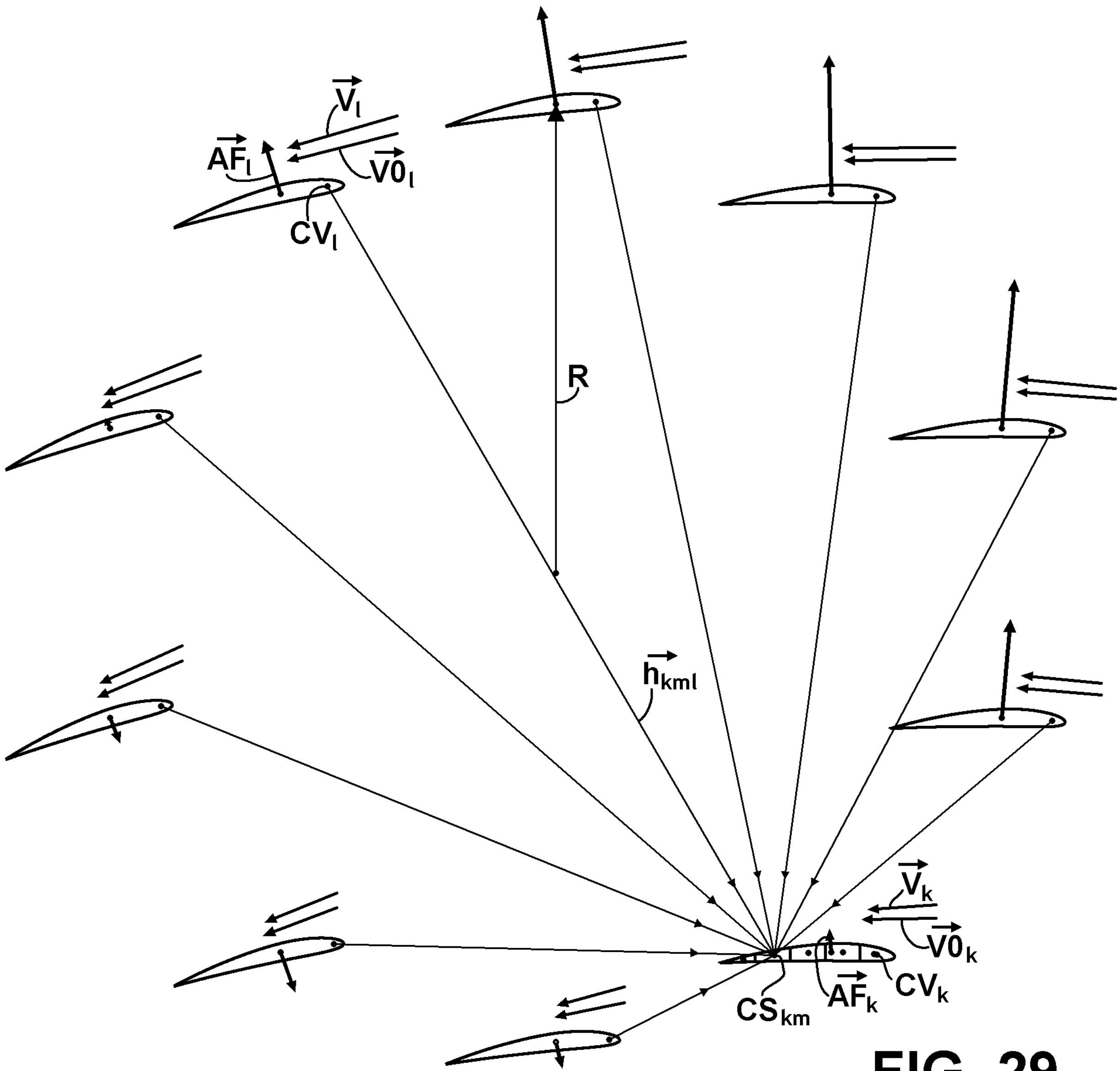

FIG. 29

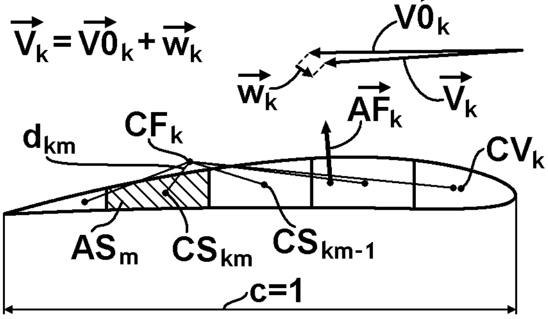

$$\vec{V}_k = \vec{V0}_k + \vec{w}_k$$

$$\vec{w}_k = \frac{\sum_{m=1}^{M} \vec{w}_{km} * AS_m /(1+d_{km})}{\sum_{m=1}^{M} AS_m /(1+d_{km})}$$

$$\vec{w}_{km} = \sum_{l=1,\ l\neq k}^{N} \vec{w}_{kml}$$

FIG. 30

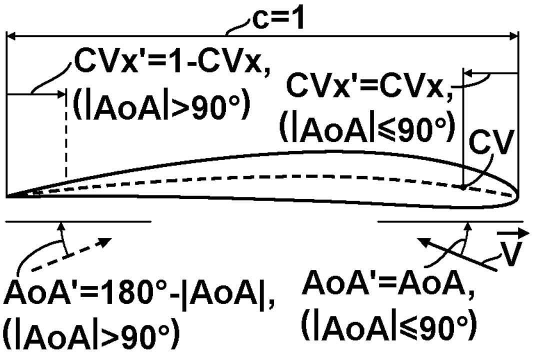

$CVx' = 0.5*(1-(\sin(|AoA'|))^{0.07})$

$CVy = \text{camberline}(CVx)$

FIG. 31

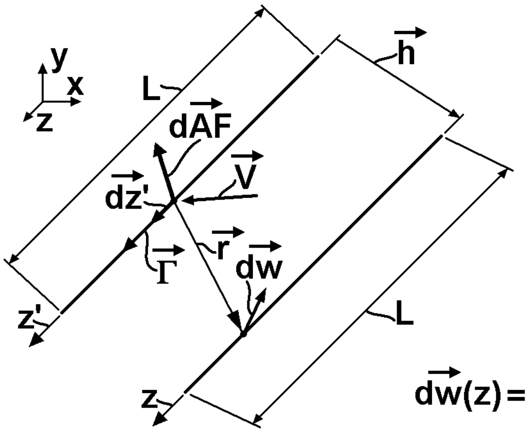

$$\Gamma = \frac{\vec{AF} \times \hat{V}}{\rho * |\vec{V}| * L} * \hat{z} \qquad d\vec{w} = \frac{\Gamma * d\vec{z}' \times \hat{r}}{4 * \pi * |\vec{r}|^2}$$

$$d\vec{w} = \frac{\Gamma * \hat{z} \times \hat{r}}{4 * \pi * |\vec{r}|^2} * dz'$$

$$\hat{\tau} = \hat{z} \times \hat{h}$$
$$h = |\vec{h}|$$
$$r = |\vec{r}|$$
$$\hat{z} \times \hat{r} = \hat{\tau} * \frac{h}{r}$$
$$r = \sqrt{h^2 + (z-z')^2}$$

$$d\vec{w}(z) = \frac{\Gamma * h * \hat{\tau}}{4 * \pi * \sqrt{h^2 + (z-z')^2}^{\,3}} * dz'$$

$$\vec{w}(z) = \int_0^L d\vec{w}(z)$$

$$\vec{w} = \langle \vec{w}(z) \rangle = \frac{1}{L} \int_0^L \vec{w}(z) * dz = \frac{\Gamma * h * \hat{\tau}}{4 * \pi * L} \int_0^L \int_0^L \frac{dz' * dz}{\sqrt{h^2 + (z-z')^2}^{\,3}} = \frac{\Gamma * \hat{\tau}}{2 * \pi * h} * \left(\sqrt{1 + (h/L)^2} - h/L\right)$$

$$a = h/L \qquad K3 = \sqrt{1 + a^2} - a \qquad w0 = \frac{\Gamma}{2 * \pi * h} \qquad \vec{w} = w0 * K3 * \hat{\tau}$$

FIG.32

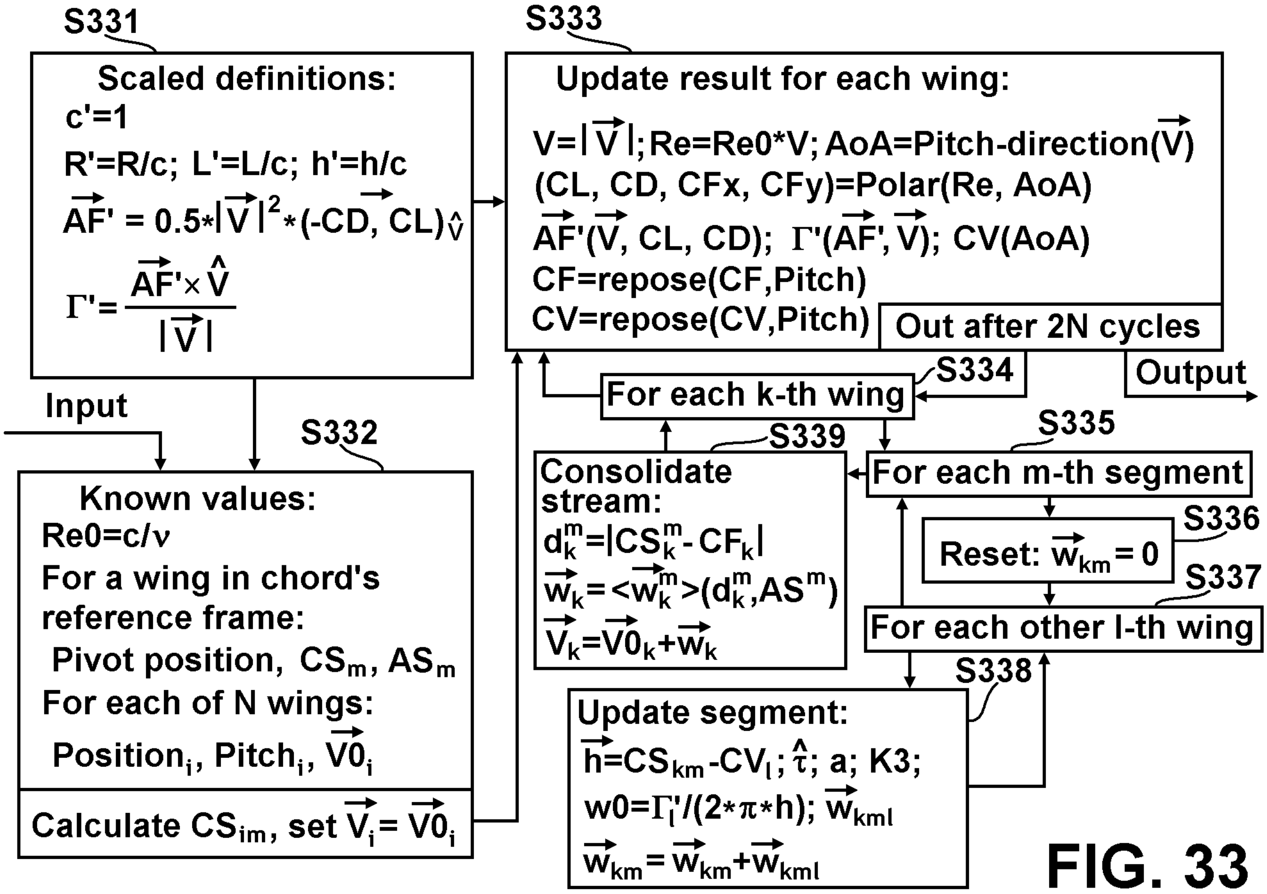

FIG. 33

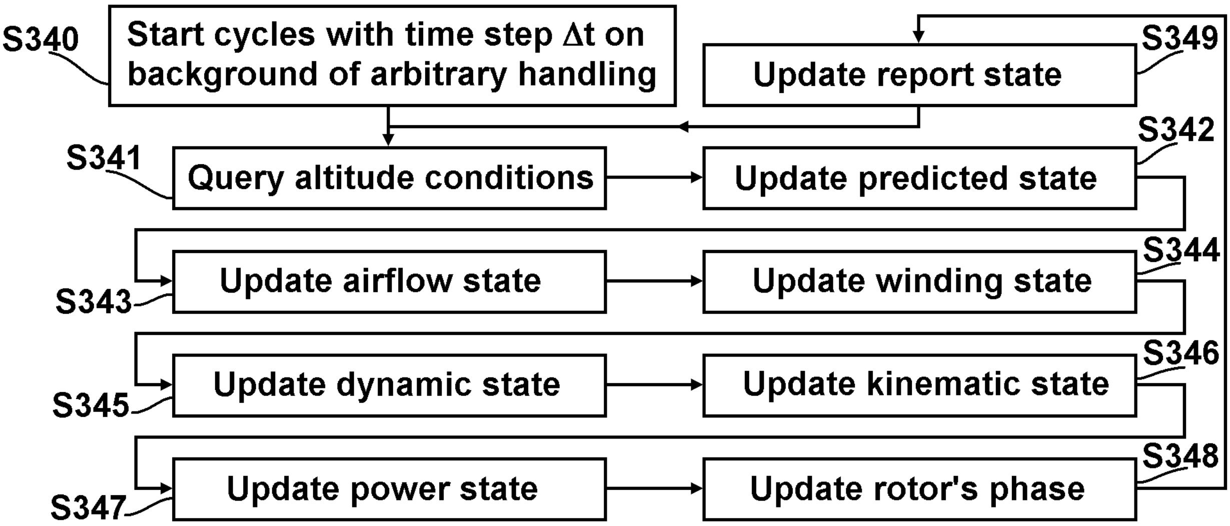
S340
Start cycles with time step Δt on background of arbitrary handling
S349
Update report state
S341
Query altitude conditions
S342
Update predicted state
S343
Update airflow state
S344
Update winding state
S345
Update dynamic state
S346
Update kinematic state
S347
Update power state
S348
Update rotor's phase

FIG. 34

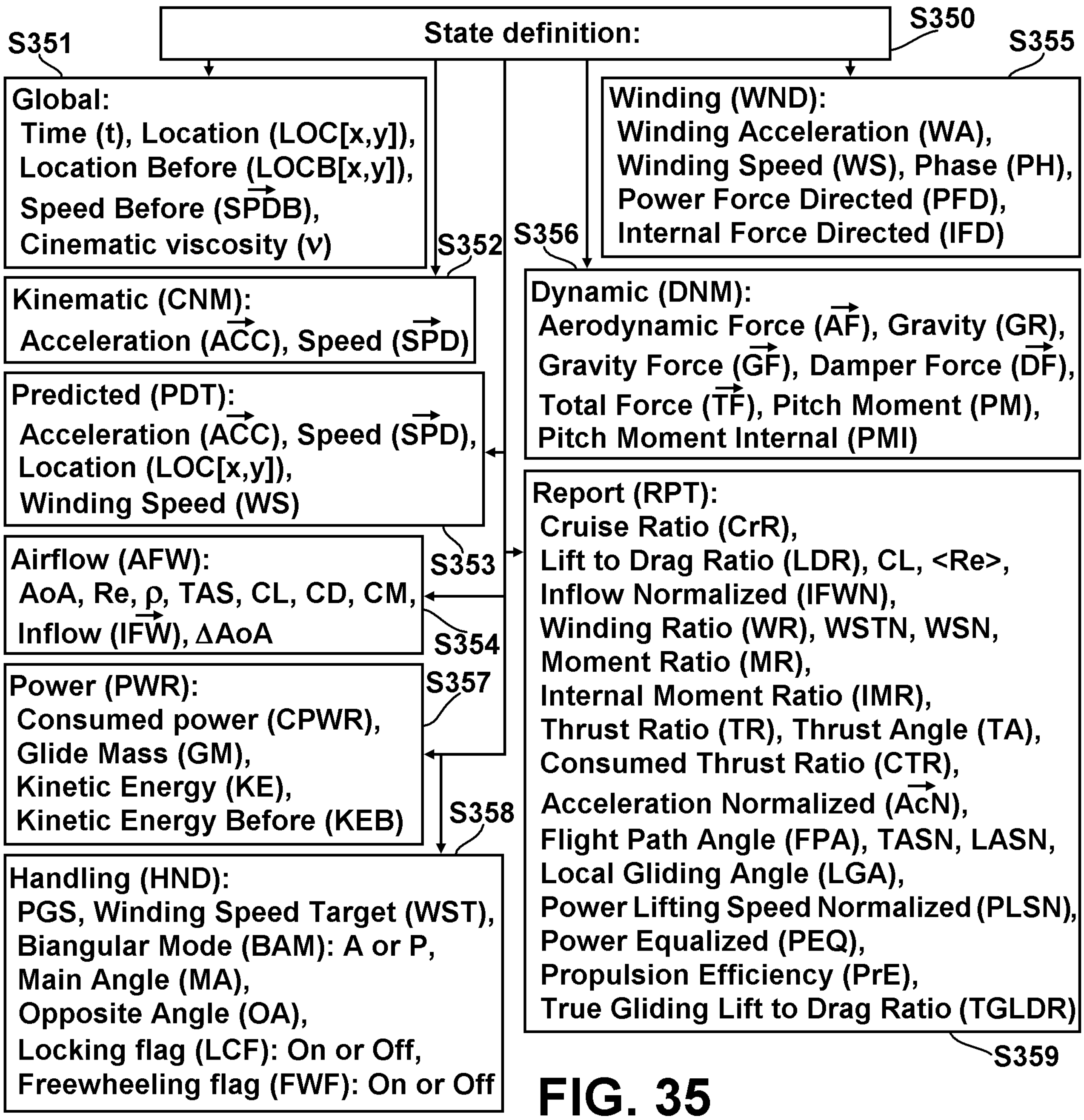
S350
State definition:
S351
Global:
Time (t), Location (LOC[x,y]),
Location Before (LOCB[x,y]),
Speed Before (SPDB),
Cinematic viscosity (ν)
S355
Winding (WND):
Winding Acceleration (WA),
Winding Speed (WS), Phase (PH),
Power Force Directed (PFD),
Internal Force Directed (IFD)
S352
Kinematic (CNM):
Acceleration (ACC), Speed (SPD)
S356
Dynamic (DNM):
Aerodynamic Force (AF), Gravity (GR),
Gravity Force (GF), Damper Force (DF),
Total Force (TF), Pitch Moment (PM),
Pitch Moment Internal (PMI)
Predicted (PDT):
Acceleration (ACC), Speed (SPD),
Location (LOC[x,y]),
Winding Speed (WS)
S353
Airflow (AFW):
AoA, Re, ρ, TAS, CL, CD, CM,
Inflow (IFW), ΔAoA
S354
Report (RPT):
Cruise Ratio (CrR),
Lift to Drag Ratio (LDR), CL, <Re>,
Inflow Normalized (IFWN),
Winding Ratio (WR), WSTN, WSN,
Moment Ratio (MR),
Internal Moment Ratio (IMR),
Thrust Ratio (TR), Thrust Angle (TA),
Consumed Thrust Ratio (CTR),
Acceleration Normalized (AcN),
Flight Path Angle (FPA), TASN, LASN,
Local Gliding Angle (LGA),
Power Lifting Speed Normalized (PLSN),
Power Equalized (PEQ),
Propulsion Efficiency (PrE),
True Gliding Lift to Drag Ratio (TGLDR)
S359
S357
Power (PWR):
Consumed power (CPWR),
Glide Mass (GM),
Kinetic Energy (KE),
Kinetic Energy Before (KEB)
S358
Handling (HND):
PGS, Winding Speed Target (WST),
Biangular Mode (BAM): A or P,
Main Angle (MA),
Opposite Angle (OA),
Locking flag (LCF): On or Off,
Freewheeling flag (FWF): On or Off

FIG. 35

FIG. 36A

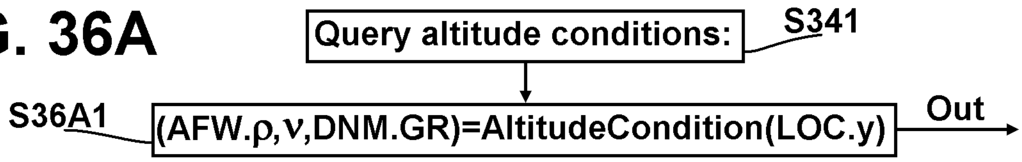

FIG. 36B

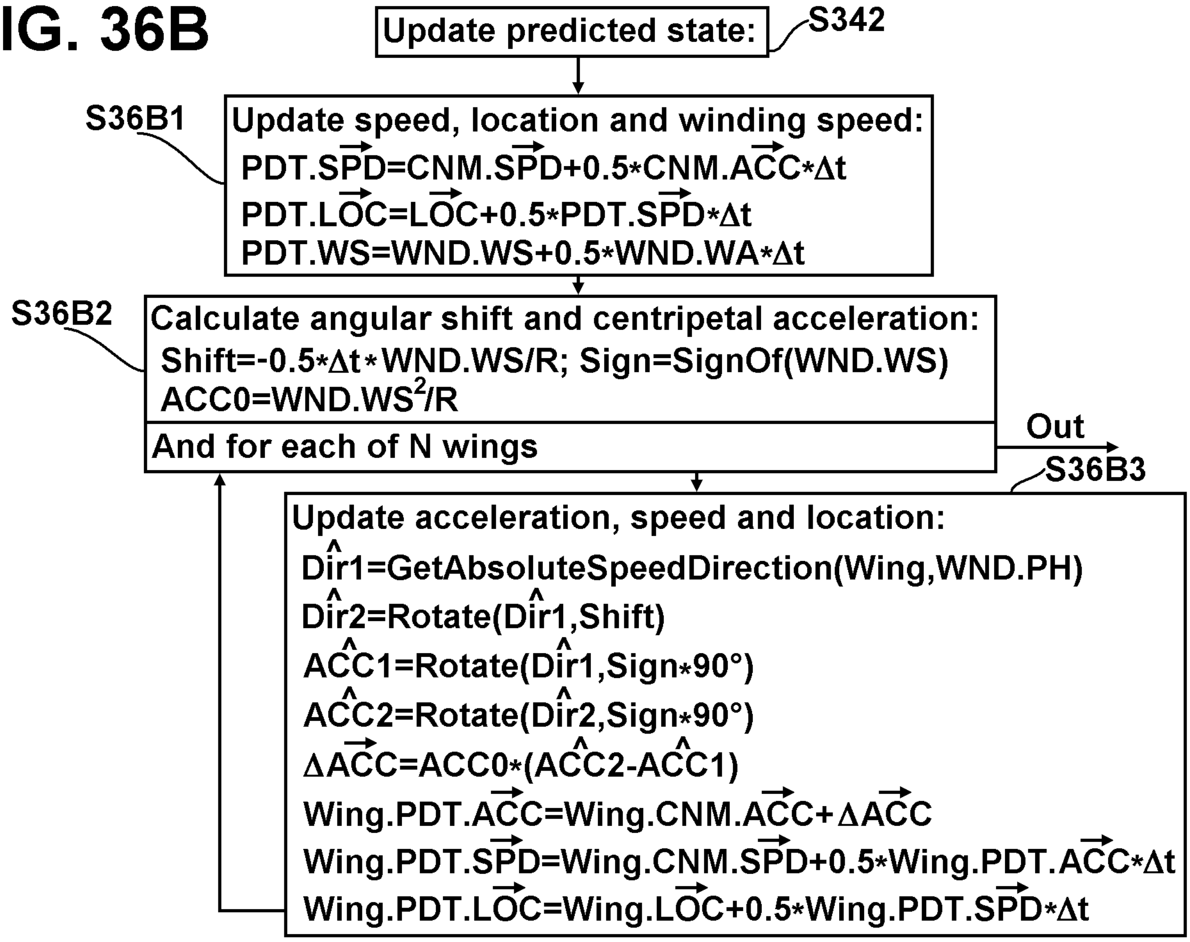

FIG. 36C

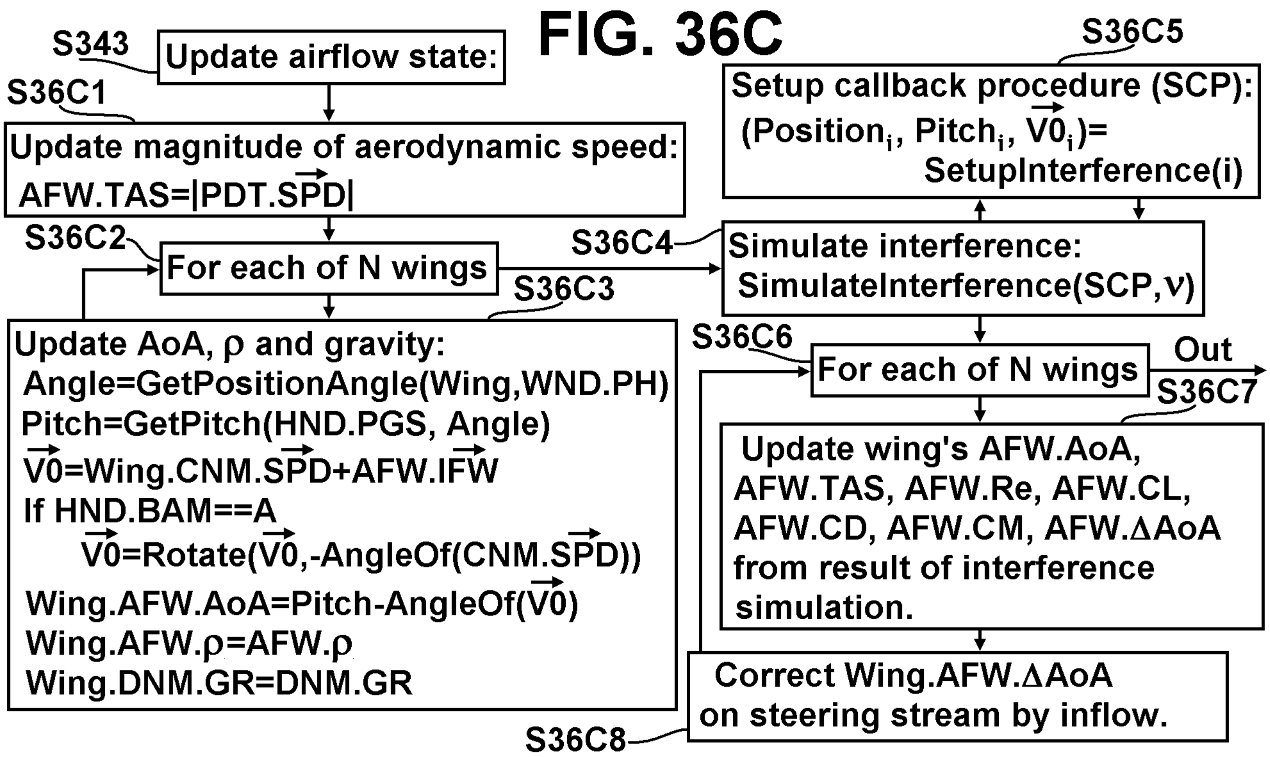

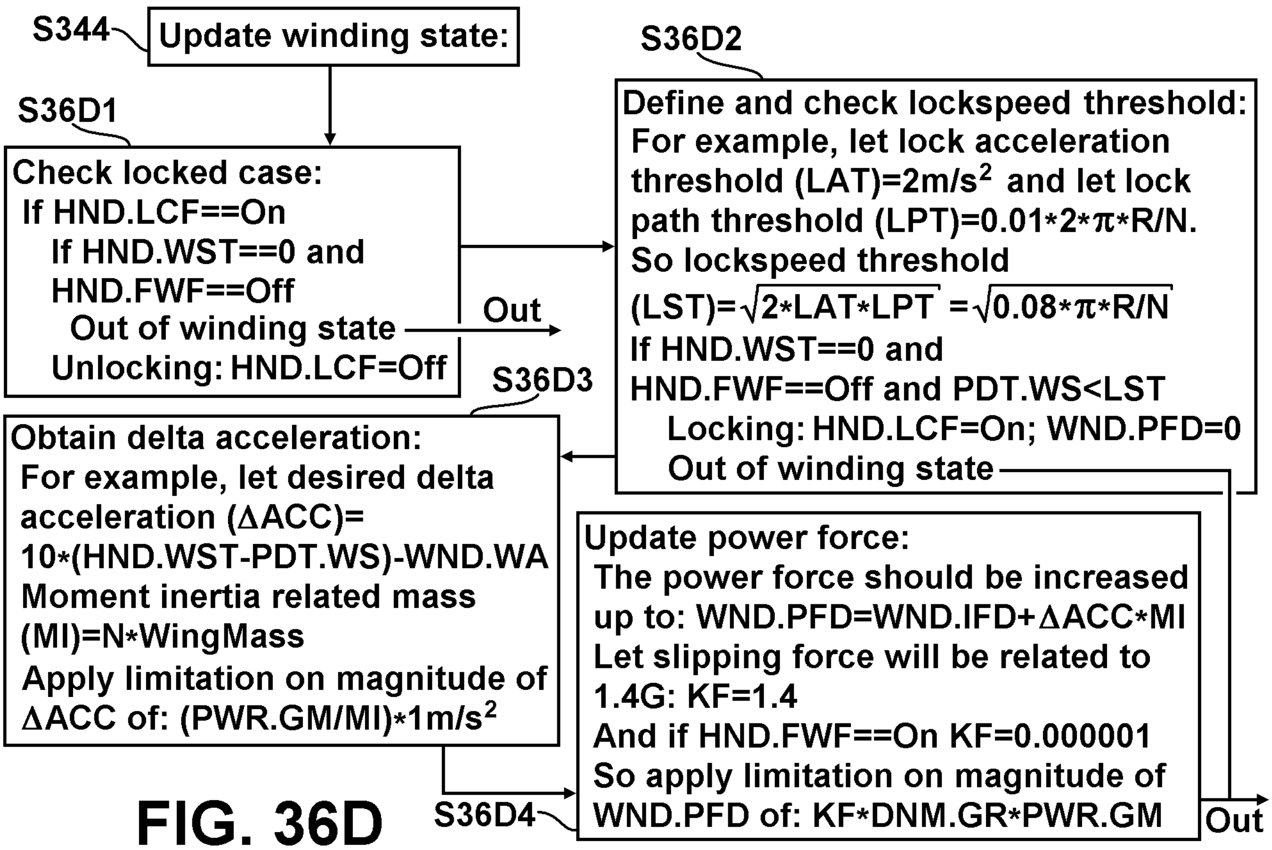

FIG. 36D

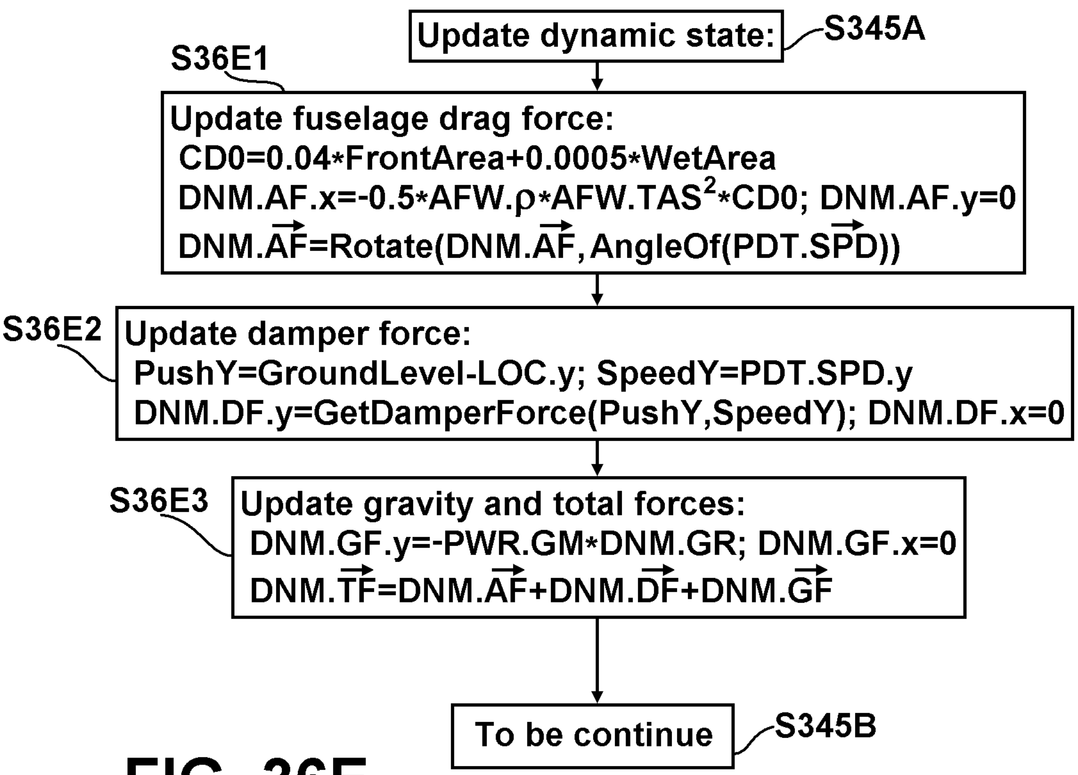

FIG. 36E

FIG. 36F

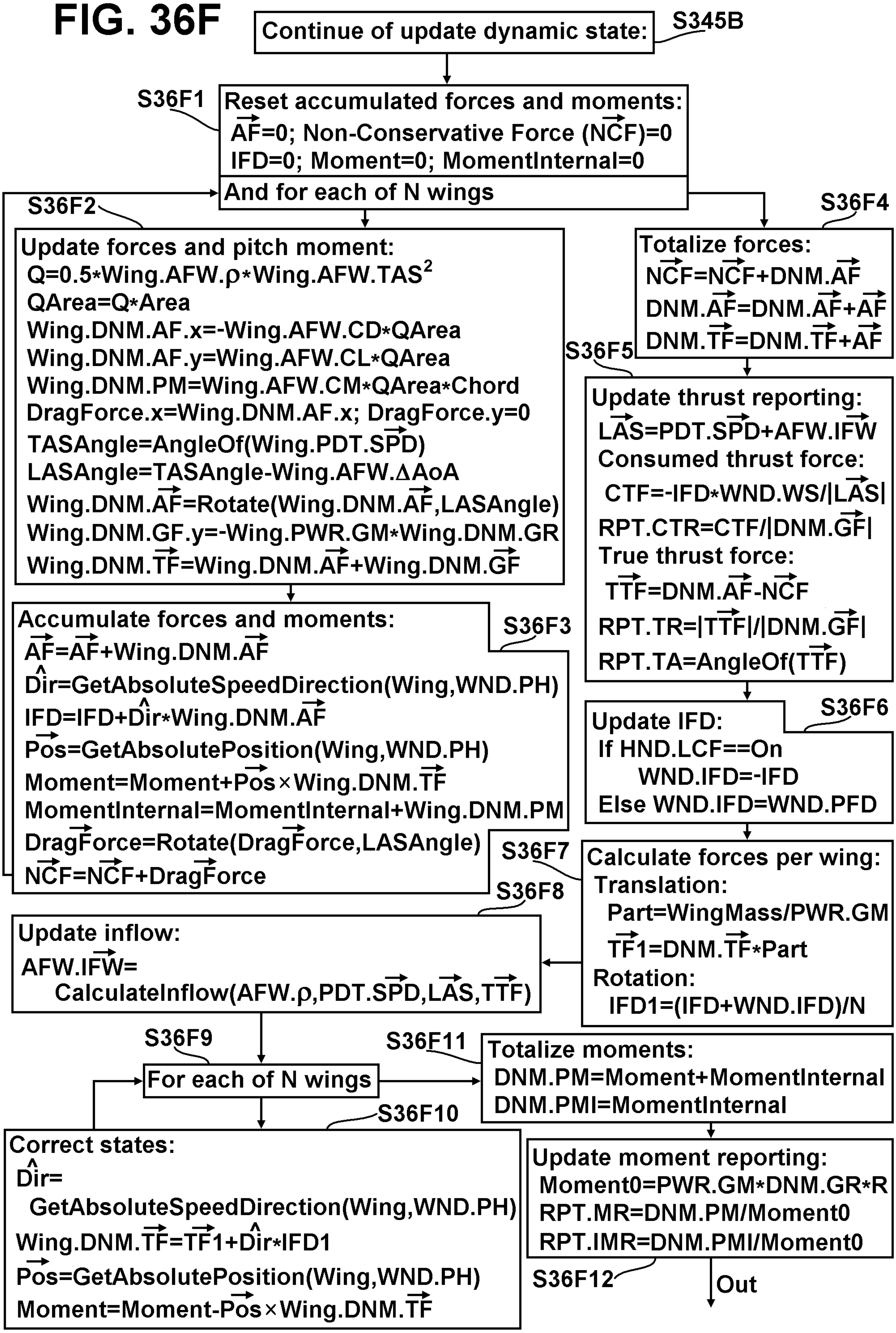
Continue of update dynamic state:
S345B
S36F1
Reset accumulated forces and moments:
AF=0; Non-Conservative Force (NCF)=0
IFD=0; Moment=0; MomentInternal=0
And for each of N wings
S36F2
Update forces and pitch moment:
Q=0.5*Wing.AFW.ρ*Wing.AFW.TAS²
QArea=Q*Area
Wing.DNM.AF.x=-Wing.AFW.CD*QArea
Wing.DNM.AF.y=Wing.AFW.CL*QArea
Wing.DNM.PM=Wing.AFW.CM*QArea*Chord
DragForce.x=Wing.DNM.AF.x; DragForce.y=0
TASAngle=AngleOf(Wing.PDT.SPD)
LASAngle=TASAngle-Wing.AFW.ΔAoA
Wing.DNM.AF=Rotate(Wing.DNM.AF,LASAngle)
Wing.DNM.GF.y=-Wing.PWR.GM*Wing.DNM.GR
Wing.DNM.TF=Wing.DNM.AF+Wing.DNM.GF
S36F3
Accumulate forces and moments:
AF=AF+Wing.DNM.AF
Dir=GetAbsoluteSpeedDirection(Wing,WND.PH)
IFD=IFD+Dir*Wing.DNM.AF
Pos=GetAbsolutePosition(Wing,WND.PH)
Moment=Moment+Pos×Wing.DNM.TF
MomentInternal=MomentInternal+Wing.DNM.PM
DragForce=Rotate(DragForce,LASAngle)
NCF=NCF+DragForce
S36F4
Totalize forces:
NCF=NCF+DNM.AF
DNM.AF=DNM.AF+AF
DNM.TF=DNM.TF+AF
S36F5
Update thrust reporting:
LAS=PDT.SPD+AFW.IFW
Consumed thrust force:
CTF=-IFD*WND.WS/|LAS|
RPT.CTR=CTF/|DNM.GF|
True thrust force:
TTF=DNM.AF-NCF
RPT.TR=|TTF|/|DNM.GF|
RPT.TA=AngleOf(TTF)
S36F6
Update IFD:
If HND.LCF==On
WND.IFD=-IFD
Else WND.IFD=WND.PFD
S36F7
Calculate forces per wing:
Translation:
Part=WingMass/PWR.GM
TF1=DNM.TF*Part
Rotation:
IFD1=(IFD+WND.IFD)/N
S36F8
Update inflow:
AFW.IFW=
CalculateInflow(AFW.ρ,PDT.SPD,LAS,TTF)
S36F9
For each of N wings
S36F10
Correct states:
Dir=
GetAbsoluteSpeedDirection(Wing,WND.PH)
Wing.DNM.TF=TF1+Dir*IFD1
Pos=GetAbsolutePosition(Wing,WND.PH)
Moment=Moment-Pos×Wing.DNM.TF
S36F11
Totalize moments:
DNM.PM=Moment+MomentInternal
DNM.PMI=MomentInternal
Update moment reporting:
Moment0=PWR.GM*DNM.GR*R
RPT.MR=DNM.PM/Moment0
RPT.IMR=DNM.PMI/Moment0
S36F12
Out

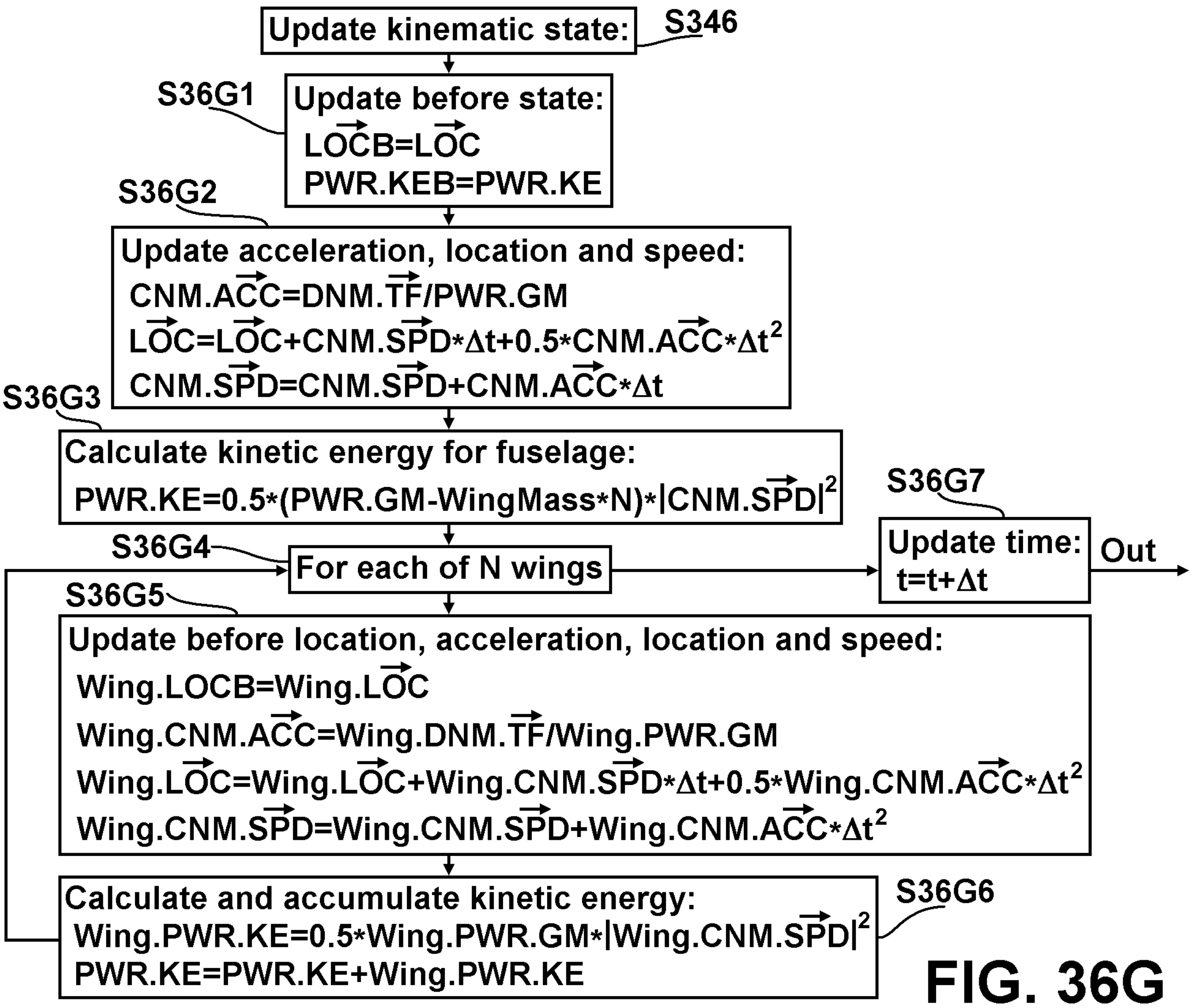

FIG. 36G

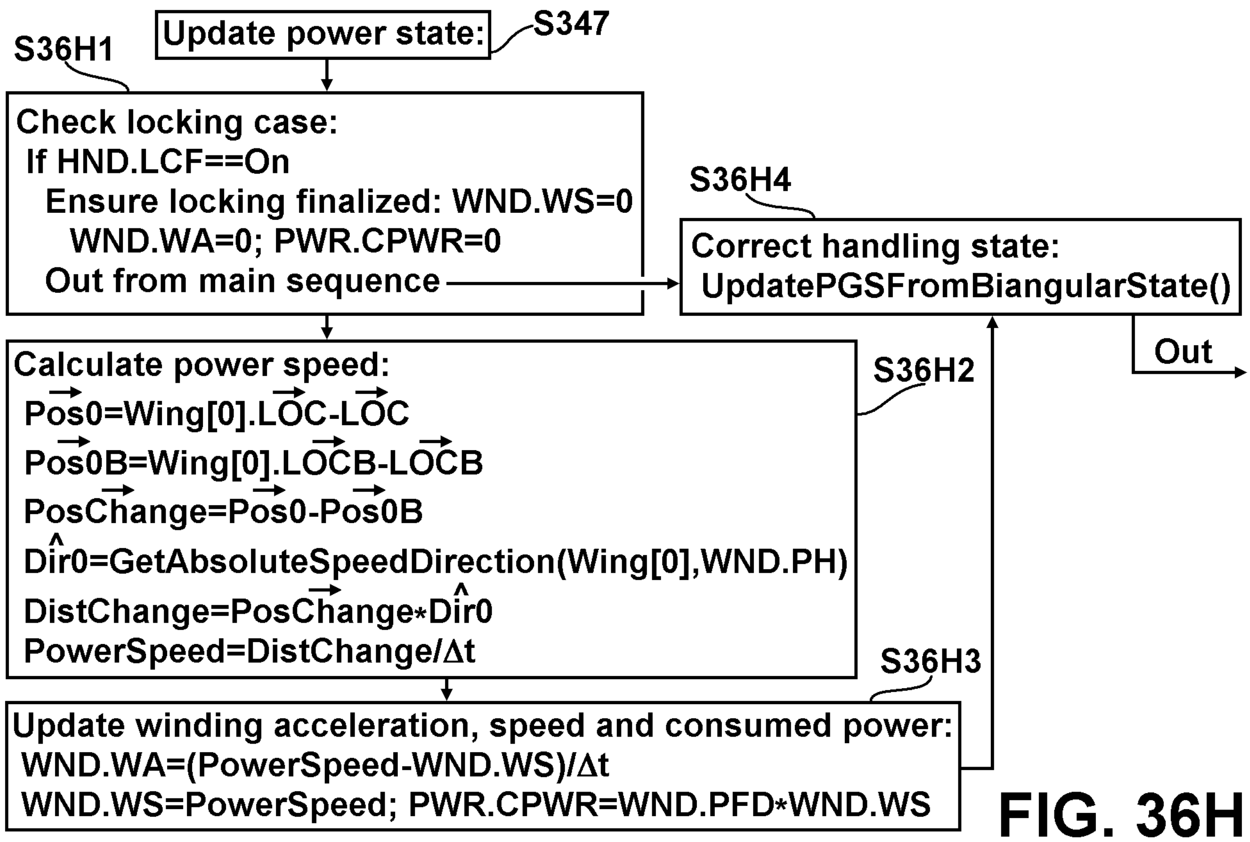

FIG. 36H

FIG. 36I

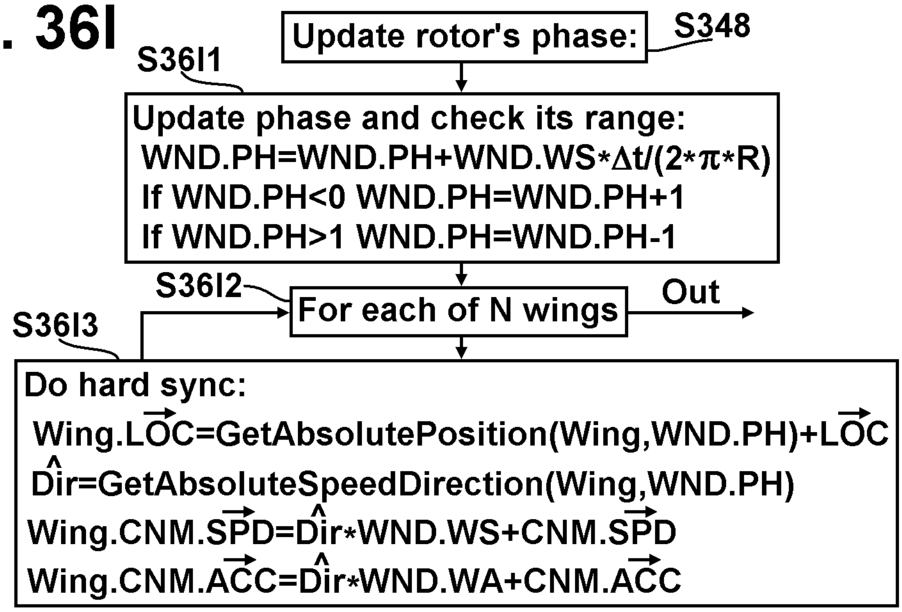

FIG. 36J

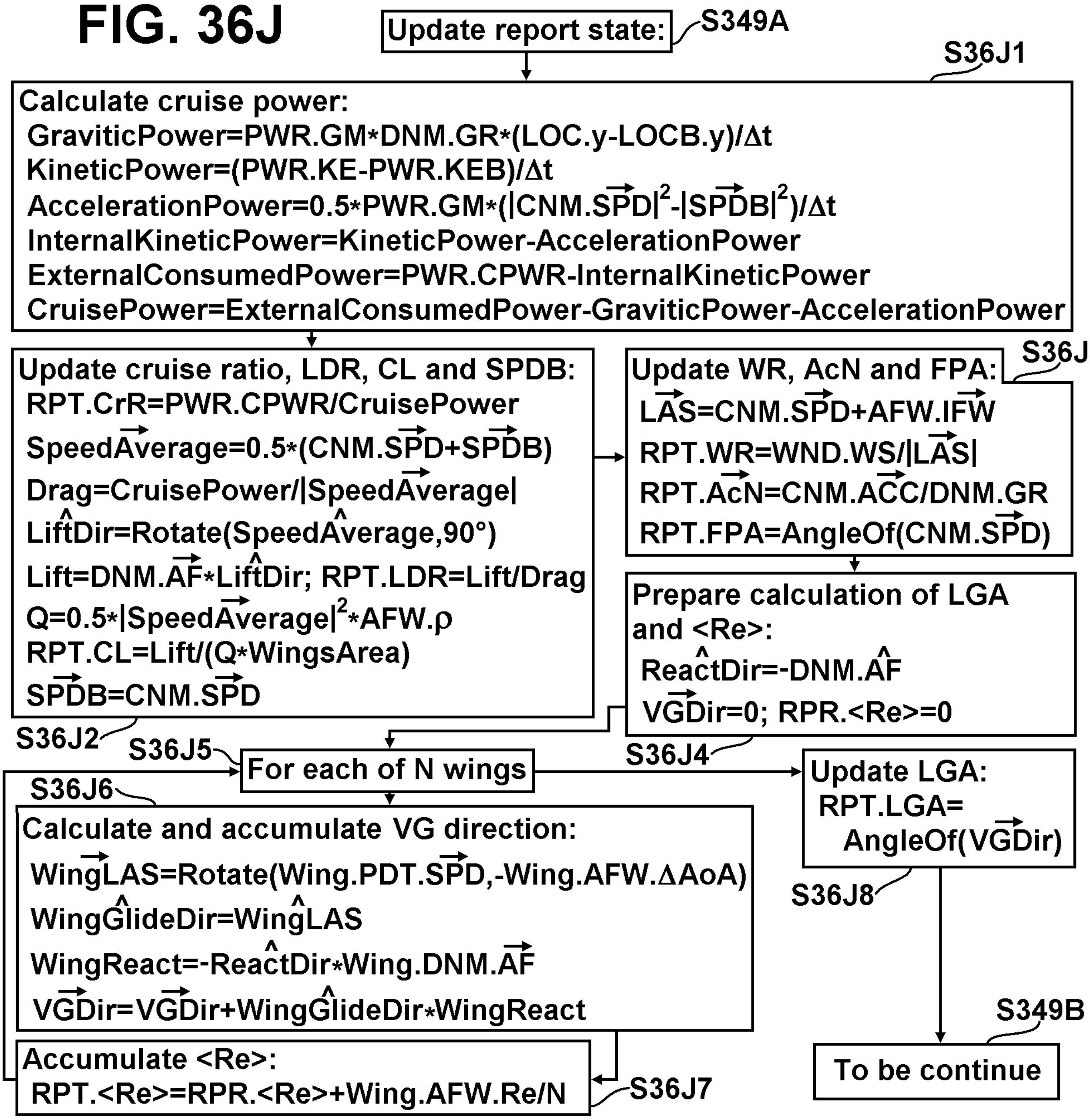

S349B – Continue of update report state:

S36K1 – Update of normalized speeds, PrE and TGLDR:
Q0=PWR.GM*DNM.GR/WingsArea
$V0=\sqrt{2*Q0/AFW.\rho}$; $P0=|DNM.\vec{AF}|*V0$
$RPT.TASN=|CNM.\vec{SPD}|/V0$; $RPT.LASN=|\vec{LAS}|/V0$
$RPT.IFWN=|AFW.\vec{IFW}|/V0$
RPT.WSTN=HND.WST/V0; RPT.WSN=WND.WS/V0
$PrInflow=AFW.\vec{IFW}*CNM.\hat{SPD}$
$RPT.PrE=|CNM.\vec{SPD}|/(|CNM.\vec{SPD}|+PrInflow)$
RPT.PLSN=RPT.PrE*ExternalConsumedPower/P0
RPT.TGLDR=RPT.LDR/RPT.PrE

S36K2 – Use specific constant:
QE=GM0*GR0/WingsArea
$VE=\sqrt{2*QE/\rho 0}$
PWR0=GM0*GR0*VE

S36K3 – Update of equalized power:
RPT.PEQ=
PWR.CPWR/PWR0

Out

FIG. 36K

Constraints used in simulation:

Entire and wings:
Aspect Ratio (AR)=LS^2/WingsArea=3.34,
where:
LS - span of wings;
WingsArea=N*WingArea;
N=10;
WingArea=2*L*Chord;
L - length of each side wing.
R/Chord=2.67
Pivot position from LE: (0.36,0.04)*Chord,
where LE - leading edge of airfoil.

Fuselage:
FrontArea/WingsArea=0.132
WetArea/WingsArea=1.53

Interference:
Number of segments M=5

Steering gear contol:
Ratios:
K=4, r1/R0=0.24, r2/R0=0.64
Assembling: inverted

Time discretization Δt:
Overall - 0.01s
Near result points - 0.001s

FIG.37

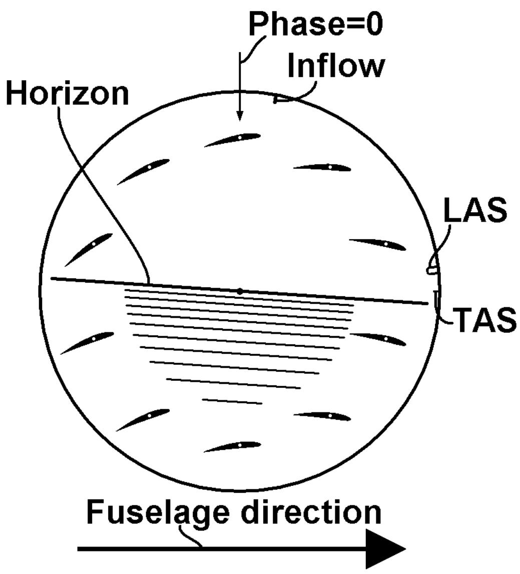

FIG. 38

Flags designation in result form:
P - Biangular Mode is Pitch based.
A - Biangular Mode is AoA based.
S - Pitch control of PGS follows Skew control, so Skew control used as main control and Gain as secondary. Simultaneously biangular values used for feedback indication.
F - Fuselage follows the TAS direction by stabilator using. Mostly used with A-flag.
L - Entire rotor is locked against rotation.
W - Entire rotor is freewheeling, without any power exchange.

FIG. 39

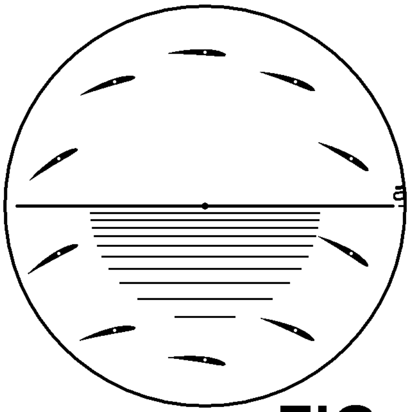

Operation: Beginning acceleration on runway

Flags: PS OA: 40.0° MA: -40.0°

PGS: (-5.6°,-66.1°,-5°) WSTN, WSN: 0.8233 , 0.8233

LASN: 0.4911 WR: 1.6765 <Re>: 429308 IFWN: 0.2791

TASN: 0.2126 FPA: 0.01° MR: 0.4130

TR: 0.3269 TA: 5.56° IMR: -0.0173

CTR: 0.7208 LGA: -18.36° AcN: (0.3024,-0.0244)

CL: 0.1278 LDR: 0.0 CrR: 1.247 PLSN: 0.4994

TGLDR: 0.0 PrE: 0.4335 PEQ: 0.3543

FIG. 40A

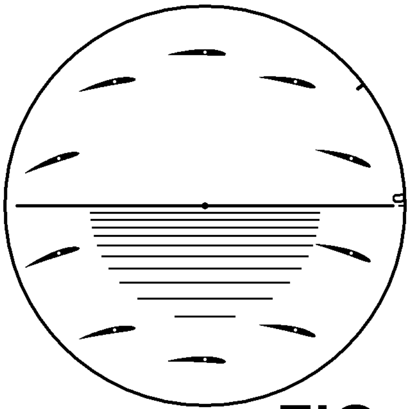

Operation: Before takeoff

Flags: PS OA: 24.6° MA: -22.0°

PGS: (-0.8°,-39.3°,-2°) WSTN, WSN: 0.6635 , 0.6636

LASN: 1.0149 WR: 0.6538 <Re>: 542325 IFWN: 0.0640

TASN: 0.9634 FPA: 0.17° MR: 0.5156

TR: 0.4091 TA: 37.62° IMR: -0.0303

CTR: 0.3549 LGA: -37.24° AcN: (0.2432,0.0601)

CL: 0.2416 LDR: 1.7 CrR: 2.928 PLSN: 1.0351

TGLDR: 1.8 PrE: 0.9499 PEQ: 0.3622

FIG. 40B

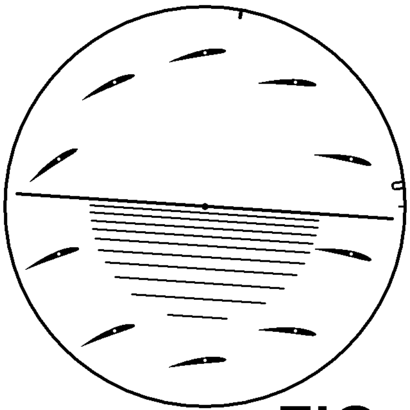

Operation: After takeoff at 0.5m

Flags: AF OA: 4.0° MA: 35.0°

PGS: (8.4°,-47.8°,-5°) WSTN, WSN: 0.6876 , 0.6874

LASN: 0.9964 WR: 0.6899 <Re>: 530918 IFWN: 0.1095

TASN: 0.9703 FPA: 3.81° MR: 0.4826

TR: 1.0977 TA: 83.16° IMR: 0.0059

CTR: 0.3250 LGA: -7.14° AcN: (0.0314,0.0933)

CL: 1.1628 LDR: 4.8 CrR: 1.467 PLSN: 0.2891

TGLDR: 4.9 PrE: 0.9796 PEQ: 0.3277

FIG. 40C

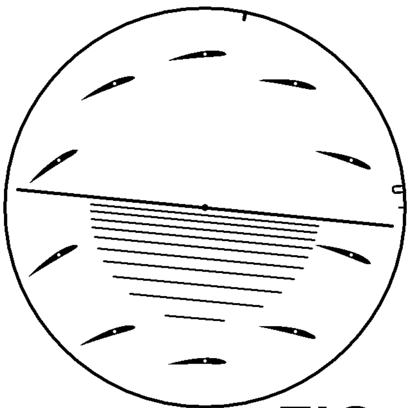

Operation: Getting initial altitude and speed at 12m

Flags: AF OA: 4.0° MA: 28.0°

PGS: (3.6°,-54.6°,-5°) WSTN, WSN: 0.6993 , 0.6994

LASN: 1.0101 WR: 0.6924 <Re>: 540478 IFWN: 0.0961

TASN: 0.9864 FPA: 5.52° MR: 0.4056

TR: 0.9763 TA: 83.96° IMR: -0.0020

CTR: 0.2836 LGA: -6.67° AcN: (0.0361,-0.0482)

CL: 0.9701 LDR: 5.7 CrR: 1.756 PLSN: 0.2967

TGLDR: 5.9 PrE: 0.9808 PEQ: 0.2852

FIG. 40D

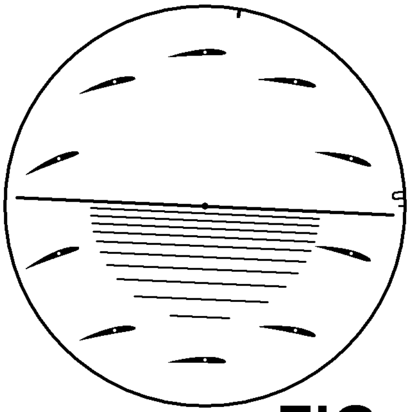

Operation: Getting cruise speed in ascent at 75m

Flags: AF OA: 2.5° MA: 12.0°

PGS: (1.9°,-38.6°,-5°) WSTN, WSN: 0.5559 , 0.5559

LASN: 1.3062 WR: 0.4256 <Re>: 653604 IFWN:

TASN: 1.2914 FPA: 2.63° MR: 0.4884 0.0742

TR: 0.9920 TA: 82.75° IMR: -0.0267

CTR: 0.2203 LGA: -7.78° AcN: (0.0708,-0.0340)

CL: 0.5767 LDR: 9.0 CrR: 2.064 PLSN: 0.2937

FIG. 40E

TGLDR: 9.0 PrE: 0.9902 PEQ: 0.2873

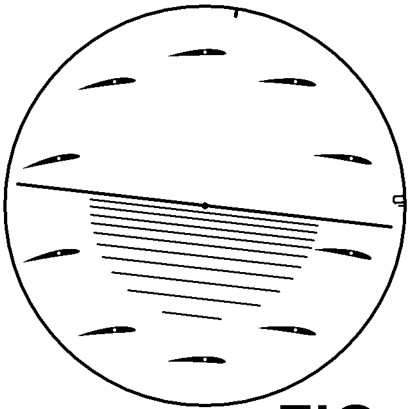

Operation: Ascending to cruise altitude at 400m

Flags: AF OA: -0.2° MA: 6.0°

PGS: (1.0°,-21.5°,-10°) WSTN, WSN: 0.4264 , 0.4264

LASN: 1.7070 WR: 0.2498 <Re>: 816858 IFWN:

TASN: 1.6970 FPA: 6.55° MR: 0.6962 0.0577

TR: 1.0154 TA: 87.55° IMR: -0.0754

CTR: 0.1927 LGA: -2.41° AcN: (-0.0002,0.0067)

CL: 0.3473 LDR: 12.6 CrR: 2.448 PLSN: 0.3250

FIG. 40F

TGLDR: 12.7 PrE: 0.9947 PEQ: 0.3353

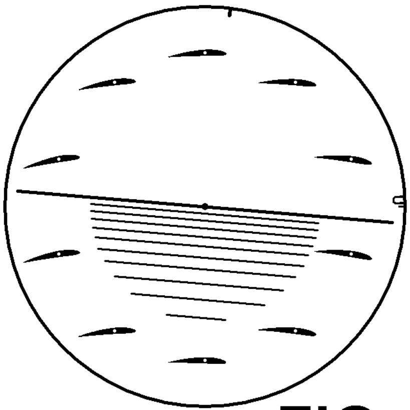

Operation: Ascending to cruise altitude at 3900m

Flags: AF OA: -0.2° MA: 6.0°

PGS: (1.4°,-18.9°,-10°) WSTN, WSN: 0.3755 , 0.3755

LASN: 1.6707 WR: 0.2248 <Re>: 714208 IFWN:

TASN: 1.6623 FPA: 4.85° MR: 0.6640 0.0581

TR: 1.0054 TA: 87.46° IMR: -0.0705

CTR: 0.1651 LGA: -2.55° AcN: (0.0027,-0.0016)

CL: 0.3600 LDR: 12.6 CrR: 2.104 PLSN: 0.2752

FIG. 40G

TGLDR: 12.7 PrE: 0.9955 PEQ: 0.3349

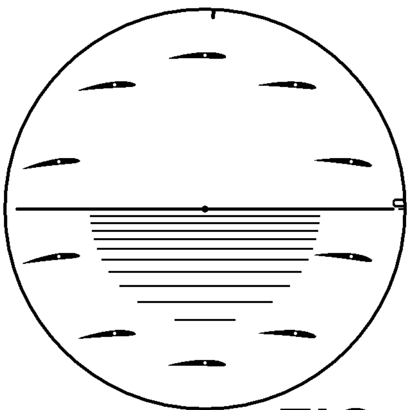

Operation: Cruise at altitude 4016m

Flags: AF OA: 0.0° MA: 3.1°

PGS: (1.0°,-14.0°,-4°) WSTN, WSN: 0.2609 , 0.2608

LASN: 1.7446 WR: 0.1495 <Re>: 743833 IFWN:

TASN: 1.7415 FPA: -0.01° MR: 0.4124 0.0549

TR: 1.0017 TA: 87.63° IMR: -0.0797

CTR: 0.0734 LGA: -2.40° AcN: (0.0006,-0.0006)

CL: 0.3295 LDR: 13.7 CrR: 1.007 PLSN: 0.1281

FIG. 40H

TGLDR: 13.7 PrE: 0.9987 PEQ: 0.1568

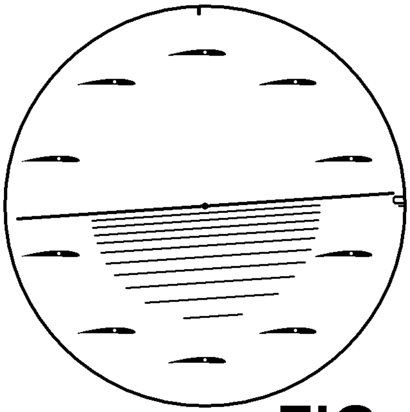

FIG. 40I

Operation: Gliding at altitude 3700m

Flags: AFL | OA: 1.0° | MA: 1.5°

PGS: (1.2°,0.5°,0°) | WSTN, WSN: 0.0000, 0.0000

LASN:	1.6990	WR:	0.0000	<Re>:	732071	IFWN:	
TASN:	1.6999	FPA:	-3.94°	MR:	0.2283		0.0561
TR:	0.9999	TA:	87.96°	IMR:	-0.0729		
CTR:	0.0000	LGA:	-2.04°	AcN:	(-0.0019,0.0010)		
CL:	0.3455	LDR:	14.1	CrR:	0.000	PLSN:	0.0000
		TGLDR:	14.1	PrE:	1.0011	PEQ:	0.0000

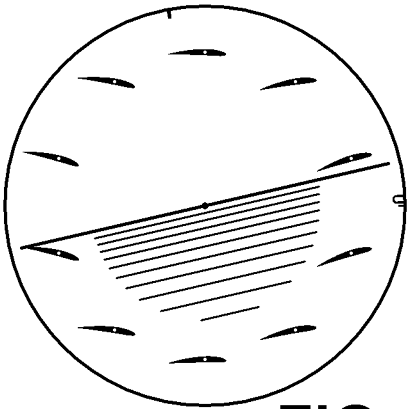

FIG. 40J

Operation: Recuperative descent at altitude 600m

Flags: AF | OA: -1.7° | MA: 5.0°

PGS: (0.7°,32.7°,-5°) | WSTN, WSN: -0.3805, -0.3806

LASN:	1.6188	WR:	-0.2351	<Re>:	789476	IFWN:	
TASN:	1.6288	FPA:	-12.98°	MR:	0.5704		0.0591
TR:	0.9935	TA:	87.76°	IMR:	-0.0583		
CTR:	-0.1477	LGA:	-2.28°	AcN:	(0.0014,0.0003)		
CL:	0.3675	LDR:	12.8	CrR:	-1.922	PLSN:	-0.2408
		TGLDR:	12.7	PrE:	1.0068	PEQ:	-0.2463

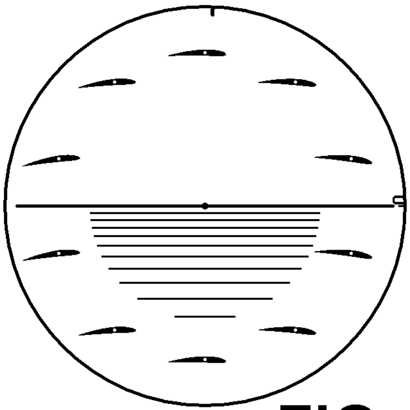

FIG. 40K

Operation: Approaching at altitude 202m

Flags: AF | OA: 0.0° | MA: 3.0°

PGS: (0.9°,-14.5°,-3°) | WSTN, WSN: 0.2669, 0.2668

LASN:	1.7518	WR:	0.1523	<Re>:	844400	IFWN:	
TASN:	1.7487	FPA:	0.02°	MR:	0.3988		0.0547
TR:	1.0023	TA:	87.68°	IMR:	-0.0819		
CTR:	0.0731	LGA:	-2.35°	AcN:	(0.0001,0.0002)		
CL:	0.3271	LDR:	13.7	CrR:	1.008	PLSN:	0.1280
		TGLDR:	13.8	PrE:	0.9987	PEQ:	0.1295

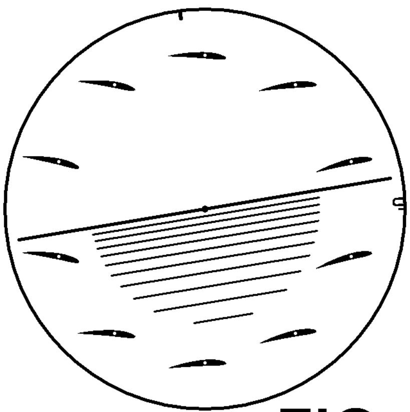

FIG. 40L

Operation: Enter in descent for landing at 165m

Flags: AF | OA: 0.0° | MA: 4.0°

PGS: (1.0°,26.9°,-15°) | WSTN, WSN: -0.3065, -0.3065

LASN:	1.5291	WR:	-0.2005	<Re>:	760234	IFWN:	
TASN:	1.5355	FPA:	-9.36°	MR:	0.3763		0.0608
TR:	0.9719	TA:	87.83°	IMR:	-0.0587		
CTR:	-0.0871	LGA:	-2.17°	AcN:	(0.0022,-0.0243)		
CL:	0.4085	LDR:	13.8	CrR:	-1.248	PLSN:	-0.1373
		TGLDR:	13.8	PrE:	1.0050	PEQ:	-0.1344

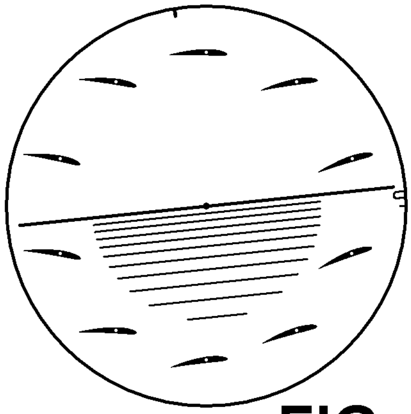

Operation: Dropping speed at altitude 82m

Flags: AF | OA: 1.0° | MA: 10.0°

PGS: (4.2°,31.2°,-15°) | WSTN, WSN: -0.2684 , -0.2685

LASN: 1.3387 | WR: -0.2006 | <Re>: 670714 | IFWN: 0.0780

TASN: 1.3488 | FPA: -5.89° | MR: 0.5417

TR: 1.0905 | TA: 93.24° | IMR: -0.0265

CTR: -0.1140 | LGA: 3.23° | AcN: (-0.0940,0.0899)

CL: 0.5906 | LDR: 11.6 | CrR: -1.226 | PLSN: -0.1406

FIG. 40M

TGLDR: 11.5 | PrE: 1.0093 | PEQ: -0.1531

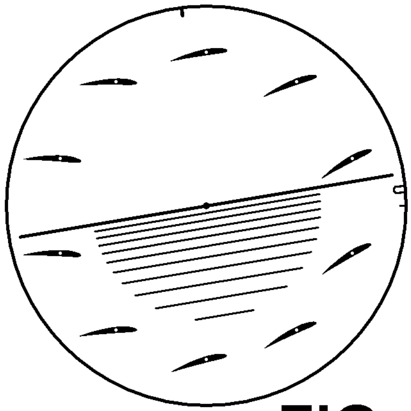

Operation: Dropping speed at altitude 30m

Flags: AF | OA: 6.0° | MA: 23.0°

PGS: (13.1°,34.3°,-10°) | WSTN, WSN: -0.1763 , -0.1761

LASN: 1.0407 | WR: -0.1692 | <Re>: 511545 | IFWN: 0.0886

TASN: 1.0480 | FPA: -9.49° | MR: 0.2245

TR: 0.9664 | TA: 87.67° | IMR: 0.0028

CTR: -0.0382 | LGA: -2.31° | AcN: (-0.0507,-0.0312)

CL: 0.8623 | LDR: 5.5 | CrR: -0.216 | PLSN: -0.0410

FIG. 40N

TGLDR: 5.4 | PrE: 1.0107 | PEQ: -0.0391

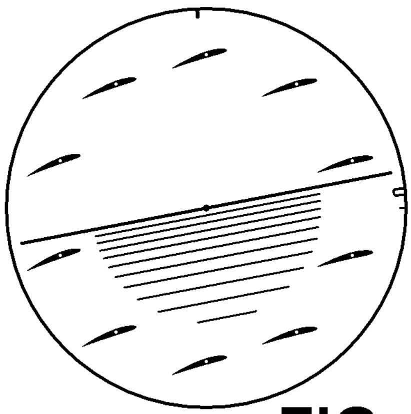

Operation: Dropping speed at altitude 20m

Flags: AF | OA: 8.0° | MA: 30.0°

PGS: (18.3°,-6.4°,-5°) | WSTN, WSN: 0.2499 , 0.2458

LASN: 1.0202 | WR: 0.2410 | <Re>: 496636 | IFWN: 0.0896

TASN: 1.0202 | FPA: -10.85° | MR: 0.2320

TR: 0.9577 | TA: 81.70° | IMR: 0.0026

CTR: 0.0463 | LGA: -8.80° | AcN: (-0.0405,0.0095)

CL: 0.9452 | LDR: 3.5 | CrR: 0.197 | PLSN: 0.0515

FIG. 40O

TGLDR: 3.5 | PrE: 1.0039 | PEQ: 0.0564

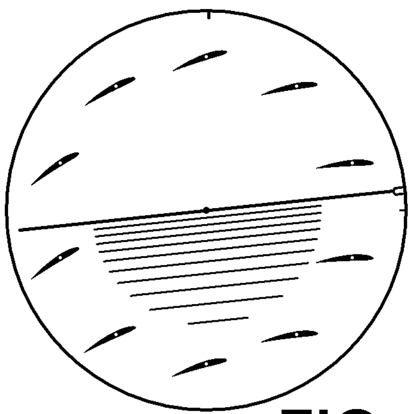

Operation: Dropping speed and descent at altitude 6m

Flags: AF | OA: 9.0° | MA: 38.0°

PGS: (17.9°,-30.5°,-5°) | WSTN, WSN: 0.4895 , 0.4895

LASN: 0.9449 | WR: 0.5181 | <Re>: 479295 | IFWN: 0.0980

TASN: 0.9385 | FPA: -5.99° | MR: 0.3011

TR: 0.9651 | TA: 83.30° | IMR: 0.0064

CTR: 0.1529 | LGA: -7.98° | AcN: (-0.0965,0.0414)

CL: 1.1643 | LDR: 2.9 | CrR: 0.429 | PLSN: 0.1377

FIG. 40P

TGLDR: 2.9 | PrE: 0.9987 | PEQ: 0.1443

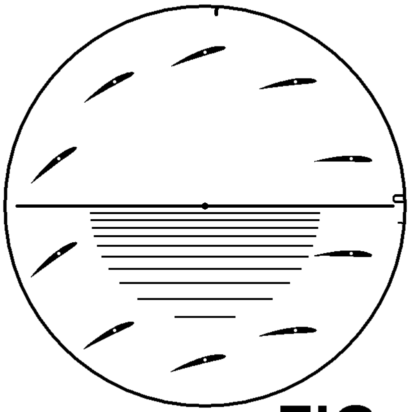

Operation: Dropping speed and descent at altitude 2m

Flags: P | OA: 42.4° | MA: -4.2°
PGS: (17.0°,-39.3°,-5°) | WSTN, WSN: 0.5809 , 0.5703

LASN: 0.8877 | WR: 0.6425 | <Re>: 468040 | IFWN: 0.1110
TASN: 0.8839 | FPA: -4.91° | MR: 0.4201
TR: 1.0288 | TA: 86.72° | IMR: 0.0092
CTR: 0.2053 | LGA: -5.69° | AcN: (-0.2247,0.1449)
CL: 1.4354 | LDR: 2.0 | CrR: 0.475 | PLSN: 0.1798
TGLDR: 2.0 | PrE: 1.0036 | PEQ: 0.2344

FIG. 40Q

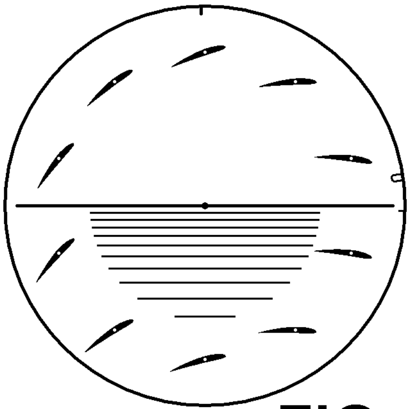

Operation: Before touchdown at altitude 0.2m

Flags: P | OA: 58.0° | MA: -14.6°
PGS: (17.0°,-60.1°,-5°) | WSTN, WSN: 0.6755 , 0.6754

LASN: 0.7551 | WR: 0.8945 | <Re>: 439250 | IFWN: 0.1281
TASN: 0.7497 | FPA: -1.38° | MR: 0.3081
TR: 1.0067 | TA: 91.11° | IMR: 0.0183
CTR: 0.2561 | LGA: -2.56° | AcN: (-0.2155,0.0768)
CL: 1.9058 | LDR: 2.1 | CrR: 0.522 | PLSN: 0.1781
TGLDR: 2.1 | PrE: 1.0075 | PEQ: 0.1957

FIG. 40R

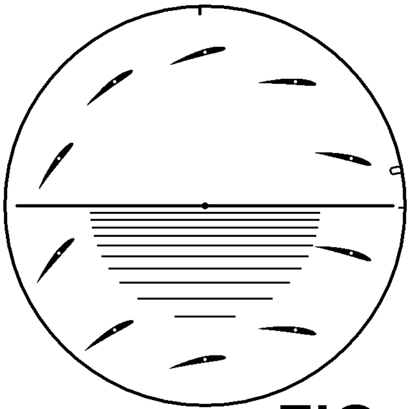

Operation: Touchdown

Flags: P | OA: 60.9° | MA: -23.8°
PGS: (12.4°,-70.0°,-5°) | WSTN, WSN: 0.6755 , 0.6756

LASN: 0.7137 | WR: 0.9465 | <Re>: 431433 | IFWN: 0.1355
TASN: 0.7055 | FPA: -0.49° | MR: 0.2679
TR: 1.0025 | TA: 91.51° | IMR: 0.0261
CTR: 0.2171 | LGA: -2.07° | AcN: (-0.1252,0.2511)
CL: 2.0453 | LDR: 2.8 | CrR: 0.642 | PLSN: 0.1553
TGLDR: 2.8 | PrE: 1.0068 | PEQ: 0.1633

FIG. 40S

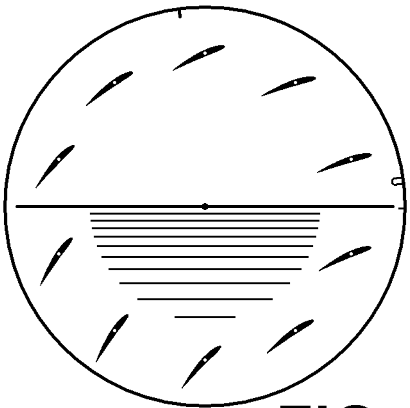

Operation: Begin aerial braking on runway

Flags: PSW | OA: 60.9° | MA: 13.5°
PGS: (35.0°,-40.0°,35°) | WSTN, WSN: 0.3395 , 0.4788

LASN: 0.6671 | WR: 0.7177 | <Re>: 365870 | IFWN: 0.0940
TASN: 0.6738 | FPA: -0.53° | MR: 0.0013
TR: 0.6595 | TA: 97.54° | IMR: 0.0013
CTR: 0.1533 | LGA: 1.18° | AcN: (-0.3784,-0.1768)
CL: 1.6879 | LDR: 1.7 | CrR: -0.000 | PLSN: 0.0607
TGLDR: 1.6 | PrE: 1.0200 | PEQ: -0.0000

FIG. 40T

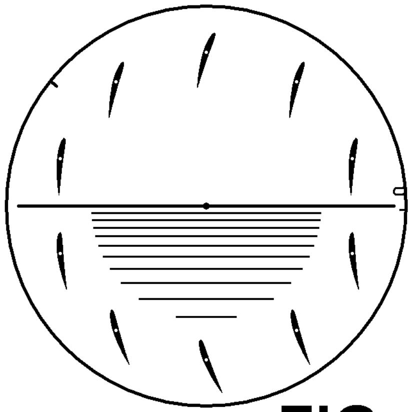

Operation: Continue aerial braking on runway

Flags: PS OA: 115.9° MA: 68.5°
PGS: (90.0°,-40.0°,90°) WSTN, WSN: 0.3395, 0.3395

LASN: 0.2629 WR: 1.2912 <Re>: 193105 IFWN:
TASN: 0.2952 FPA: -1.14° MR: 0.1732 0.0422
TR: 0.0814 TA: 141.35° IMR: -0.0122
CTR: 0.2410 LGA: 0.78° AcN: (-0.2817,0.0242)
CL: 0.6322 LDR: 0.1 CrR: 0.414 PLSN: 0.2467
TGLDR: 0.1 PrE: 1.1280 PEQ: 0.0630

FIG. 40U

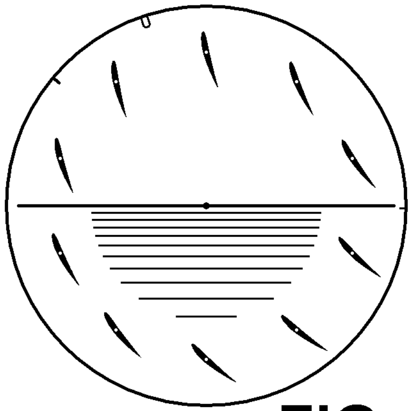

Operation: Finalizing aerial braking on runway

Flags: PS OA: 145.9° MA: 98.5°
PGS: (120.0°,-40.0°,120°) WSTN, WSN: 0.3395, 0.3395

LASN: 0.0660 WR: 5.1434 <Re>: 163692 IFWN:
TASN: 0.0549 FPA: -0.70° MR: 0.0965 0.0985
TR: 0.0385 TA: 140.02° IMR: -0.0005
CTR: 0.5048 LGA: 37.83° AcN: (-0.0435,0.0254)
CL: 6.8794 LDR: 0.0 CrR: 0.911 PLSN: -1.7638
TGLDR: -0.0 PrE: -2.5784 PEQ: 0.0330

FIG. 40V

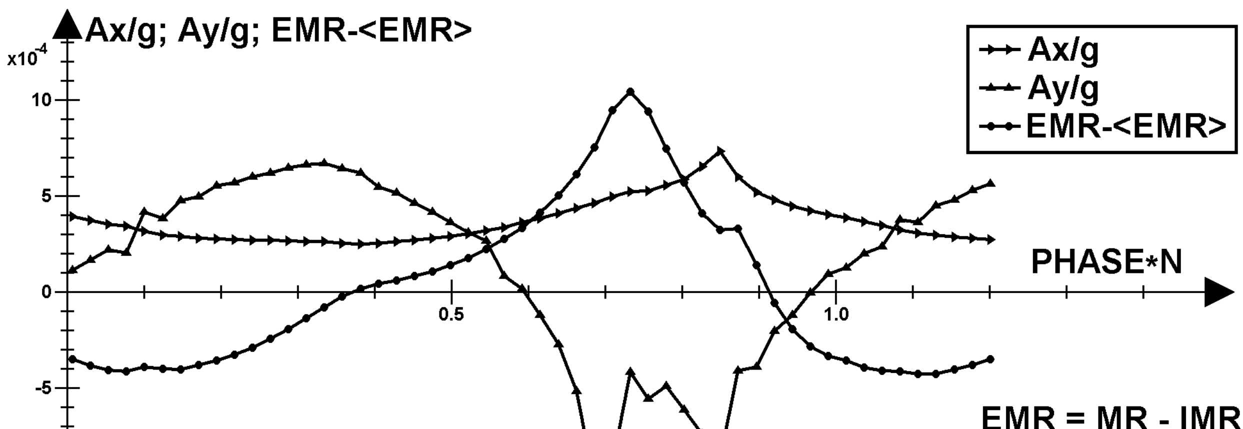

FIG. 41A

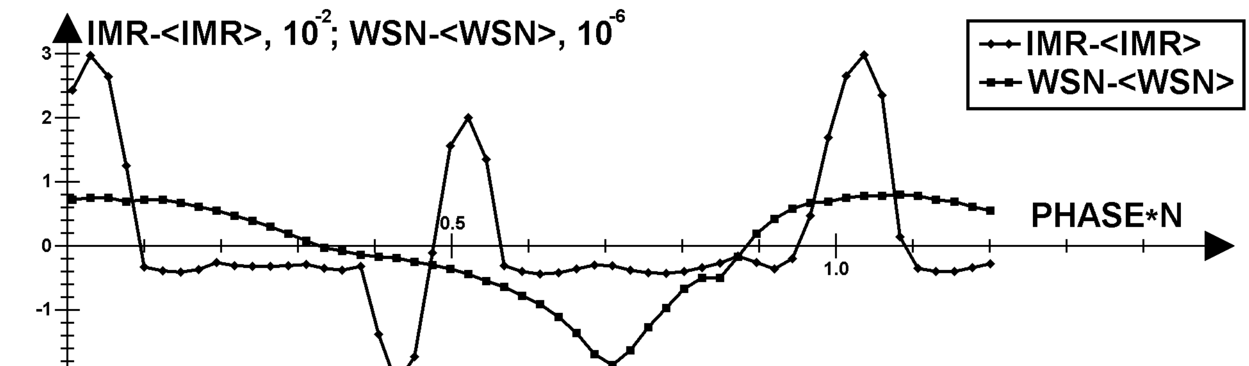

FIG. 41B

Turning on operation	Side	ΔOA	ΔMA	ΔP	ΔG	ΔAcN
1: Getting initial altitude and speed at 12m						
See FIG. 40D	Inside	+1°	-2°	-1.1°	-2.9°	(-0.0153,-0.0364)
	Outside	-1°	+2°	+1.1°	+3.0°	(+0.0097,+0.0307)
	Difference	-2°	+4°	+2.2°	+5.9°	(+0.0250,+0.0671)
2: Getting cruise speed in ascent at 75m						
See FIG. 40E	Inside	+1°	-2°	-0.9°	-2.7°	(-0.0264,-0.0489)
	Outside	-1°	+2°	+0.8°	+2.7°	(+0.0277,+0.0255)
	Difference	-2°	+4°	+1.7°	+5.4°	(+0.0541,+0.0744)
3: Ascending to cruise altitude at 3900m						
See FIG. 40G	Inside	+1°	-2°	-0.7°	-2.6°	(-0.0272,-0.0396)
	Outside	-1°	+2°	+0.7°	+2.7°	(+0.0275,+0.0377)
	Difference	-2°	+4°	+1.4°	+5.3°	(+0.0547,+0.0773)
4: Cruise at altitude 4016m						
See FIG. 40H	Inside	+1°	-2°	-0.7°	-2.7°	(-0.0253,-0.0376)
	Outside	-1°	+2°	+0.6°	+2.7°	(+0.0241,+0.0368)
	Difference	-2°	+4°	+1.3°	+5.4°	(+0.0494,+0.0744)
5: Gliding at altitude 3700m						
See FIG. 40I	Inside	+0°	-1°	-0.5°	-1.0°	(+0.0018,-0.0654)
	Outside	-0°	+1°	+0.5°	+0.9°	(-0.0028,+0.0681)
	Difference	-0°	+2°	+1.0°	+1.9°	(-0.0046,+0.1335)
6: Recuperative descent at altitude 600m						
See FIG. 40J	Inside	-1°	+1°	-0.1°	+1.8°	(-0.0300,-0.0371)
	Outside	+1°	-1°	+0.2°	-1.7°	(+0.0300,+0.0356)
	Difference	+2°	-2°	+0.3°	-3.5°	(+0.0600,+0.0727)
7: Dropping speed at altitude 82m						
See FIG. 40M	Inside	-1°	+1°	-0.1°	+1.7°	(-0.0125,-0.0271)
	Outside	+1°	-1°	+0.1°	-1.8°	(+0.0131,+0.0278)
	Difference	+2°	-2°	+0.2°	-3.5°	(+0.0256,+0.0549)
8: Dropping speed and descent at altitude 6m						
See FIG. 40P	Inside	-1°	+2°	+0.9°	+2.7°	(-0.0169,-0.0012)
	Outside	+1°	-2°	-0.8°	-2.8°	(+0.0161,-0.0008)
	Difference	+2°	-4°	-1.7°	-5.5°	(+0.0330,+0.0004)

FIG. 42

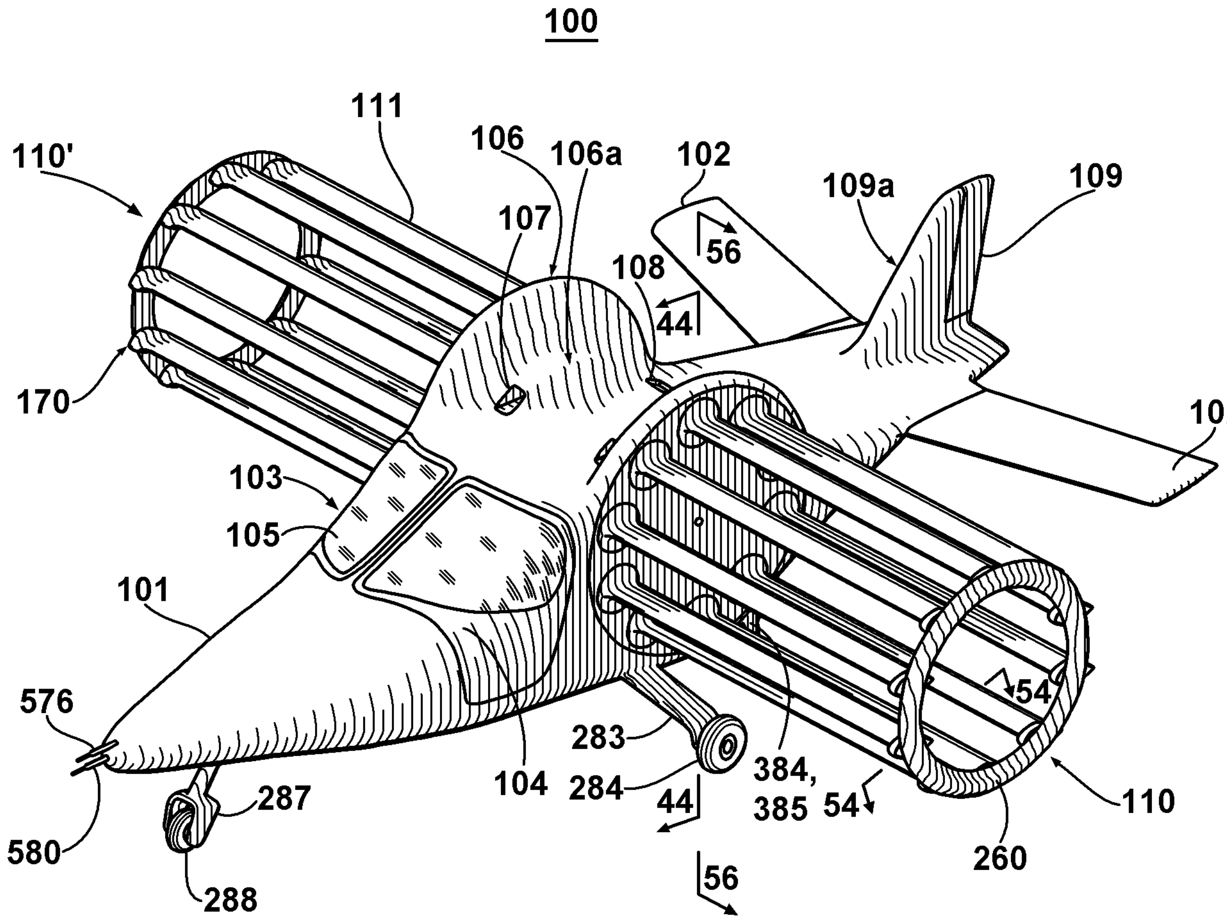
100
111
110'
106
106a
102
109a
109
107
56
108
44
170
102
103
105
101
54
576
283
384,
385
580
287
104
284
44
54
110
260
288
56

FIG. 43

FIG. 44A		
	FIG. 44D	
FIG. 44B	FIG. 44E	
FIG. 44C	FIG. 44F	

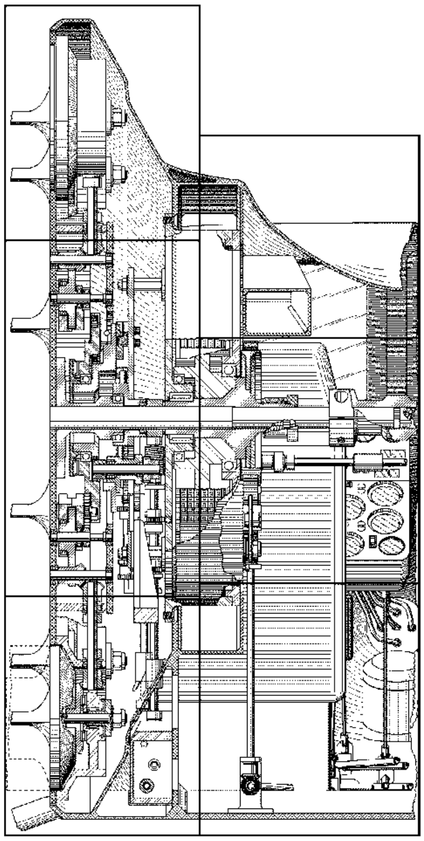

FIG. 44

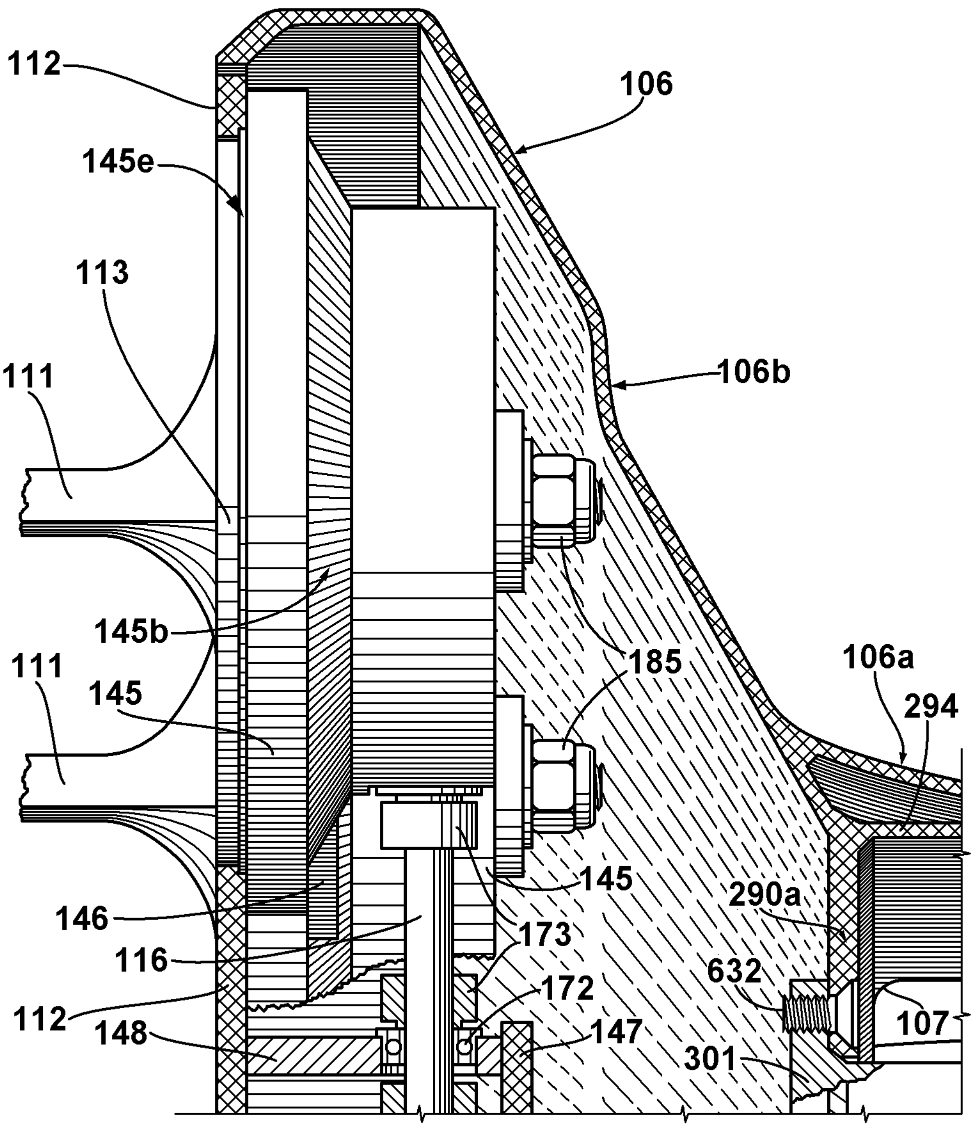
112
106
145e
113
111
106b
145b
185
106a
111
145
294
145
290a
146
173
116
632
172
112
107
148
147
301

FIG. 44A

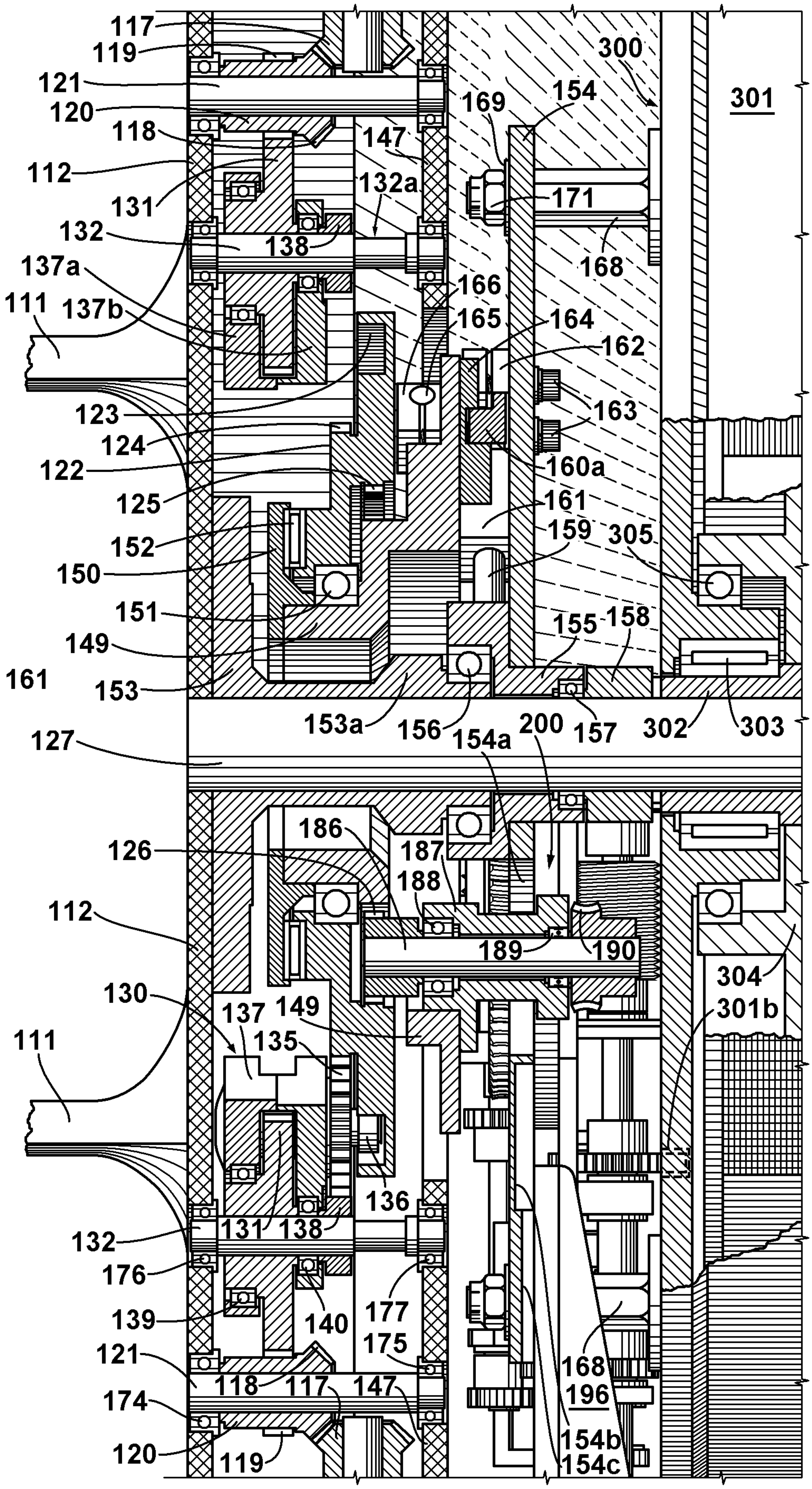
117
119
121
120
118
112
131
132
137a
111
137b
123
124
122
125
152
150
151
149
161
153
153a
156
154a
200
157
302
303
127
300
301
169
154
147
132a
171
138
168
166
165
164
162
163
160a
161
159
305
155
158
126
186
187
188
189
190
304
301b
130
137
149
135
136
131
138
132
176
139
140
177
175
121
118
117
147
174
120
119
168
196
154b
154c

FIG. 44B

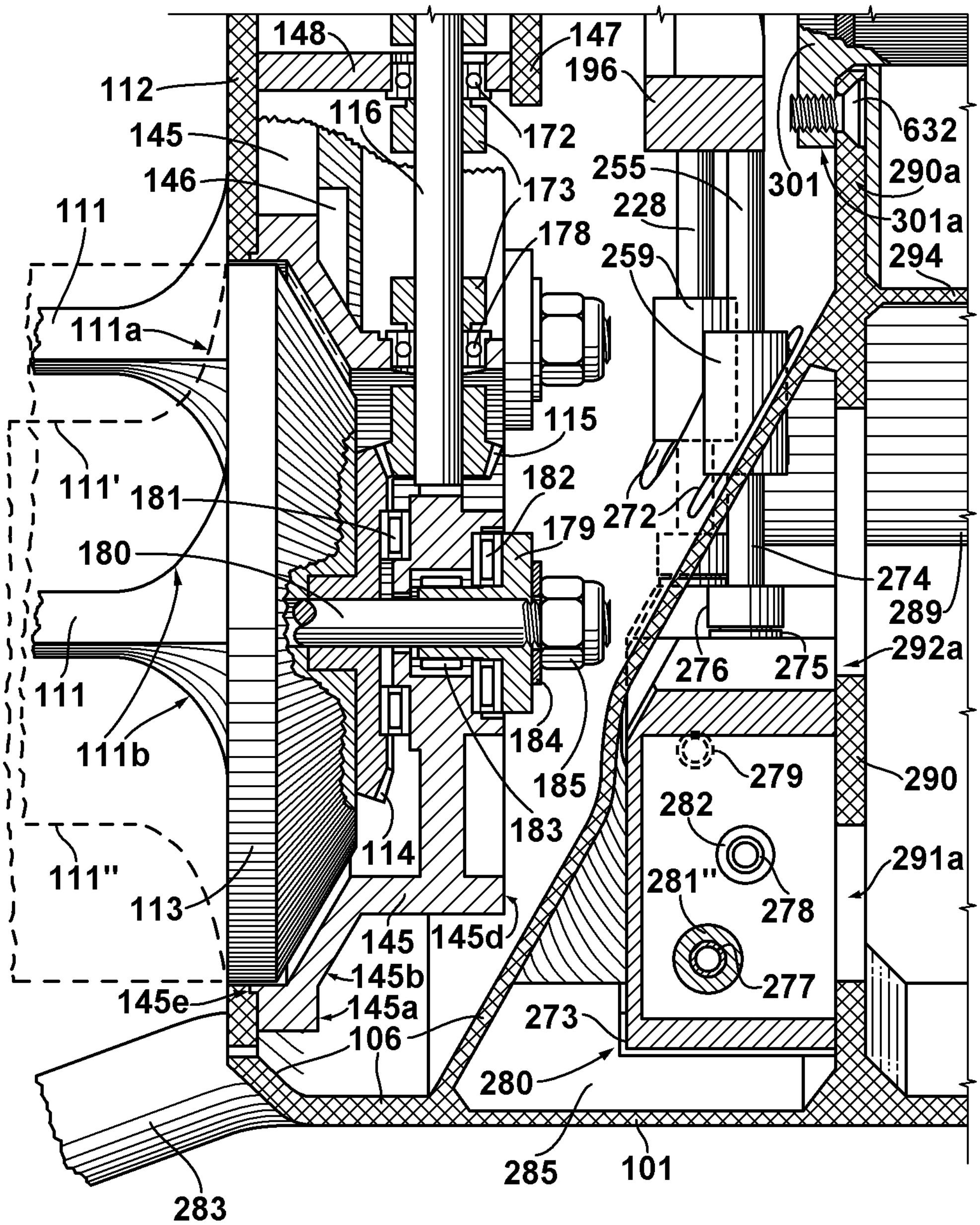
148
147
196
112
116
172
632
145
173
255
301
290a
146
228
301a
111
178
259
294
111a
115
111'
181
182
179
272
180
274
289
111
276
275
292a
111b
184
185
279
290
282
183
114
291a
111''
281''
278
113
145
145d
145b
277
145e
145a
273
106
280
285
101
283

FIG. 44C

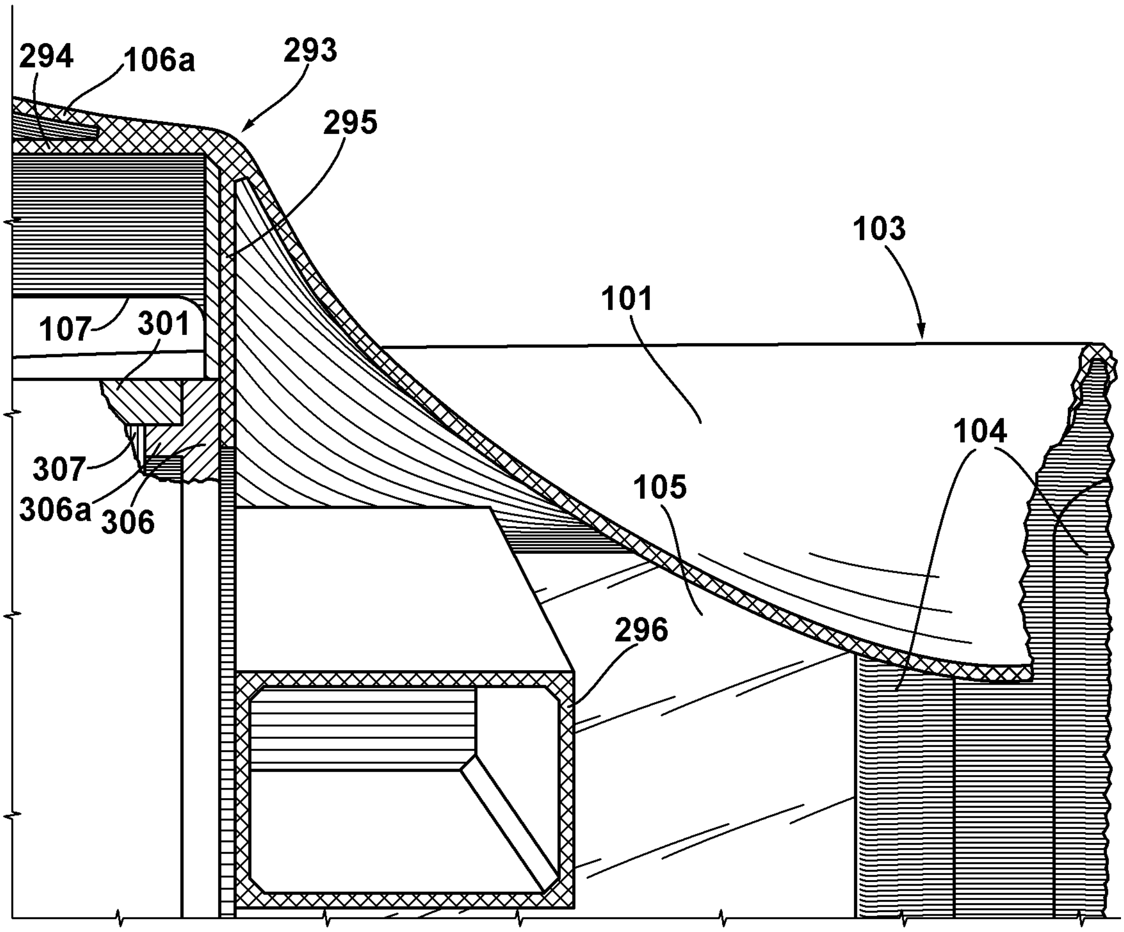

FIG. 44D

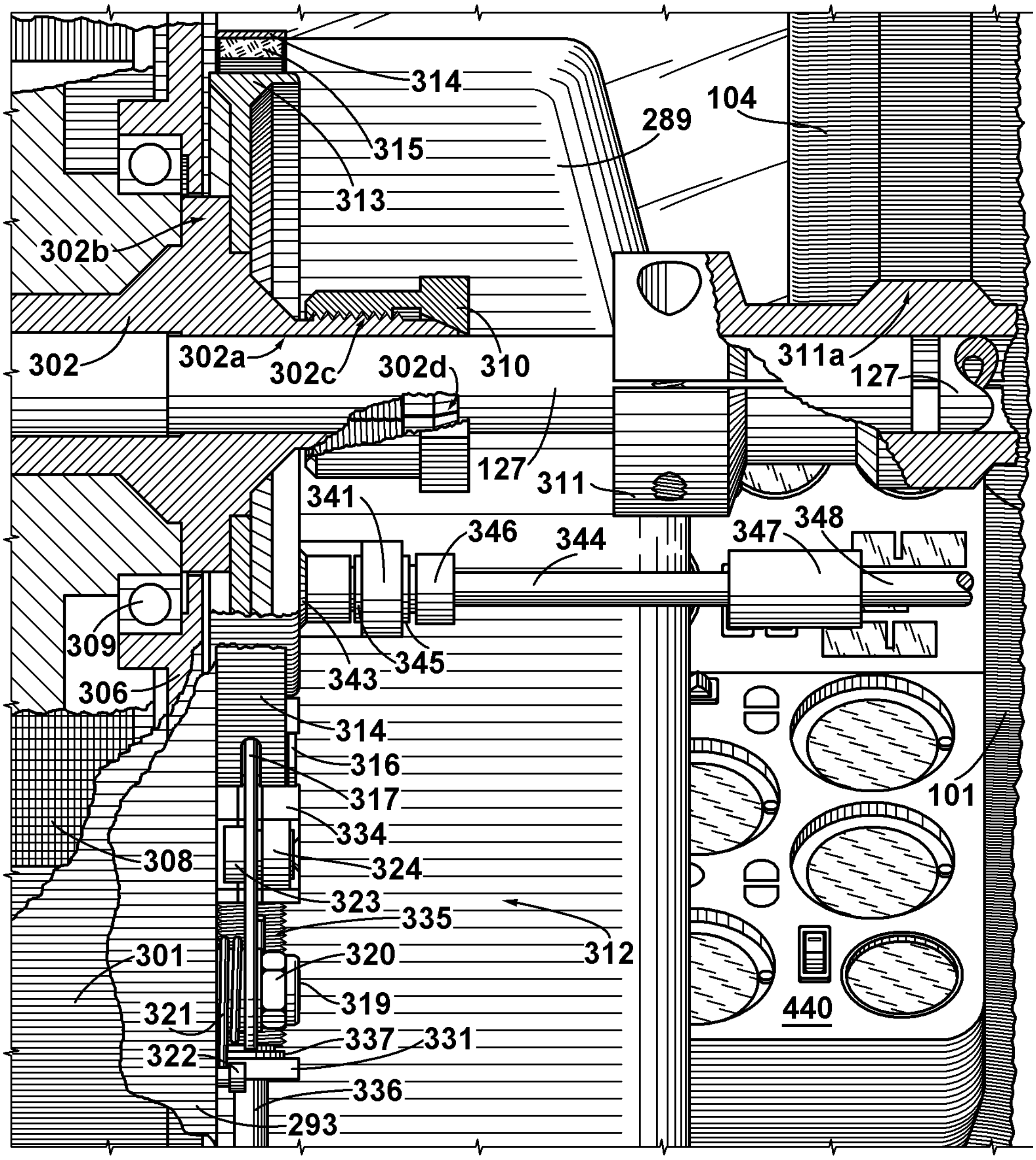
314
315
313
289
104
302b
302
302a
302c
302d
310
311a
127
127
311
341
346
344
347
348
309
343
345
306
314
316
317
334
324
308
323
335
301
320
312
319
321
337
331
322
336
293
101
440

FIG. 44E

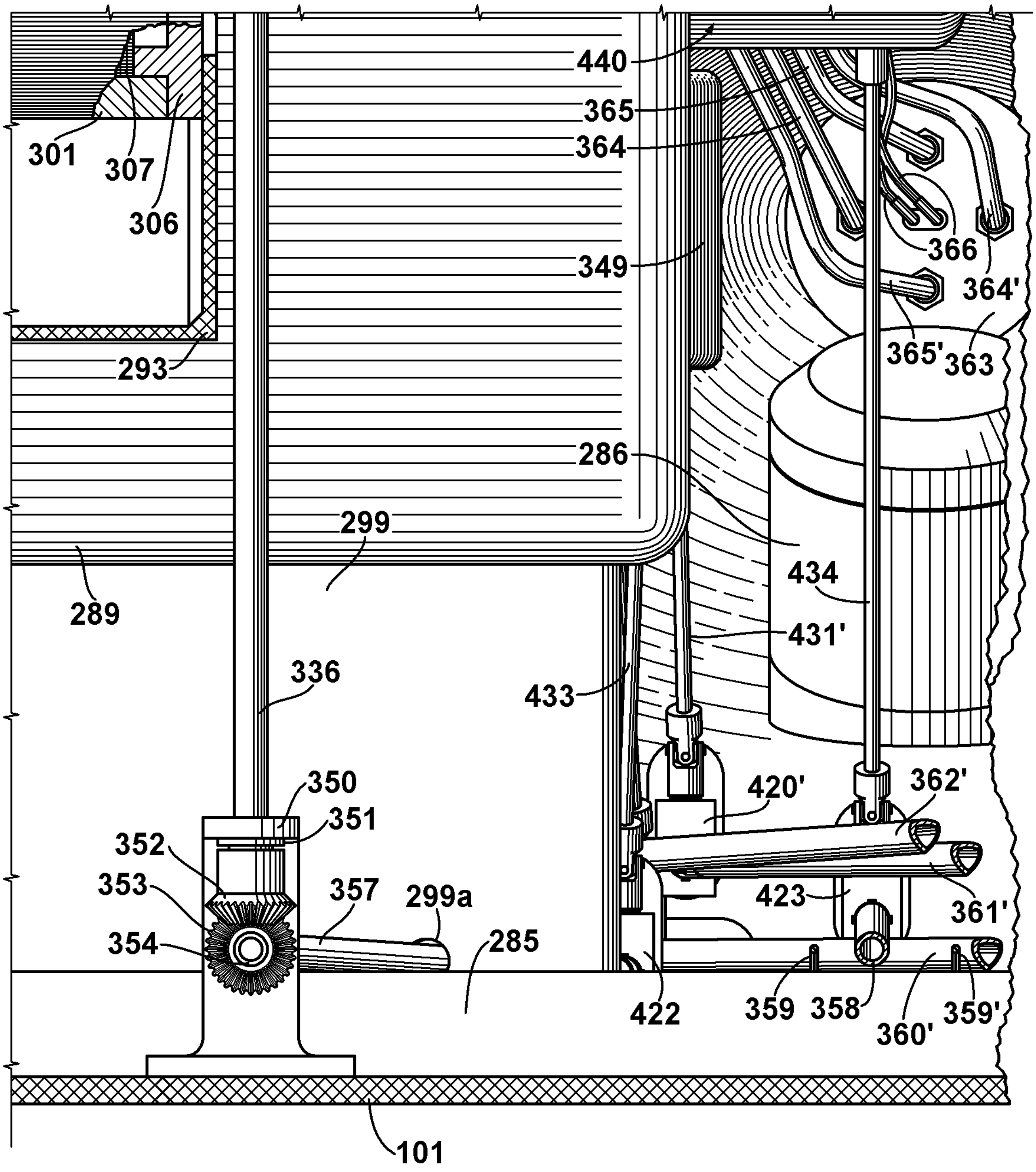
440
365
364
301
307
306
366
349
364'
365'
363
293
286
299
434
289
431'
336
433
420'
362'
350
351
352
353
357
299a
423
361'
354
285
422
359
358
359'
360'
101

FIG. 44F

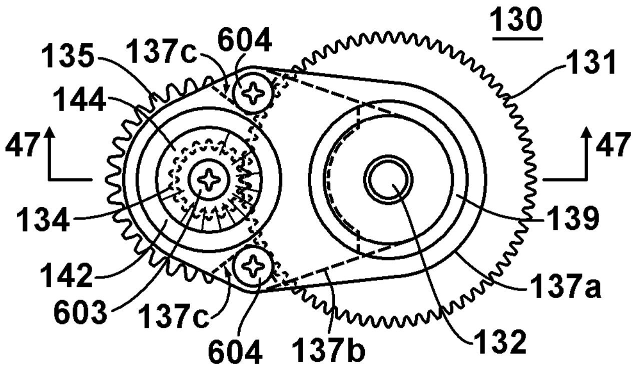

FIG. 45

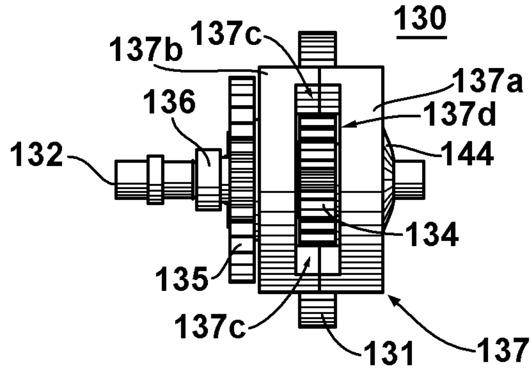

FIG. 46

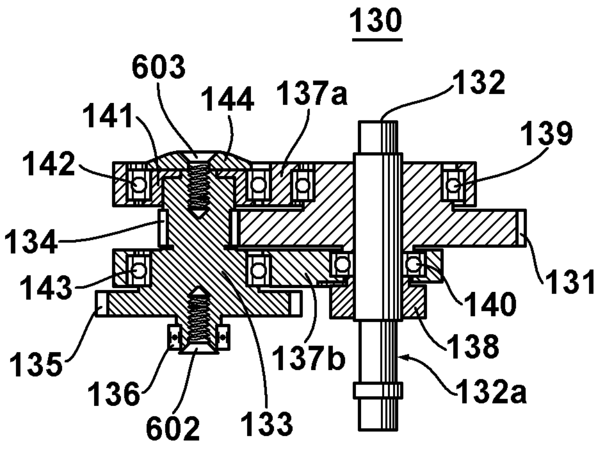

FIG. 47

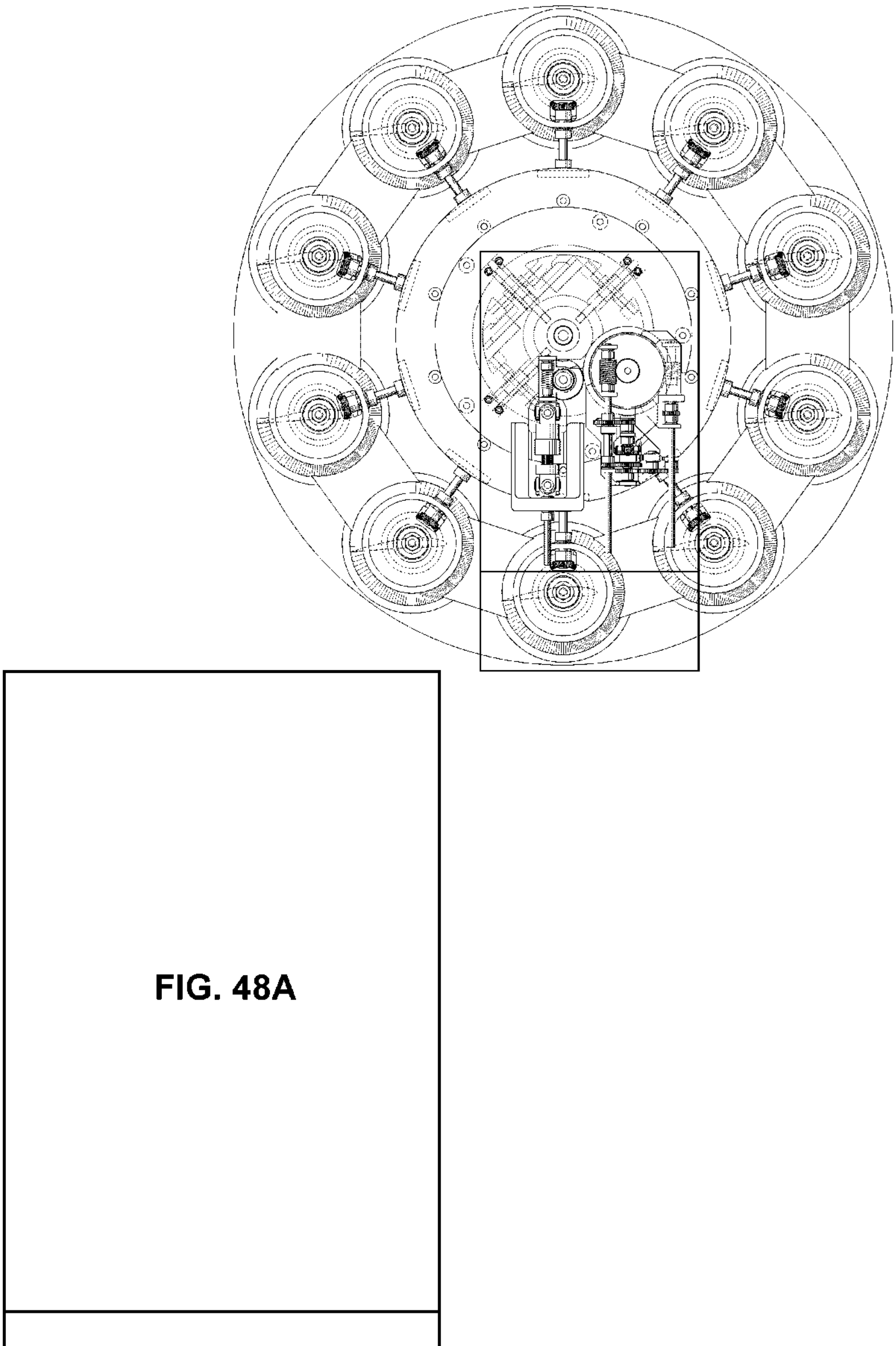

FIG. 48

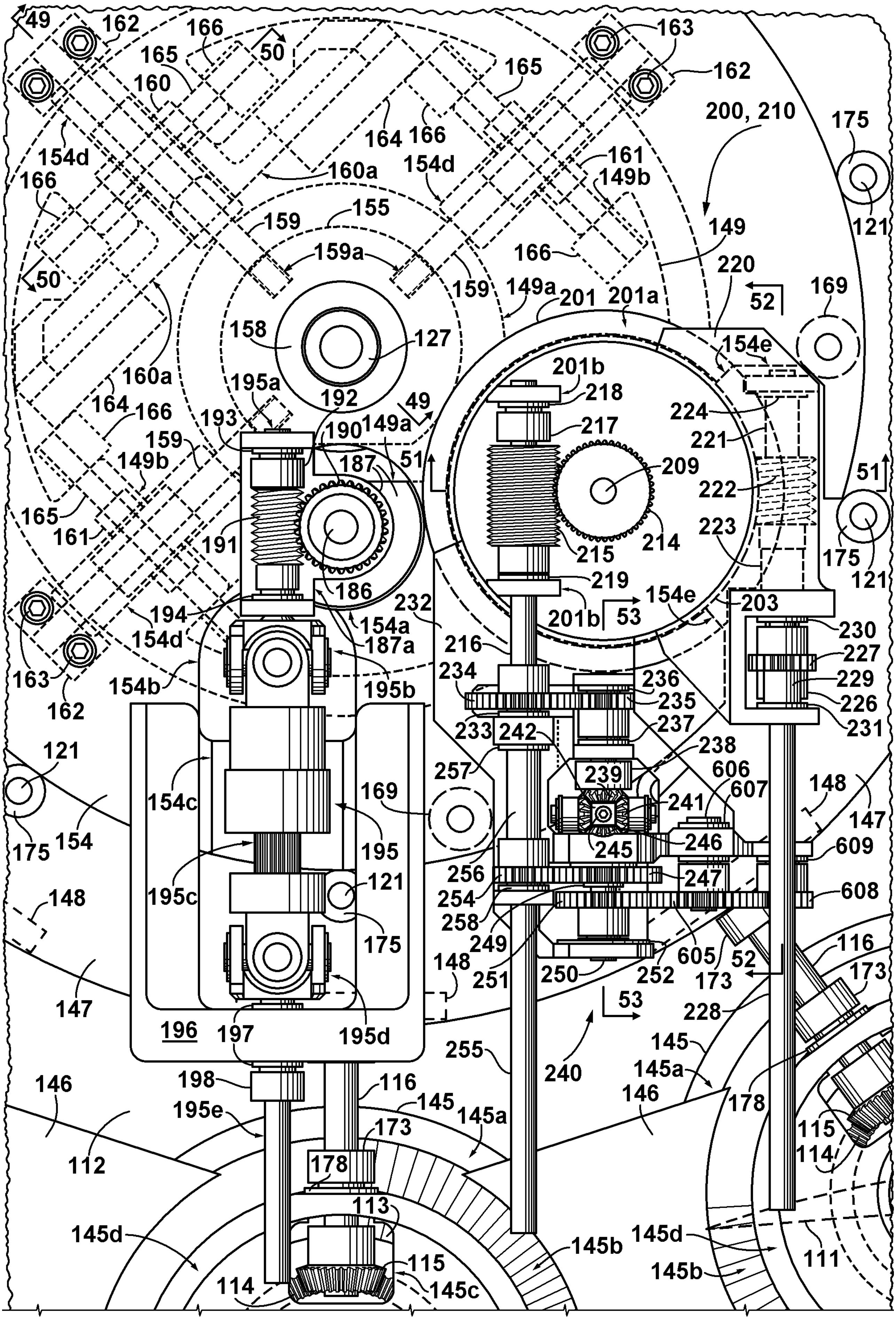

49
162
166
50
165
160
163
165
162
200, 210
175
164
166
154d
160a
154d
161
149b
121
166
155
149
159
159a
159
149a
201
201a
220
52
169
50
158
127
154e
160a
201b
218
164
166
195a
192
49
224
217
193
190
149a
221
159
187
51
149b
209
51
222
165
191
161
215
214
223
175
121
219
186
154e
203
194
154a
232
201b
53
230
154d
187a
216
227
163
195b
234
236
229
154b
235
226
162
233
242
237
231
121
238
257
239
606
148
607
154c
169
241
147
175
154
246
609
195
245
256
247
195c
121
254
608
148
258
175
249
605
52
116
173
148
251
250
252
173
147
53
228
196
197
195d
145
255
240
198
116
145
145a
146
146
195e
145a
178
173
112
178
115
113
114
145d
145d
145b
111
145b
115
114
145c

FIG. 48A

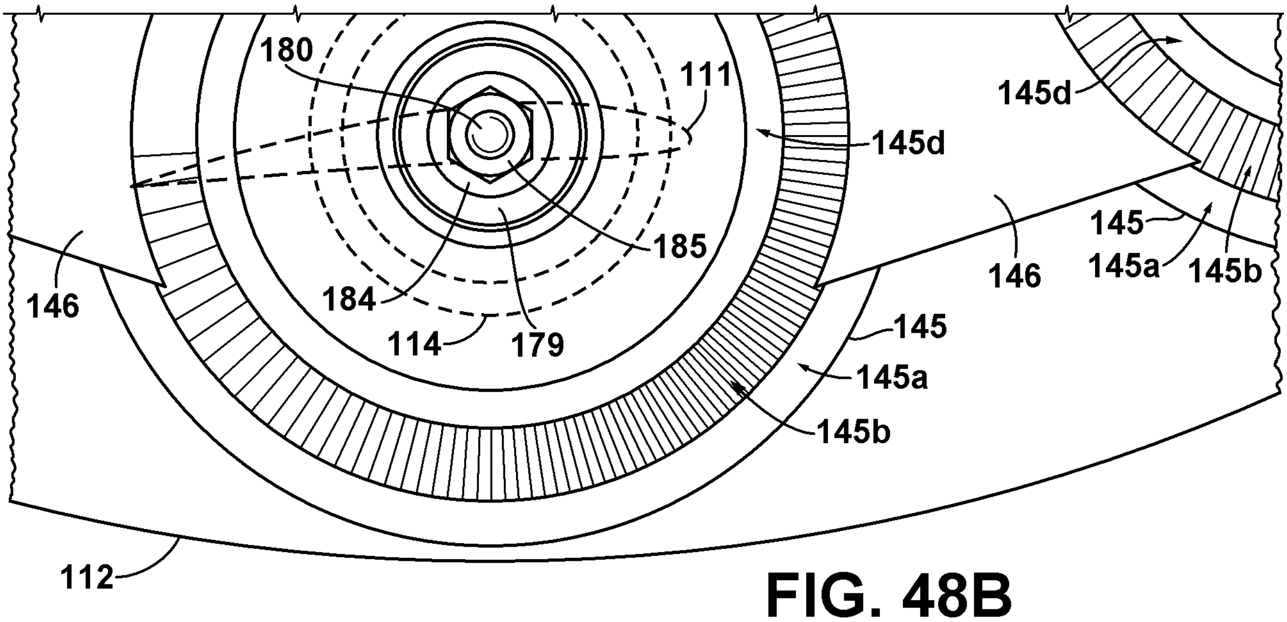

FIG. 48B

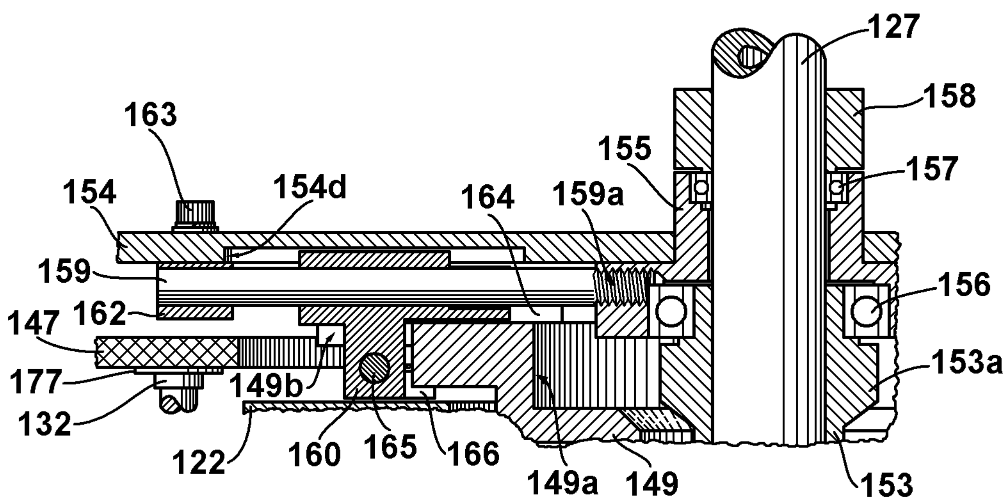

FIG. 49

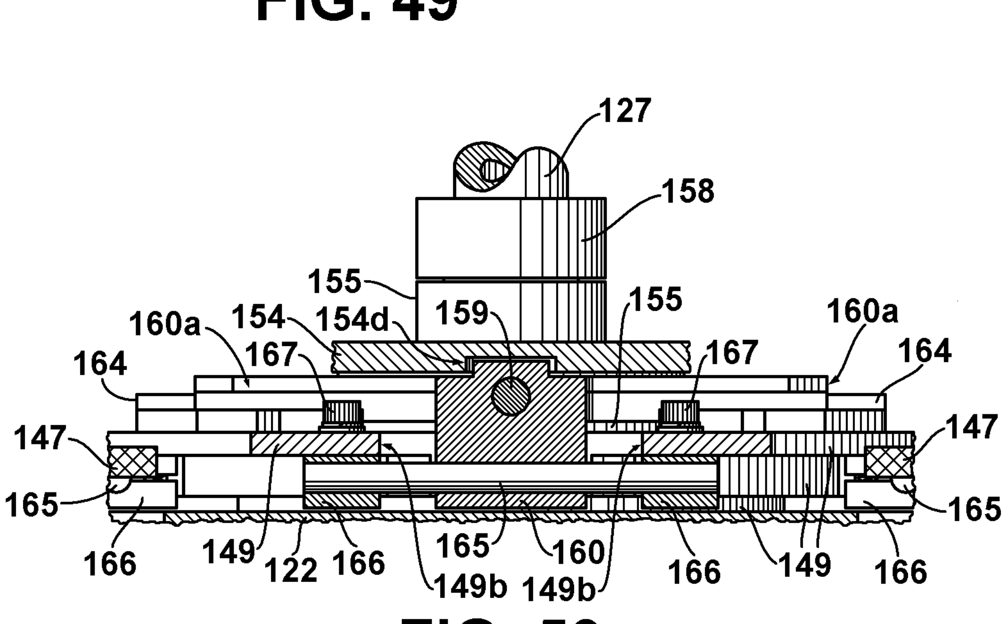

FIG. 50

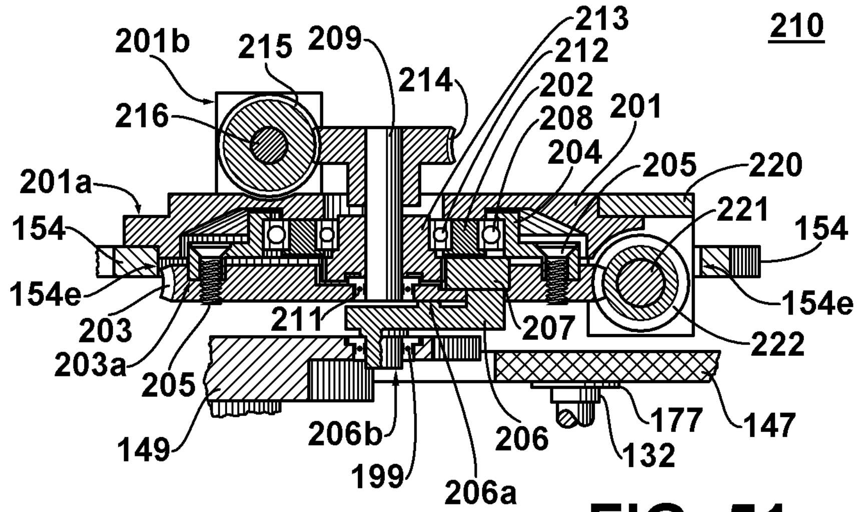

FIG. 51

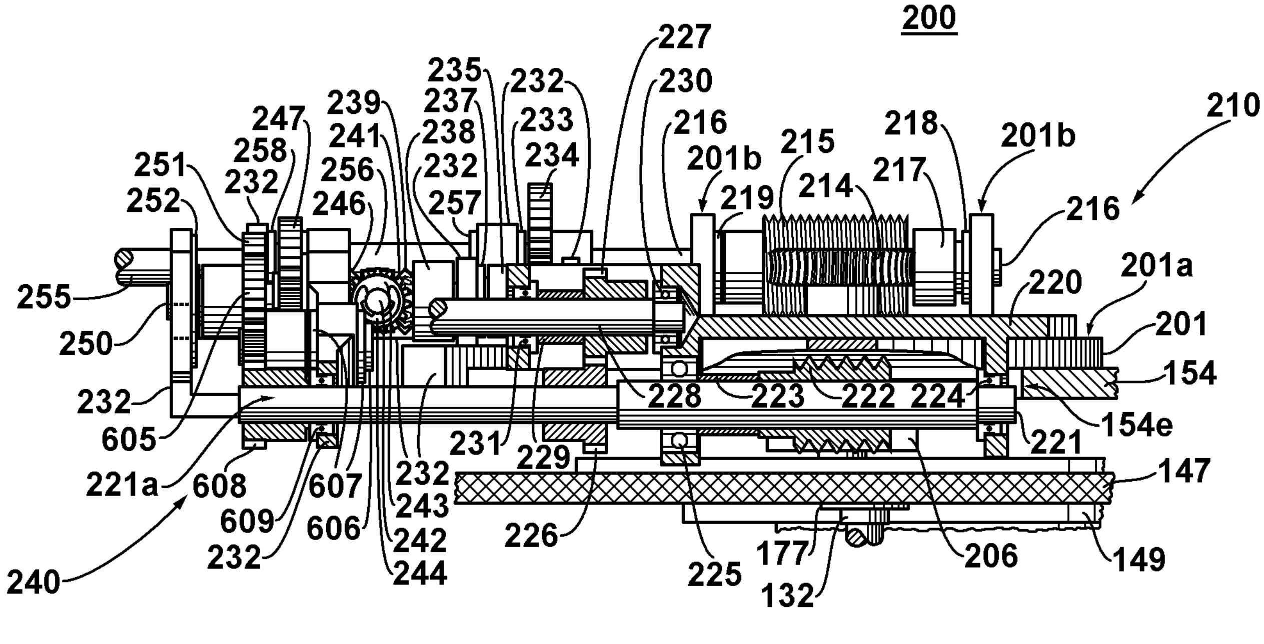

FIG. 52

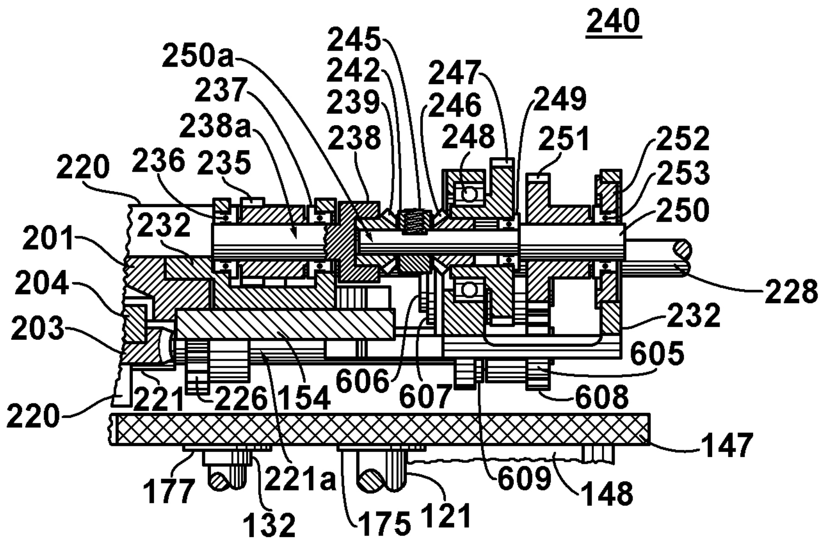

FIG. 53

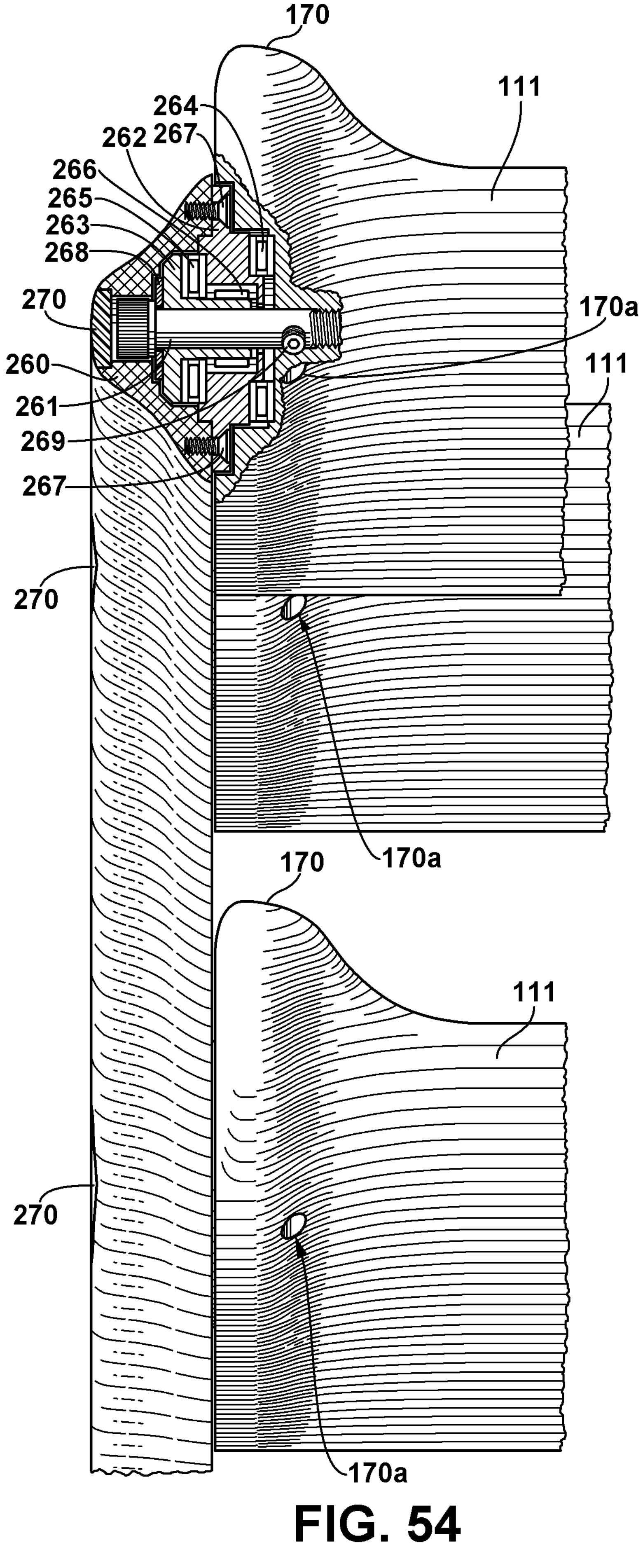
170
111
264
267
262
266
265
263
268
270
170a
111
260
261
269
267
270
170a
170
111
270
170a

FIG. 54

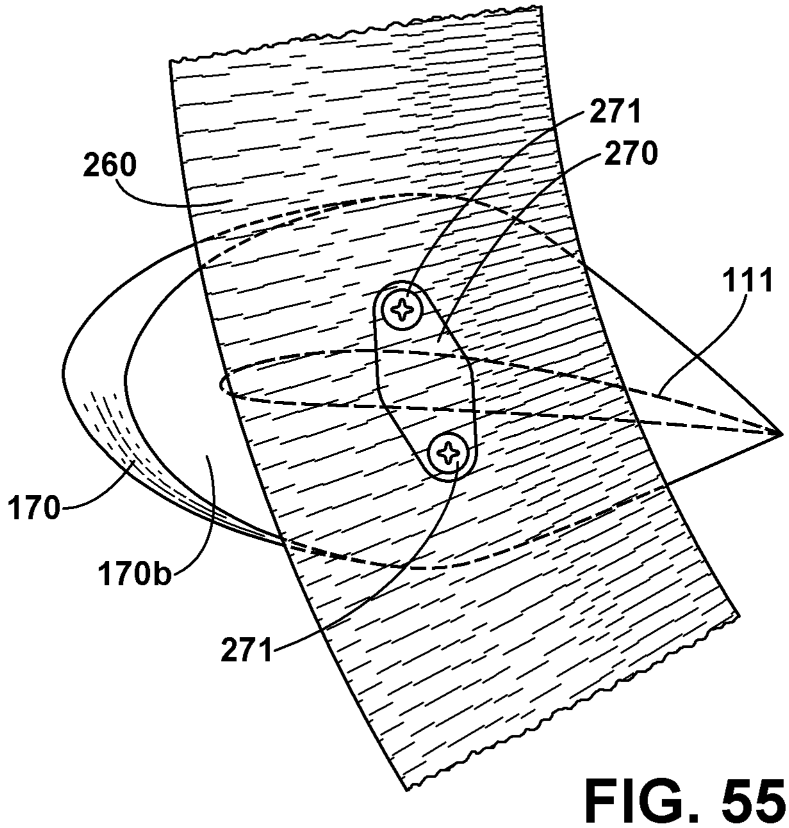

FIG. 55

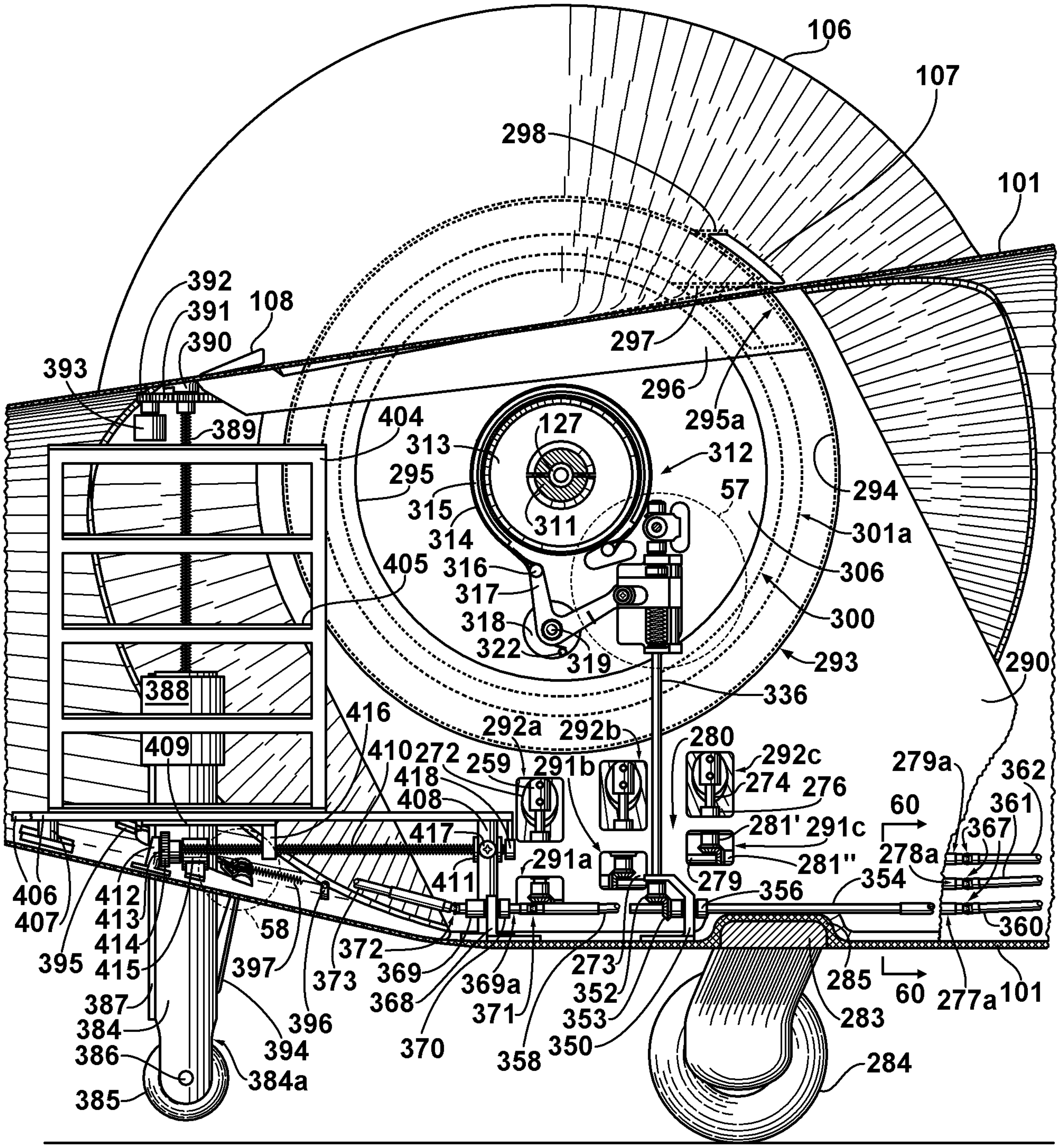

FIG. 56

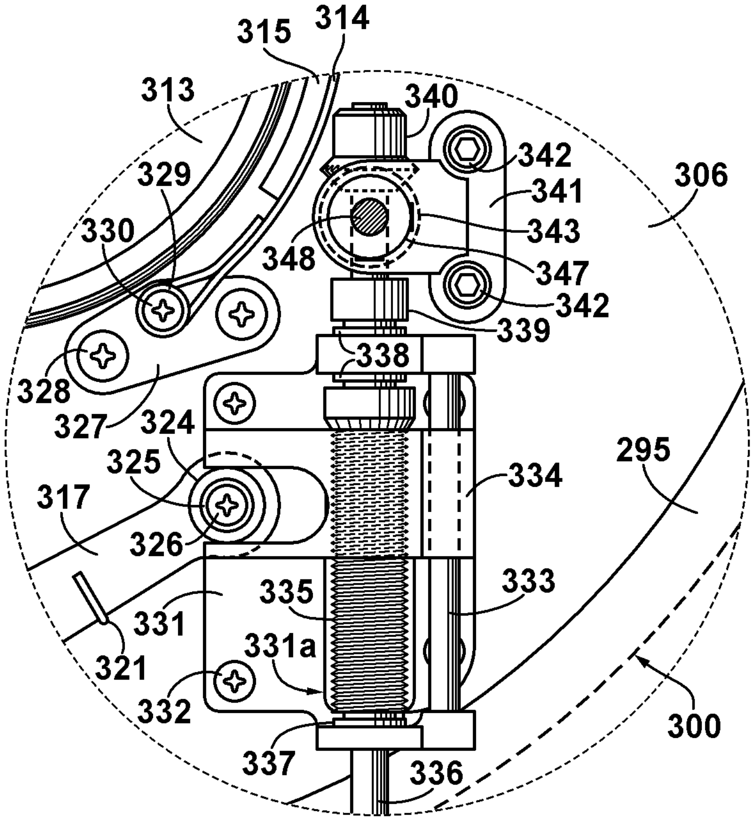
315
314
313
340
342
341
306
329
343
330
348
347
342
339
338
328
327
324
334
295
325
317
326
333
335
331
331a
321
332
300
337
336

FIG. 57

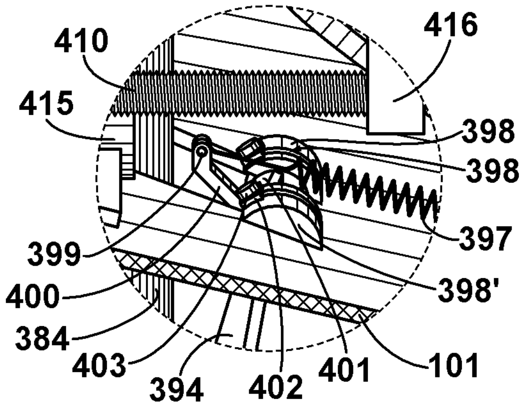
416
410
415
398
398a
397
399
398'
400
384
403
394
402
401
101

FIG. 58

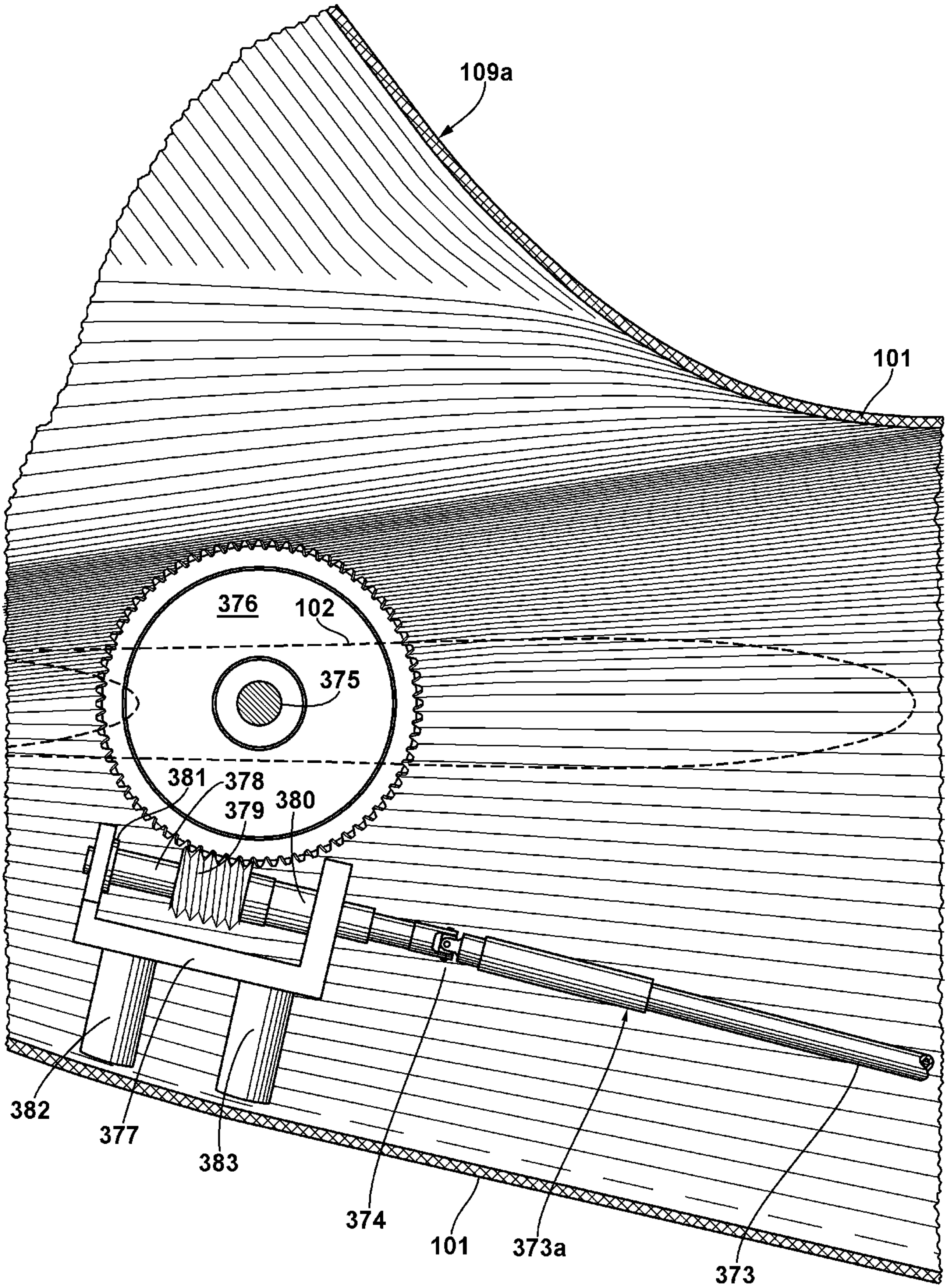
109a
101
376
102
375
381
378
379
380
382
377
383
374
101
373a
373

FIG. 59

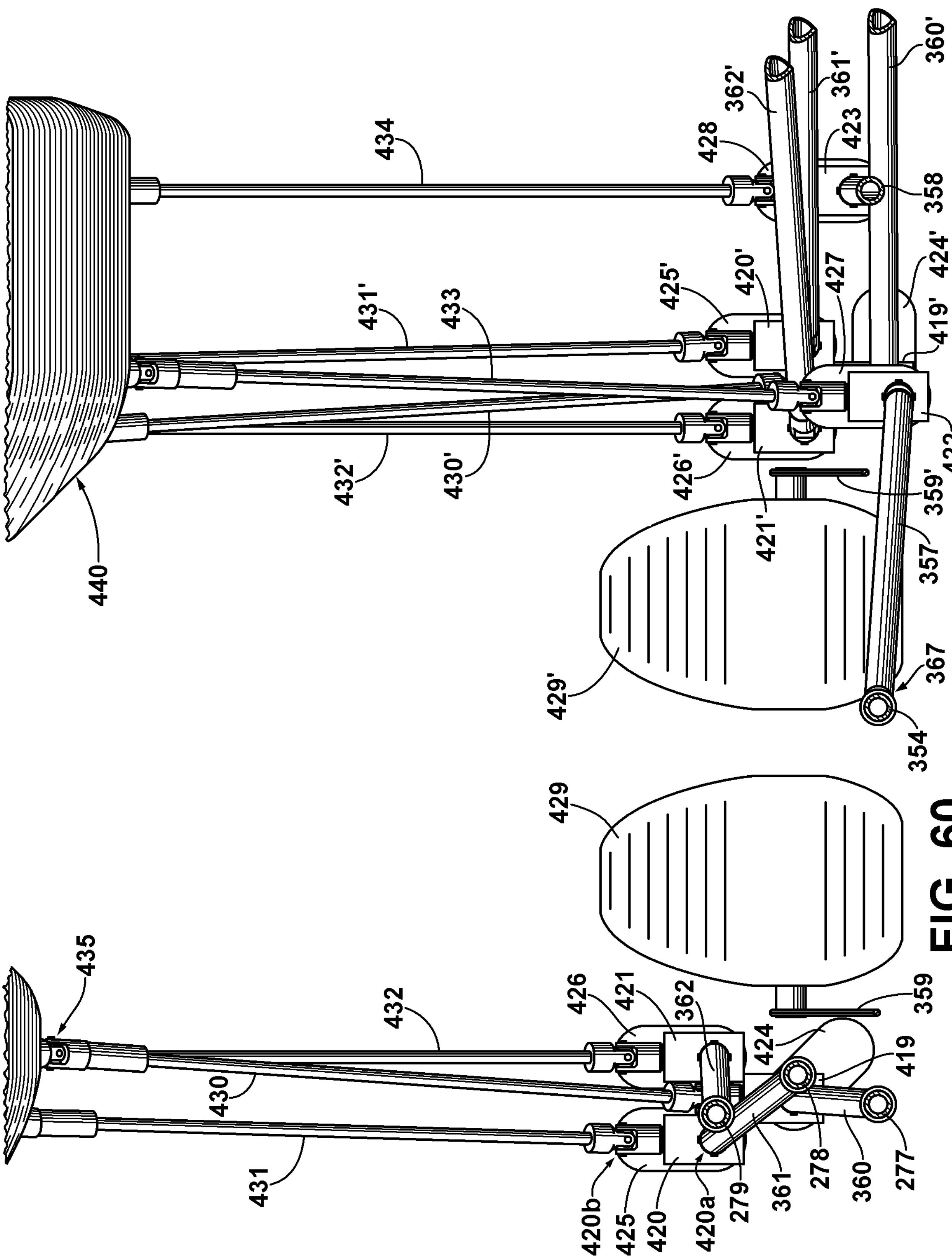
434
428
362'
361'
360'
423
358
425'
420'
431'
433
427
424'
419'
422
359'
357
421'
426'
430'
432'
440
429'
367
354
429
435
432
426
421
362
424
359
419
430
431
420b
425
420
420a
279
361
278
360
277

FIG. 60

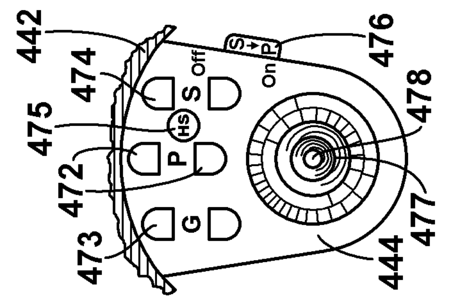

FIG. 62

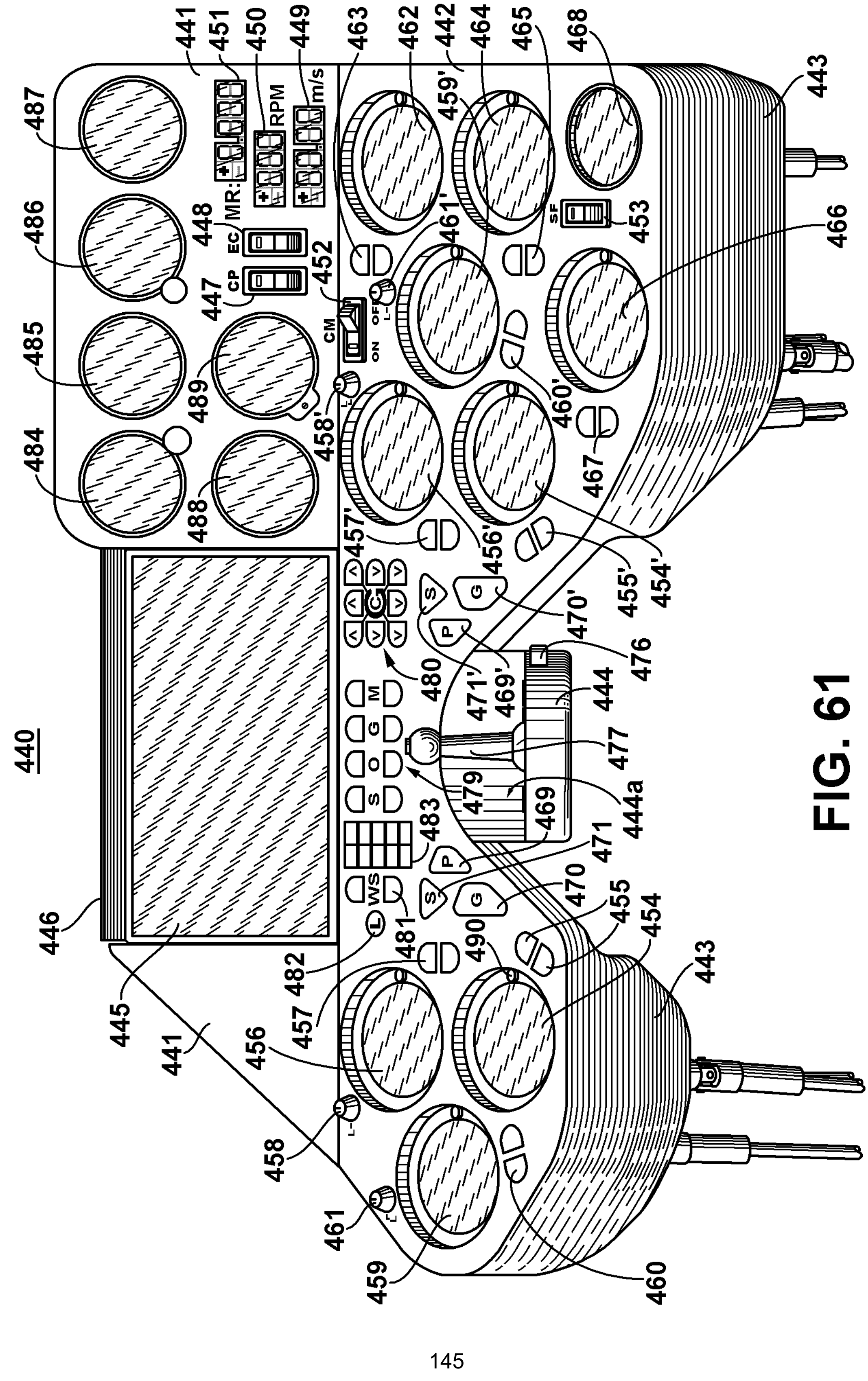

FIG. 61

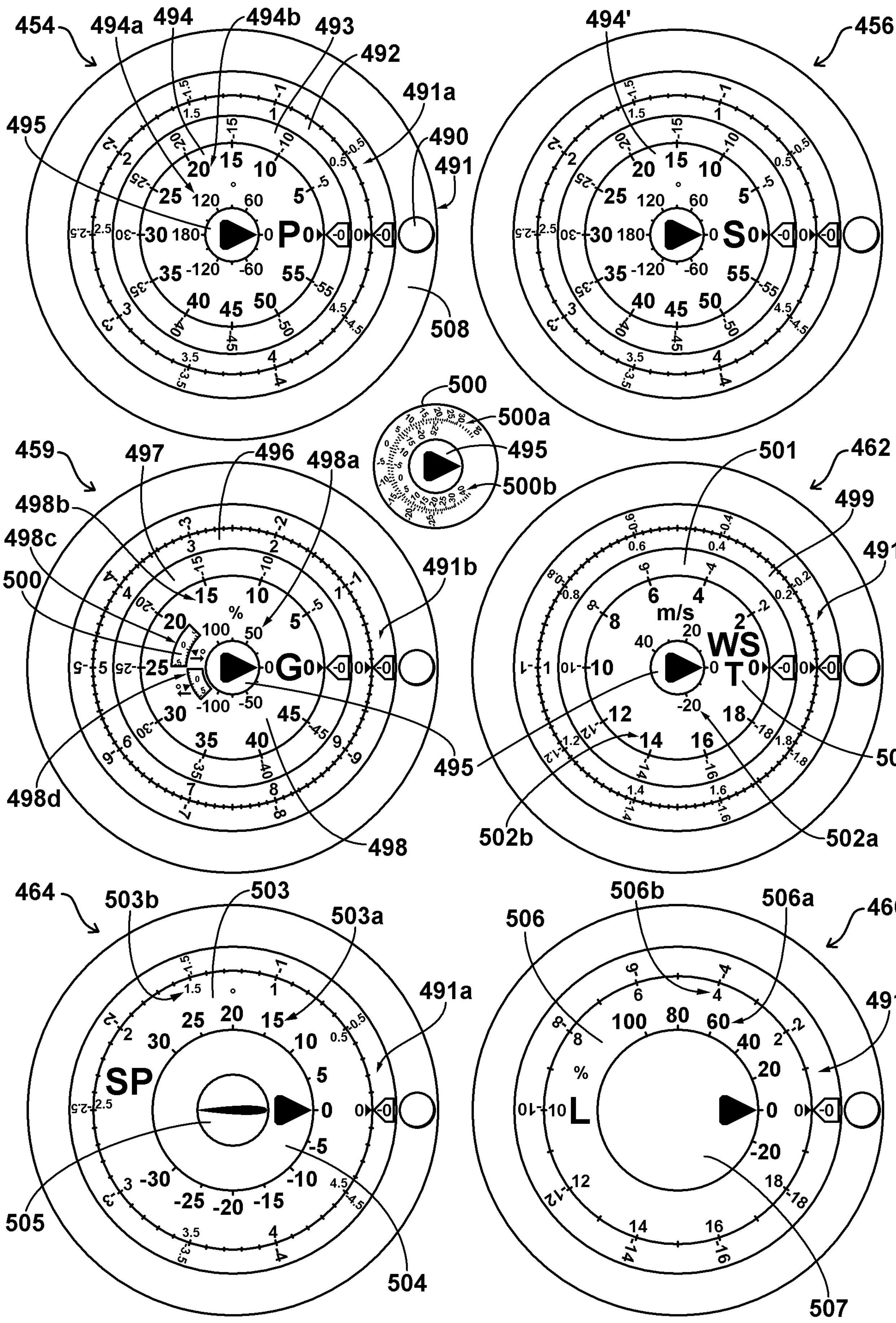

FIG. 63

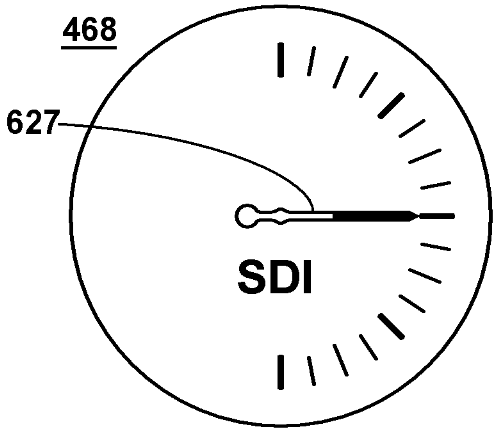

FIG. 64

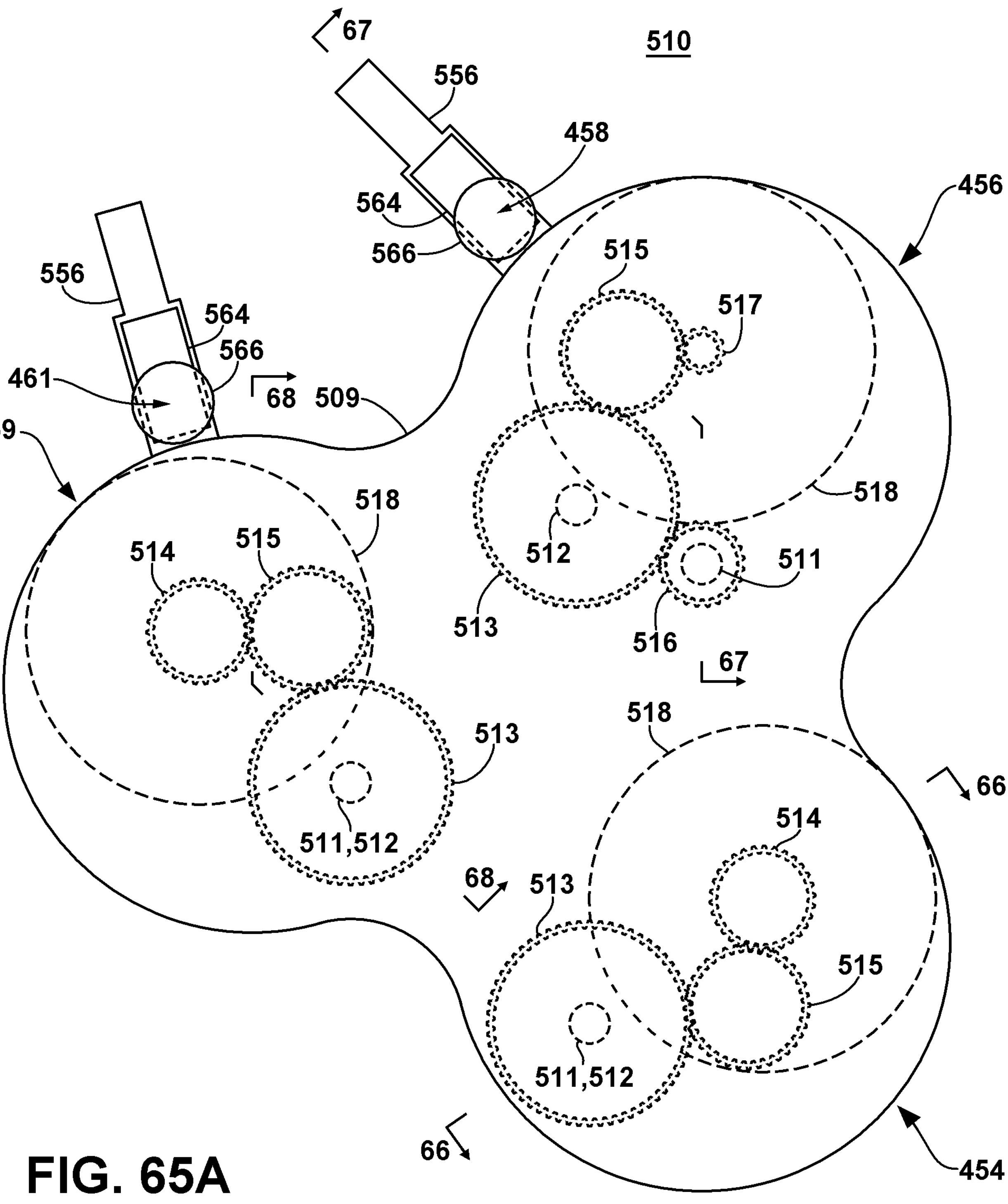

FIG. 65A

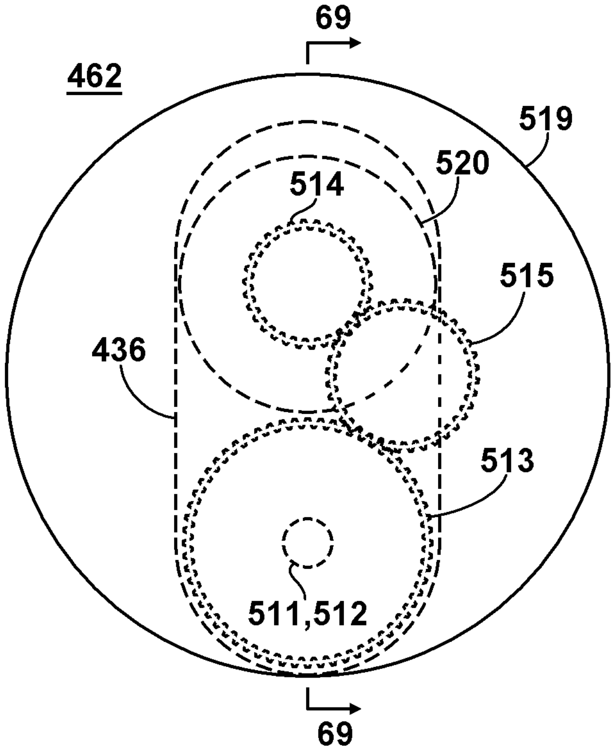

FIG. 65B

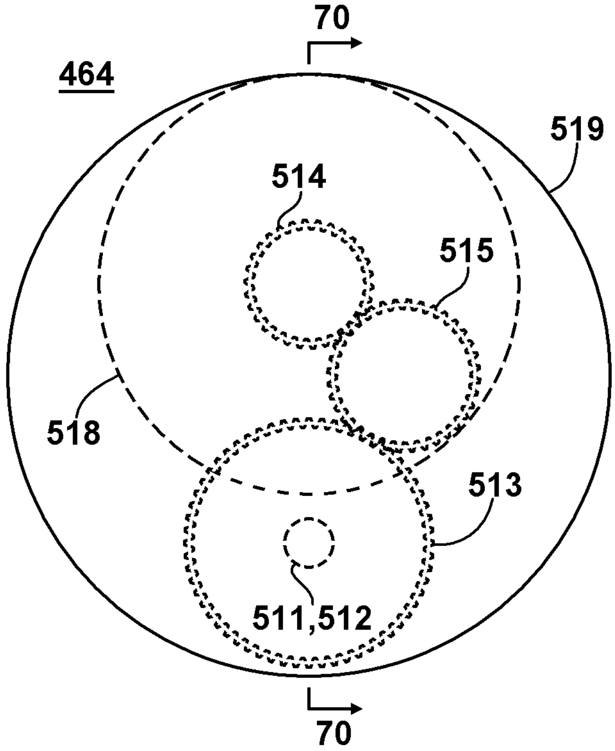

FIG. 65C

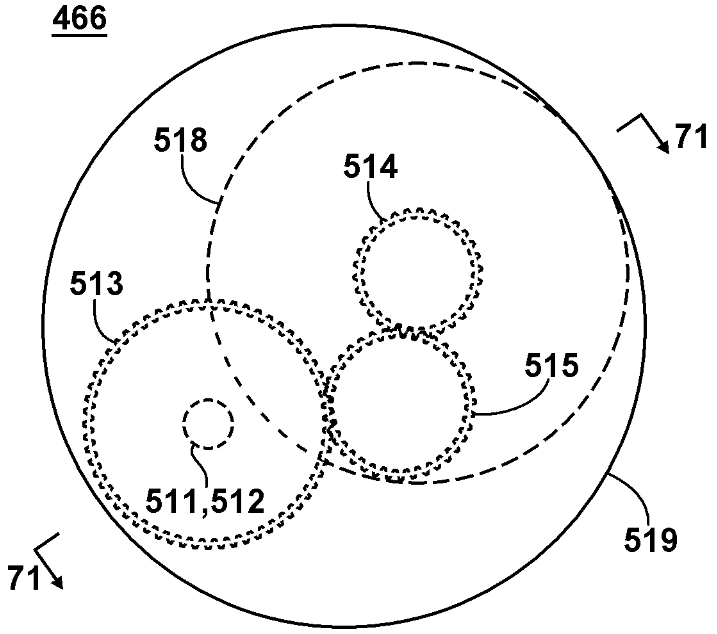

FIG. 65D

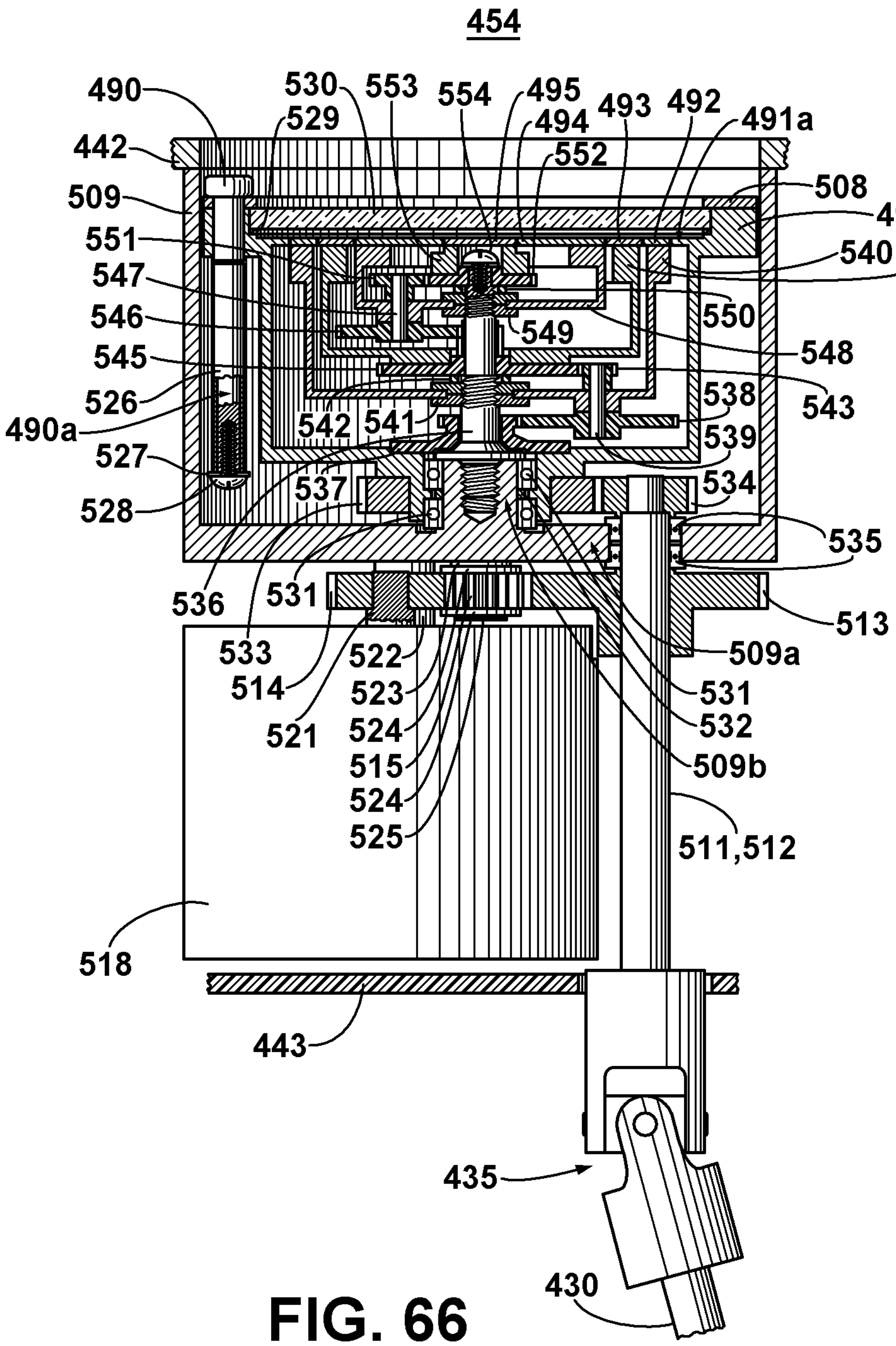
454
490
530
553
554
495
494
493
492
491a
529
442
552
509
508
491
551
540
544
547
550
546
549
548
545
543
526
538
490a
542
541
539
527
537
534
528
535
536
531
513
533
522
509a
514
523
531
521
524
532
515
509b
524
525
511,512
518
443
435
430

FIG. 66

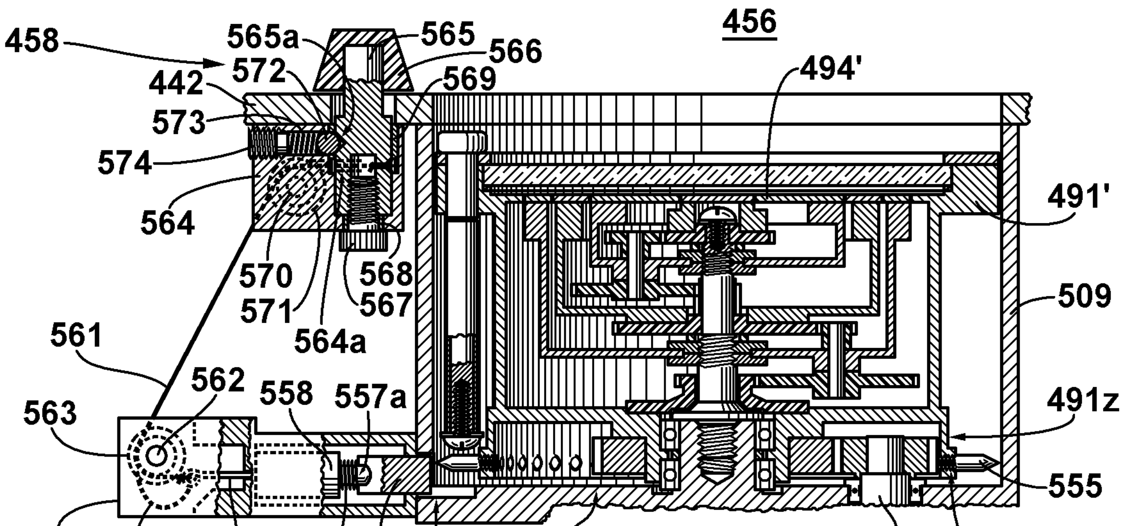
456
458
565a
565
566
442
572
569
494'
573
574
564
491'
570
568
571
567
509
564a
561
491z
562
558
557a
563
555
556
561'
560
559
557
509c
509a
511
555a

FIG. 67

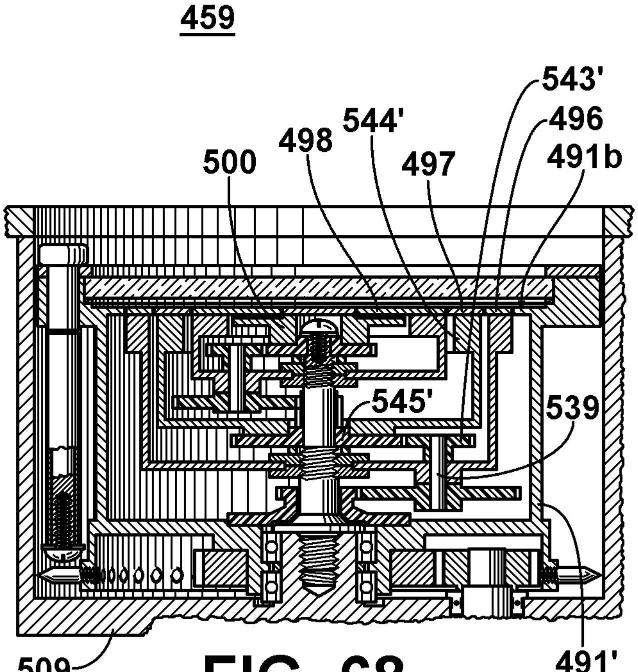

FIG. 68

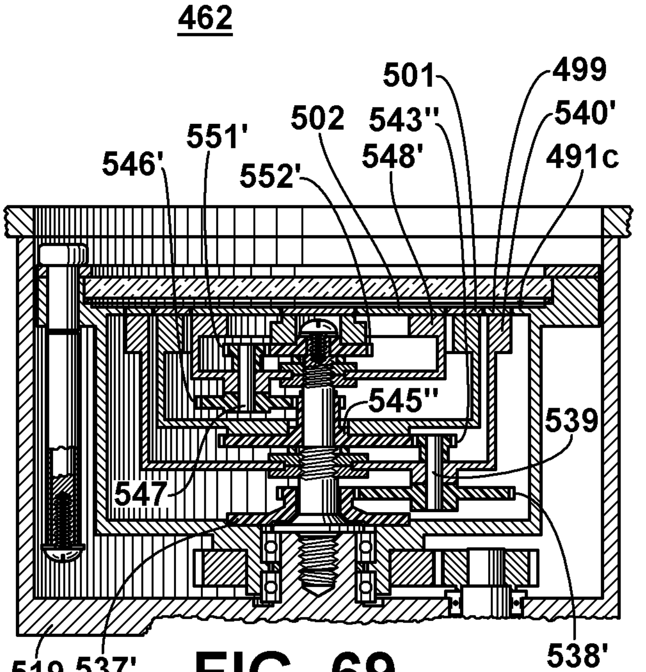

FIG. 69

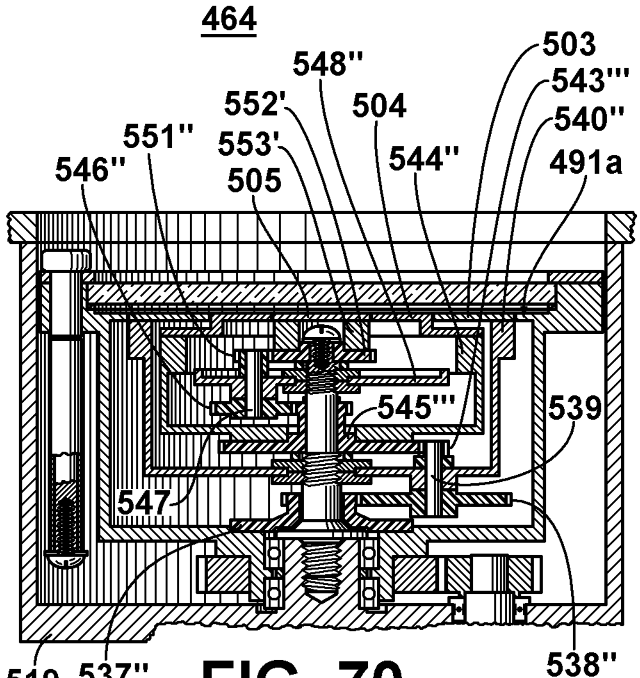

FIG. 70

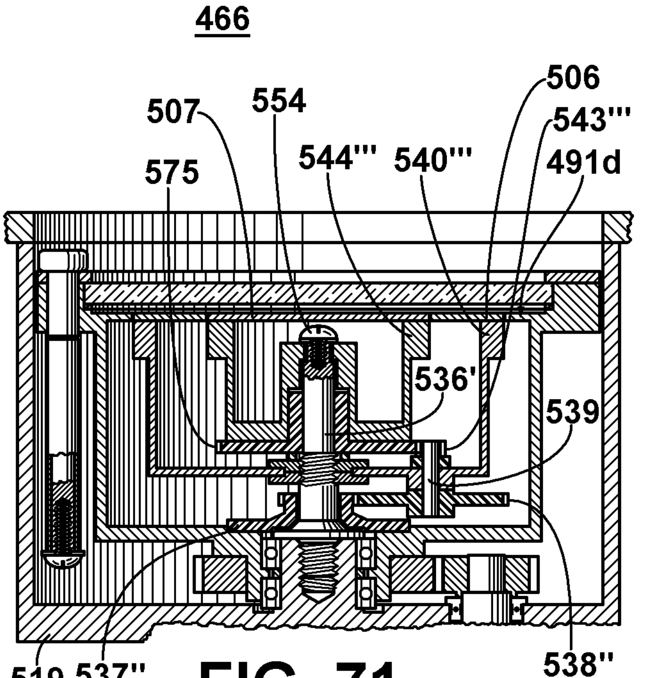

FIG. 71

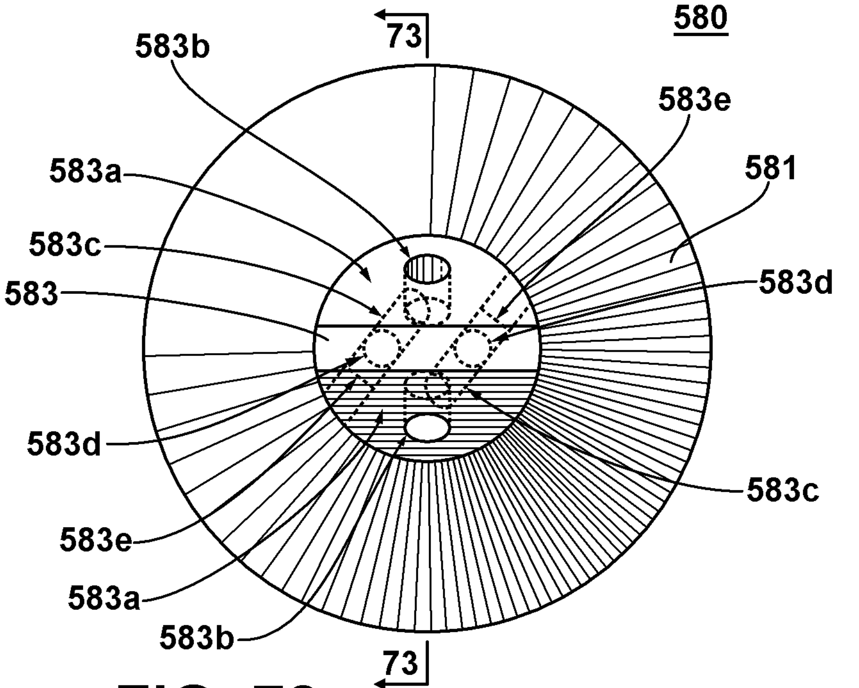

FIG. 72

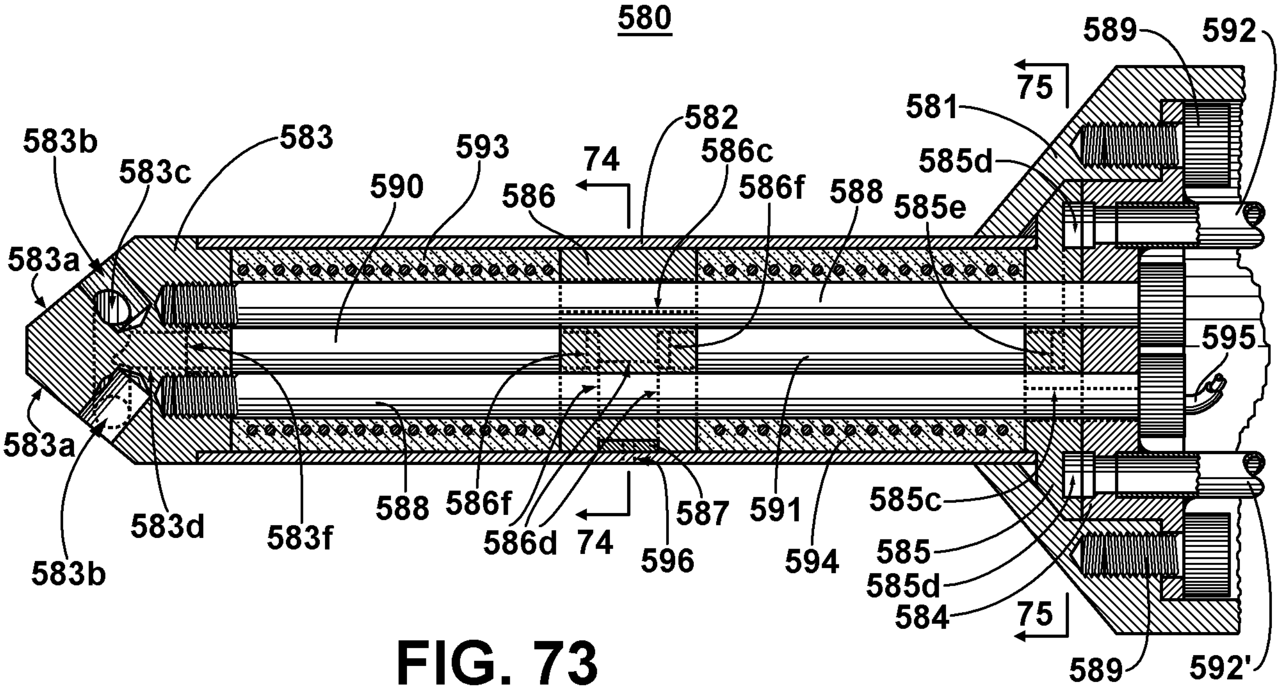

FIG. 73

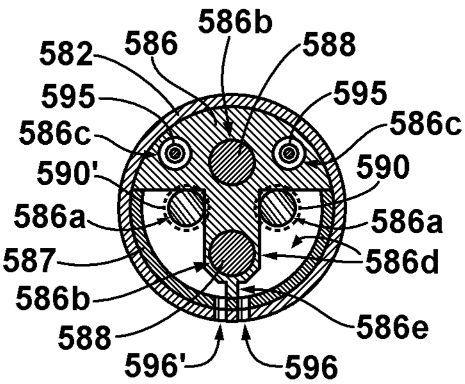

FIG. 74

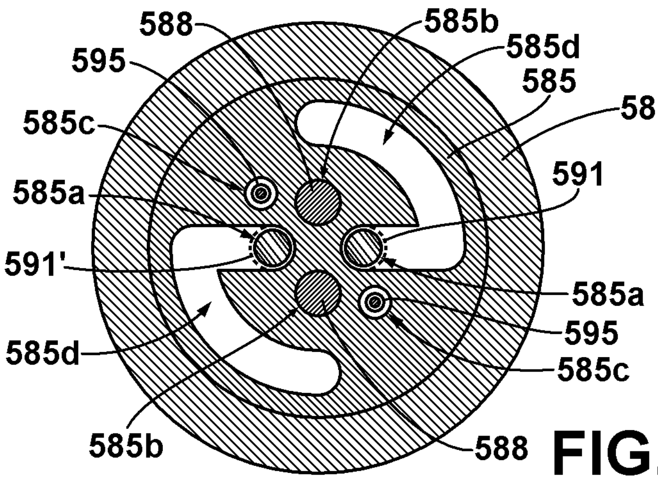

FIG. 75

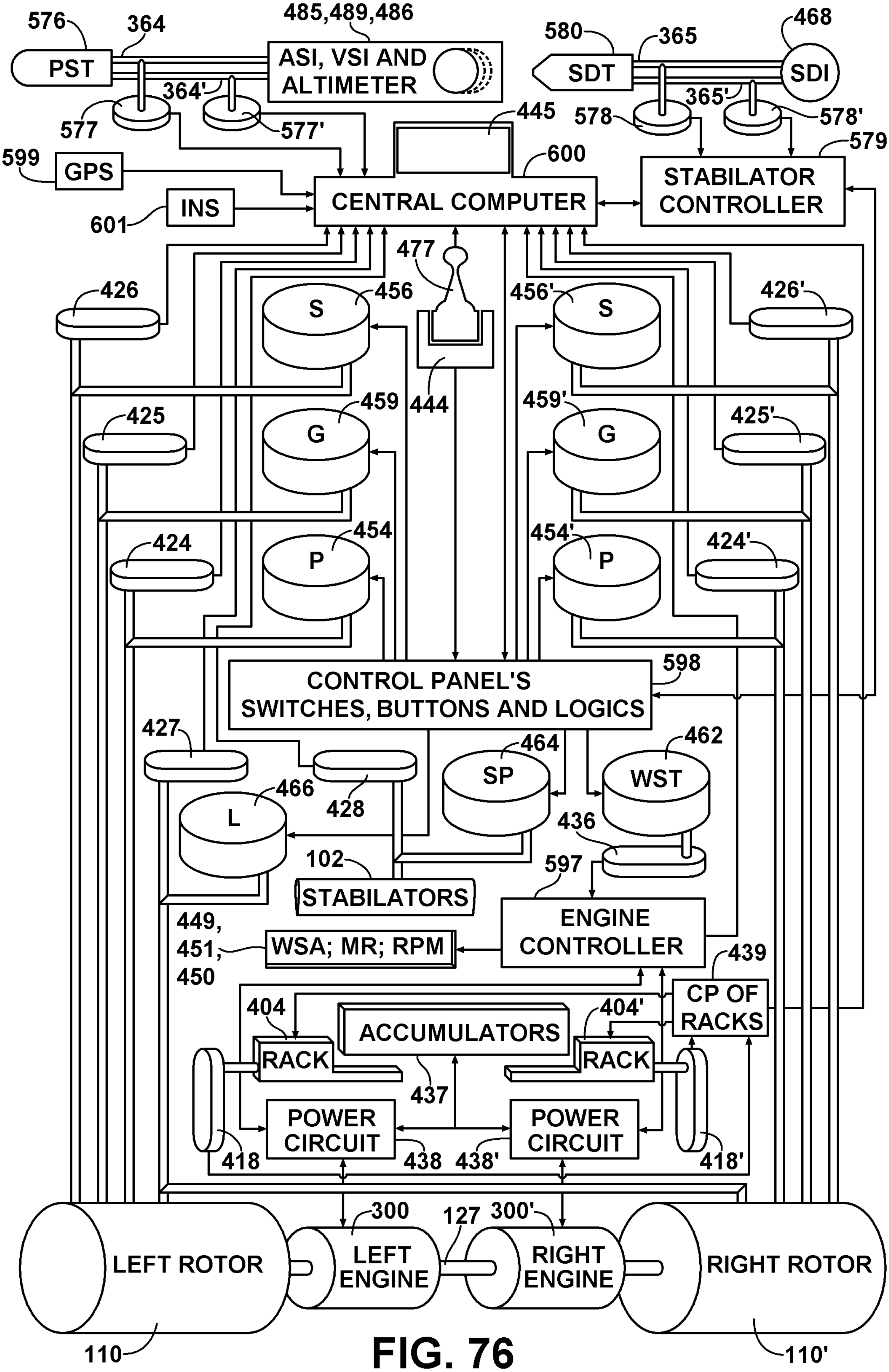
576
364
485,489,486
PST
ASI, VSI AND ALTIMETER
364'
577
577'
580
365
468
SDT
SDI
365'
578
578'
445
599
GPS
600
579
STABILATOR CONTROLLER
INS
CENTRAL COMPUTER
601
477
426
456
S
456'
S
426'
444
459
459'
425
G
G
425'
454
454'
424
P
P
424'
CONTROL PANEL'S SWITCHES, BUTTONS AND LOGICS
598
427
464
462
SP
WST
466
L
428
436
102
STABILATORS
597
ENGINE CONTROLLER
449, 451, 450
WSA; MR; RPM
439
CP OF RACKS
404
404'
ACCUMULATORS
RACK
RACK
437
POWER CIRCUIT
POWER CIRCUIT
418
438
438'
418'
300
127
300'
LEFT ROTOR
LEFT ENGINE
RIGHT ENGINE
RIGHT ROTOR
110
110'

FIG. 76

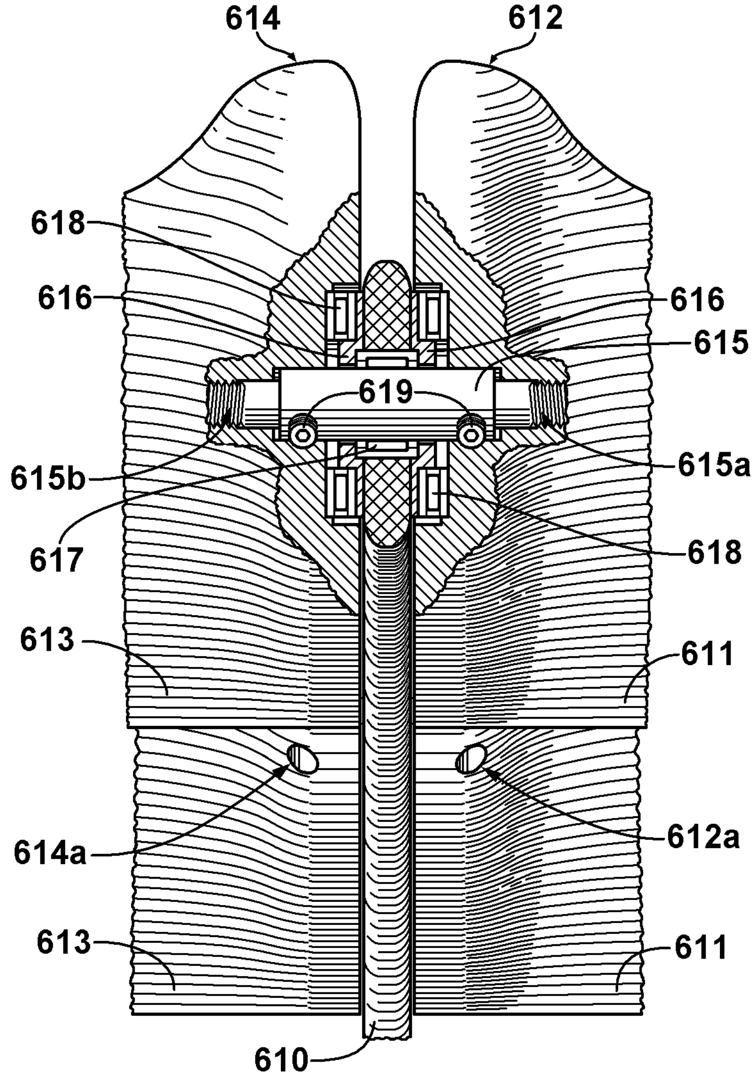

FIG. 77

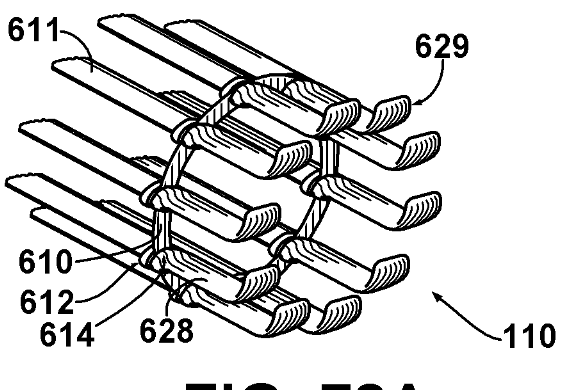

FIG. 78A

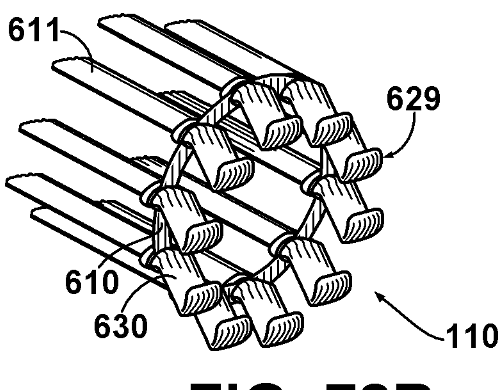

FIG. 78B

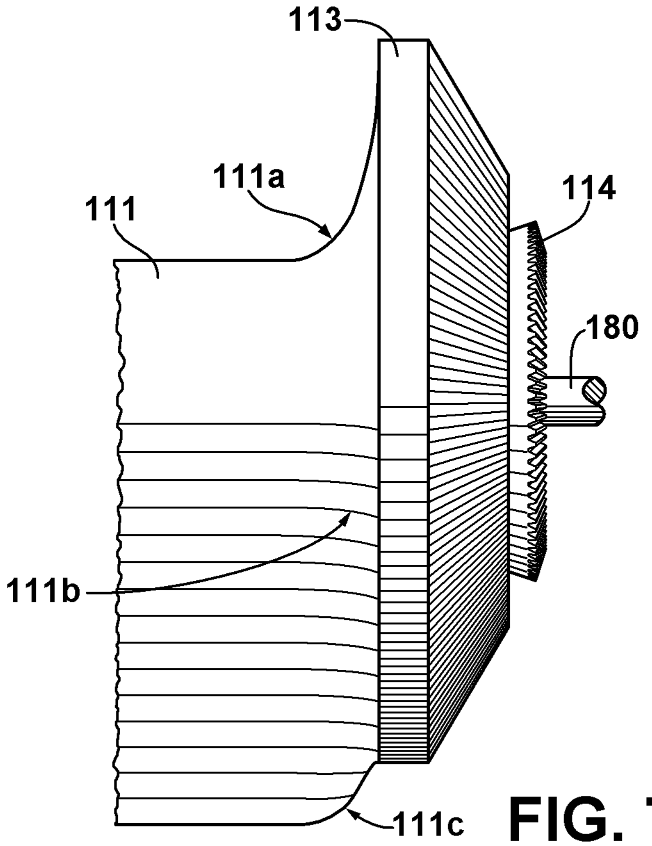
113
111a
111
114
180
111b
111c

FIG. 79

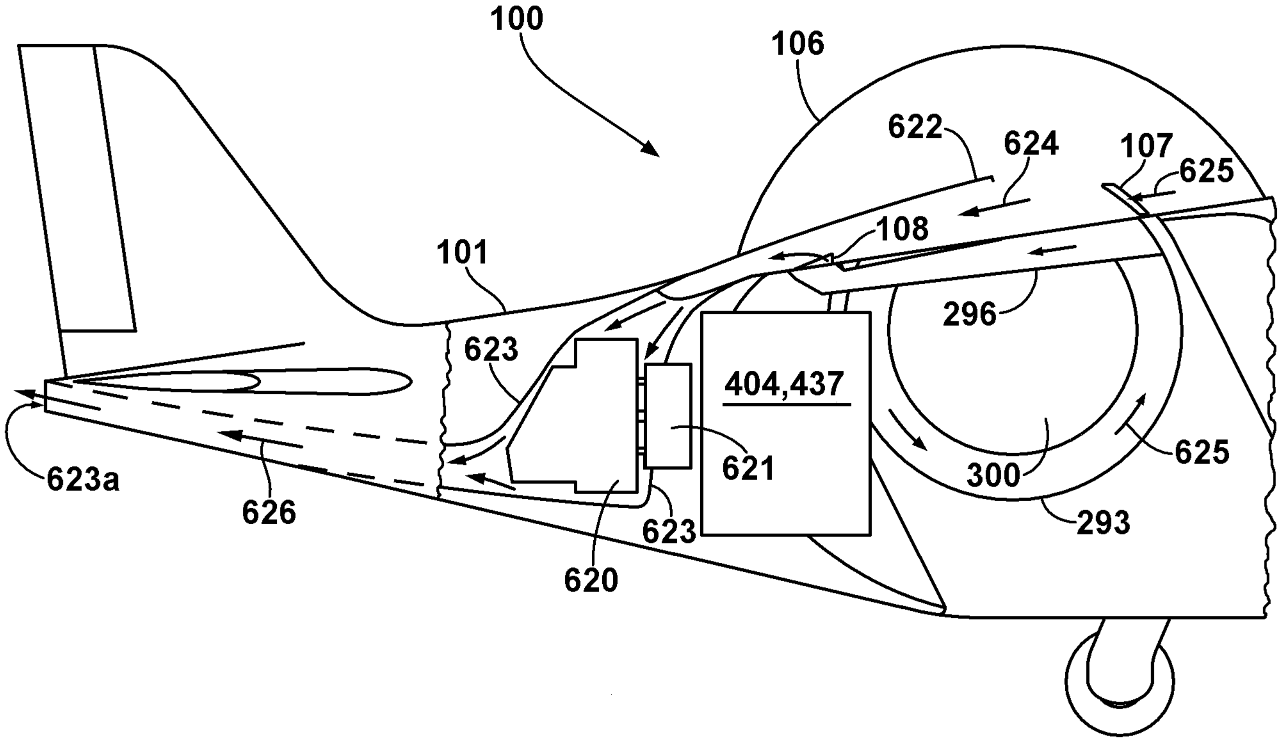
100
106
622
624
107
625
108
101
296
623
404,437
623a
626
621
300
625
293
623
620

FIG. 80

REFERENCES CITED IN THE DESCRIPTION

Patent documents cited in the description

- US2045233 1936-06-23, Kurt F.J. Kirsten et al, PROPELLER FOR AIRCRAFT **[0180]**
- US5100080 1992-03-31, Pierre Servanty, ROTOR FOR DEVELOPING SUSTAINING AND PROPELLING FORCES IN A FLUID, STEERING PROCESS, AND AIRCRAFT EQUIPPED WITH SUCH ROTOR **[0181]**
- US6932296 2005-08-23, Glenn Martin Tierney, CYCLOIDAL VTOL UAV **[0182]**

Non patent literature cited in the description

- Prandtl, L. (1924). Induced drag of Multiplanes, published as NACA TN 182, 1924 from Technische Berichte, Vol. III, No. 7, 1924 **[0205]**